ANL-7582

ANL-7582

proposal for a regional accelerator facility

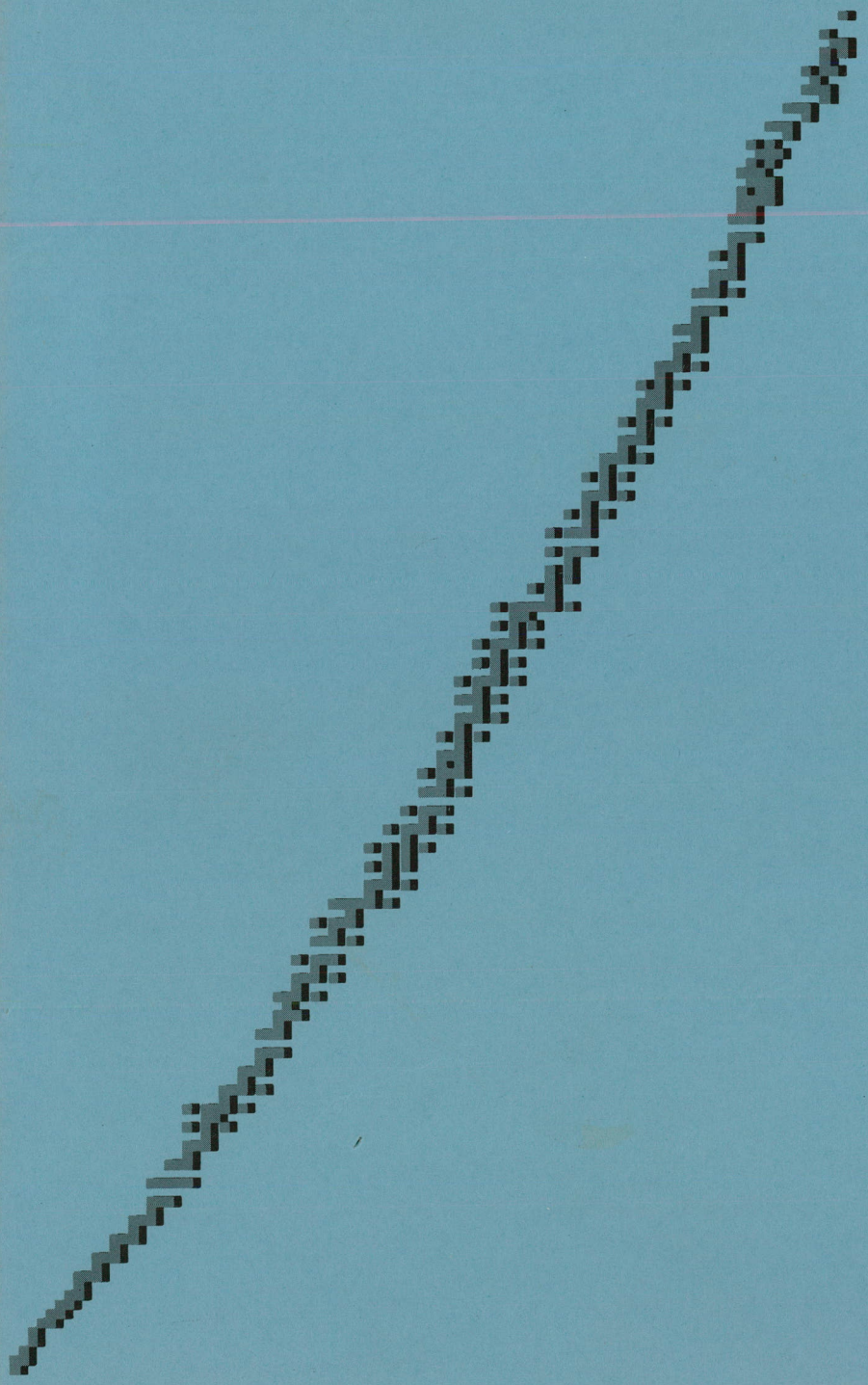

MIDWEST
TANDEM
CYCLOTRON

DISCLAIMER

The facilities of Argonne National Laboratory are owned by the United States Government. Under the terms of a contract (W-31-109-Eng-38) between the U. S. Atomic Energy Commission, Argonne Universities Association and The University of Chicago, the University employs the staff and operates the Laboratory in accordance with policies and programs formulated, approved and reviewed by the Association.

MEMBERS OF ARGONNE UNIVERSITIES ASSOCIATION

The University of Arizona
Carnegie-Mellon University
Case Western Reserve University
The University of Chicago
University of Cincinnati
Illinois Institute of Technology
University of Illinois
Indiana University
Iowa State University
The University of Iowa
Kansas State University
The University of Kansas
Loyola University
Marquette University
Michigan State University
The University of Michigan
University of Minnesota
University of Missouri
Northwestern University
University of Notre Dame
The Ohio State University
Ohio University
The Pennsylvania State University
Purdue University
Saint Louis University
Southern Illinois University
University of Texas
Washington University
Wayne State University
The University of Wisconsin

Printed in the United States of America
Available from
Clearinghouse for Federal Scientific and Technical Information
National Bureau of Standards, U. S. Department of Commerce
Springfield, Virginia 22151
Price: Printed Copy $3.00; Microfiche $0.65

ANL-7582
Physics

MIDWEST TANDEM CYCLOTRON

a Proposal for a Regional Accelerator Facility

June 1969

Prepared by the
Chemistry and Physics Divisions
Argonne National Laboratory

THIS PAGE

WAS INTENTIONALLY

LEFT BLANK

PREFACE

This Proposal for a regional accelerator system was developed by staff members of the Argonne Chemistry and Physics Divisions, with the advice and assistance of the AUA Ad Hoc Committee on a Heavy-Ion Accelerator, whose members are listed in Sec. IV. So many individuals contributed to the effort that it is feasible here to list only those who played a major role in the preparation of the technical portions of this document.

The section on the TU tandem was written by D.S. Gemmell. The cyclotron section was prepared by members of the design group (listed in Sec. III); T. K. Khoe, J. J. Livingood, and W. J. Ramler played a major role in the preparation of the material for this document. The sections on the building and the beam-transport system were written by T. H. Braid, with assistance from R. H. Siemssen on the shielding calculations. Others who contributed to parts of Sec. II are A. M. Friedman, A. H. Jaffey, and others who have already been mentioned. The construction schedule and cost estimates were worked out by T. H. Braid, F. P. Mooring, W. J. Ramler, and C. B. Webster.

The description of the experimental program was organized by P. R. Fields and J. P. Schiffer, with contributions from a very large number of interested associates both at Argonne and in the universities, as indicated on the first page of Sec. V.

The document as a whole was organized by L. M. Bollinger and J. P. Schiffer, and it was edited by F. E. Throw.

THIS PAGE
WAS INTENTIONALLY
LEFT BLANK

TABLE OF CONTENTS

ABSTRACT

The Midwest Tandem-Cyclotron is proposed as a regional facility to be built at Argonne National Laboratory for advanced research in nuclear chemistry and nuclear physics. The accelerator system would consist of a large 6-sector ring cyclotron whose injector is either a TU tandem Van de Graaff (for heavy ions) or a 4-sector cyclotron (for light ions). When not in use as an injector, the tandem would be used separately for research. The system would accelerate ions in all regions of the periodic table, providing continuously-variable beam energies up to 350 MeV for protons and up to 8—10 MeV per nucleon for ions of the heaviest elements. After a brief general description (Chap. I) of the proposed accelerator system and its use, Chap. II describes the accelerators, the building, and the associated experimental facilities. Chapters III and IV indicate the relevant research capabilities currently existing at Argonne and in the universities of the Midwest. Finally, the character of the anticipated research on super-heavy elements, other experiments with heavy-ion beams, and research with light-ion beams are discussed in Chapter V.

I. INTRODUCTION AND SUMMARY

The Midwest Tandem-Cyclotron accelerator system is proposed as a facility to be built at Argonne National Laboratory and operated by the Laboratory as a regional facility for advanced research in nuclear chemistry and nuclear physics. The research to be carried out at the proposed accelerator will encompass much of basic nuclear science, with special emphasis on (a) the search for the predicted "islands" of stable superheavy elements, (b) the investigation of the nuclear structure revealed by energetic collisions between complex nuclei, and (c) the elucidation of momentum distributions of nucleons and the correlation between nucleons in nuclear matter. The proposed accelerator system is believed to be the next logical step in the development of the experimental apparatus needed to attack these frontier problems of nuclear science.

As its name suggests, the proposed Midwest Tandem Cyclotron (MTC) complex consists of two major components—a TU tandem Van de Graaff and a variable-energy open-sector ring cyclotron. These two accelerators would be operated in two alternative modes, as is illustrated in Fig. I-1. For the acceleration of heavy ions to high energy, the tandem must serve as an injector for the cyclotron. Alternatively, the tandem and the cyclotron can be used independently and simultaneously.

Consider first the independent mode of operation. Here the TU tandem will accelerate hydrogen ions to 32 MeV (or perhaps 40 MeV) and almost all heavier ions to higher energies. At the same

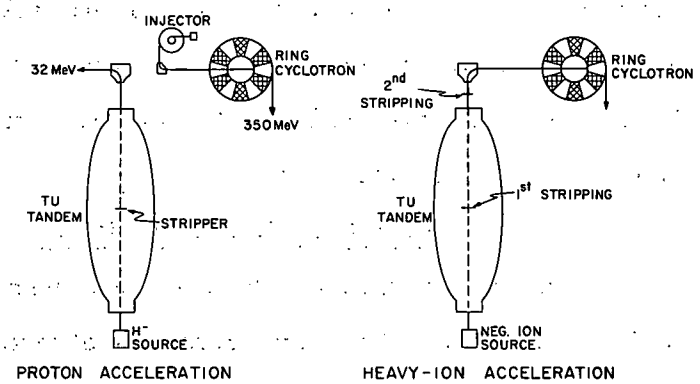

Fig. I-1. The two alternative modes of operation of the MTC system.

time, the cyclotron will provide protons over a wide energy range up to a maximum energy of 350 MeV, deuterons to 200 MeV, He^3 to 516 MeV, and He^4 to 400 MeV. In the alternative injection mode of operation, intended primarily for heavy-ion acceleration, energetic ions issuing from the tandem are stripped to a high charge state before they enter the cyclotron, where they are accelerated on up to energies well above the Coulomb barrier for interactions on any target nucleus. For both light- and heavy-ion acceleration, the MTC will provide beams with high intensity, high resolution, high maximum energy, and an energy that is continuously variable over a wide range. The maximum energies and currents of the system for representative projectiles are given in Sec. II. F.

The MTC accelerator system is designed to have unexcelled research capability in a very wide range of nuclear investigations. The heavy-ion beams will have energies and intensities far greater than any that have yet been achieved; these properties are essential for an effective investigation of the predicted new superheavy elements and will also provide a probe with which to investigate the nucleus in entirely new ways. Similarly, the light-ion beams will have much better intensity and energy resolution than any now available in the range covered by the MTC; these features and the variable energy will permit many qualitatively new investigations in a broad energy range which (for protons) extends well above the pion-production threshold.

The availability of two machines that can be used simultaneously for independent experiments will allow the system to support a large volume of research, an important consideration for a regional facility that is intended for the use of some 200 experienced scientists from 25 or more institutions.

Scientific Considerations. Although the proposed facility will have characteristics that make it very well suited to a wide variety of investigations, the requirements of two areas of investigation have

had a determining influence on the parameters of the accelerator system. The primary requirement is that the system should provide intense, energetic beams of heavy ions over the full range of the periodic table. These heavy ions are intended largely for the study of very heavy elements and especially for the search for the widely discussed "islands" of stability that are predicted to occur at masses considerably heavier than any that have yet been identified experimentally. An island of this kind is expected to result from the influence of closed nuclear shells, and currently it is thought that closed shells of 114 and perhaps 126 protons and of 184 neutrons will have a dominating influence on stability. The discovery and understanding of superheavy nuclides of this kind, if they can be produced, would have a profound influence on our understanding of the nucleus; and it could also have major consequences for applied science.

Finding effective ways to produce enough of the predicted superheavy nuclei for study is a considerable technical and scientific challenge. It seems clear that efficient production will require nuclear reactions between two heavy nuclei. However, one of the intriguing aspects of the problem is that we have little solid information on what kind of reactions are most effective, what energies are required, or indeed on what product nucleus to strive for. Consequently, an accelerator intended for the production of superheavy nuclei should have rather general capabilities that will allow all reasonable approaches to be explored. It should provide intense, high-energy beams of ions throughout the periodic table, and in particular it should be able to accelerate the heaviest ions (U^{238}) well above the Coulomb barrier for an interaction with a uranium target. Exactly what the desirable upper energy limit is for the uranium ion is not clear. The energy needed to overcome the Coulomb barrier in an interaction between two spherical nuclei of mass 238 is only about 6 MeV per nucleon, but the deformation of actual heavy nuclei is likely to increase this to about 8 MeV per nucleon. Also, the recent indication that heavy-ion-induced fission is an effective way to

produce superheavy nuclei and that the production cross section increases with increasing projectile energy up to well above the Coulomb barrier suggests that it may be important to be able to accelerate U^{238} up to energies of 10 or 15 MeV per nucleon. These considerations suggest that most of the accelerators now being actively considered for heavy-ion acceleration have too low an upper energy limit for the heaviest projectiles. It is to achieve the desired high energy that we use a TU tandem (rather than the smaller MP model) as the injector and that our cyclotron is larger than the 200-MeV four-sector Indiana cyclotron.

The prospect of using heavy ions for other nuclear investigations is also exciting, since we now have very little knowledge of what can happen in energetic collisions between complex nuclei. Undoubtedly this field will prove to be a rich source of qualitatively new information for our understanding of the nucleus. There are also interesting new possibilities for the use of energetic heavy-ion beams for investigations in atomic and solid-state physics and in biology and medicine.

The second area of research that has had a major influence on the design of the new accelerator system is the kind of nuclear-physics research done with light ions in the medium-energy range. Here the determining considerations are that it is important to be able to explore the region of energy up to and through the meson threshold much more thoroughly than will be practical with accelerators in existence or under construction. The physics of this region is interesting because of the presence of the meson threshold (at about 290 MeV for nucleon-nucleon interactions) and because the region links two fundamentally different sorts of nuclear physics. At the low-energy end of the region one studies the energy levels one by one and attempts to describe the level structure in terms of nuclear models; the models themselves have to be related to the nucleon-nucleon forces, a connection that must necessarily be indirect. At high energies ($>$100 MeV for protons) interest shifts to pair-correlation functions, momentum distributions,

etc.; these are related more directly to the nucleon-nucleon forces, although virtually nothing is now known about them. Our accelerator complex may well turn out to be the ideal system for the study of nuclear structure in that it is equally well suited for both kinds of physics— its energy is low enough to permit the good energy resolution required to study individual states and at the same time its maximum energy is high enough to permit a thoroughgoing investigation of the more general features of nuclear matter. Thus, the MTC may allow the gulf between the two areas of nuclear physics to be bridged.

Accelerator Considerations. The MTC accelerator complex combines two modern accelerators, each of which would be a valuable research tool by itself; when used as a system, they will provide a unique and powerful probe for nuclear research.

The TU tandem is the largest of the tandem Van de Graaff accelerators; a prototype is nearing completion. The choice of this tandem is dictated by the need to inject highly-stripped heavy ions into the cyclotron so as to minimize the radius of curvature (and thus the size and cost) of the cyclotron. The use of the smaller MP model would require the construction of a substantially larger cyclotron; and the even smaller FN tandem probably would not be suitable at all, because it could not provide the required intensity of heavy-ion beam. Moreover, the TU by itself will be much more valuable than the smaller tandems in many areas of research.

The TU will be used in its tandem mode of operation at all times. That is to say, negative ions will be injected into the machine from an ion source near ground potential, and these ions are accelerated to the terminal, where they pass through an electron-stripping medium. An alternative, and superficially attractive, possibility is to produce highly-stripped heavy ions in a source mounted in the terminal of the TU. This possibility was rejected partly because of questions regarding its feasibility and partly because of our judgement that a terminal source would severely prejudice the reliability of the system for heavy-ion

acceleration, in view of the short lifetimes of all known sources producing usable intensities of ions in the required high charge states. In contrast to these problems with the terminal source, the planned external source at ground potential is much more reliable and its accessibility makes all technical problems much easier to solve. The reliability of the external source is essential for our system, which (because of its regional character) must support the work of a very large number of users.

The open-sector cyclotron with free-standing magnet sections has characteristics that make it especially suitable for the proposed application. In particular, the space between magnets allows the problems of beam injection and extraction, vacuum pumping, and the design of the accelerating structure to be solved much more easily than in a conventional cyclotron. The technology of open-sector cyclotrons is relatively well understood now, and the experience gained at the machine now under construction at Indiana University should provide answers to many of the remaining questions.

The size of the proposed cyclotron was set by the dual requirements that the upper energy limit for protons should be well above the meson threshold and that the cost of the cyclotron should not be substantially higher than would be required for heavy-ion acceleration alone. Both four-sector and six-sector designs were carefully considered. A six-sector design was chosen because orbit calculations showed that resonance instabilities in a four-sector machine could cause unsatisfactory operation for both protons and heavy ions. Such resonances are unimportant for the proposed six-sector machine, which will reliably accelerate protons up to at least 350 MeV.

Construction and Operation. The way in which the proposed facility will be constructed can only be specified in general terms at this time. Consider first the TU tandem. The major responsibility for the construction of this accelerator will, of course, rest with the manufacturer (High Voltage Engineering Corporation). However, in order to minimize the cost, we propose to take on a limited responsibility

for the design and development of some parts of the tandem system that do not interact in a fundamental way with the basic characteristics of the accelerator. Also, this experience will prove valuable later, since an effective use of a machine of this magnitude will require an operating staff that is fully competent in all aspects of electrostatic-accelerator technology, especially in view of the potential of the system for future improvements. Because of the experience gained from constructing and operating a Van de Graaff accelerator (starting in 1948) and from operating a tandem since 1962, Argonne already has on its staff men with many of the technical skills that will be needed for the development and operation of the TU-tandem system.

The conceptual design of the proposed cyclotron has been carried out by the accelerator design group in the Argonne Chemistry Division, who have had the previous experience of designing several other cyclotrons and who for many years have had the broadening experience of being responsible for the operation and development of several different kinds of accelerators—a cyclotron, a Van de Graaff, a high-current electron linac, and a Cockcroft-Walton. In view of this existing competence, the Laboratory plans to take on the prime responsibility for the design and assembly of the proposed cyclotron, although major mechanical construction will be done outside and major components will be purchased from commercial sources, when possible. An important aspect of this approach is the backup provided by the pool of skilled manpower concerned with the operation and improvement of the ZGS. Also, the universities in the area have staff members with demonstrated competence in cyclotron technology.

Building. The great range of experiments for which the accelerator system may be used places severe demands on the beam-handling system and on the building that houses the facility. It would not be justifiable to make full provision initially for all of the many experiments for which the system is well suited. Nevertheless, it is important that the design of the supporting facilities and especially the

building should not preclude the possibility of exploiting the accelerator fully in any area of science that might become especially interesting in the future. Thus, we have attempted to lay out the facility in such a way as to permit the future development of many features of the system that do not appear to be of primary importance now. In general terms, this has been done by considering what would be required to emphasize various characteristics of the accelerated projectiles (energy resolution, time resolution, etc.) and the building has been designed to make it feasible to satisfy these requirements later, if it becomes desirable. Similarly, the building was planned to permit the simultaneous use of several ion beams from the tandem in several independent experiments.

Since the proposed accelerator complex is to be a regional facility, some office and laboratory space for outside users is provided in the accelerator building. Additional space will be made available in existing buildings such as those that house the Chemistry and Physics Divisions.

Supporting Facilities. Existing equipment and auxiliary facilities at Argonne will contribute greatly to the effective use of the proposed accelerator complex. For experiments tied directly to the accelerator, the existing items consist of major pieces of equipment (magnetic spectrograph, etc.) now being used in nuclear-physics experiments at the present cyclotron and tandem; also, the Sigma-7 multiple-task computing system now being developed by the Chemistry Division will serve initially as an on-line data-handling facility. The existing auxiliary facilities available for off-line experiments are even more valuable. The most notable of these is the M-wing "hot laboratories" of the Argonne Chemistry Division, probably the world's most sophisticated research facilities for carrying out laboratory operations on high-activity materials, particularly heavy elements. Other major facilities that will play an important role in off-line experiments are a mass separator, a high-resolution alpha spectrometer, and a double

high-resolution high-transmission beta-ray spectrometer. The existence of these major facilities will greatly extend the research capability of the MTC.

Research Personnel. One of the most important justifications for the construction of the MTC is the large and outstanding group of nuclear chemists and physicists eager to use it—perhaps the largest group of experienced scientists who have ever banded together to support the construction of an accelerator to be used in nuclear science. This pool of manpower skilled in research consists of nuclear chemists and nuclear physicists both at Argonne and at universities in the area.

The nuclear chemists from the Argonne Chemistry Division constitute one of the largest and most productive groups of its kind and, of central importance for this proposal, it has had years of experience in heavy-element and nuclear chemistry. An approximately equal number of nuclear chemists are distributed over seven Midwestern universities. They provide a wide range of competence in nuclear chemistry. The large group of nuclear physicists in the Argonne Physics Division are an essential ingredient for an effective use of the MTC for physics since, as members of the operating institution, they will establish the core of the physics research program. The largest group of all consists of the nuclear physicists from the AUA universities (and a few others)—about 135 physicists with long-term appointments. Associated with these groups of experienced scientists are a total of about 500 postdoctoral fellows and graduate students.

Allocation of Experimental Time. In view of the large number of scientists who have already indicated a desire to use the proposed facility, it is clear that running time on the new facility will be in great demand and that no single institution should control its use. Thus, although the facility will be built and operated by Argonne, it is assumed that its use will be governed by a representative group of users from the Midwest in somewhat the way the ZGS is.

A necessary implication of the concept that the MTC will be a regional facility used by a very large number of investigators is that, in spite of its capacity to support a large volume of research, the new system cannot be expected to support the entire research programs of many users. Thus, much of the research that is now carried out at other accelerators in the area will need to continue. Indeed, an important aspect of this proposal is that the new accelerator system will be effectively used because most of the users have smaller accelerators at their home institutions and their research can be effectively extended and complemented by experiments at the MTC.

Cost. The estimated cost for the construction of the proposed facility is $24.4 million. This total allows $6.8 million for the TU tandem, $8.6 million for the cyclotron and its light-ion injector, $7.3 million for the building, and $1.7 million for beam-handling and other equipment. The accelerator system will be operational in 1975 if the project is authorized and funded in fiscal year 1971.

II. THE ACCELERATOR SYSTEM

The proposed tandem-cyclotron system consists of a TU-model tandem Van de Graaff and a variable-energy 6-sector isochronous cyclotron. These accelerators will be used both independently and as a coupled system in which the tandem injects into the cyclotron.

The TU tandem is guaranteed by its manufacturer (High Voltage Engineering Corporation) to operate with at least 16 million volts on its terminal and it is designed to operate at 20 MV. Thus, it will accelerate hydrogen ions to 32 MeV (or perhaps 40), helium ions to 48 MeV (or 60), and a heavy ion such as I^{127} to about 150 MeV. The ion beams may be either dc or pulsed, as required, and they will have the good energy resolution and emittance that are characteristic of tandem Van de Graaffs.

When the 6-sector cyclotron is operated independently of the tandem, it will be used primarily to accelerate light ions. These ions will be injected into the main machine from a small injector cyclotron, as is planned at Indiana University. The system is designed to provide variable-energy beams with maximum energies of 350 MeV for protons, 200 MeV for deuterons, 520 MeV for He^3, and 400 MeV for He^4. Other relatively light ions can also be accelerated by the cyclotron alone.

The acceleration of heavy ions to very high energies requires that the tandem serve as an injector for the cyclotron. In this mode of operation (as shown in Fig. I-1) negatively-charged ions from a source at approximately ground potential are accelerated to the positive terminal of the tandem. There they pass through a gas stripper in which many electrons are removed from each atom, and the resulting positively-charged particles are accelerated back to ground potential. Here the projectiles pass through a foil stripper to form the very highly stripped ions that are injected into the cyclotron. The high charge of

these injected ions allows a cyclotron of moderate size to accelerate the ions on up to very high energies.

For both light- and heavy-ion acceleration and in both the independent and injection modes of operation, the proposed accelerator system provides beams with high maximum energy, high intensity, high resolution, and an energy that is continuously variable over a wide range. A carefully planned building and some essential auxiliary equipment will allow the accelerator to be used effectively in a varied research program.

II. A. THE TU TANDEM

The model-TU tandem Van de Graaff is the latest in a series of tandem accelerators being developed and manufactured by High Voltage Engineering Corporation (HVEC) of Burlington, Massachusetts. The most significant feature of the new accelerator is its high terminal voltage (16 MV guaranteed, 20 MV design aim). This will permit the acceleration of heavy ions to sufficiently high energies so that, after passage through a thin stripping foil, a high charge-to-mass ratio will result, thus allowing very efficient acceleration of the ions to high energies in a cyclotron.

In the course of the past decade, HVEC has successfully incorporated the tandem principle into a series of accelerators, and as of May 1969, has sold 54 of these machines to laboratories in many parts of the world. The company's program of research and development in accelerator technology has enabled it to progressively raise the voltage sustainable on the center terminal of the tandem. The series includes the models EN (maximum guaranteed terminal voltage 6 MV), FN (7.5 MV), MP (10 MV), and TU (16 MV). Voltage tests on the first TU tandem are scheduled to take place at HVEC's Burlington plant in the fall of 1969. Strictly speaking, this first machine will be a model XTU. This is HVEC's nomenclature for that version of the accelerator having a guaranteed proton performance only. In order to provide a capability for the acceleration of high currents of heavy ions, the XTU

will require some additions and alterations (described later in this section). The resultant accelerator having both a light-ion and a heavy-ion capability is termed the model TU. In the accelerator facility being proposed here, the TU tandem will be able to be used either as a "stand-alone" accelerator or as an injector for an open-sector cyclotron.

When operated in the stand-alone mode, the TU will be a very useful accelerator in its own right, capable of producing high-quality beams of both light and heavy ions for a variety of experimental purposes. The virtues of the tandem as a tool in experimental nuclear physics are now widely recognized. They include excellent energy resolution and stability, continuous and easily-controlled energy variability over a wide range, intense beams (either dc or pulsed) with good emittance properties, the ability to accelerate a large variety of ions, and readily accessible ion sources at or near ground potential. The energy of a beam (injected as atomic negative ions) emerging from a tandem is $V(q + 1)$ plus a small injection energy, where V is the terminal voltage and q is the charge state of the ions in the second (high-energy) half of the accelerator following the stripping process in the center terminal. The terminal voltage of the TU will be variable from 3 to 16 MV, thus providing hydrogen-ion beams of from 6 to 32 MeV and helium-ion beams of from 6 (He^{+}) to 48 (He^{++}) MeV. A detailed list of the beams, energies, and intensities which are expected from the TU is given in Table II-A-VII. For light-ion beams, either a gas or a foil stripper can be used in the center terminal of the machine, but for heavy ions only a gas stripper is presently contemplated.

These same beam properties that make the TU such a desirable experimental tool also make it well suited for use as an injector to an open-sector cyclotron. One of the great advantages of this type of cyclotron construction is that it permits the use of an external source of ions for injection. In addition to benefitting other aspects of the cyclotron operation (e.g., reducing the gas load in the cyclotron, etc.) this arrangement permits detailed preparation of the ion beam before injection.

Pre-acceleration of the ions in the tandem is beneficial both from a beam-optics standpoint and by virtue of the high charge-to-mass ratio obtainable for the beam injected into the cyclotron. The importance of this latter factor can be realized when one notes that for a given cyclotron of fixed maximum diameter and maximum average field, the maximum energy per nucleon attainable for heavy ions is approximately proportional to $(q/m)^2$, where q is the charge of the particle and m is its mass. The high-quality beams (good emittance and energy resolution) from the TU tandem are also important properties in connection with its use as an injector.

The cyclotron is an rf machine and is designed to provide beams of readily variable energy. This means that the TU tandem will have to supply a pulsed beam at a frequency which can be varied to be kept equal to the cyclotron rf frequency (or to a subharmonic of it), and with a pulse width suitably short in order to achieve good energy resolution in the beam extracted from the cyclotron. It is proposed to achieve these requirements for a pulsed beam by means of velocity modulation of the negative-ion beam entering the tandem. This technique has been used in several existing tandems to produce pulsed beams with pulse widths of about 1 nsec, which is about the value required for the proposed cyclotron. The requirement of producing such pulsed beams at variable frequencies and for a great range of ion masses poses some difficult but nevertheless solvable technical problems.

The responsibilities for the development and construction of the TU tandem described in this proposal will be divided between HVEC and ANL in the following way. HVEC will be responsible for the accelerator as a voltage generator and for its meeting (as minimum requirements) the guaranteed specifications of an XTU tandem (HVEC equipment specification number V-117). These specifications include the delivery from the accelerator of 5 μA of 32-MeV protons. HVEC will also be responsible for the additions and improvements to the vacuum system required in order to achieve satisfactory performance for the intense heavy-ion beams discussed in this proposal. ANL will

be responsible for the beam optics and the transmission of the various beams through the accelerator. The ANL responsibility will include such items as the pulsing and bunching system, the charge-state selector in the center terminal of the machine, additional ion sources, beam-handling equipment, etc.

In what follows, the TU tandem will be described and various aspects of its expected performance discussed. Some topics of crucial importance to the present proposal (e.g., vacuum problems, beam pulsing, etc.) will be treated in detail.

1. General Description of the TU Tandem

Figure II.A-1 shows two photographs of the tank of a TU assembled at the Burlington plant of HVEC. Because of the size of the tank, its sections must be welded together near the accelerator site, hydrostatically pressure tested, and then moved inside the building. Figure II.A-2 shows plan and elevation drawings of a possible arrangement for the proposed TU installation.

As an illustration of the way in which the TU will be used in conjunction with the cyclotron, let us consider the acceleration of bromine. Negative bromine ions emerging from an ion source fall through a potential drop of 150 keV and are directed towards the tandem by an inflection magnet which also serves as a mass analyzer. Thus in our example, Br^{79} could be accepted for acceleration while Br^{81} would be rejected. This negative-ion beam then enters a klystron buncher which applies a suitable velocity modulation to the beam so that it will arrive at the cyclotron in short bursts at an appropriate frequency to match the rf frequency of the cyclotron. This velocity-modulated beam now enters the first (low-energy) half of the tandem accelerator and on reaching the center terminal it has increased its energy by an amount corresponding to the terminal voltage.

Inside the terminal, the beam passes through a gas stripping canal and becomes fractionated into a roughly Gaussian distribution of

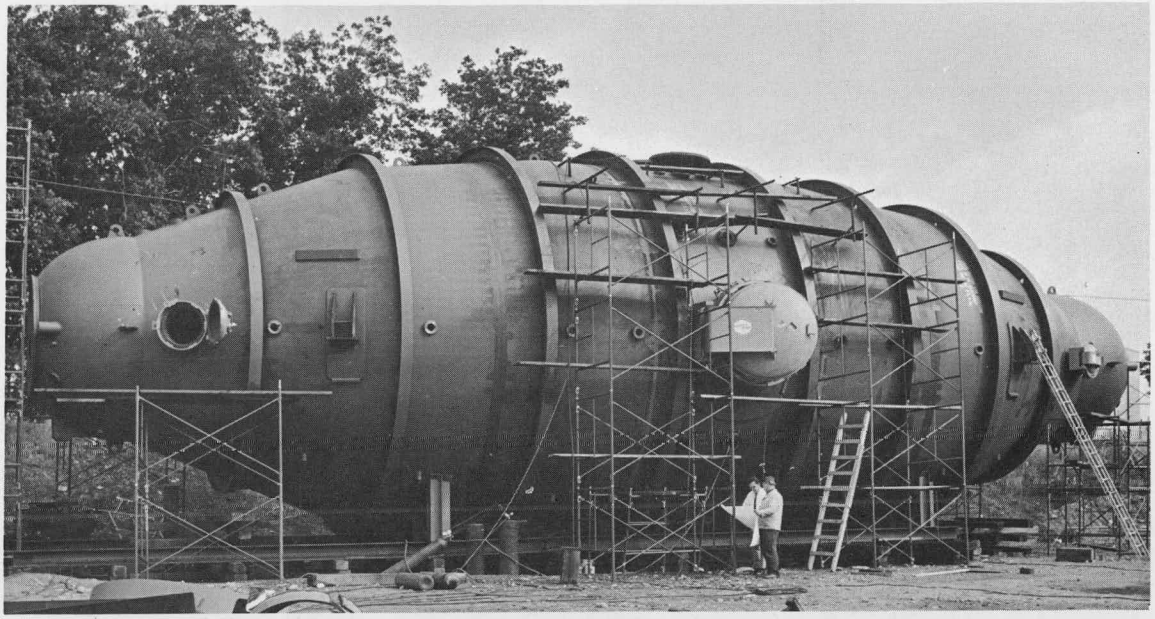

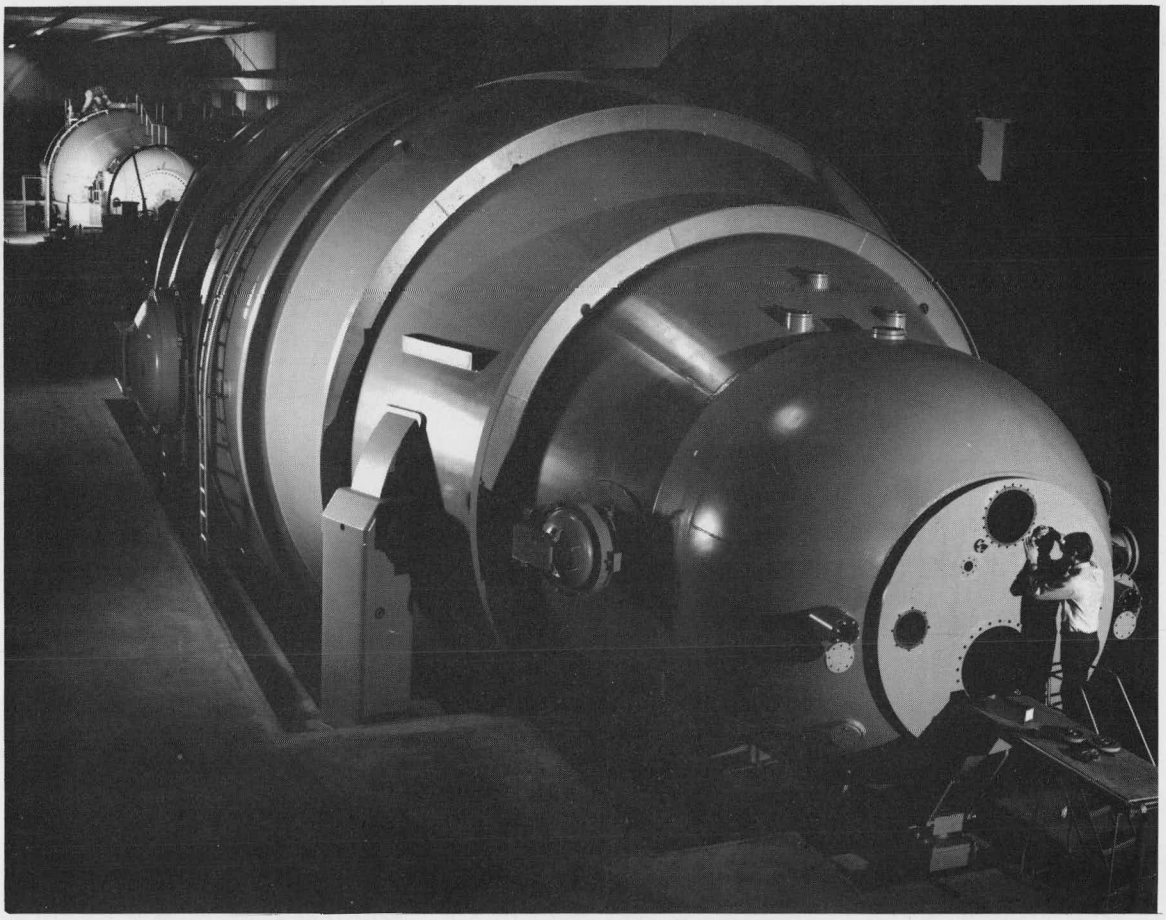

Fig. II. A-1. Views of the tank of a TU tandem being assembled at the Burlington plant of High Voltage Engineering Corporation.

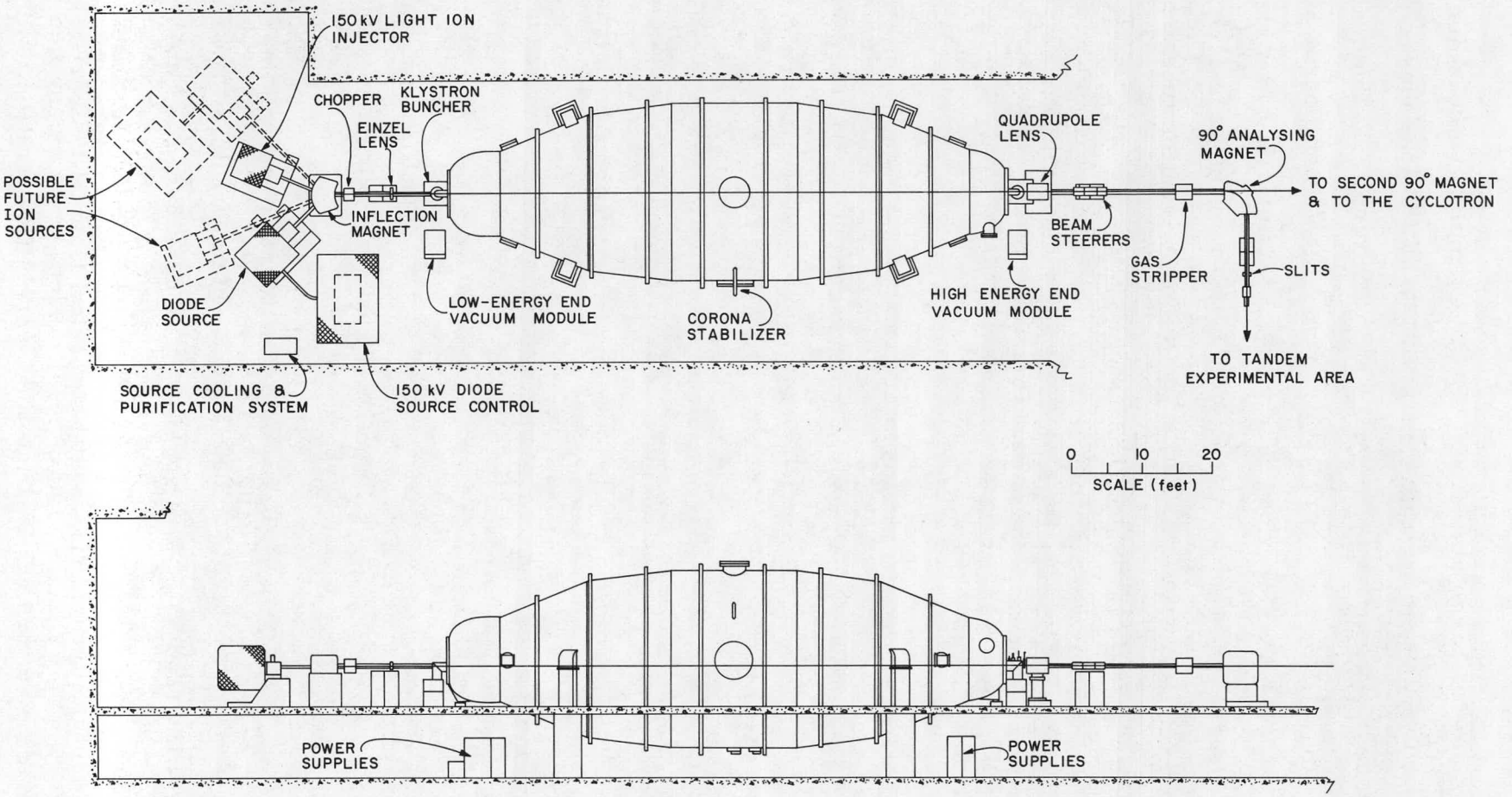

Fig. II. A-2. Diagram of the proposed TU tandem installation.

several positive charge states. If, in our example, we consider a terminal voltage of 16 MV, then the mean charge state of the ions emerging from the stripper will be about 6.3. Still within the terminal, the beam enters a device that selects one charge state (e.g., the 7+ component) of the beam for further acceleration. (This is done primarily to increase the useful beam current available from the TU by preventing undesired charge states from entering and loading the acceleration tubes in the second half of the machine.) The beam in the desired charge state is then focused into the high-energy tube and, in our example, would emerge from the accelerator as Br^{79} (7+) ions at 128 MeV.

This beam is now transmitted towards the cyclotron via an isochronous beam-transport system, passes through a thin foil stripper located near the injection point of the cyclotron, and undergoes a further fractionation into several more highly stripped charge states. For the example chosen, the charge state for which the particle current is highest would be 23+. This charge state would be selected magnetically by the cyclotron's inflection system and would then be accelerated up to a final energy of 2.2 BeV (27.5 MeV/nucleon).

For the stand-alone mode of operation of the TU, the beam from the tandem would be transported via an analyzing magnet directly into one of the target areas. (A second stripper would then be required only for the most energetic beams of the heavier ions. This stripping would increase the charge-to-mass ratio so that these beams can be handled by the 90° magnet. There would be an accompanying loss in beam intensity by about a factor of five.)

An alternative to using an external negative-ion source would be to employ a positive-ion source contained within the center terminal of the tandem. This approach was considered in connection with this proposal, but discarded for the following principal reasons. In order to obtain useful currents (i.e., at least a few times 10^{13} particles/sec) in high positive charge states (e.g., 9+ for uranium), one requires a high-power source such as the Penning type used with the Berkeley HILAC.

Unfortunately, the filament lifetime in this type of source is very short (typically about half an hour). The source is a complicated one to operate and requires frequent adjustment. If one adds pulsing and bunching components and some beam optical elements, it is clear that this would create quite a complex ion-source system. If a system like this were readily accessible, its complexity would be acceptable. But contained within a terminal structure operated at megavolt potentials and surrounded by a large tank full of high-pressure gas, such a source could scarcely be termed accessible. The delivery of the needed high power levels (~40 kW) to the terminal and the dissipation of the associated heat would give rise to serious technical problems. The large quantities of gas consumed by the source would also present problems and require a substantial amount of additional pumping power supplied in the terminal. These various difficulties, coupled with the fact that the lack of accessibility to the source would tend to seriously reduce both the flexibility and the useful beam time available for the entire accelerator system, were considered convincing arguments against such an ion source. Viewed somewhat differently, it was thought that the costs involved in making such a source useful were not warranted. These considerations are reinforced by the fact that the maximum beam currents achievable with the two types of sources (positive and negative) are the same since each is determined by the current-carrying capability of the tandem's acceleration tubes. A system using an external negative-ion source and bunching system is greatly to be preferred because of the accessibility of the source, its flexibility (in that one can have several sources and service and test all except one of them while the accelerator is running with a beam), and its far less stringent space and power requirements.

To illustrate the great importance for heavy-ion acceleration of being able to achieve high terminal voltages on the tandem injector, Fig. II.A-3 shows the results of some calculations for the case of bromine acceleration. In the figure, the final energies per nucleon obtainable from the proposed cyclotron are plotted as a function of the voltage on the

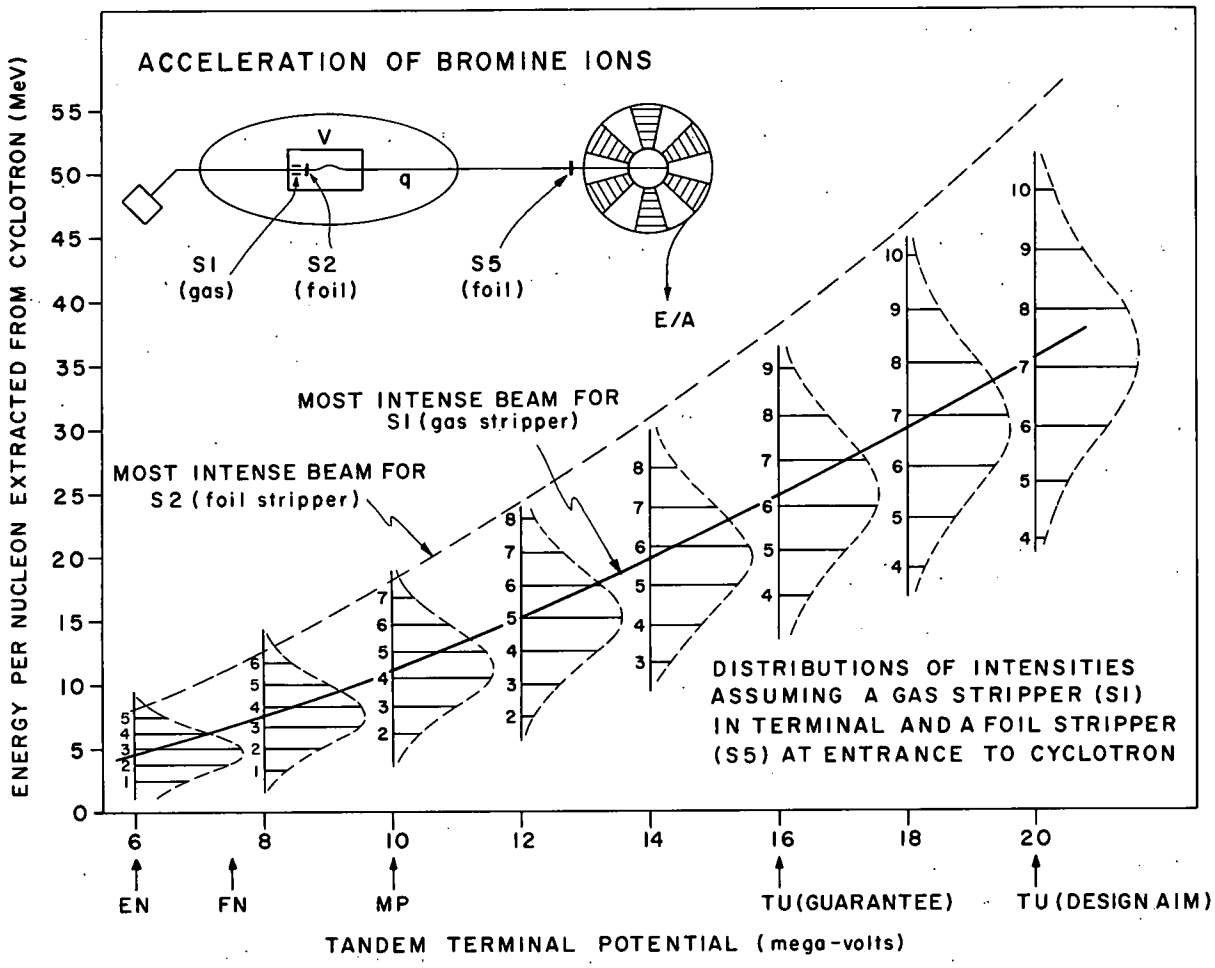

Fig. II. A-3. Illustration of the improvement in performance of the cyclotron for heavy-ion acceleration as the voltage on the terminal of the tandem injector is raised. The indicated charge-state values are those applying during acceleration in the second half of the tandem.

center terminal of the tandem. Also indicated are the relative beam intensities expected for different choices of the charge state selected for acceleration in the second half of the tandem. It is assumed, for the purposes of the figure, that one always selects the most intense charge state following the final (foil) stripper for acceleration in the cyclotron. (If one did not do this, but instead selected a less intense but higher charge state emerging from this final stripper, the energy achieved from the cyclotron would be unchanged but, because of the higher charge/mass ratio, would be achievable with a lower magnetic field.) It is clear from the figure that there is a dramatic improvement in the performance of

the overall (tandem plus cyclotron) system as the voltage on the tandem terminal is raised. The rated terminal voltages of the various models of tandem accelerator are also marked on the abscissa in the figure. Figure II. A-3 also points out the significant improvement in performance to be obtained should the TU reach its design aim of a 20-MV terminal voltage. A further advantage is gained from high terminal voltages in the acceleration of beams injected as negative molecular ions. For instance, in the case of UF_5^- beams, the uranium nucleus acquires only about 72% of the energy of the negative molecule. Thus with a terminal voltage of 16 MV, the uranium would attain only 11.4 MeV in the low-energy section of the tandem. The molecule, of course, would disintegrate in the gas stripper and the uranium ions would then receive the full benefit of the acceleration voltage in the second half of the machine.

The solid line running across Fig. II. A-3 shows, as a function of terminal voltage, the energy/nucleon attainable for the beam of highest intensity coming out of the cyclotron. The broken line shows the same thing but calculated under the assumption of a foil stripper in the tandem terminal. This would result in still higher energies—a consequence of the higher charge states attained in foil stripping as opposed to gas stripping. However, for reasons explained later in this section, it is presently considered unfeasible to use a foil stripper in the terminal for heavy-ion acceleration.

2. Voltage Performance and Stability

The TU tandem is designed to operate at a maximum voltage of 20 MV. HVEC will guarantee operation at voltages up to 16 MV. These high operating voltages, which have not previously been achieved in electrostatic generators, are possible as a result of many advances in accelerator technology—e.g., improvements in acceleration tubes, insulating gases, electrostatic structure, and column resistors. The acceleration tubes will have stainless steel electrodes and will use the

"inclined-field" type of construction which has proved highly successful in reducing electron-loading effects. The tubes for both the negative and positive stages will be constructed in four 6-ft sections. Between each pair there will be a 2-ft drift section permitting the inclusion of items such as additional pumping on the tubes, an electrostatic focusing lens ("funnel lens") between two of the low-energy tube sections, and perhaps at some later date a foil stripper assembly in the high-energy tube if it should be found desirable. The insulating gas in the pressure vessel will be a mixture of 30% sulphur hexafluoride (SF_6), and 70% of the usual mixture of nitrogen and carbon dioxide. Tests conducted on existing tandems indicate that this mixture of three gases at a pressure of about 200 psi should lead to optimum voltage performance and stability. The major factors limiting the voltage attainable on the MP tandem (run without tubes) are thought to be the movement of the column rings as a result of the large electrostatic forces between them and the ionization currents produced at the ends of the rods that form the terminal cage. In the TU, these difficulties are being corrected by using column rings that withstand movement under electrostatic stress and by reducing the localized field concentrations by constructing the terminal with a continuous skin. The maximum diameter of the center terminal will be 7 ft and it will have an overall length of 8 ft. Inside the tank, the high-voltage terminal is supported by insulating column structures, mounted horizontally under compression. The columns are of a truss construction and are assembled in place in the tank. Each consists of four 8-foot-long sections, of which 6 ft is insulating length.

In stand-alone operation of the TU, the terminal voltage will be controlled to within 1.5 kV. This will be accomplished by deriving an amplified signal from the slit edges at the image point of the 90° beam-analyzing magnet. Beam motion on the slit will provide a signal which will be amplified to control the corona load on the center terminal via a corona-point assembly on the tank. When the TU is used as an injector for the cyclotron, the stabilization system will use a

generating voltmeter located in the pressure vessel near the center terminal. As a result, the voltage of the tandem terminal will be stable to about 1 part in 10^3.

3. Negative-Ion Injection

It is planned to install two negative-ion sources initially. The inflection magnet will, however, have extra ports to permit later addition of other sources. (This is a factor that strongly affects the time the accelerator is available for use. The running time for experiments can be maximized by having several sources arranged so that while one is being used, the others can be worked on.) The two initial sources will probably be a duoplasmatron with charge exchange (used mainly for beams of hydrogen and helium ions) and a direct-extraction diode source which is known to provide copious negative beams of many elements. Another promising type of source presently under development is the sputtering type designed by Hortig.[1] In this source, the material from which negative ions are to be produced is evaporated and is condensed on a spinning disk. A thin layer of cesium is then evaporated over it, and both layers are then bombarded with a beam of 25-keV positive krypton ions. The resulting negative ions emerge with a low energy spread and good emittance characteristics. The layers of material on the spinning disk are constantly replenished by continuous evaporation.

In this way, Hortig has achieved negative-ion beam currents of 24 μA for oxygen, 5 μA for copper, 11 μA for silver, and 12 μA for gold. The beam currents available from the source are presently limited by the bombarding krypton current (0.6 mA). It can reasonably be expected that much higher bombarding currents will be attained and that still larger negative-ion currents will then be produced.

Until now there has been little demand for negative beams of the heavier elements. This situation will certainly change with the

---

[1] G. Hortig, P. Mokler, and M. Müller, Z. Physik 210, 212 (1968).

advent of the TU tandem. A study of the more recent information on atomic negative ions[2-4] shows that—with the exception of the rare gases, the alkaline earths (Be, Mg, etc.), nitrogen, and possibly scandium—all elements up to atomic number 36 (krypton) form stable atomic negative ions. The behavior of the remainder of the periodic table in this respect is not as thoroughly known. However, there is no distinct trend of the electron affinity with atomic number within the various groups of elements for which data are available. The theoretical calculations on the lighter elements also show that electron affinities, which are of the order of about 1 eV, result from a delicate balance of factors and no distinct trend can be expected. (It has been noted[4] that there is a very small general increase in electron affinity as one goes from the first period to the second period.) Thus it is highly probable that the great majority of the remaining elements also form stable atomic negative ions. The major uncertainty concerns the lanthanide and actinide elements, particularly the first half of each series. Those elements for which a stable atomic negative ion does not exist can often be accelerated as metastable negative ions (e.g., He, N, Mg, Ca) or as negative molecular ions. When the use of molecular negative ions is included, it is very likely that practically every element can be accelerated as a negative ion. At least one of the rare gases, xenon, forms large amounts of negative molecular ions by electron impact on the fluorides and oxy-fluorides.[5] Krypton probably behaves similarly although its fluoride is extremely reactive chemically. Some molecular negative ions are very stable and have high electron affinities (e.g., CN has a higher electron affinity than any atom, forms a very stable negative

---

[2] R. S. Berry, "Small Free Negative Ions," in Chemical Reviews 1969, (in press).

[3] B. Moiseiwitsch, in Advances in Atomic and Molecular Physics, edited by D. R. Bates and I. Estermann (Academic Press, New York, 1965), Vol. 1, p. 61.

[4] E. Clementi et al., Phys. Rev. 133, A419 (1964); Phys. Rev. 133, A1274 (1964); Phys. Rev. 135, A980 (1964).

[5] M. Studier (private communication).

ion, and can be produced in high abundance). Volatile compounds of many refractory metals exist (e.g., UF_6, WF_6) and at least some are known to form negative molecular ions containing the metal when subjected to electron impact.

It is more difficult to predict the currents that might be obtained for the various negative ions that have not yet been employed in accelerators. While there is a fairly good correlation between high electron affinity and high negative-ion current, there are numerous exceptions such as hydrogen and helium. The substantial currents obtained for Ag^- and Au^- beams by Hortig[1] with a sputtering technique are highly encouraging, since a fair number of other elements should have comparable electron affinities and should therefore lend themselves to this technique. Certainly the various plasma and discharge sources should produce useful currents of molecular negative ions from many of the volatile or moderately volatile oxides and halides of many elements.

Uranium beams are of particular interest in this proposal. Negative beams of several microamperes have been obtained from a diode source[6] (UF_5^-) and a Penning source[7] (UF_2^-). The prospects for obtaining larger negative beams are quite good. So far there has been little interest in uranium beams because existing tandem accelerators could not accelerate such ions to energies sufficient to overcome the Coulomb barrier; and consequently relatively little effort has been spent on obtaining such beams. It is encouraging, however, that in the report on the Manhattan Project, where considerable effort was put into developing positive-ion sources suitable for use in the electromagnetic separation of large quantities of uranium, intensities of the negative ions UCl_n^- and UF_n^- were found to be comparable to positive-ion intensities.[8] For these reasons it seems eminently reasonable to expect

---

[6] P. H. Rose (private communication).

[7] K. Bethge (private communication).

[8] E. H. S. Burhop, H. S. W. Massey, and C. Watt, in The Characteristics of Electrical Discharges in Magnetic Fields, edited by A. Guthrie and R. K. Wakerling (McGraw-Hill Book Co., Inc., New York, 1949), p. 145.

50 μA of UF_5^- from an ion source injecting into the TU tandem. The beam-current calculations presented in this proposal are based on this expectation for uranium beams.

Table II. A-I shows data (largely supplied by HVEC) on the currents of negative ions which have been achieved as of May 1969. It is reasonable to expect that increased interest in this topic will lead to significantly larger negative-ion beam currents in the next few years. (One has only to consider the history of the development of negative beams of helium ions. A few years ago the attainment of such beams was considered most unlikely. Largely spurred on by tandem accelerator requirements, research work led quite rapidly to the development of beams of tens of microamperes.)

It is quite possible that the technology of negative-ion sources will receive considerable impetus and assistance from the related technology involved in electrostatic-propulsion engines for rockets. This has been a topic of great interest in space research during recent years. The development of very large negative-ion currents is of importance in this field because of the necessity of neutralizing the ion beam ejected from such engines.

A possible layout of the negative-ion injection system for the TU tandem is included in Fig. II. A-2. In this arrangement, each source is mounted on a short section of acceleration tube and is capable of being operated at voltages of up to 150 kV. The beam from the source is focused by an einzel lens which permits better focusing of the ion beam for optimum transmission through the injection system. The sources are mounted on the $+45^\circ$ and -22.5° entrance ports of the inflection magnet. The magnet (shown in Fig. II. A-2) has five ports so the beam can be inflected at angles of $\pm 45^\circ$, $\pm 22.5^\circ$, and 0°. The radius of curvature of the magnet is 40 in., and at 45° its mass-energy product is 60 so it can inflect all negative ions or molecular ions with masses up to A = 400 at energies up to 150 keV. The inflection magnet also serves as a mass analyzer with resolution width ($\Delta m/m = 1/150$).

TABLE II.A-I. Presently achievable negative-ion beam currents. Where an element is listed but no current is given, this indicates merely that a negative-ion beam has been identified. Parentheses indicate tentative identification of an ion species.

Period	Group 0	Group I	Group II	Group III	Group IV	Group V	Group VI	Group VII	Group VIII
1		H, 700 μA							
2	He, 12 μA	Li, 2 μA	BeH^-, 0.2 μA	B, 0.7 μA BF^-, 15 μA	C, 10 μA C_2^-, 4 μA	N, 0.25 μA NH^-, 1 μA CN^-, 30 μA	O, 24 μA	F, 250 μA	
3		Na, 0.5 μA	MgH^-, 0.3 μA	Al, 0.1 μA	Si	P, 3 μA	S, 50 μA	Cl, 250 μA	
4		K, < 1 μA	Ca, < 1 μA		Ti		CrO_3^-, 0.8 μA	Mn	FeO_2^-, 1 μA Co | Ni
		Cu, 5 μA		Ca, 0.1 μA $GaCl_2^-$, 10 μA		AsH^-	Se	Br, 100 μA	
5		Rb					Mo		
		Ag, 1 μA				Sb	Te, 2 μA	I, 50 μA	
6		Cs				TaF^-, 2 μA TaO_2^-, 4 μA	WO^-		
		Au, 12 μA	Hg, 0.5 μA			Bi, (2 μA)			
Lanthanides									
Actinides		UF_5^-, 5 μA UF_2^-, 2 μA							

Unwanted ions from the source can be largely rejected here and prevented from loading down the accelerator. This will be particularly useful, for instance, in accelerating low-abundance isotopes from a source containing other isotopes of the same element.

The helium injector shown in Fig. II. A-2 provides microampere levels of He^- beam for injection into the TU. The helium source is a lithium charge-exchange source in which positive helium ions extracted from an ion source are converted to negative ions. The source and its associated supplies are mounted in an enclosure at 150 kV potential.

After leaving the inflection magnet, the negative-ion beam enters the klystron buncher. At this point the beam is focused to a crossover to minimize any aberrations the buncher may produce in the beam optics. From the buncher the beam enters the low-energy section of the tandem, at which point it is again focused by means of a gridded entrance lens.

Also located in the low-energy extension of the accelerator are a beam-profile monitor, an aperture, and an insertable Faraday cup. These are provided to monitor and properly focus the injected negative-ion beam.

4. The Beam-Pulsing System

The requirements of the cyclotron lead to a set of conditions imposed upon the beam injected into it. These are listed in Table II. A-II.

The primary function of the pulsing system on the TU tandem is to fulfill the time and frequency requirements for the beam injected into the cyclotron—without violating the other restrictions on the allowable energy and emittance properties of the beam. It is clear from Table II. A-II that if the rf voltage in the cyclotron can be "flat-topped," then the pulsing requirements for the TU will become much less stringent. (Without flat topping, the 0.5-nsec pulse width is required only to achieve the best possible energy resolution for the beam extracted from the cyclotron.)

TABLE II.A-II. Requirements for beams injected into the cyclotron.

Cyclotron rf frequency range	(a) light ions	~11 to 22 MHz
	(b) heavy ions	~11 to 15.6 MHz
Phase stability of injected beam pulses		$< 2 \times 10^{-3}$
Pulse width of injected beam	(a) without "flat-topping"	< 0.5 nsec
	(b) with "flat topping"	< 2 nsec
Energy resolution and stability of injected beam	$\Delta E/E$	$< 3 \times 10^{-3}$
Emittance of injected beam (for all injection energies)		< π cm-mrad

Considerable experience has been accumulated over many years at ANL in connection with pulsed-beam and time-of-flight techniques. This experience should be of great value in connection with the TU tandem's beam-pulsing system which will be developed and constructed by Argonne personnel.

Klystron bunchers have been used successfully on several existing tandems (including the one at Argonne). For example, at the MP tandem at the University of Rochester, proton beams with pulse widths of 0.8 nsec and oxygen beams with pulse widths of 2 nsec have been achieved[9] on targets.

The bunching system that most probably will be used with the TU will employ a 3-gap klystron buncher located shortly before the entrance to the low-energy section of the tandem. This type of buncher consists of four cylindrical drift tubes mounted along the beam axis and separated from one another by short gaps (typically a little less than 1 cm). The outer two drift tubes are grounded and the inner two are driven with a periodic voltage. The voltages applied to the two inner tubes are the same but their phases differ by 180°. The beam optics for the negative-ion beam would be arranged to form a crossover at the center gap of the buncher, and this would then act as object point for the TU accelerator. The use of

[9] K. H. Purser (private communication).

such a buncher with a sine-wave voltage applied to it presents no particular difficulties for bunching ions of a fixed mass at a fixed frequency. However, the need in the present proposal for a wide variability in ion mass and in bunching frequency does raise some problems.

The drift tubes of the conventional buncher normally form part of a tuned circuit in an rf oscillator. Thus the frequency of the applied voltage can be varied only over a fairly limited range. Furthermore, the maximum efficiency attainable with the sinusoidal buncher is about 1/3. That is, about 2/3 of the beam from the ion source is wasted because it does not coincide with the proper "ramp" section of the sine-wave bunching voltage. Both of these difficulties can be overcome if one can use linear circuit techniques to generate a more suitable voltage waveform (ideally this waveform approximates an isosceles triangle). Since the drift tubes would then not be part of a resonant system, the frequency could be varied easily over a wide range. The bunching efficiency would go up to about $\frac{1}{2}$. For heavy ions the bunching voltages required are low enough (about 5—10 kV) for linear circuit techniques to be usable.[10] For light ions, the required bunching voltages are in excess of 20 kV and sinusoidal excitation will probably be necessary. In the event that sinusoidal waveforms have to be used for all ion species, there are enough variable parameters (e.g., ion-source voltage, drift-tube length, harmonic operation, etc.) in the bunching system that one can still expect to be able to bunch beams of all masses over the required frequency ranges.

To avoid undesirable de-bunching effects for that portion of the beam that enters the buncher during the wrong phase of the bunching voltage, a beam chopper is required. This would be located ahead of the buncher and synchronized with it. It would consist of a set of deflecting electrodes which apply a periodic square-wave voltage normal to the beam as it emerges from the inflector magnet. Because of the low velocity of the heavier ions, a series of short deflection plates would be used. By use of appropriate delay lines, the deflecting voltage would be made to travel along the plates at the same velocity as the ion.

---

[10] F. J. Lynch (private communication).

The frequencies at which this type of buncher operates are usually less than 5 MHz. One would like to maintain fairly low bunching frequencies in order to keep the period of the bunching voltage large relative to the transit time of the ions crossing the gap. (It takes about 35 nsec for a 150-keV UF_5^- ion to cross a 1-cm gap.) Thus it seems clear that the buncher will have to operate on a subharmonic of the cyclotron's rf frequency. (The orbit frequency of the ions in the cyclotron will also be a subharmonic of the rf frequency. However, there seems to be no compelling reason for making the buncher operate on the same subharmonic.) The distance between the outer gaps of the buncher must be an odd-integral multiple of the distance traveled by the ion in one period of the buncher excitation signal. To accommodate the variations in this distance required for various ion species and various operating frequencies of the cyclotron, the buncher would be constructed so that the lengths of the two inner drift tubes are continuously variable over a factor of about two.

Small changes in injection voltage, terminal voltage, or voltage distribution in the accelerator tubes can cause unacceptable changes in transit time through the accelerator. (Experience at Rochester[9] has demonstrated that because of fluctuations in the voltage distribution in the tubes, variations of several nanoseconds can occur in the transit time through the tandem.) Fortunately, these fluctuations occur on a time scale that is long compared with the buncher period. Thus the phasing of the buncher can be continuously corrected relative to the phase of the cyclotron rf frequency by using a device that detects the beam bursts as they arrive at the cyclotron, compares their phase with that of the cyclotron's rf, and then feeds back a phase-correcting signal to the buncher.

The bunching voltages required are such that the energy spreads introduced are always less than 20 keV, a value acceptably small for the various beams to be injected into the cyclotron.

A source of time spread that may be expected to become significant at low bunching frequencies (i.e., at high peak pulse currents)

is the space-charge repulsion between ions within a bunch. Estimates,[10] based on the expression derived by Inman and Murray[11] for the growth of an oblate spheroid of charge with time, indicate that in the worst case expected to be encountered in the TU system (low-energy heavy ions) the time spread due to space-charge effects will be less than 0.2 nsec.

For the case in which negative molecular ions are accelerated, an additional time spread will be introduced because of the break-up energy of the molecules in the stripper gas in the tandem terminal. For UF_5^- ions, this effect will cause an energy spread of about 10 keV and contribute about 0.2 nsec time spread to the pulsed beam.

Calculations have been made[10] to evaluate the expected performance of a 3-gap buncher used with the TU tandem. The results show that with a diode ion source and with a triangular voltage waveform to excite the buncher, the requirements listed in Table II. A-II can be met for all ion species. Typical bunching factors of 40 to 50 should be attainable.

Table II. A-III lists the various contributions to the pulse width calculated for an iodine beam arriving at the cyclotron. A tandem terminal voltage of 16 MV is assumed. It is also assumed that the beam-transport system (length 110 ft) between the TU and the cyclotron is isochronous (i.e., that ions following different paths through the system take the same time).

5. Stripping

During passage through the accelerator complex, ion beams will undergo stripping. The responsibility for the construction and location of the various strippers will lie with ANL. It is proposed to install five strippers placed as shown in Fig. II. A-4. These will be used in varying combinations for different modes of operation of the accelerator facility as indicated in Table II-A-IV.

---

[11] F. W. Inman and J. J. Murray, IEEE Trans. Nucl. Sci. NS-13, 1 (April 1966).

TABLE II.A-III. Contributions to the pulse width of an iodine beam from the TU tandem (terminal voltage 16 MV).

Source of time spread	Time spread (nsec)
Energy spread of diode source (50 eV)	0.6
Time spread due to buncher (triangular-waveform excitation)	0.8
Energy straggling in gas stripper (~0.7 keV)	0.01
Anisochronism of charge-state selector system	0.1
Energy straggling and variation in thickness of foil stripper (~100 keV)	0.2
Space-charge effects	0.1
Pulse width (fwhm) of pulses arriving at the cyclotron	1.1

The first two strippers will be located within the center terminal of the TU. Here there will be both a gas stripper S1 and a foil stripper S2. Gas strippers S3 and S4 will be located at the object points of the two 90° analyzing magnets for use in stand-alone operation of the TU. These two strippers serve to increase the charge-to-mass ratio for beams of heavier ions. Without strippers S3 and S4, the magnets (mass-energy products of about 200) would be unable to bend these beams into the TU experimental areas. For example, a 91-MeV beam of U^{5+} ions (corresponding to a terminal voltage of 16 MeV and UF_5^- injection) would require a bending magnet with a mass-energy product of about 870.

Present theories of stripping are not able to predict accurately the charge-state distributions expected when ion beams pass through various materials. These distributions depend in a rather complicated manner on the cross sections for electron capture and loss, which themselves can be only roughly calculated. Some of these cross

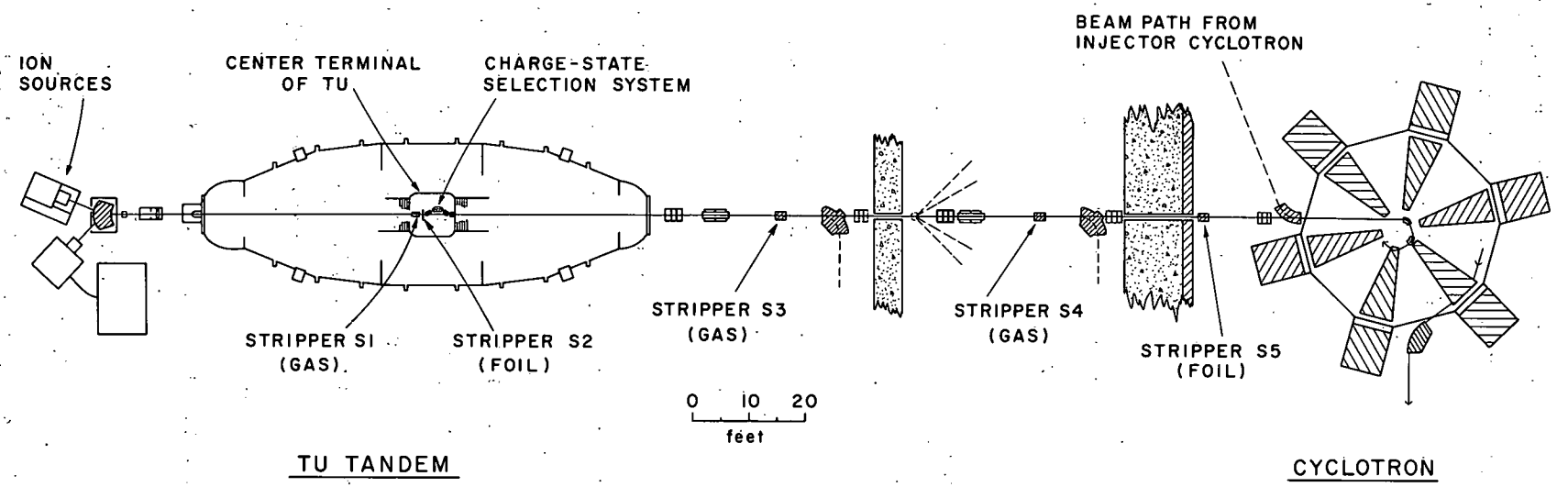

Fig. II. A-4. Diagram showing the relative positions of the TU tandem and the cyclotron together with the locations of various magnets, quadrupole lenses, and strippers.

TABLE II.A-IV. Stripper combinations for various operating modes.

	TU alone	TU + cyclotron
Light ions ($Z \lesssim 3$)	S2	S2
Intermediate ions ($3 \lesssim Z \lesssim 40$)	S1	S1 + S5
Heavier ions ($Z \gtrsim 40$)	S1 + (S3 or S4)	S1 + S5

S1 = Gas stripper in center terminal.

S2 = Foil stripper in center terminal.

S3, S4 = Gas strippers ahead of the two 90° analyzing magnets of the TU.

S5 = Foil stripper at entrance to cyclotron.

sections have been measured over limited energy ranges, but the data are so scarce that their use for calculating charge-state distributions is very limited.

In a few cases, the actual charge-state distributions have been measured. (See, for example, Refs. 12–16 and references contained therein.) Again, the experimental data are not extensive enough to cover all of the combinations of ion species, energy ranges, and stripping media of interest here. It is fairly well established, however, that a dynamically stable charge distribution is rapidly reached when ions pass through matter and that this distribution is independent of the initial charge of the ion beam. It has further been found that the true equilibrium distributions

---

[12] G. Ryding, A. B. Whittkower, and P. H. Rose, Phys. Rev. (to be published).

[13] C. D. Moak et al., Phys. Rev. 176, 427 (1968).

[14] I. S. Dmitriev and V. S. Nikolaev, Soviet Phys.—JETP 20, 409 (1965).

[15] H. D. Betz et al., Phys. Letters 22, 643 (1966).

[16] E. Leischner, UNILAC Bericht Nr. 1-66, Universität Heidelberg (1966).

may be approximated roughly by a Gaussian when, for ions of atomic number Z, the average charge $\bar{q}$ lies in the range $1 \ll \bar{q} \ll Z$ and when the ion velocity is given by $v \gtrsim v_0 = e^2/\hbar = 2.2 \times 10^8$ cm/sec (i.e., for energies greater than about 25 keV/nucleon). These conditions are satisfied for most of the cases of interest in connection with this proposal and so, in what follows, Gaussian distributions will be assumed. That is, the charge distributions will be taken to be of the form

$$F_i(q_i) = \text{const.} \times \exp\left[-(q_i - \bar{q})^2/2\sigma^2\right],$$

with the constant chosen to make $\sum_i F_i = 1$. The values of $\bar{q}$ and σ are taken from the work of Betz et al.[15] and Leischner.[16] Two sets of values are used—one set for a gas stripper (air) and one set for a foil stripper (Formvar). The values for $\bar{q}$ are calculated from the empirical formula given by Betz et al.,[15] which they found gave good agreement with their measured values. Their work, like that of others, shows clearly that the effect of stripper density is quite important for heavy ions. They find, for instance, that $\bar{q}_{foil}/\bar{q}_{gas} \approx 2$ for 70-MeV uranium ions. This effect makes it highly desirable to use stripping foils wherever possible in the proposed accelerator.

Measurements[17] at HVEC have shown that the lifetime of stripper foils is unfortunately very short (~1 hour at particle currents of about 6×10^{12} particles/sec) for beams of low-energy heavy ions. Stripper S1 in the tandem terminal is therefore a gas stripper because low-energy ($\leq$ 20 MeV) heavy-ion beams are anticipated there with currents up to 4×10^{14} particles/sec. By the time these beams encounter stripper S5, their energies will be sufficiently high and their intensities sufficiently reduced that foil stripping will then be feasible. (Furthermore, even if a high failure rate for these foils should be encountered, their location outside of the tandem tank renders them easily accessible for renewal.) It is envisaged that foil strippers S2 and S5

---

[17] F. Chmara, G. Ryding, and J. Shaw, contribution to the Washington, D.C. Accelerator Conference, March 1969 (IEEE Trans. Nucl Sci., June 1969).

will each be an assembly containing perhaps 100 foils, any one of which can be remotely selected for insertion into the beam.

The variance σ^2 of the Gaussian approximation to the charge distribution is known[16] to be almost energy independent. It is larger for heavier ions and for foils than for gas strippers. Figure II. A-5 shows some representative Gaussians calculated for various ion beams in an air stripper. The increased width of the distributions for the heavier ions is useful in this accelerator design because it permits higher charge-to-mass ratios to be accelerated in the cyclotron without a prohibitive reduction in current intensity.

Measured charge-state distributions are known (e.g., Refs. 12 and 13) to vary in shape quite markedly as a function of ion energy for different combinations of ions and stripping materials. These variations are thought to result from atomic shell effects and also from the influence of collisions in which more than one electron is captured or lost. The departure from a Gaussian distribution is usually in the direction of a skewing towards higher charge states—a tendency which helps the aims of the proposed accelerator. As an example of the variations to be expected in the charge-state distributions, Fig. II. A-6 shows some measured values for 12-MeV iodine ions in hydrogen and oxygen together

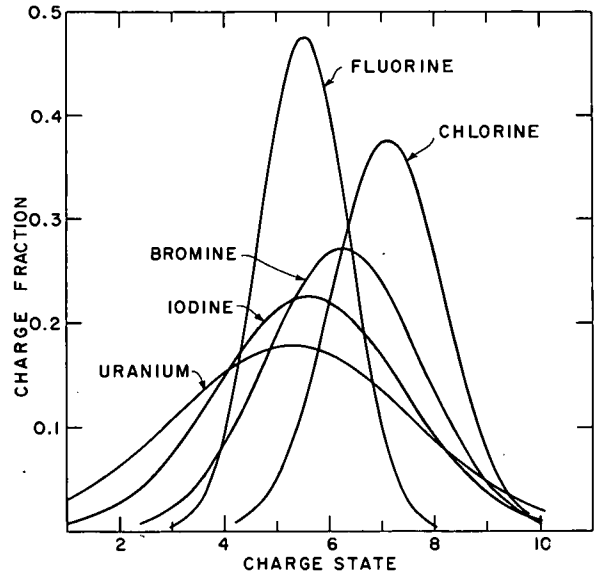

Fig. II. A-5. Equilibrium charge-state distributions (Gaussians) calculated from values of $\bar{q}$ and σ determined from the empirical formulae and results given in Refs. 15 and 16. The curves are for 16-MeV ions in a gas (air) stripper.

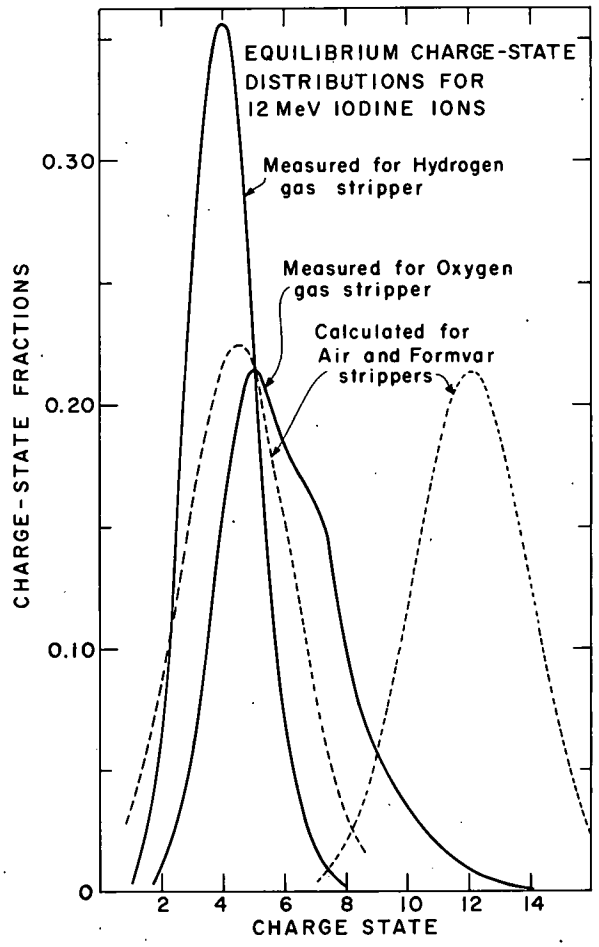

Fig. II. A-6. Equilibrium charge-state distributions for 12-MeV iodine ions. The curves shown are those measured (Ref. 12) for hydrogen and oxygen gas strippers together with the Gaussian approximations calculated for a gas (air) and a foil (Formvar) stripper.

with the calculated Gaussian distributions in air and in a Formvar foil.

The calculated values given in this proposal for the expected particle energies and beam currents from the accelerator complex are based on the Gaussian approximation to the equilibrium charge-state distributions in air and Formvar strippers. It should be noted that, in practice, significantly improved values may be obtained in many instances as a result of the skewing of the actual distributions and also by the use of other stripping materials chosen to provide values of $\overline{q}$ and σ optimized for a specific type of beam.

For foil strippers, a material of low atomic number will usually be preferred. This results in a higher mean charge for the stripped ions[15] and minimizes the scattering in the foil, which can be a very significant factor to be considered for a heavy-ion beam.

It has been suggested by Bohr and Lindhard[18] that the increase in mean charge $\bar{q}$ with stripper density is the result of an increased probability for the loss of electrons from excited atomic states of the ions in the beam. In low-density gas strippers, the average time between successive collisions will be long compared to the lifetimes of these excited states and the equilibrium charge-state distribution will be independent of density. As the density increases, the time between collisions decreases and when this time is comparable to the lifetimes of the excited states, an increase in the mean charge will result. The magnitude of this increase was estimated[18] to be about 20%. Ryding et al.[12] have measured a 15% increase in $\bar{q}$ for a high-density gas stripper. Because of restrictions in space available in the center terminal of the TU, stripper S1 will necessarily be small (about 20 in. long by 0.2 in. diameter) and will be operated as a high-density gas stripper. This provides a further likely source of improvement for the overall performance of the accelerator because of the production of higher charge states.

Bohr and Lindhard further suggested that adjustment processes, in which the excitation energy of an ion is redistributed amongst its electrons, have lifetimes much shorter than those for radiative transitions. Consequently, a further increase in mean charge is to be expected (and is observed) in a solid where the mean time between successive collisions is comparable to the short lifetimes of these events. Many of these lifetimes have been measured by beam-foil spectroscopy[19] (a field which has much to offer to and much to gain from the construction of this accelerator). It is likely that the relatively high charge states obtained for beams passing through foils are due to the loss of electrons from excited states soon after the beam leaves the foil. If this is so, then it is possible that by using two or more thin foils spaced a short

---

[18] N. Bohr and J. Lindhard, Kgl. Danske Videnskab. Selskab, Mat.-Fys. Medd. 28, 7 (1954).

[19] See, for example, Beam Foil Spectroscopy, edited by S. Bashkin (Gordon and Breach, Science Publishers, New York, 1968); Sec. V.B6c in the present proposal.

distance apart, the mean charge attainable may be still further increased. Experiments[20] to test this possibility are now in progress at HVEC.

Measurements[12] indicate that over 90% of a 16-MeV iodine beam reaches charge-state equilibrium in passage through 100 micron-cm of oxygen gas. This is about 10^{16} atoms/cm^2 and corresponds to less than a microgram per cm^2 of stripping material. Thus there emerges a further point in connection with stripper S1: even if it were possible to use a foil stripper here, about a factor of ten too much material would have to be inserted in the beam since the thinnest self-supporting foils are in the 5—10 μg/cm^2 range. This would produce additional scattering and energy spreads (worse in any case for a foil, which cannot be made as uniform as a gas stripper). These effects would be particularly deleterious for low-energy heavy-ion beams.

6. Charge-State Selection and Positive-Ion Acceleration

Since only one of the ion charge states emerging from stripper S1 will contribute usefully to the beam accepted either for acceleration in the cyclotron or for most experiments employing only the TU, some form of charge-state selection is desirable in the terminal of the TU. This would prevent loading the high-energy acceleration tubes with unwanted beams and thus permit the acceleration of more beam in the desired charge state. This is an important point because the beam current in the accelerator tubes will probably be limited to about 60 μA (metered current). Without terminal charge selection, the multiplication of ion charge (typically a factor of about 5) which occurs in the terminal stripper would restrict the negative-ion current injected into the TU to about 10 μA. With charge selection it is expected that about 60 μA can be injected, resulting in an (electrical) current of about 60 μA in the high-energy section. (This is due to the approximately canceling effects of the charge multiplication and the

[20] P. H. Rose, J. P. Schiffer, and A. B. Whittkower (private communication).

reduction in particle current as a result of fractionation of the beam into several charge states.)

It is planned to accomplish the charge selection by means of a magnetic analysis system. This is illustrated schematically in Fig. II.A-7. The system shown contains three magnets giving consecutive deflections of -14°, $+28^{\circ}$ and -14° and is capable of handling U^{5+} at 16 MeV. It will completely separate I^{7+} (16 MeV) from its neighboring charge states. (Complete separation is not a necessity since further separation will occur in the magnetic analysis following tandem acceleration.) The magnets and power supplies will weigh about 900 lb. Power consumption will be about 15 kW. (The terminal of the TU will support up to 3000 lb and 25 kW of power will be provided.)

The beam in the selected charge state will be focused into the high-energy acceleration tube by a magnetic quadrupole doublet. This (remotely adjustable) lens does not preserve the axial symmetry of the beam profile, but instead will produce a beam having an elliptical cross section, which is better matched to the oval shape of the beam aperture in the acceleration tube.

The angular spread of the beam emerging from gas stripper S1 is expected to be less than ± 0.005 radian. Under these conditions, the anisochronism introduced by the terminal charge-state selection system will always be less than 0.1 nsec.

It is planned to provide two paths for the beam through the center terminal—one through the charge-selection system and one direct straight-line path to be used in light-ion applications and in adjustment procedures for heavy-ion beams.

Figure II.A-8 shows a possible arrangement for the components inside the center terminal of the TU.

The limitation of (metered) current to 60 μA in the acceleration tubes of the TU is a figure which HVEC expects as an extrapolation from their previous experience with tandem accelerators. The limitation is determined by a complex mixture of many factors,

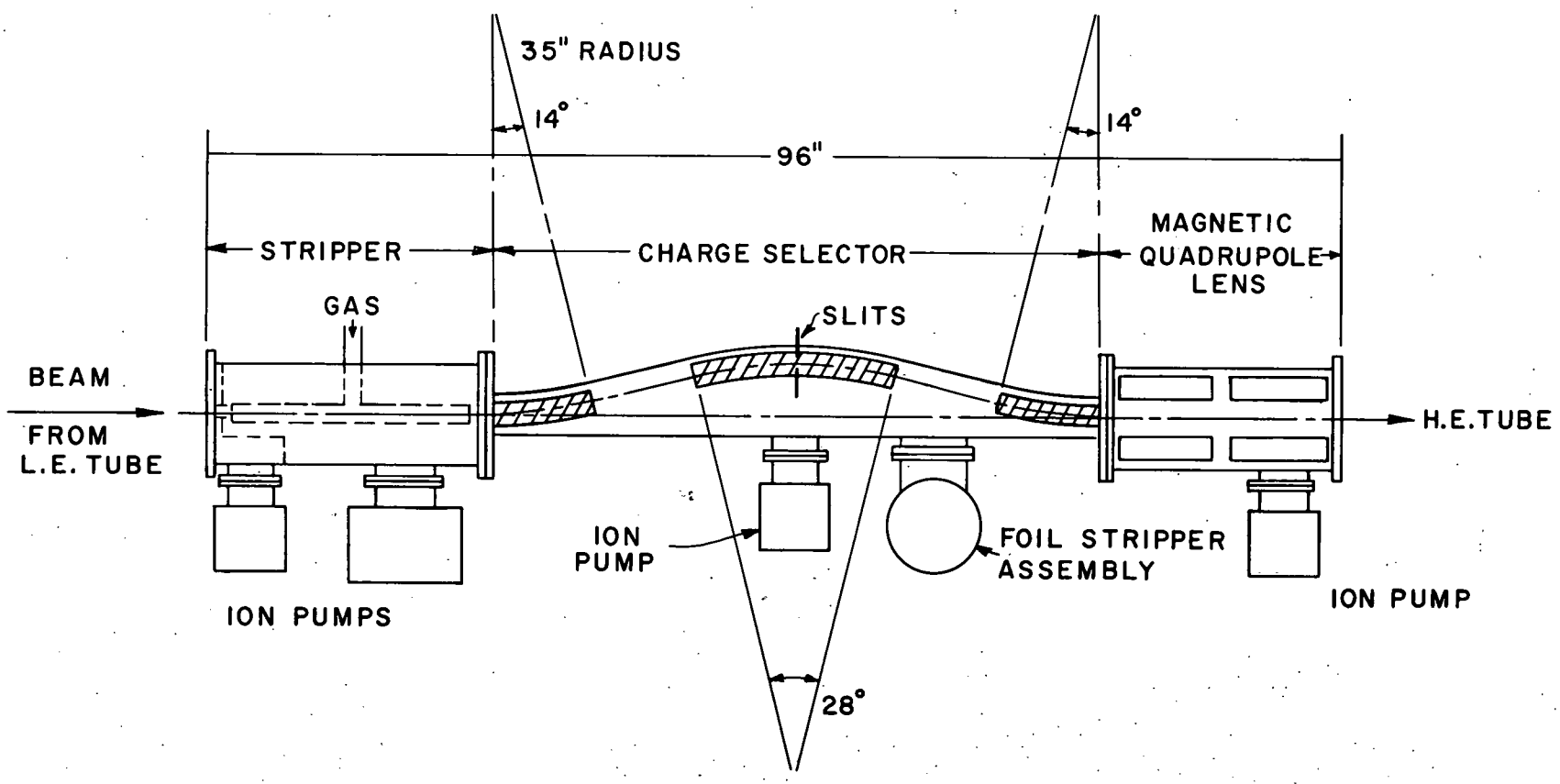

Fig. II. A-7. An arrangement for magnetic selection of one charge state of the ion beam emerging from the gas stripper S1 in the center terminal of the TU.

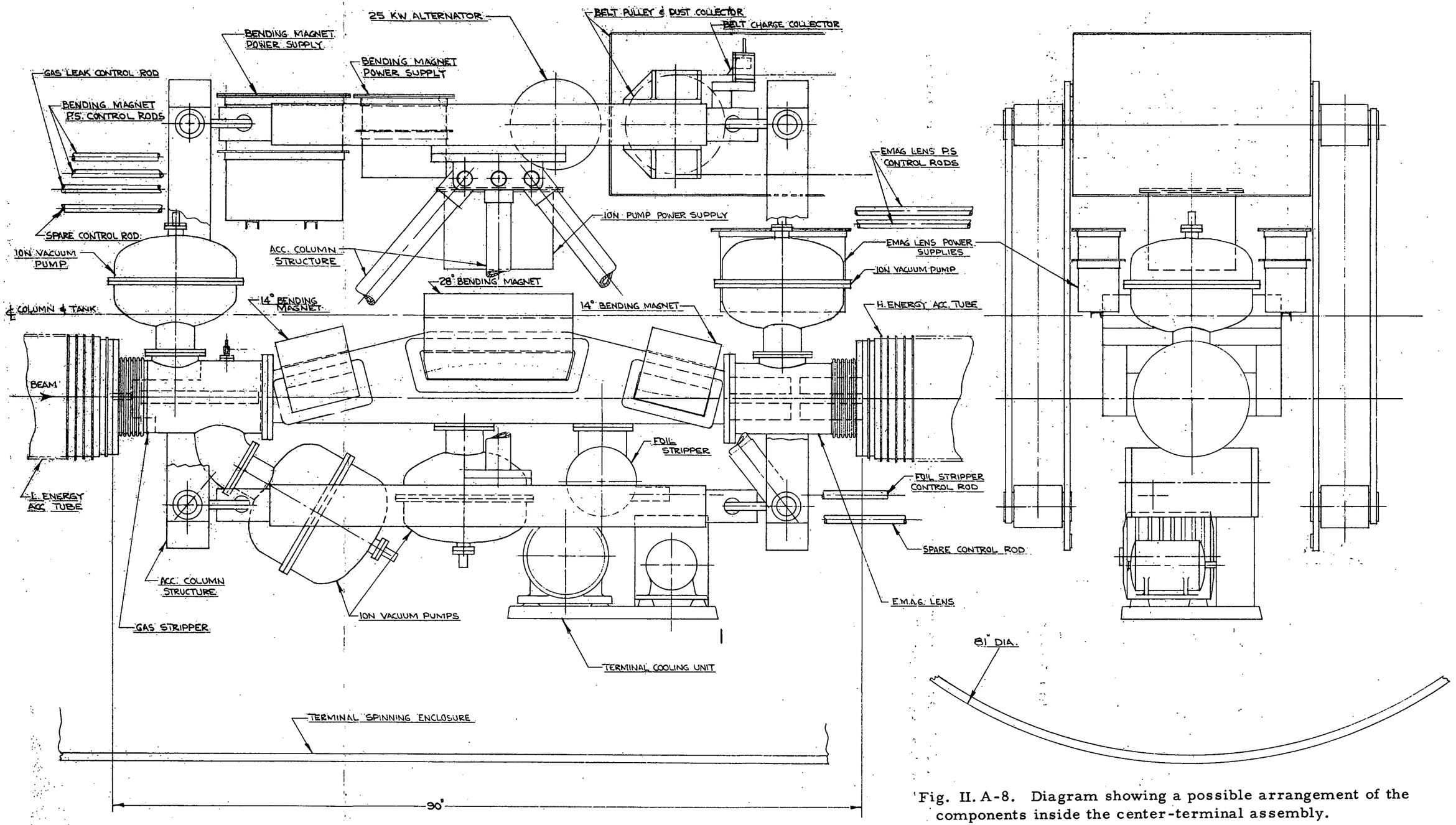

Fig. II. A-8. Diagram showing a possible arrangement of the components inside the center-terminal assembly.

including voltage gradient, vacuum conditions, and ion optics. The same limiting value for the time-averaged current is expected for both dc and pulsed operation of the TU.

7. Vacuum Conditions

For the acceleration of intense heavy-ion beams in the TU, it is clear that the required vacuum conditions must be better than those hitherto regarded as "normal" in tandem accelerators. In the "normal" operation of tandems, high vacuum is achieved in the acceleration tubes by diffusion pumps at the low- and high-energy ends of the machine only. A pressure gradient then exists within the tubes, pressure being highest at the center terminal and lowest at each end of the accelerator. This residual pressure is predominantly due to the gas load from a gas stripper and to continuing outgassing of the various constituents of the tubes (mainly incompletely polymerized vinyl acetate sealing material). Usually the gas flow from the stripper is pumped out through the tubes at the high-energy end of the machine. Pressures as high as 10^{-4} Torr may exist at the terminal end of the high-energy tube under conditions of maximum gas flow.[9, 17]

With these conditions, attenuation of the primary beam components due to charge-changing collisions in the accelerator tubes is expected to be pronounced for slow-moving heavy ions. Experience at the University of Rochester MP tandem with a sulphur beam has shown[9] that with a terminal voltage of 10 MV and an oxygen gas stripper, but with no pumping in addition to the normal pumps external to the pressure vessel, it was not possible to operate with an injected negative-ion current greater than 2 μA. When higher injection currents were attempted, the transmission of the accelerator went down rapidly. It is thought[9] that this was due to ionizing effects of the beam in the residual gas existing in the poor vacuum in the terminal region. This causes local loading currents which upset the potential distribution in the tubes, giving

undesirable electrostatic steering and consequent rapid deterioration of the transmission.

The beam apertures in the electrodes of the acceleration tubes of the TU will be smaller than those of the MP tandem in order to achieve the higher voltage gradients required. As a consequence, the TU tubes have about half the gas conductance of those in the MP. These considerations make it apparent that additional pumping will be required if the TU is to be operated with high currents of heavy ions.

To determine what operating pressures are required, calculations have been performed[21] to establish the beam attenuation under various pressure conditions. A particle in an ion beam is assumed to be lost if it changes its charge in a collision with a molecule in the residual gas in the acceleration tubes. Such collisions cause particles to be removed from the desired discrete energy spectrum of the accelerated beam and to appear as a "smeared" energy continuum. The dominant charge-changing processes are expected to be the capture and the loss of single electrons. (Multiple electron transfers may occur with lower but still appreciable probabilities.[22]) The calculations are complicated by the fact that the values of σ_c and σ_ℓ, the cross sections for electron capture and loss, are poorly known; they vary drastically with the charge state and velocity of the projectile ion and the chemical nature of the collision partner. Furthermore, both the concentration and composition of the gas may vary considerably along the ion trajectory. To simplify the computations, the assumptions were made that the gas concentration is uniformly distributed throughout each tube section and that the residual gas is air.

Presented in Table II.A-V are the transmission efficiencies of the two (low- and high-energy) sections of the TU for ionic uranium and iodine species, calculated for two conditions of pressure. In the

---

[21] S. Wexler (private communication).

[22] See, for example, B. Franzke et al., Phys. Letters 25A, 769 (1967).

TABLE II. A-V. Calculated transmission of uranium and iodine ions through the TU tandem (terminal voltage 16 MeV). HVEC will make provision that the pressure in the acceleration tubes will be $< 2 \times 10^{-6}$ Torr.

Accelerator section	Path length (cm)	Pressure (Torr)	Ion species	Average $\sigma_c + \sigma_\ell$ (cm^2/molecule)	Transmission (percent)
Low-energy	1100	(a) 2×10^{-6}	UF_5^- or I^-	55×10^{-16}	65
		(b) 2×10^{-5}			1.4
High-energy	1100	(a) 2×10^{-6}	U^{5+}	10×10^{-16}	93
		(b) 2×10^{-5}			46
		(a) 2×10^{-6}	I^{6+}	6×10^{-16}	96
		(b) 2×10^{-5}			63
Complete TU tandem		(a) 2×10^{-6}	Uranium		60
		(b) 2×10^{-5}			0.6
		(a) 2×10^{-6}	Iodine		62
		(b) 2×10^{-5}			0.9

table, the estimated average cross sections for the sum of capture and loss of electrons are the properly weighted averages taken over the range of velocities of the species in each section of the accelerator. Data for the positively charged species were taken from theoretical curves prepared by Betz and Schmelzer.[23] Since relevant data for negative ions were not available, an "educated guess" of 55×10^{-16} cm^2/molecule

[23] H. D. Betz and C. Schmelzer, Charge Exchange Cross Sections of Fast Heavy Ions, UNILAC Bericht, Nr. 1-67, Universität Heidelberg (1967).

was taken for the average cross section for electron loss by them. (Cross sections for collisional detachment of electrons from negative ions have been determined for relatively few ions, mainly H^- and O^-, and only at low energies—almost entirely in the energy region below 15 keV. At the higher energies in this range, the cross sections can be as high as 40×10^{-16} cm^2/molecule. At energies above 15 keV, very few data exist. Results[24] for 560-keV O^- impinging on N_2 show that the cross section for single electron loss is 3.0×10^{-16} cm^2/molecule and for double electron loss 2.0×10^{-16} cm^2/molecule. The cross sections increase with the mass of the target species. Since in the calculations air was assumed to be the residual gas although the vapor in a vacuum-tight machine consists mostly of hydrogen, water, carbon monoxide, and hydrocarbons, and because nothing is known about electron detachments from UF_5^- and I^- on collision with H_2O, CO, or hydrocarbon molecules, it was deemed desirable to assume that the total cross sections will be very large—100×10^{-16} cm^2/molecule at the beginning of their acceleration and 10×10^{-16} cm^2/molecule as they enter the center terminal.)

The results of the calculation, shown in Table II. A-V, indicate that if the pressure in the acceleration tubes can be maintained at 2×10^{-6} Torr or less, then the transmission efficiencies for uranium and iodine beams can be expected to be 60% or more. For higher pressures, the transmission gets rapidly worse, particularly for the low-energy section. (The calculation may be somewhat pessimistic here since the gas concentration will be highest at the terminal end of the low-energy tube and the electron-loss cross section is least there, varying approximately inversely as the ion velocity.)

Thus, to achieve high transmission efficiencies for the TU tandem, HVEC will provide for operating pressures under 2×10^{-6} Torr in the accelerator tubes. This will be achieved by differentially pumping the gas stripper in the terminal, thereby greatly reducing gas

---

[24] J. B. Hasted, Physics of Atomic Collisions (Butterworth Scientific Publ., Ltd., London, 1964), pp. 298 et seq.

flow into the tubes, and by the use of additional pumping located in the six "dead sections" in the accelerator tubes. The vacuum chamber of the terminal charge-state selector will also be pumped.

All of the pumps located within the pressure tank will be of the Vac-Ion (getter) type. Those inside the center terminal will draw their power from an alternator driven by the charging belt of the accelerator and those located at the "dead sections" will be powered by alternators driven by rotating Lucite rods. These pumps are reliable and have long lifetimes. Tests made on a pump of this type at Brookhaven National Laboratory[25] have shown it to be capable of pumping 50 atmospheric cc/hour of hydrogen at pressures of 10^{-6} Torr for periods in excess of 1000 hours before maintenance is required.

In the beam-transport system external to the tandem, it is relatively easy to maintain pressures less than 2 or 3 $\times$ 10^{-7} Torr and consequently the transmission efficiencies for the various ion beams will always be greater than 90% in these regions.

8. Emittance of the Ion Beam

On the basis of measurements with a diode source used in conjunction with an MP tandem, HVEC expects the emittance of negative heavy-ion beams leaving the 150-keV injector to be about 2 cm-mrad-$(MeV)^{1/2}$. The optics at the injector will provide a crossover at the klystron buncher which then acts as object point for the tandem. The beam diameter at this point will be about 0.5 cm. The entrance to the low-energy tube will be gridded (leaving approximately 90% transparency to the ion beam) so as to provide a well-defined controllable electrostatic lens at this point. This, together with the action of the "funnel lens" (an electrostatic quadrupole lens located between sections 2 and 3 of the low-energy tube) will provide a magnification of about

---

[25] J. A. Benjamin, Selection of An Ion Pump for a Terminal Ion Source, Brookhaven National Laboratory Report BNL-13511.

0.35 for the beam focused at the stripper in the center terminal when the terminal is at 16 MV. Thus the beam at the stripper should be about 0.18 cm (0.07 in.) in diameter and therefore should pass cleanly through the stripper canal whose inner diameter will be approximately 0.2 in.

The half-angle of convergence at the stripper will be about 1.4 mrad. Calculations[6] on the plural scattering of heavy ions in gases indicate that this half angle will be increased to about 5 mrad for the beam leaving the stripper. Thus the emittance of the beam entering the HE tube will be about 7 cm-mrad-$(MeV)^{1/2}$. This value should be conserved throughout the acceleration in the high-energy section of the machine and hence should result in a compression in transverse phase space to less than 1 cm-mrad, a value quite adequate for the beam to be injected into the cyclotron. (Passage through stripper S5 will slightly worsen the emittance properties of the beam; but by arranging the ion optics so that a beam crossover occurs at this stripper, the increase in emittance due to scattering in the stripper can be held down to an acceptable level.)

9. Energy Spreads in the Ion Beam

Table II.A-VI lists the sources and magnitudes of the various contributions to the energy spreads expected for an iodine beam accelerated in the TU tandem. The estimates for spreads due to straggling in the strippers are obtained through use of the relationships given by Lindhard et al.[26] and the energy-loss data measured by Pierce and Blann[27] (for gases) and by Moak and Brown[28] (for foils).

---

[26] J. Lindhard, M. Scharff, and H. E. Schiott, Kgl. Danske Videnskab. Selskab, Mat.-Fys. Medd. 33, No. 14 (1963).

[27] T. E. Pierce and M. Blann, Phys. Rev. 173, 390 (1968).

[28] C. D. Moak and M. D. Brown, Phys. Rev. 149, 244 (1966).

TABLE II. A-VI. Estimated energy spreads (keV) introduced into iodine beams from the TU tandem (terminal voltage 16 MV).

Source of energy spread	TU only	TU injecting into cyclotron
Straggling in gas stripper S1	0.7	0.7
Instability of terminal voltage	11 (I^{6+})	112 (I^{6+})
Straggling in strippers S3 or S4 (gas) and S5 (10-$\mu g/cm^2$ carbon foil)	~1 (S3 or S4)	40 (S5)
Thickness variation (10%) in foil stripper	. . .	75 (S5)
Total energy spread	12	140
Ion energy (MeV)	112	112
Relative energy spread	10^{-4}	1.3×10^{-3}

When the TU is operated in its stand-alone mode, a 90° analyzing magnet can be used to stabilize the terminal voltage to less than 1.6 kV. When the tandem is used as an injector to the cyclotron, however, this magnet will not be used and the tandem terminal voltage will be stabilized by using a generating voltmeter in the pressure vessel. This will then permit the terminal voltage of the TU to be stabilized to 1 part in 1000.

The percentage energy spreads given in the last row of Table II. A-VI are acceptably low both for experiments using the TU alone and for the beam injected into the cyclotron.

10. Particle Energies and Intensities Available from the TU Tandem

The terminal voltage of the TU is continuously variable from 3 to 16 MeV. This, together with the fact that a wide variety of

charge states can be chosen for heavy ions accelerated in the high-energy section of the tandem, means that a very large energy range is attainable for the ion beams from the machine. Furthermore, because of the fractionation into charge states as the ions go through strippers S3, S4, and S5, a wide range of charge-to-mass ratios is obtainable; and this range could be further increased if desired by providing for optional gas stripping at S5.

For each of several ion species, Table II.A-VII lists the particle intensities, maximum energies, relevant charge states, and (electrical) currents in various sections of the TU accelerator. The bunched current injected into the TU was calculated on the assumptions that the bunching efficiency factor is 0.3 and that separation of isotopes

TABLE II.A-VII. Particle intensities and maximum energies estimated for various pulsed ion beams accelerated in the TU tandem (terminal voltage 16 MV). The figures given for the pulsed-beam currents are based on presently achievable currents from negative-ion sources (except in the case of uranium beams, where it is expected that 50 μA of UF_5^- should be readily attainable). In some instances, the maximum source currents cannot be used because of the expected 60-μA limitation in the current-carrying capability of the low-energy acceleration tubes (e.g., for hydrogen beams) or the high-energy tubes (for F^{6+} and Cl^{7+} beams). Provided that this limitation is not exceeded, dc beam currents may be expected to be about a factor of 3 higher, since a bunching efficiency of 0.3 was assumed for the pulsed beams. A transmission factor of 70% is assumed for each half of the TU, so the overall transmission factor is 0.5. Unless indicated in the first column, the ion sources are assumed to contain elements in their natural isotopic abundances. For ionic masses lower than 150, the inflection magnet will separate out one isotope for acceleration.

Ion	Negative-ion current from source (μA)	Bunched current injected into TU (μA)	Terminal stripper	Charge state selected	Electrical current in high-energy tube (μA)	Energy (MeV)	Particles per second ($\times 10^{12}$) from TU (pulsed beam)	Most intense charge state following foil stripper S5
p, d	180	60	S2	1	43	32	180	—
He^3, He^4	12	4	S2	2	6	48	12	—
Li^6, Li^7	2	0.6	S2	3	1.3	64	2	—
C	2	0.6	S1	5	1.0	96	1	6
O	24	7	S1	6	15	112	12	8
F	117	35	S1	6	60	112	43	9
S	20	6	S1	7	12	128	7	14
Cl	143	32 (Cl^{35})	S1	7	60	128	37	15
	250	57 (Cl^{35})	S1	9	28	160	14	16
Br	100	15 (Br^{79})	S1	6	17	112	13	23
	100	15 (Br^{79})	S1	8	11	144	6	24
I	50	15	S1	6	14	112	10	28
	50	15	S1	8	8	144	4	30
U	50 (UF_5^-)	15	S1	5	9	91	8	28
	50 (UF_5^-)	15	S1	8	4	139	2	34

occurs in the inflection magnet. A transmission factor of 0.5 was assumed for the TU. This factor is intended to account for losses due to such causes as gas scattering and beam optics. For the heavier ions listed in the table, two rows of data are given: one for the most intense charge state leaving the center-terminal stripper and one for a higher, less-intense charge-state component. Since a Gaussian distribution of charge states was assumed, it is quite possible that the intensities of these higher-charge-state components are somewhat underestimated.

II. B. CYCLOTRON

1. Summary

The basic design criteria for the proposed accelerator are that it should accelerate ions in all regions of the periodic table, providing energetic ion beams with variable energy, high intensity, and good energy resolution. The energy requirements are that the system must accelerate uranium ions to at least 9 MeV/nucleon and protons to well above the meson threshold, say to 350 MeV, at minimum cost. The system chosen to meet these requirements consists of a large open-sector isochronous cyclotron with two alternative injectors—one a modified TU tandem Van de Graaff for the injection of heavy ions and the other a much smaller cyclotron for the injection of light ion species. This section will be devoted to a technical discussion of the large cyclotron and its injector for light ions.

The open-sector design for a cyclotron has many excellent characteristics for its intended use. The projectiles enter the cyclotron with a substantial energy (acquired in the injector) and with a very small energy spread and emittance. Thus, focusing forces are present in full strength even on the first turn and there is no loss in intensity like that in the central region of an ordinary cyclotron. The good quality of the incident beam and the focusing forces also allow the beam to be well confined throughout its trajectory, so that the magnet gap may be small (for a substantial saving in cost) and the beam can be extracted from the cyclotron without much loss in intensity. The space between the magnetic sectors makes the injection and extraction processes relatively easy and allows ample space for the accelerating structure and for vacuum pumps. Since there is no load of un-ionized gas from the ion source, which is far upstream in the injector, the vacuum can be excellent. The diameter (and hence cost) of the magnets required for heavy-ion acceleration may be minimized by using highly stripped incident ions. The ion source is not limited in bulk to the finger-sized unit of the ordinary cyclotron, since it is located at the input of the injector or pre-injector.

Both four-sector and six-sector designs of the large cyclotron were seriously considered. The four-sector machine is somewhat less expensive, since it has fewer major components. However, orbit calculations show that a six-sector machine is vastly superior in every other respect—in freedom from resonance instabilities for both light and heavy ions, higher energy for light ions, superior performance in beam extraction, lower rf power, ease of construction with non-spiraled magnets and less stringent tolerance in placement. Thus a six-sector design (N = 6) was chosen for the main cyclotron.

This design reliably satisfies both the heavy-ion and light-ion requirements. The maximum value of the field rigidity $B\rho$ with conventional copper coils is 1160 kG-in. (2946 kG-cm), corresponding to an energy of 350 MeV for protons and 10.6 MeV/nucleon for uranium (charge 38+) obtained with the TU operated at the guaranteed terminal potential of 16 MV. The energy is variable over a wide range, typically 7:1. With the exception of the protons, the lowest energy of the light ions slightly overlaps or approaches the maximum energy provided by the tandem.

Figure II·B-1 illustrates the maximum energy achievable by the cyclotron as a function of the final charge-to-mass ratio Z/A of the projectile. These energies are based on a field rigidity of 1160 kG-in. If superconducting main coils are adopted, as is being considered, the field rigidity for heavy ions will be increased to about 1290 kG-in. The maximum energy for the uranium 38+ ion would then increase to about 13.1 MeV/nucleon (and the present injection radius would have to be decreased or the TU would have to operate at $>$ 16 MV), but the maximum energy of the proton and other somewhat relativistic projectiles would remain unchanged.

When a light-ion beam is required to have good energy resolution, it can have only modest intensity, namely, about 10 μA average current. However, we believe this can be increased substantially for experiments that do not require stringent energy resolution. The intensity of a heavy-ion beam cannot be stated so simply, because it

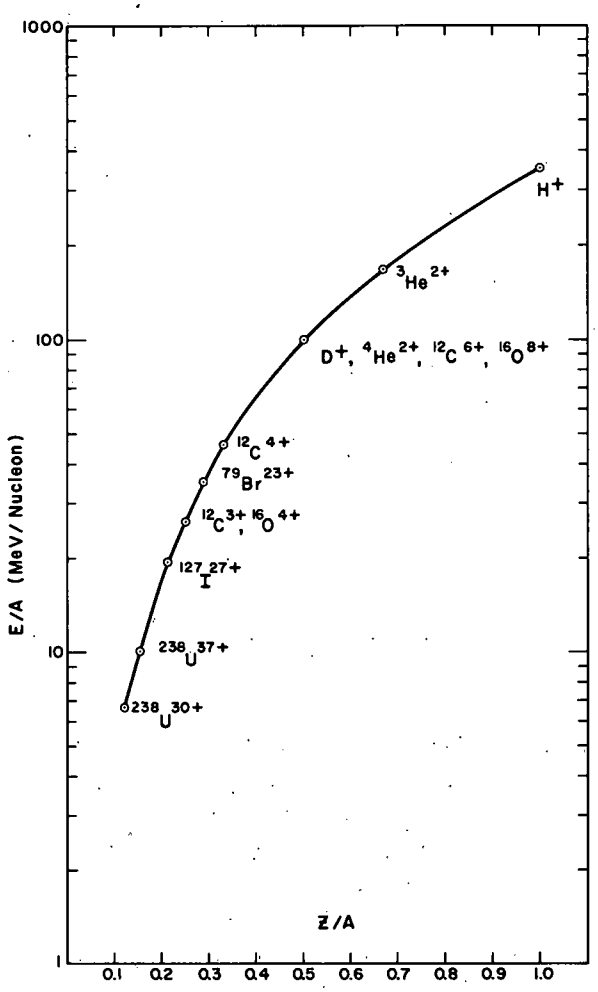

Fig. II. B-1. The energy per nucleon as a function of the charge-to-mass ratio in the N = 6, $\theta = 20^{\circ}$ cyclotron at maximum excitation (Bρ = 1160 kG-in.).

depends on the value of Z/A for any given species and on the characteristics of the tandem and its ion source. Figure II. B-2 is a plot of particle intensity as a function of energy per nucleon and final Z/A for uranium, iodine, and bromine. As previously discussed in connection with the tandem (Sec. II·A), these currents are limited either by ion-source technology or by the beam-current capacity of the tandem.

A vacuum of about 1×10^{-7} Torr will be provided in the cyclotron. This will permit more than 80% of the heavy ions to be accelerated without charge-exchange collisions.

The design aim for the energy resolution of the extracted beam is better than 1 in 10^3; hopefully, a resolution approaching 1 in 10^4 will be attained. Energy analysis of the extracted beam is planned to

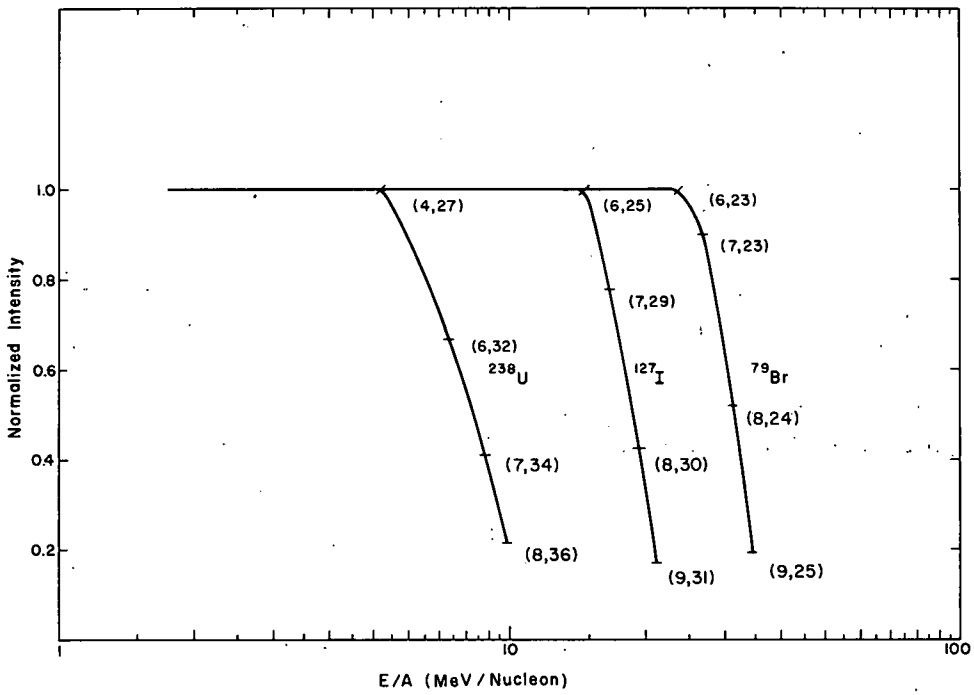

Fig. II·B-2. Beam intensities from the N = 6 cyclotron—calculated for a bunching efficiency of 30%, a tandem transmission of 50%, and a cyclotron efficiency of 50%. The isotopic species of the ion is indicated for each curve, and its charge state at each calculated point is given in parentheses—the first number being the charge number after gas stripping in the terminal of the tandem, the second being the state selected after the second (foil) stripper. The normalized intensities are I/I_{max}, where the maximum expected intensities I_{max} are 7×10^{11} pps for uranium, 1×10^{12} pps for iodine and 1.5×10^{12} pps for bromine.

assure the experimenter a beam of good resolution, namely, better than 1 in 10^4.

The emittance of the extracted beam will be about 1.5π mm-mrad.

Auxiliary dees tuned to the second harmonic of the rf frequency will be used to increase the duty factor of the beam without sacrificing energy resolution. Although the scheme entails mechanical and electrical complication, it is feasible. For a modest voltage on the auxiliary dees, the duty factor can be extended from about 1.5% (main dees only) to almost 10% without changing the energy resolution of 1 in 10^3. The rf design utilizes the advantages inherent in a 3-dee 3-phase

rf system. The maximum voltage will be 250 kV on the main dees and about 80 kV on the secondary dees. The fundamental frequency will be variable from about 9 to 22 MHz. The total power required (main and auxiliary dees) will be about 1 MW.

The magnetic guide field will be provided by 6 radial-sector magnets weighing 450 tons each (total weight 2700 tons). With conventional copper coils, the maximum gap field will be 18 kG. The total required power for magnet excitation, including trim coils, is 1200 kW. The overall diameter of the large cyclotron is 51 ft.

The energy amplification factor for the cyclotron is about 26 for 350-meV protons; hence, the required injector energy is 13.8 MeV. Tentatively, the light-ion injector will be an open-sector cyclotron with four sectors. It will have an energy amplification factor of about 4.5 and the pre-injector will have a dc terminal that operates at 3 MV. Main and auxiliary dees are planned for the injector cyclotron, and klystron bunching will be utilized on the pre-injector terminal.

The characteristics of the main cyclotron and of its injector cyclotron (to be described in Sec. II·B9) are summarized in Table II·B-I.

TABLE II·B-I. Tentative parameters of the main and injector cyclotron.

	Main cyclotron	Injector cyclotron
No. of sectors N	6	4
Injector	N = 4 cyclotron or tandem	3-MV dc pre-injector
Overall diameter	51 ft	15 ft
Magnet		
Iron width	20°	35°
Magnet gap	4 in. (10.16 cm)	2 in. (5.08 cm)
Total weight of iron	2700 tons	72 tons
Maximum power including trim coils	1000 kW	66 kW

TABLE II· B-I (cont'd)

		Main cyclotron	Injector cyclotron
Main dees			
Number		3	2
Width		30°	40°
Max. voltage		250 kV	100 kV
Frequency range		22 to 9 MHz	22 to 9 MHz
Auxiliary dees (for flat topping)			
Number		3	3
Width		15°	
Max. voltage		80 kV	33 kV
Frequency range		44 to 18 MHz	44 to 18 MHz
Max. power (60 Hz), main and auxiliary dees		1 MW	150 kW
Energy resolution		Better than 1 in 10^3	Only 1 in 300 req'd
Emittance of external beam at 1160 kG-in.		1.5π mm-mrad	8.2π mm-mrad required
Radius of final orbit	ρ_{max}	64.4 in. (164.0 cm)	19.3 in. (49.0 cm)
Radius of initial orbit	ρ_{min}	16.0 in. (40.6 cm)	9.1 in. (23.1 cm)
Final orbit length/2π	R_{max}	185.5 in. (471.2 cm)	46.0 in. (116.8 cm)
Initial orbit length/2π	R_{min}	46.0 in. (116.8 cm)	21.6 in. (54.9 cm)
With copper coils			
Max. field at final orbit	B_{max}	18.0 kG	14.8 kG
Max. final rigidity	$B_{max}\rho_{max}$	1160 kG-in. (2946 kG-cm)	285 kG-in. (724 kG-cm)
Max. average field	$\langle B \rangle_{max}$	6.25 kG	6.20 kG
With superconducting coils*			
	B_{max}	20.0 kG	
	$B_{max}\rho_{max}$	1290 kG-in. (3277 kG-cm)	
	$\langle B \rangle_{max}$	6.95 kG	

*To obtain maximum advantage, the TU terminal must exceed 16 MV or else R_{min} must be decreased.

After the operating parameters of the entire accelerator complex have been determined for a variety of particles and energies, automatic return to these values will be controlled by a small computer. The extent of this automation and the installation of the needed interface equipment will be set by experience as the individual accelerators are brought into use.

2. The Choice of the Number of Sectors

a. The Hazards of Resonance

In all magnetically-guided accelerators, stabilizing forces are present to keep the projectiles on course. As a result, the orbits weave back and forth about an ideal path, the number of vertical and radial oscillations per turn being denoted by ν_z and ν_x.

These necessary guiding forces are accompanied by hazards in that resonances can develop that vastly increase the amplitudes of the oscillation, so that particles may be lost by collision with the structure of the accelerator. Not all of the resonances are equally serious; some are trivial, some can be eliminated by extremely rigid tolerances in magnet construction and placement (at a very high additional cost); the cause of others can be compensated by currents flowing in auxiliary coils, while still others form impassible barriers.

Plots of ν_z vs ν_x are valuable since they disclose the resonant conditions that must be traversed successfully if an intolerable loss of particles is not to be suffered.

b. The Calculation of the Oscillation Frequencies ν_z and ν_x

Without a detailed knowledge of the fringing fields near the edges of the magnets (such knowledge can be acquired only by study of model or full-scale magnets), one may obtain rough values of ν_z and ν_x by calculations based on the so-called "hard edge" approximation, in which the magnetic fields are assumed to terminate abruptly. An orbit through the remainder of the inter-magnet space (a "valley") is then a straight line.

The more accurate "soft edge" calculations involve a reasonable estimate of the rate at which the field gradually dies out as the ions advance into a valley. At small radii, no portion of the path in a valley is straight, since the magnets are so close together that their

fringing fields overlap. The values of ν_z and ν_x are then significantly different from the values if a hard edge had been assumed. At large radii, where the magnets are much farther apart, the changes in ν_z and ν_x are less pronounced.

Our earliest thoughts on the open-sector cyclotron, presented at the ANL-AUA meeting of 11 January 1969, were based on the hard-edge approximation. Machines of N = 4, with angular magnet widths $\theta = 38^\circ$ and $\theta = 45^\circ$ were considered; to reach the goal of high-energy protons without crossing resonances that would cause a severe loss of particles, it was necessary to add spiraling to the magnets. This would increase the problems of design and raise the cost. A six-sector magnet, with $\theta = 20.5^\circ$ and no spiraling, was also considered—again in the hard-edge approximation; this appeared very attractive.

Our recent studies, here presented in both the hard- and soft-edge form, indicate that for 350-MeV protons the N = 6 machine with θ reduced to 20° offers many advantages over the N = 4 designs, although the latter could be employed for machines of lesser energy.

In Sec. II. B2 we discuss the resonances that must be traversed by two N = 4 machines and one of the N = 6 variety.

c. Resonances with N = 4 Magnets

In Fig. II. B-3, counting from the top downwards, the first and third heavy curves are plots of ν_z vs ν_x for protons with hard-edge N = 4 magnets of angular widths $\theta = 38^\circ$ and 45°, respectively. The second and fourth heavy curves show the results with soft edges, and are characterized by an initial rise in ν_z at low energy because of the considerable trespass of the fringing fields into the valleys when the hills are close together. We note two general trends: the curves are lowered by the soft-edge effect and by an increase in the angular width θ.

We will discuss the various resonances encountered by protons (with remarks on heavier ions where appropriate), starting at the left where the energy is approximately that of injection. Remarks always apply to the soft-edge situation.

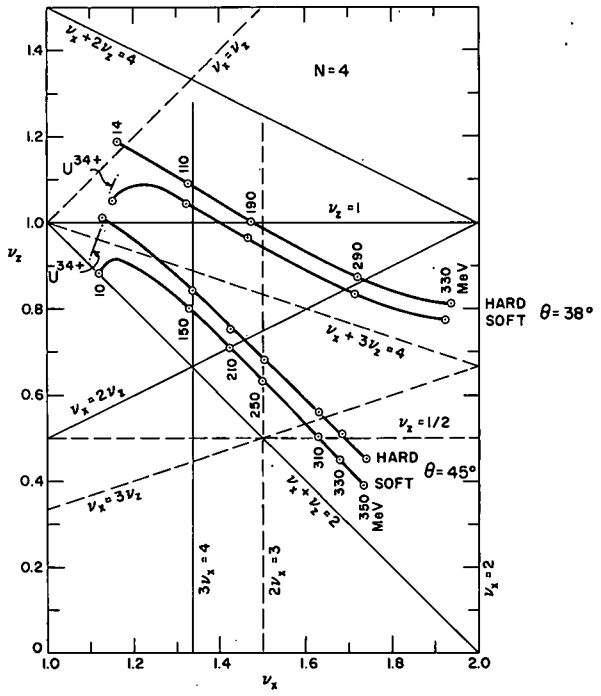

Fig. II. B-3. Resonances that must be crossed by protons and U^{34+} in a four-sector cyclotron with magnet angular widths 38° and 45°. Energies in MeV are indicated at selected points for protons. "Hard" implies a simple analysis in which the field at a magnet edge is assumed to terminate abruptly; "soft" means that a reasonable estimate of a gradually-decreasing edge field has been assumed. Dashed lines, in general, represent resonances that are trivial, though in some cases they could be troublesome. In gaining energy from 14 to 350 MeV, protons must cross two very serious resonances.

$\nu_x + 3\nu_z = 4$. This is a cubic, non-linear, imperfection resonance driven mainly by the fourth harmonic of d^3B_z/dx^3, and by a median-plane error. With N = 4 and $\theta = 45°$, it must be crossed by uranium and slightly less heavy ions; medium-light particles will be in its neighborhood for a considerable time. It is not expected to be troublesome.

$3\nu_x = 4$. For the N = 4 magnet, this is a quadratic, non-linear, intrinsic resonance driven by the fourth harmonic of d^2B_z/dx^2 and of $dB_z/\rho\, dx$. It should not be difficult to pass, in view of the large energy gain per turn that is planned.

$\nu_z = 1$. (Traversed by N = 4 with $\theta = 38°$, but not with $\theta = 45°$.) This is a linear imperfection resonance arising from error in the magnetic median plane. The driving force is the first harmonic of the horizontal component of the field on the geometric median plane. This is an extremely difficult resonance to traverse (and it must be traversed for $\theta = 38°$ at energies exceeding 200 MeV) since an error of 0.1 in. in the first harmonic of the median plane will cause a vertical displacement of 1 in., for 800-keV energy gain per turn. For $\theta = 45°$,

heavy ions will be dangerously close to this resonance during most of the time, as indicated by the short path labeled U^{34+}.

$\nu_x = 2\nu_z$. This, known as the Walkinshaw resonance, is a quadratic, non-linear coupling resonance, driven by the average values of d^2B_z/dx^2 and $dB_z/\rho\, dx$. It can generate a vertical oscillation amplitude twice as large as any existing radial amplitude. This can be serious, since the coherent radial amplitude may not be small, because of the discrete nature of the energy gain per dee-gap crossing. (This will be discussed later.)

$2\nu_x = 3$. This is a linear imperfection resonance driven by the third harmonics in the field and in its radial gradient. Their effect can be eliminated by harmonic correction coils.

$\nu_x = 3\nu_z$. An imperfection, cubic, non-linear coupling resonance that can be traversed without difficulty.

$\nu_z = \frac{1}{2}$. A linear imperfection resonance due to the first harmonic of the gradient dB_z/dx. Harmonic coils can correct this.

In a four-sector machine, the value $\nu_x = 2$ represents the impassable "π-mode stop band" at which radial stability disappears completely.

The very short lines, labeled U^{34+}, indicate the soft-edge values of ν_z and ν_x (for $\theta = 38^\circ$ and $\theta = 45^\circ$) as uranium and other heavy ions are accelerated to full energy. For $\theta = 45^\circ$, the trajectory is never very far from the serious $\nu_z = 1$ resonance.

d. Resonances with N = 6 Magnets

After several trials, the angular width $\theta = 20^\circ$ has been found to be most suitable for the attainment of 350-MeV protons. The ν_z vs ν_x plots for protons are shown in Fig. II. B-4 for hard and soft edges. Only three resonances need be crossed, and none of these are serious.

$\nu_x = \nu_z$. This represents a linear-coupling resonance caused by an error in the median plane such that on the geometrical (not

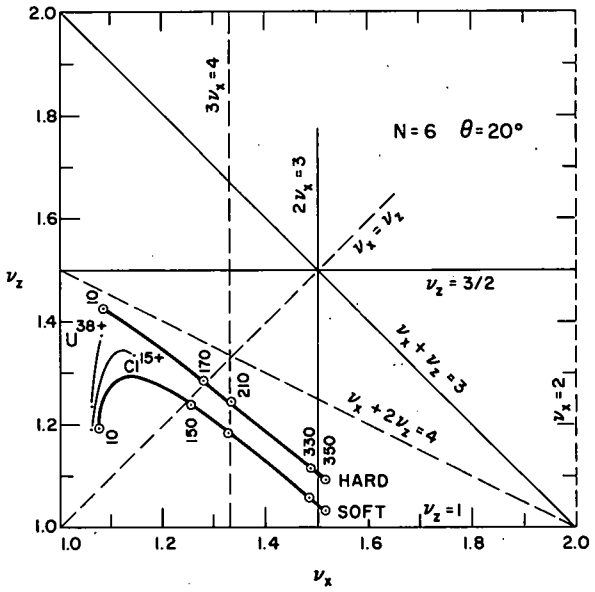

Fig. II. B-4. Resonances relevant to the performance of a six-sector cyclotron with magnet width $\theta = 20^{\circ}$. (See Fig. II. B-3 for an explanation of the symbolism.) Note that protons cross only three unimportant resonances from 10 to 350 MeV, and that the heavy ions from chlorine to uranium cross none at all.

magnetic) median plane B_x and B_θ are finite and proportional to x. In an open-sector cyclotron, the amplitudes of the vertical and radial oscillations are comparable, so an exchange of energy from one mode to the other will be harmless. Furthermore, the error in the median plane can be corrected by using different currents in the upper and lower trim coils.

$3\nu_x = 4$. Here we have a non-linear, quadratic imperfection resonance for the N = 6 magnet. It is driven chiefly by the fourth harmonic of the sextupole component of the field; and since the lowest harmonic of a perfect N = 6 magnet is the sixth, the force due to imperfections should be small.

$2\nu_x = 3$. This resonance (for an N = 6 machine) is actually a combination of two: (a) The linear-imperfection parametric resonance $2\nu_x = 3$, driven by a third-harmonic error in the radial gradient. (This is also encountered in the N = 4 machine.) Harmonic coils can eliminate it. (b) The non-linear, cubic, intrinsic resonance $4\nu_x = 6$, driven mainly by the sixth harmonic of d^3B_z/dx^3. It will not be troublesome. Both of these resonances can be completely avoided by making the field slightly non-isochronous for the last 20 turns. This lowers ν_x and makes ν_z increase rapidly, so that the path in the ν_z vs ν_x space turns upward without crossing the $2\nu_x = 3$ line.

On the other hand, this resonance may possibly be put to use: control of the phase and amplitude of the third harmonic of the field and its gradient will bring the resonance into prominence and result in a coherent oscillation that will increase the separation of orbits at the entrance to the extractor channel, should this be necessary.

It will be observed from Fig. II. B-4 that the design goal of 350 MeV is attained just before reaching the very serious resonance at $\nu_z = 1$.

Heavy ions (of which we show Cl^{15+} to 62 MeV/A and U^{38+} to 10.6 MeV/A) cross no resonances at all nor do they come within the vicinity of any. Somewhat lighter particles follow ν_z vs ν_x paths that lie between the hard- and soft-edge curves for protons (but terminate sooner), and so run into no serious difficulties.

The "π-mode stop band" for N = 6 occurs at $\nu_x = 3$, far off to the right beyond the edge of Fig. II. B-4.

As the above discussion and Fig. II. B-4 show, the design goal of 350 MeV is attained without much trouble from resonances. However, if it had been necessary to construct the 6-sector machine so that it would accelerate protons to substantially higher energies, then it would be necessary to cross the extremely serious resonances at $\nu_z = 1$. In principle this resonance could be crossed by exceptionally careful machining and location of the magnets and by correction coils, but the expense of this solution and the risk of failure would be substantial.

e. Orbit Scrambling with N = 4 and N = 6

Since energy is given to the ions in discrete and finite quantities at each dee-gap crossing, no particles ever travel on an equilibrium orbit. After each energy increment, this ideal orbit suddenly jumps to a location to the outside of the particle's existing position—so an oscillatory path about this new ideal orbit is generated, the jump becoming more pronounced with increased dee potential. The

effect on the amplitude of motion is cumulative when the radial oscillation frequency is close to the value $\nu_x = \frac{1}{2}N$. The result is that the oscillations become so large that successive turns are sometimes far apart and sometimes close together, which is to say that coherent oscillations are engendered. It is even possible for an orbit of given energy to lie, for a short space, inside an orbit of lesser energy. All this is true even if the ions travel in single file, thus forming a beam of zero width.

Such a "scrambling" of orbits raises two worrisome points. (1) Since the oscillatory paths are longer than the ideal equilibrium orbits, the basic criterion for isochronism is violated, and (2) the length of each bunch of ions is increased. Fortunately, calculations show that both of these effects are negligible if the beam is injected with the right initial conditions; the necessary adjustments to the inflector are less critical with N = 6 than with N = 4.

On the other hand, scrambling is most undesirable if it occurs near the final orbits, since it permits particles of differing energy to enter the extraction channel, thereby increasing the energy spread of the external beam.

For N = 4 and $\theta = 38^\circ$, a glance at Fig. II. B-3 shows that at the final energy of 330 MeV, ν_x has the value 1.92, which is very close to the critical number $\nu_x = N/2 = 4/2 = 2$. Hence scrambling will be very severe. A means of circumventing this can be devised by arguing backward; we assume no scrambling at the final energy and then trace the paths backward, to discover how far off the ideal course, at injection, the ions would have had to be, in order to cause this desirable final condition. Unfortunately, if care is taken to inject with this needed initial oscillation, the ions will still have considerable amplitude left by the time they reach 290 MeV. This is the energy at which the $\nu_x = 2\nu_z$ (Walkinshaw) resonance occurs, and it can be passed without serious loss only if the radial amplitude is small. Thus, for the intended

goal of high-energy protons with little energy spread in the extracted beam, the N = 4, $\theta = 38^{\circ}$ magnet is not suitable.

With N = 4 and $\theta = 45^{\circ}$, the scrambling would be less since ν_x is only 1.75 at the final energy of 350 MeV.

Even less mixing of ions with different final energies will occur for N = 6 and $\theta = 20^{\circ}$, since the value of ν_x at 350 MeV is about 1.5 (as seen in Fig. II. B-4) and this is far removed from the critical value $\nu_x = N/2 = 6/2 = 3$. Furthermore, what little mixing might exist can be removed by the earlier device of injecting deliberately off-course by the requisite amount to reduce the oscillations to zero at extraction, remembering that the Walkinshaw resonance ($\nu_x = 2\nu_z$) is not crossed in the N = 6 machine.

All this supplies a very compelling argument for six sectors.

f. Beam Envelopes with N = 4 and N = 6

When a realistic beam of finite width, divergence, and energy spread is injected into an open-sector cyclotron, its radial envelope is wider when in a magnet than when in a valley. The extent of this widening is much more pronounced with four sectors than with six. This is indicated in Fig. II. B-5, where the ratio (beam width in a magnet)/(beam width in a valley) is shown as a function of azimuth for N = 4 and N = 6 machines. At comparable final energies, the envelope expands by the factor 3.6 in going from valley center to magnet center for N = 4 and $\theta = 45^{\circ}$, and by the factor 5.5 for N = 4 and $\theta = 38^{\circ}$, whereas with N = 6 and $\theta = 20^{\circ}$, the expansion is by only the factor 1.4.

The point of importance is that there is a much greater length of no overlap of envelopes in a valley for a machine with N = 6 than with N = 4. For extraction, this is a critical matter. This process will be started in a valley center by introducing the inner electrode of an electrostatic deflector between the envelopes, which will be

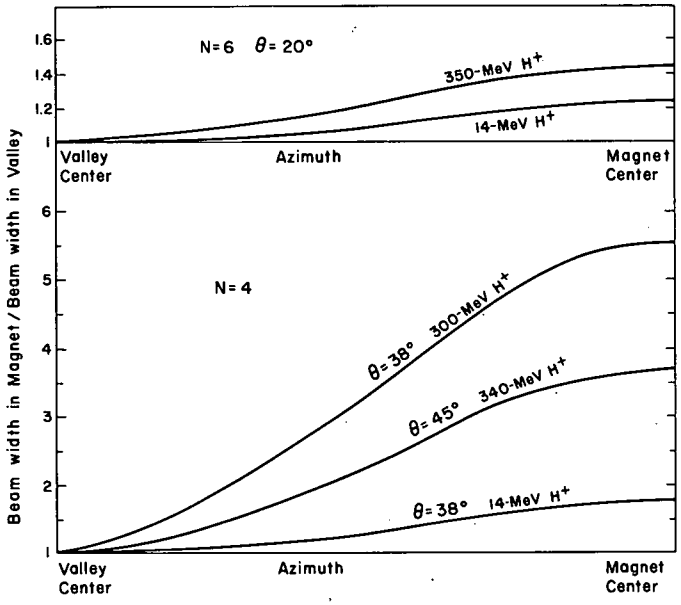

Fig. II. B-5. Ratio of beam width in a magnet to that in a valley. The relative expansion of the beam envelope in going from valley center to magnet center is much less with N = 6 than with N = 4 at the final energy. This reduces losses in the electrostatic deflector and eases the extraction problem.

separated at this point with either N = 4 or N = 6. With N = 4, the deflector must be short; otherwise the inner plate may intercept particles of the rapidly widening envelope of the previous orbit. On the other hand, with N = 6 the envelope expands very little between valley center and magnet, so that a long deflector may be used without intercepting particles of the preceding orbit. Since the lateral deflection varies with the square of the deflector length, N = 6 will give a much larger displacement at the position of the next element in the extraction complex, thereby easing the problem of obtaining an external beam and promising fewer losses in the process.

g. RF Power with N = 4 and N = 6

With N = 4 and each of two dees at potential V_4, the power is $P_4 \propto 2\,V_4^2$, while with N = 6 and three dees we have $P_6 \propto 3\,V_6^2$. But for the same energy gain per turn, it follows that $2V_4 = 3V_6$, so that $P_6 = \frac{2}{3} P_4$; i.e., less rf power is required for N = 6 than with N = 4. Further, the lessened dee voltage with N = 6 implies a smaller sudden shift in the equilibrium orbit at each gap traversal, so that orbit scrambling is reduced.

h. Summary: N = 4 vs N = 6

N = 4. A non-spiraling N = 4 magnet with $\theta = 38^{\circ}$ or slightly less, would be an excellent choice for protons of 200 MeV or a little more, and it also would be satisfactory for heavy ions. With a larger magnet width, say $\theta = 45^{\circ}$, resonances would seriously threaten the acceleration of heavy and light particles.

For greater proton energy, with N = 4 and either value of θ, some of the hazards could be avoided by adding a spiral to the magnet structure, but only at a greater cost of iron fabrication and increased complexity of dee structure.

N = 6. On the other hand, 350-MeV protons accelerated in a non-spiraling N = 6, $\theta = 20^{\circ}$ magnet traverse no troublesome resonances that cannot be eliminated by harmonic and trimming coils. No resonances at all threaten heavy ions.

With no resonance problems, the N = 6 machine will lose no ions from this cause and hence will give a larger yield of particles per second than an N = 4.

N = 6 affords less stringent tolerances in magnet construction and placement.

N = 6 exhibits a lesser degree of overlap of orbits at the extractor, so losses will be diminished and the extraction problem will be easier.

The three dees of N = 6 require less rf power for the same energy gain per turn, and reduce the magnitude of coherent oscillations.

i. Conclusion

Although the N = 6 design involves 50% more magnets than the N = 4 variety, on all other counts it is far superior for use with the variety of particles and energy ranges contemplated in this proposal.

Note, however, that for the small injector cyclotron with a maximum proton energy of about 15 MeV, the N = 4 design is entirely

suitable. The operating path on the ν_z vs ν_x diagram does not cross any resonances at all.

3. Beam Quality

In this section and those that follow, the beam quality and the design features related to the beam quality are discussed under two alternative assumptions about the rf voltage on the acceleration structure. In conventional accelerators, a sinusoidal voltage is applied to the accelerating dees, with the result that the ions injected during a finite time receive different gains in energy per turn and have a corresponding energy spread in the extracted beam. Following a discussion of this effect, we will describe a technique (called energy flat-topping) that gives almost constant energy gain per turn to all ions and a consequent reduction in the energy spread.

a. Energy Spread

(i) Effect of pulse length and errors in magnetic field. A pulse of ions entering the cyclotron will have a time duration. If the dee voltage is sinusoidal, not all the ions will receive the peak energy gain at each crossing of a dee gap. After K turns, when the most favored ion has reached the output radius, the others will have accumulated energy deficits so that the beam passing through the extraction channel will have a spread in energy. Furthermore, the magnetic field surely will not have the exact value demanded by the frequency of the dee voltage, so that the bunches will slip in phase with respect to the peak voltage, thereby increasing the energy spread.

We define the duty factor as DF = (pulse length)/(oscillator period) = τf, where f is the oscillator frequency. Then the energy spread of the extracted beam at final energy can be shown to be

$$\frac{\Delta E_f}{E_f} = \frac{\pi^2}{2} \left(K \frac{|\Delta B|}{B} + DF \right)^2$$

if $DF \geq K |\Delta B|/B$, as is usually true. Experience shows that a long-term field stability $|\Delta B|/B = 10^{-5}$ can be obtained routinely. A pulse length of

0.5 nsec is possible with a buncher, so for 350-MeV protons (for which K = 350 turns and f = 20 MHz), we find that DF = 1%. Hence

$$\frac{\Delta E_f}{E_f} = \frac{\pi^2}{2}(0.0035 + 0.01)^2 = 9.0 \times 10^{-4}.$$

It would be extremely difficult to obtain a better resolution so long as the dee voltage is sinusoidal. The dominant term is the duty factor, and further shortening of the beam pulse (whether obtained by a klystron or by sweeping the beam across a slit) involves very serious problems associated with linearity of the voltage, timing, etc. Even if the pulse length could be reduced, its peak current would have to increase proportionally to maintain the same average current and this would cause difficulties from space charge.

Figure II. B-6 is a plot of $\Delta E/E$ for two values of field regulation and with K = 350 turns (as for protons) and K = 70 (as for heavy ions, which take fewer turns to reach full energy because of their high charge). For a given $\Delta E/E$, heavy ions place less stringent demands on field stability and permit a larger duty factor.

(ii) Effect of energy spread in the injected beam. Since the directional deviations of ions in the injected beam are expected to be uncorrelated with their energy deviations, the energies gained at gap crossings will not be correlated with input energies. Optimistically, the overall total energy spread at the final energy will be

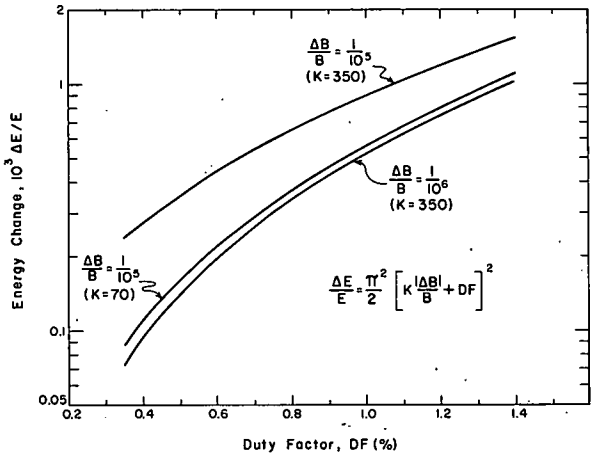

Fig. II. B-6. Energy change as a function of percent duty factor, for two values of error in the magnetic field. For protons, the number of turns to reach final energy is K = 350, while for heavy ions it is K = 70.

$$\left(\frac{\Delta E_f}{E_f}\right)_{\text{total}} = \left\{\left[\frac{\pi^2}{2}\left(K\frac{|\Delta B|}{B} + DF\right)^2\right]^2 + \left[\frac{\Delta E_i}{E_f}\right]^2\right\}^{1/2}.$$

The injection energy for 350-MeV protons is 13.8 MeV. Let us suppose that the energy spread from the injector is as bad as $\Delta E_i/E_i = 1/300$ so $\Delta E_i/\Delta E_f = 1.3 \times 10^{-4}$. Then for the earlier example we have

$$\left(\frac{\Delta E_f}{E_f}\right)_{\text{total}} = \left\{\left[9.0 \times 10^{-4}\right]^2 + \left[1.3 \times 10^{-4}\right]^2\right\}^{1/2}.$$

Thus, even so wide a spread in the injection energy is of small consequence.

(iii) Effect of changes in dee voltage. Although the energy spreads discussed thus far are those found in a single pulse of particles, there is another disturbance that can cause the pulse energy to shift along the energy scale.

If the dee voltage is lowered, then in the same number of turns less energy is acquired. If this voltage change is small enough that the ions of reduced energy will still pass through the extraction channel of the cyclotron, then this effect will cause an energy spread

$$\frac{\Delta E}{E} = \frac{\Delta V}{V}.$$

The dee voltage can be stabilized to 1 part in 10^4 if care is exercised to reduce voltage ripple in the power supply and if the filaments of power tubes are heated by direct current. But changes in dee voltage caused by sparks (whether major or minuscule) cannot be compensated quickly enough because of the millisecond time constant of the rf system. Fortunately, the tendency to spark will be reduced by the large clearances available around the dees in the open-sector cyclotron.

(iv) Effect of instability in frequency and phase. Modern low-level frequency synthesizers and phase controllers are so precise that no measurable contribution to energy spread will be encountered because of lack of stability in these devices.

In summary, with the use of sinusoidal dee potentials, it appears possible to obtain day-to-day energy spreads as small as 1 part in 10^3 in the external beam from the cyclotron provided the pulses are very short, corresponding to a duty factor of 1%. It would be extremely difficult to attain 1 part in 10^4. Our design aim is to achieve a resolution width that is less than 1 part in 10^3 for a sinusoidal wave form and to obtain much less than 1 part in 10^3 by flat-topping. External analyzing magnets will be used to obtain energy spreads better than 1 part in 10^4.

b. Duty Factor and Energy Flat-Topping

If the wave form of the dee voltage were square, rather than sinusoidal, and if the duration of the pulse of ions did not exceed the duration of the flat top of the voltage, then all the particles in the bunch would receive the same energy at every traversal of a dee gap. Hence, no energy spread would develop.

A truly square voltage wave can be produced only by the superposition of an infinite number of sinusoidal voltage waves with frequencies that are harmonics of the fundamental, but a useful approximation to a flat top can be attained by using only two frequencies.

It is difficult to impress voltages of different frequencies on the same dee; but the same effect can be obtained by applying sinusoidal voltages to several sets of dees at such frequencies, amplitudes, and relative phases that the energy gained per turn is almost constant for all ions in a pulse of finite but limited length. Analysis indicates that the flat-topping effect will be significant even with only two sets of dees. The main dees operate on the fundamental frequency, supplying the major part of the accelerating voltage. Auxiliary dees are tuned to the second harmonic. They subtract from the energy gained by ions that cross the main gaps at peak potential, and add to it for ions that receive only a small fraction of peak voltage at the main gaps. The auxiliary dees may

be nested inside the main ones, or they may be displaced in azimuth; proper control of voltage amplitude and relative phase is necessary in either case.

In an ideal rf structure the voltage could be independent of radius within each dee set; and in this case it can be shown that the resolution width would be 10^{-4} for a duty factor of 11% if the peak voltage V_2 on the auxiliary dees is one quarter of the peak voltage V_1 on the main set. In practice, however, the radial lengths of both sets of dees are appreciable fractions of the rf wavelengths, so that the voltages are not constant with radius and the energy spread is somewhat greater than for the ideal case. This can be partially compensated by judicious choice of the shape and position of the stub that supplies the rest of the resonant circuit.

To determine the effect of radial dee-gap voltage distributions on flat-topping, a $\frac{1}{5}$-scale rf strip-line model was constructed to measure such distributions for both the fundamental and the second-harmonic frequencies. At the highest frequency, the distribution along the accelerating gap of the second harmonic varied from V at the extraction radius to a minimum of 0.3 V at the position of the stub, and then increased to 0.75 V at the injection radius. As the frequency was reduced to the low end of the range, the minimum value of voltage increased from 0.3 V to 0.7 V. The voltage distribution along the fundamental dee was found to be more nearly uniform, the minimum never being less than 0.8 of the voltage at the extraction radius. These distributions were used to calculate the effect of adding the auxiliary dee, assuming negligible variations in all other accelerator parameters.

The results of the calculation are given in Fig. II·B-7. Here E_t is the final energy of an accelerated particle injected at a time t (relative to the peak of the fundamental rf mode) and E_0 is the final energy of a particle injected at t = 0. In the figure, the injection time is given in percent of the fundamental cycle time T, i.e., as 100 t/T = 100 tf.

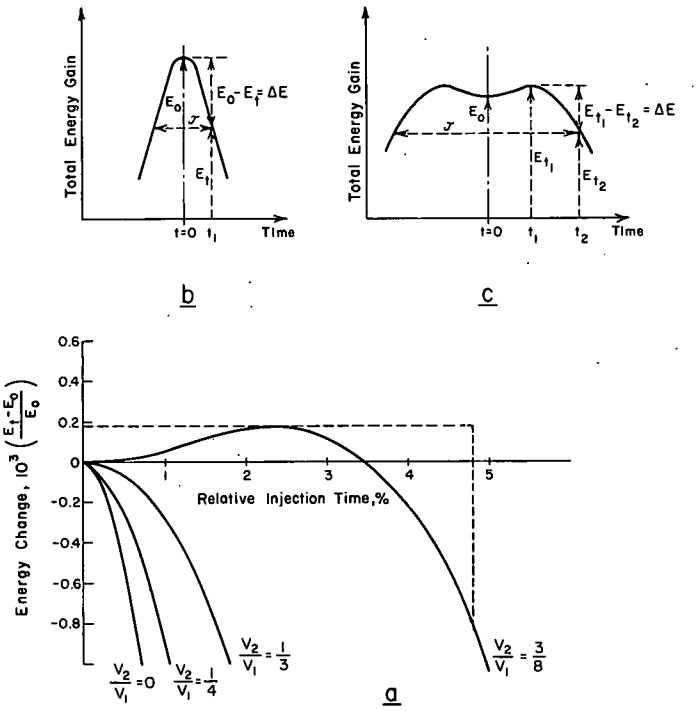

Fig. II. B-7. Effect of injection time. (a) Particle energy change as a function of injection time for three sets of main and auxiliary dees for which the voltages V_1 and V_2 vary along the radial dimensions. (b) A partially-flattened energy-gain wave where the energy change is $\Delta E = E_0 - E_t$ for a pulse of duration $\tau = 2t_1$. (c) An overcompensated energy-gain wave.

The curves in Fig. II· B-7 may be used to calculate the effect of duty factor on resolution width. First note that numerically the duty factor is just twice the relative injection time for the end of the pulse, since the total spread in time is twice the deviation from zero. Then for $V_2/V_1 = 0$, one sees from the figure that the relative energy at the end of the pulse decreases by 1×10^{-3} when the relative injection time varies from 0 to 0.7%; and this implies that the total relative energy spread $\Delta E/E$ of the extracted beam is 1×10^{-3} when the duty factor is $2 \times 0.7\%$.

When flat-topping is applied, the permissible duty cycle (for a given energy spread) increases rapidly, as may be seen from the figure. For example, to obtain $\Delta E/E = 10^{-3}$ requires DF = $2 \times 1\%$ if $V_2/V_1 = 1/4$ and DF = $2 \times 1.85\%$ if $V_2/V_1 = 1/3$. When $V_2/V_1 = 3/8$, the maximum energy gain is not at t = 0, and consequently the curve of $(E_t - E_0)/E_0$ goes through a maximum at a nonzero time. As in the other cases, however, the total energy spread of the extracted beam may be read from the curve; for example, as shown by the dashed lines, $\Delta E/E = 10^{-3}$ if DF = $2 \times 4.8\% = 9.6\%$. Note that the pulse widths

corresponding to these duty cycles are a few nanoseconds, wide enough to be easily realized. Alternatively, the resolution width can be made much smaller than 10^{-3} by using a very narrow incident pulse. So long as $K \cdot \Delta B/B \ll DF$, the overall energy spread may be read from Fig. II. B-7 with acceptable accuracy; otherwise, a much more involved procedure is necessary.

The variation in rf voltage with radius raises the hope that it will be possible to find dee shapes and stub locations that will give a large maximum main dee voltage and very little auxiliary dee voltage near the extraction radius, since this combination would increase the separation between the final turns.

All in all, energy flat-topping by the use of auxiliary dees is of great value in extending the duty cycle (thereby raising the number of particles per second) without increasing the energy spread. (It must be noted, however, that variations of energy arising from changes in the dee voltage will still exist.)

The benefits of energy flat-topping are obtained at a price. The net energy gain per turn is reduced, unless the voltage on the main dees is raised; and a higher voltage will increase the rf power and demand greater clearances to prevent sparking. Twice as many dees and resonant structures are needed. The mechanical and electrical problems are formidable if the auxiliary dees lie within the main dees; and if they are located in adjoining valleys, they lead to difficulties with injection and extraction of the particles.

c. Beam Emittance

This quantity is here defined as the area of the phase-space ellipse, namely $\epsilon = \pi y_0 y_0'$, where y_0 and y_0' are respectively the half width (or height) and the maximum divergence (in the appropriate plane) of the beam envelope at a "waist", i.e., at a point where the envelope has the least width. At a fixed momentum, emittance is a constant; so a decrease

in beam width is accompanied by an increase in divergence and vice versa. Since one desires both of these parameters to be small, the emittance should also be small.

For 350-MeV protons, the emittance needed for efficient beam extraction is about 1.5 π mm-mrad in both the radial and vertical planes.

When the large N = 6 cyclotron is used with light ions, it will be preceded (as explained in Sec. II·B9) by a smaller cyclotron—and this in turn by a pre-injector, probably a 3-MV one. By the principle of adiabatic invariance it can be shown that the product of emittance × momentum (i.e., $\epsilon \times B\rho$) is a constant. Hence, if we are to have ϵ = 1.5 π mm-mrad for 350-MeV protons (for which $B\rho$ = 1160 kG-in.), then for injection into the N = 6 machine at 13.8 MeV ($B\rho$ = 212.4 kG-in.) the emittance will be 8.2 π; and at injection into the N = 4 machine at 3 MeV ($B\rho$ = 99 kG-in.), the emittance will be 17.6 π mm-mrad. Therefore the emittance of the beam from the pre-injector must not exceed 17.6 π mm-mrad; if it can be made less than this, all subsequent values will be less (i.e., better) than those quoted.

The ion source and the Cockcroft-Walton accelerator that are used in conjunction with the ZGS proton synchrotron give 120 mA of protons at 750 keV with an emittance of 76 π mm-mrad. If this beam were accelerated to 3 MeV, the emittance would become 38 π mm-mrad. This is 2.2 times (i.e., worse than) our required figure of 17.6 π. However, we need only 5 mA, rather than 120, and it is known that emittance decreases more than linearly as less current is drawn from a source. Hence we have complete confidence that the required 17.6 π mm-mrad for 5 mA at 3 MeV can be obtained.

We note that all of the light ions have the same momentum (1160 kG-in.) at their maximum energies, so all will have the same final emittance of 1.5 π mm-mrad. A significant deterioration will occur only at minimum energy; thus for 50-MeV protons (for which $B\rho$ = 406 kG-in.) the emittance will rise to 4.3 π mm-mrad.

When heavy particles are injected from the tandem into the large cyclotron, the emittance of the ions on leaving the TU will be somewhat less than 3 π mm-mrad, as was shown in Sec. II·A.* Some worsening will occur at the second (foil) stripper, but this will be small since this stripper will be located near the crossover in trajectories following a quadrupole triplet in the transport system, so that scattering in the foil will be small compared to the existing divergence. Consequently the emittance at injection into the N = 6 machine will be close to or less (i.e., better) than 17.6 π mm-mrad. This will again be the required (maximum) value, since the heavy ions will surely be used near to their maximum energies (for which the momentum is Bρ = 1160 kG-in. or only slightly less).

---

*Unfortunately, there are several definitions of emittance in current use. In the terminology used in Sec. II·A (the TU section of this proposal), the value quoted as 10 mm-mrad at emergence from the tandem is the area of a rectangle that bounds the phase-space ellipse. Hence the area of the ellipse will be somewhat less than 10 mm-mrad. In the terminology of this section, this emittance is less than (10/3.14)π, i.e. less than 3.2 π mm-mrad.

4. Sector Magnets

In the design of an open-sector cyclotron, the interacting magnetic parameters of sector width and field strength must satisfy the isochronous and focusing requirements for each type of projectile. Through a program of orbit computations, it was ascertained that a magnet of 6 sectors would be best in accelerating protons to an energy of 350 MeV. These magnets are straight radial sectors of 20° azimuthal width. Each magnet is about 22 ft long, 19 ft high, and 7 ft wide and weighs 450 tons; the total for six is 2700 tons. The central region of the magnet arrangement has an inner diameter of 78 in. and is free of iron. The maximum diameter of the assembly is 51 ft.

The maximum magnetic field in the gap has been set at 18 kG and the computed soft-edge effect is illustrated in Sec. II·B2b. With the basic parameters of the poles established by the desired projectile energies and orbit properties, the other parameters of the magnet were selected on the basis of a cost-optimization study.

A plan view of the magnet is shown in Fig. II·B-8, the dimensions of a sector being given in Fig. II·B-9.

a. Magnet Gap

There are several advantages in having a small magnet gap. Excitation power is reduced, both for the main and the trim coils, and field flutter is increased. In addition, the extent of the fringing field is lessened, so the angular width θ of the magnets can be increased; this reduces the outside radius of the machine with a substantial reduction in weight. But there are other considerations that suggest a large gap: possible orbit-plane displacement, trim-coil space requirements, voltage-holding clearance for electrostatic deflectors, accuracies in the machining and installation of the poles of the magnet, and the conductance of the gap for high-speed vacuum pumping. When these factors were all taken into consideration, the gap dimension

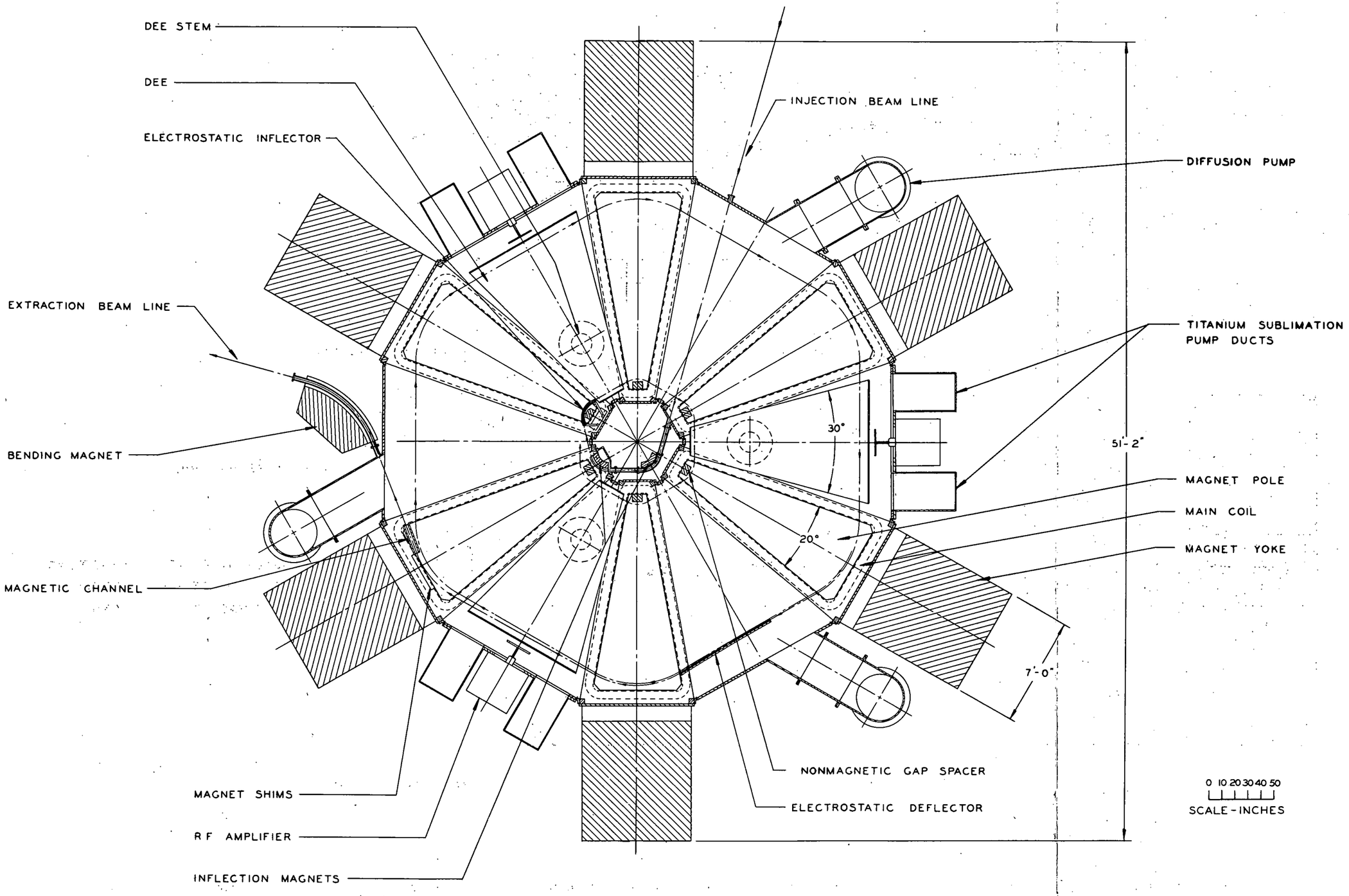

Fig. II. B-8. Plan view of proposed 6-sector cyclotron.

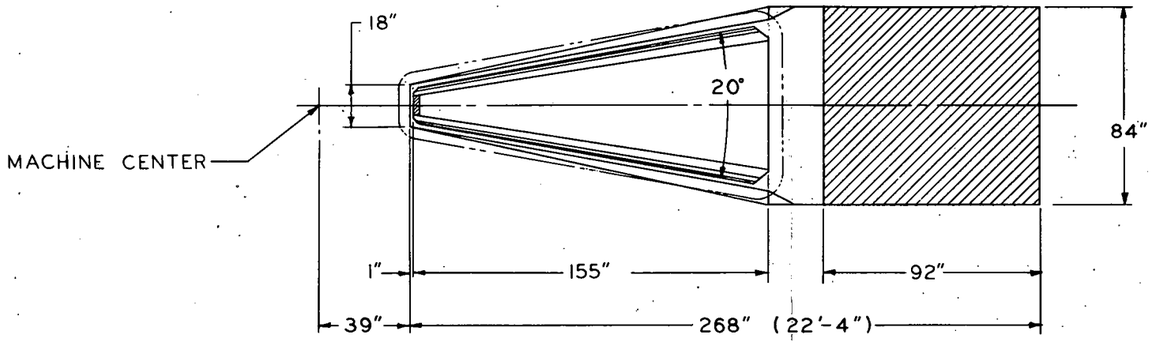

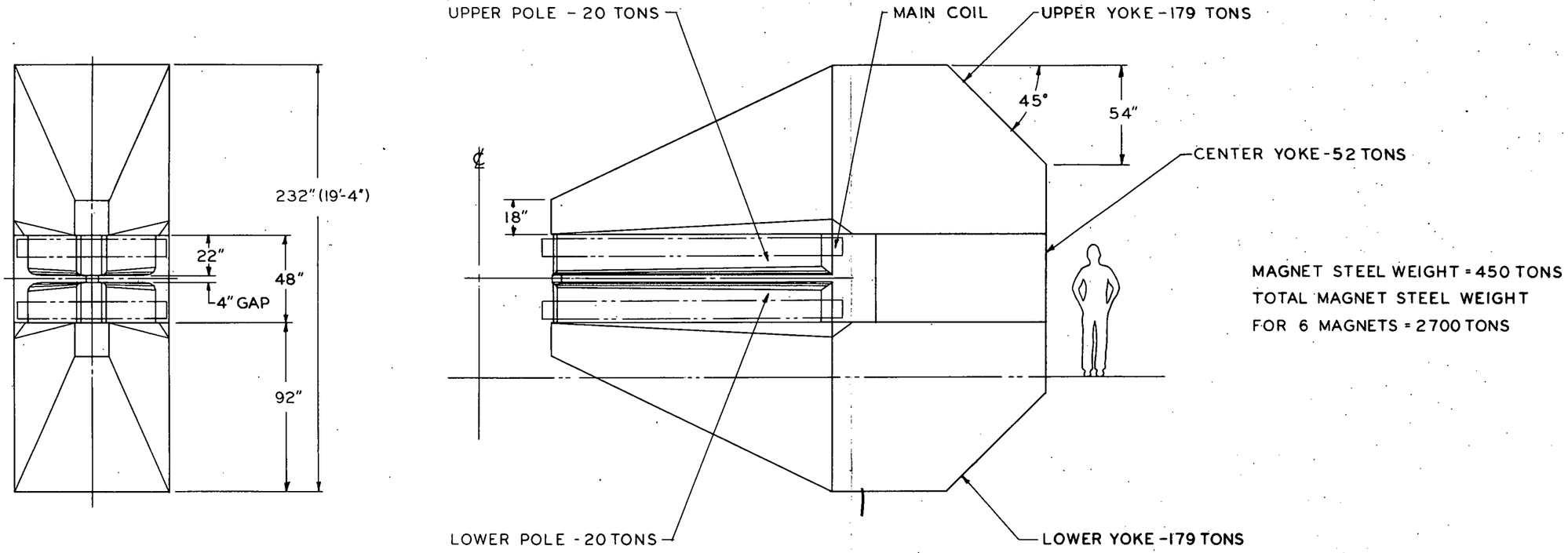

Fig. II. B-9: Proposed design for one magnet sector in the N = 6 cyclotron. The copper coils are suitable for B_{max} = 18 kG. Weight of steel in each magnet = 450 tons. Total weight of steel for six magnets = 2700 tons.

of the iron was chosen to be 4 in. This leaves a clear aperture of 2.5 in. for beam traversal.

b. Poles

The poles will be straight radial sectors, 20° in azimuthal width, 22 in. high, and extending from a radius of 40 to 195 in. The material will be 0.10% maximum carbon steel forgings, specially processed for homogeneity and high permeability. Each pole will weigh about 20 tons.

All pole faces will be machined flat to within 0.005 in. and parallel to within 0.010 in. The gap height of any one magnet will be within 0.010 in. of the average gap of all six magnets.

To minimize the mechanical deflection of the open C portion of the magnet, a nonmagnetic stainless steel spacer will be inserted between the two poles at the inner radius. The combined load will be about 1.3×10^{6} lb, primarily due to the magnetic attraction of the two poles and the atmospheric pressure on the evacuated chamber.

The radial edges of the poles will be contoured to minimize the change in the effective width of the azimuthal field with a change in field intensity. The desired theoretical contour is complex in shape but can be adequately approximated by three plane chamfers for easier and less expensive machining.

c. Upper and Lower Yokes

The upper and lower horizontal yoke members are sized to provide a flux density in the yokes of about 16 kG when the gap field is 18 kG; a 10% leakage factor has been estimated for the poles and 7% for the yokes. Total weight for each yoke is 179 tons.

Possible techniques of yoke construction have been studied to determine whether plate, forgings, or castings will offer the best quality magnet for the least cost. The quality of the iron, ease of

forming, handling and assembly, delivery time, and cost have been considered. Technical discussions were conducted with three independent steel companies and the spread in estimated cost among the three possibilities appears to be no greater than 10%. In any case, the material for the yokes will be a low-carbon steel with approximately the following analysis: carbon, 0.12% max.; manganese, 0.50%; phosphorus, 0.04%; sulphur, 0.04%; and silicon, 0.20%.

In the use of plate, the upper and lower yokes would be radially laminated with seven vertical plates. The faces of all plates would be rough machined to minimize possible gaps between laminations, and tie rods would clamp the assembly together. A flat surface would be machined on each laminated yoke, and accurate location of the poles would be achieved by use of half-and-half parting-line dowels and guide holes in mating pieces.

The main advantages of plate construction are: the basic price of steel is lower, the yoke can be laminated into pieces weighing less than 50 tons so that handling and shipping is easy, and the machining of the plates is relatively simple and can be accomplished at a high rate of metal removal with a resulting low cost per unit.

The principal disadvantages are the large number of surfaces that require machining, the need for tie rods and associated holes through the width of the yoke, and the large amount of material that is lost when developing the double taper in the yoke.

When considering either forgings or castings, the question of size must be considered. It has been found that a single piece weighing 179 tons is not a prime problem. Several of the steel manufacturers have the capabilities for making each yoke in one piece. Railroad cars are available that will carry these weights, and with proper routing these yokes can be shipped to Argonne by rail. Mobile cranes are available that can handle such a weight, so that unloading and erection at the site is quite feasible. Erection would be completed prior to the erection of the walls of the cyclotron vault.

Since the manufacturing, shipping, and erection can be readily accomplished for one-piece yoke construction, this is the preferred method.

With forgings, the yokes would be rough shaped on a flat, open die press; additional shaping would be done by flame cutting. The external surfaces would be finished to size by relatively rough machining techniques.

If cast, a pit mold would be used and the top surface would be the one to which the pole would be attached. The external surfaces of the yokes would require no additional machining. In cooling, the casting would be given the equivalent of an annealing cycle by controlled heating of the mold so that the unit would cool slowly over a period of several weeks. With proper casting techniques, the possibility of detrimental porosity is not considered a serious problem in view of the experience recently gained in casting the large pieces for the yoke of the Argonne 12-ft Hydrogen Bubble Chamber.

A final decision as to the preferred method of construction still requires further evaluation.

d. Center Yoke

The flux return between the top and bottom yokes is a 53-ton rectangular block of 0.12% maximum carbon steel, 92 in. × 85 in. × 48 in. high. Because of its simple shape, it could be made more economically as a forging than as a casting. The other possibility is to laminate it with vertical plates welded or bolted together.

The principal requirements for this center yoke are that its top and bottom surfaces be parallel, and that its height be equal to the sum of the two pole heights plus the magnet gap to within a very small tolerance.

e. Main Coils

The six sectors can be excited with conventional copper coils requiring about 1 MW of dc power to produce an 18-kG field, and 3.5 MW for 20 kG. (It is possible that instead of copper coils, superconducting coils will be used. The latter would require only 200 kW of refrigeration power to produce a 20-kG field. The superconducting coils are described in Sec. II·B5.)

Two coils are required for each magnet sector: 9.9×10^4 ampere-turns per pole, i.e., 60 turns and 1650 A. This is based upon an estimated effective flux leakage of 10% for the poles and 7% for the yokes. Each copper coil has a rectangular cross section measuring 5.6 in. wide × 9.4 in. high overall and consists of 5 two-layer pancakes of 0.921 in. square × 0.521 in. i.d. hollow conductor forming a single coil assembly that is 10 turns high × 6 turns wide. Conventional insulation of epoxy-impregnated fiberglass tape will be used.

The coils will be water cooled at a pressure of 125 psi. The temperature rise of the water will be 10°C for maximum power.

Excitation will be possible with a single silicon-controlled rectifier or transistorized type power supply providing a current regulation of $\Delta I/I \leq 1$ in 10^5 over a current range from $0.3\, I_{max}$ to I_{max}. The power supply will be programmed with fixed rise and fall rates dI/dt to achieve a predictable field-current relationship.

f. Trim Coils

Pole-face windings (i.e., trim coils) are located on the top or bottom surfaces of each pole. These coils are necessary to isochronize the magnetic field for a wide variety of ions and energies.

Ideally, the magnetic field within a magnet sector should be constant along each equilibrium orbit and should drop off to zero at the edges of the magnet where the ion would then follow a straight line trajectory. Since this is an impractical set of conditions because

fringing fields do exist at the edge of the magnet, reasonable compromises must be reached. First, on the basis of orbit calculations it has been decided that all the trim coils can be made as circular arcs centered on the mechanical center of the cyclotron rather than that each coil should describe an arc about an appropriate one of the many orbit centers. Second, there will be only one trim coil per 12 orbits. The radial width of each coil will be governed by the width of the orbit group.

The field for the 350-MeV protons is the most difficult to isochronize because its increase with radius (by a factor of 1.373) is greater than for any other projectile. A current gradient of about 120 ampere-turns/in. will be provided at the inner radius, increasing to 1080 ampere-turns/in. at the outer radius. This requires 32 trim-coil pairs per sector, at 900 A regulated to 1 part in 3×10^4. The power will then be 585 kW in the trim coils and 620 kW in the main coils.

Further magnet studies are required to optimize the combined use of iron and trim coils. For example, it is quite reasonable to plan that the gap should decrease and the field increase toward larger radii. The trim coils would then be used to superimpose a positive or negative gradient as the particle requires. This is one of the prime reasons for model-magnet studies; but the present design, although not optimized, is a reasonable one on which to establish feasibility and cost.

Several designs for the trim coils have been studied, taking into account the problems of insulation, accuracy of position, and the passage of 128 electrical leads per sector through the vacuum wall. At this time, it is believed that the best design will be one in which all the 32 trim coils on one pole are completely "canned" in a vacuum-tight, welded, nonmagnetic stainless steel jacket. One large conduit can then carry all 128 leads through the wall of the vacuum chamber. The jacket will be continuously rough pumped to reduce the effect of differential pressure. Such canning will minimize the problem of vacuum outgassing.

The trim coils on the face of a pole will be made up of wide flat copper conductors to which are brazed square hollow copper tubing that serves as input and output leads for both water and current.

The trim-coil straps will lie in grooves machined in a stainless steel base plate. Insulation capable of withstanding high temperature will permit welding on a cover plate and a radial conduit that contains the copper tubes. The total thickness of the package will be about $\frac{3}{4}$ in. This is small enough that the assembly can be attached to one of the poles when its mate is already in position on the other facing the same gap. This will then permit the removal or installation of the trim coils without disturbing the magnet poles or yoke.

Shunts will be used on the trim coils to correct a tilt in the median plane of a sector or a local variation of its azimuthal width.

g. Harmonic Coils

Harmonic coils can compensate the effects of certain mechanical and magnetic imperfections in the full-scale magnet.

A few of these errors are that: the gap of a sector magnet may be different from that of its mates, though uniform as a function of radius; the width of the azimuthal field of a sector may differ from that of other sectors; and the position of the magnetic median plane may be uniformly displaced.

On the basis of reasonable assumptions as to the size of such errors, it is calculated that one pair of harmonic coils per sector will suffice. Each member of a pair will consist of 75 turns of solid No. 8 square copper conductor wound around a pole, outside of the vacuum. At 20 A, there will be 3000 ampere-turns per sector, and the 550 W will be dissipated by proximity to the water-cooled main coils.

The harmonic coils will be connected in a 3-phase configuration such that a first-harmonic corrective field can be introduced at any

azimuth without altering the average field strength around the orbit. In addition, the current in each coil will be independently variable.

h. Adjustable Magnet Supports

The necessary symmetry of the magnetic field requires the sector magnets to be independently adjustable in azimuth, radius, height, and parallelism to the overall median plane of the cyclotron.

(i) Vertical adjustment. To raise or lower the individual magnets or to achieve a pitch or roll adjustment, each unit will be supported on two screw jacks at the outer radius and one at the inner radius. Mating spherical surfaces will be provided to allow a small amount of tilt before binding can occur in the screw jack. Driveshafts will be provided with brakes to lock the jacks in position.

(ii) Horizontal adjustment. For movements in azimuth, radius, or yaw, a means for moving each magnet in the horizontal plane will be provided. The plan being considered is a high-pressure oil film between flat bearing surfaces that will be machined into the support assemblies between the jacks and magnet. The central region of the plane bearings will be undercut to provide sufficient area to lift the weight of the magnet when an oil pressure of 1000 psi is applied. The hardened and ground mating surfaces around the periphery of the bearing will form a self-regulating orifice, maintaining only just enough pressure to float the load.

There will be x- and y-direction screws to translate horizontally one or both ends of the magnet on these oil-film bearings.

When the proper position is attained, the oil pressure will be removed, and the weight of the magnet will rest on the large area provided at the periphery of the bearing. The use of this large bearing area precludes the possibility of later settling of a magnet due to indentation or brinelling, such as might occur if balls or rollers were used to support the weight of the magnet.

i. Model Magnet

Magnetic measurements on a 1/5 scale model will have to precede the final design of the full-scale magnet. The model will have 3 sectors so that mutual effects will be present. Measurements will include precise determination of the soft-edge effect, properties of the trim coils, required edge-shaping of the poles, and the combined optimization of the iron and of trim coils to achieve efficient utilization of power.

5. Superconducting Coils for the Main Magnet

The use of superconducting coils to excite high-field magnets has recently emerged[1] as an attractive alternative to copper coils, both from the economic viewpoint and from the prospect of increasing the maximum useful field attainable with iron magnets. Both aspects reflect the fact that the field-generating current involves very little power loss; thus, higher fields may be usefully generated even when the permeability of the magnet iron is not large. Whereas the operating cost for ordinary copper coils is primarily due to the power lost by the magnet current, power for refrigeration dominates the operating cost of superconducting coils.

In view of the potential gains, it seemed appropriate to examine the application of this scheme to the six-sector cyclotron, comparing the merits of the traditional copper coil structure to the use of superconductors. The results of our preliminary investigation indicate that a completely stabilized superconductor coil holds certain advantages over its copper counterpart, not the least of which is its ability to raise the maximum useful magnetic field from 18 kG to 20 kG (and possibly higher), with a marked decrease in the power consumption.

The feasibility of operating the cyclotron at 20 kG has been examined. The most serious problem arises from the decrease in the permeability μ of the iron, particularly in regions of high flux concentration. The usual saturation of the poleface edge by fringing flux is controlled through shaping the edge to a surface of constant flux density (based on a 2-dimensional calculation with hydrodynamic analogy). Although azimuthal variation of the field shape is thereby expected to be made almost independent of flux density up to 20 kG, there will be somewhat more fringing field at this high field. However, since the 20 kG is used only for heavy ions, the softer field edge will have no

---

[1] John R. Purcell, "The Superconducting Magnet System for the 12-foot Bubble Chamber," Argonne National Laboratory Report ANL-HEP-6813, June 1968.

detrimental effect on the ion orbits. Although the decrease in μ will markedly affect the radial field variation, this is easily compensated with the 32 trim coils.

With the present cyclotron concept, increasing the maximum field to 20 kG would improve performance only for the heavy-ion beams. The trim coils will not carry enough power to adjust for proton isochronosm over a wider velocity range than the present design permits; further, the $\nu_z = 1$ resonance at a proton energy of 360 MeV is a barrier which may be difficult to cross.

In joining the output of the TU tandem to the input of the 6-sector cyclotron, the injection radius R_{min} is fixed by the maximum magnetic field B_{max} in the cyclotron and the TU terminal voltage V. For the accelerator design considered in this proposal, V = 16 MV, $B_{max} = 18$ kG, and $R_{min} = R^0_{min}$. It is not possible to increase the output energy by increasing B_{max} to 20 kG while keeping the same V and R_{min}, though some increase in intensity is possible. However, if B_{max} were increased to 20 kG, the maximum possible improvement in performance would require changes in V or R_{min} or both. Some possible ways of exploiting an increase to $B_{max} = 20$ kG are the following. (1) With a higher field, but the same cyclotron and TU design, the same maximum energy may be achieved with a lower charge state and hence with higher yield. Thus, increasing the field from 18 kG to 20 kG allows the use of uranium ion with charge 33+ rather than 37+, with a corresponding intensity increase of about a factor of 2.5. (2) If the TU-terminal voltage remains at 16 MV, but the inner radius is made smaller than R^0_{min}, then with the same charge state (37+) the output energy is increased by the factor 1.23. (3) If the TU terminal voltage is capable of going to 20 MV, and the same charge state is used, then the inner radius remains at R^0_{min} and the output energy is increased by the factor 1.23. (4) If the TU terminal voltage is capable of going to 20 MV, the foil stripper yields the 41+ uranium ion at the same intensity as the 37+ uranium ion from a 16-MV terminal. With the 41+ uranium ion, the

inner radius is smaller than R^0_{min}, and the output energy is increased by the factor 1.52.

If further design studies confirm the practicality of the 20-kG superconducting system, this may be the most suitable means for attaining the highest energies for the heavy-ion beams without increasing costs through increasing the size of the magnet, the rf system, and the building housing the accelerator. The total capital costs for a 20-kG superconducting system is estimated to be approximately the same as the costs for an 18-kG conventional coil system. However, the power costs for operating the copper system are estimated to be about $45 000 per year as against $25 000 for the superconducting system.* While it is technically feasible to design a 20-kG copper system, it is uneconomic since capital costs exceed those for either the 18-kG copper or 20-kG superconducting systems, while operating costs are considerably larger than either.

Although this is a large system for the use of superconducting coils, systems of approximately this magnitude have already been built.[1, 2] Furthermore, engineering experience and facilities for fabricating such coils exist at Argonne, in addition to considerable experience in large-scale handling of helium and other cryogenic liquids for cooling. Good coil designs may be made with materials and techniques now known. Moreover, the rate of development in this field is quite rapid, particularly in improved methods for manufacturing superconductor cables; one may expect that even better and cheaper conductors will be available when these coils are designed.

---

*For the copper system, these operating costs are primarily for the power dissipated in exciting the magnet and for cooling the magnet. Reasonable estimates of the particles and energies to be used and of the down time indicate a duty factor (fraction of maximum power dissipatable) of 50%. For the superconducting system, the costs are largely for refrigerating power but include the cost of liquid nitrogen and makeup helium. The cooling system is assumed to run 100% of the time.

[2] J. R. Purcell and A. Herve, "Test of the 12-foot HBC Magnet," Argonne National Laboratory Report ANL-BBC-133, February 1969.

Safe and reliable operation of large superconducting magnets have been achieved[2] by paralleling the superconductor with an appropriate amount of normal conductor (such as OFHC copper) to stabilize the superconductor. The copper provides a low-resistance electrical path around any part of a superconductor strip that, due to a flux jump, has made the transition from the superconducting to the resistive state. When the copper carries the full current around this resistive strip, the heat produced must be dissipated by the liquid helium without raising the system temperature by more than $0.5^{\circ}K$. The copper strips are made large enough to provide local cooling adequate to prevent local temperature rises with consequent propagation of normal (non-superconducting) regions.

A conceptual design of the superconducting coil has been made and it appears to be quite feasible. In this design, each of the six sector magnets has six pancakes containing 21 turns in each. Alternate pancakes are wound in opposite directions to allow close interconnections with vertical jumpers of stabilized superconductors. The necessary support structure has been evaluated through calculation of the vertical and radial forces on the coil with the TRIM computer program. A 20-V 1550-A power supply will be adequate; with this, the time to bring the magnet to full field would be 10 min. Except during the exciting period, the supply would operate at 1 V and the final field could be regulated by turning the supply on or off. Regulation of 1 in 10^5 or better is achievable.

Although the potential damage to superconductors from radiation needs consideration, the evidence now available indicates that this will not be a problem. In reactor experiments in which a Nb-Zr superconducting coil received a fast-neutron exposure far exceeding the expected exposure during the lifetime of the cyclotron, Benaroya _et al._[3] observed no deterioration in the coil properties. It is to be expected

---

[3] R. Benaroya, T. H. Blewitt, J. M. Brooks, and C. Laverick, "Effect of Fast Neutron Irradiation at Low Temperature on Nb-Zr Coil Performance," IEEE Trans. NS-14 (No. 3) 383 (1967).

from the solid-state physics of such superconductors that these results may be readily extrapolated to the Nb-Ti proposed for the magnet coils.

6. Radio-Frequency System

In the design of the rf system for the 6-sector cyclotron, several choices are available as to the number of main accelerating structures to be used. Considerations of orbit stability dictate that these should be placed symmetrically, so the number is limited to 2, 3, or 4. A three-dee (three-phase) system was chosen for the proposed design. It is superior to a two-dee system, because it offers a 50% greater energy gain per revolution. On the other hand, it is more flexible than a four-dee system, since three field-free sectors are left open for the placement of guide magnets and electrostatic deflectors for injection and extraction of the beam, or for installation of auxiliary dees for energy flat-topping.

The three-dee system has several other advantages over two dees. Its power efficiency is 1/3 greater than that of the conventional two-dee arrangement, because the voltage per dee can be less for the same energy gain per revolution. With less voltage on each dee, the distance required for voltage insulation can be smaller and the design-construction constraints will be less severe. In addition, the energy imparted to the ion per gap crossing is less; hence the amplitude of the induced coherent betatron oscillation is smaller, and thus the characteristics of the trajectories are more desirable.

These advantages of a three-dee structure far outweigh the problems introduced by the increased complexity of the three-phase system.

a. Frequency

The resonance (cyclotron) frequency of an ion is directly proportional to the average magnetic field existing over the orbit path. This field is lower than that of a conventional cyclotron, in which the magnet exerts its field over the full 360° of the orbit. Since only 120° of the orbit is occupied by the magnet sectors, the 18-kG maximum

field yields a 6-kG average field. Hence, the resonance frequency of the ion is much lower than that of a conventional cyclotron—e.g., 6.94 MHz for a 350-MeV proton. This has a very important effect upon the design of the rf system. Now, acceleration may be achieved by making the rf frequency on the dees equal to the cyclotron frequency or some multiple (harmonic) of it—e.g., with the 6.94-MHz cyclotron frequency, the rf frequency may be 6.94 or 13.88 or 20.82 MHz, etc. At the fundamental value (6.94 MHz), the size of a resonant structure is uncomfortably large (about 10.7 m long for a quarter-wavelength resonator); but with harmonic acceleration, the dimensions of the structure can be reduced to a practical size.

It is proposed in our design that harmonic acceleration be used for both the light and heavy ions. This requires that for each ion, the ratio of the rf radian frequency ω_{rf} to cyclotron radian frequency ω_{ion} be an integer equal to or greater than 1. That is, $\omega_{rf}/\omega_{ion} = h = 1, 2, 3$, etc. We have chosen the highest available rf frequency to be 22 MHz (20.82 MHz actually required); the corresponding harmonic acceleration number h is 3 for a 350-MeV proton. To allow acceleration of other light ions and to provide for varying the energy, the frequency will be continuously variable from 22 to 13.8 MHz with a single resonator length. With this range in rf frequency, protons can be accelerated in the h = 3 mode over the range from 350 to about 115 MeV; for lower energies (to 50 MeV), the h = 5 mode will be used.

Since resonance frequencies are very low for heavy ions (e.g., 1.52 MHz for $^{238}U^{38+}$), the harmonic number must be large ($h \geq 10$) unless the resonant structure is lengthened. Provision is made to decrease the lower limit for rf frequency to values less than 13.8 MHz by opening a fixed electrical short (without breaking the vacuum), thereby increasing the length of the resonant structure; the lowest frequency will then be about 9 MHz, and the upper value 14 MHz. With this system, a $^{238}U^{38+}$ ion can be accelerated in the h = 6 mode to an energy of about 10.6 MeV/A. For variable-energy operation, the harmonic number will

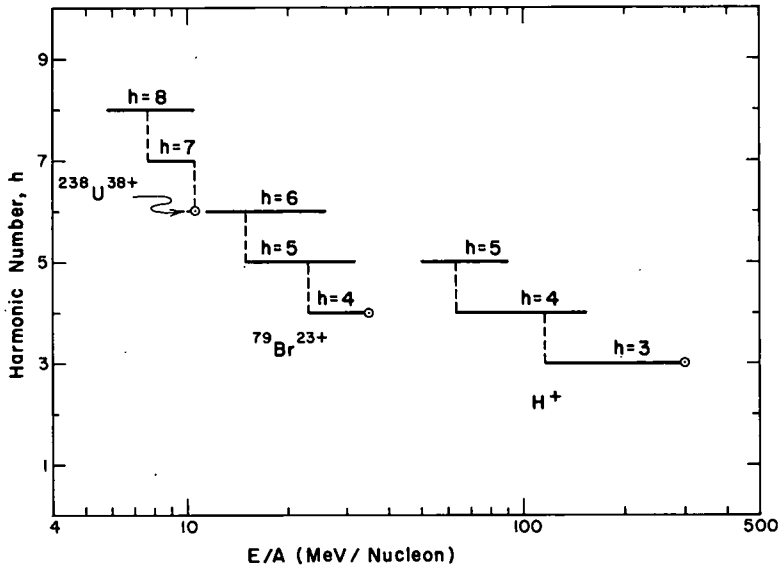

Fig. II. B-10. Harmonic numbers for several typical ion beams. The harmonic number h is the number of rf cycles for each complete orbit of the ion. For a given accelerated ion, h can be made smaller at higher energies.

have to be increased up to 8 for energies as low as 6 MeV/A. For a lighter ion, such as $^{79}Br^{25+}$, an energy of 34.7 MeV/A can be reached on the h = 4 mode.

If the size of the rf structure is increased further, even lower harmonic numbers could be used, and there would be an attendant relaxation of the magnetic-field tolerances. Such a possibility has been considered, but calculations show that if the 9—14-MHz frequency range (h = 6—10) is used, it will be no more difficult to achieve the required tolerances in the isochronous magnetic field for accelerating heavy ions than to come within the field tolerances for accelerating protons to 350 MeV (h = 3). Hence, we believe the proposed structure is adequately large, and any further size increase would entail unnecessary costs.

Figure II. B-10 relates harmonic number to the energy per nucleon (MeV/A) for protons, bromine, and uranium ions.

b. RF Generation and Control

Figure II. B-11 illustrates the tentative design of the system for the generation and control of the dee voltages. The primary rf signal is generated from a precision variable-frequency oscillator

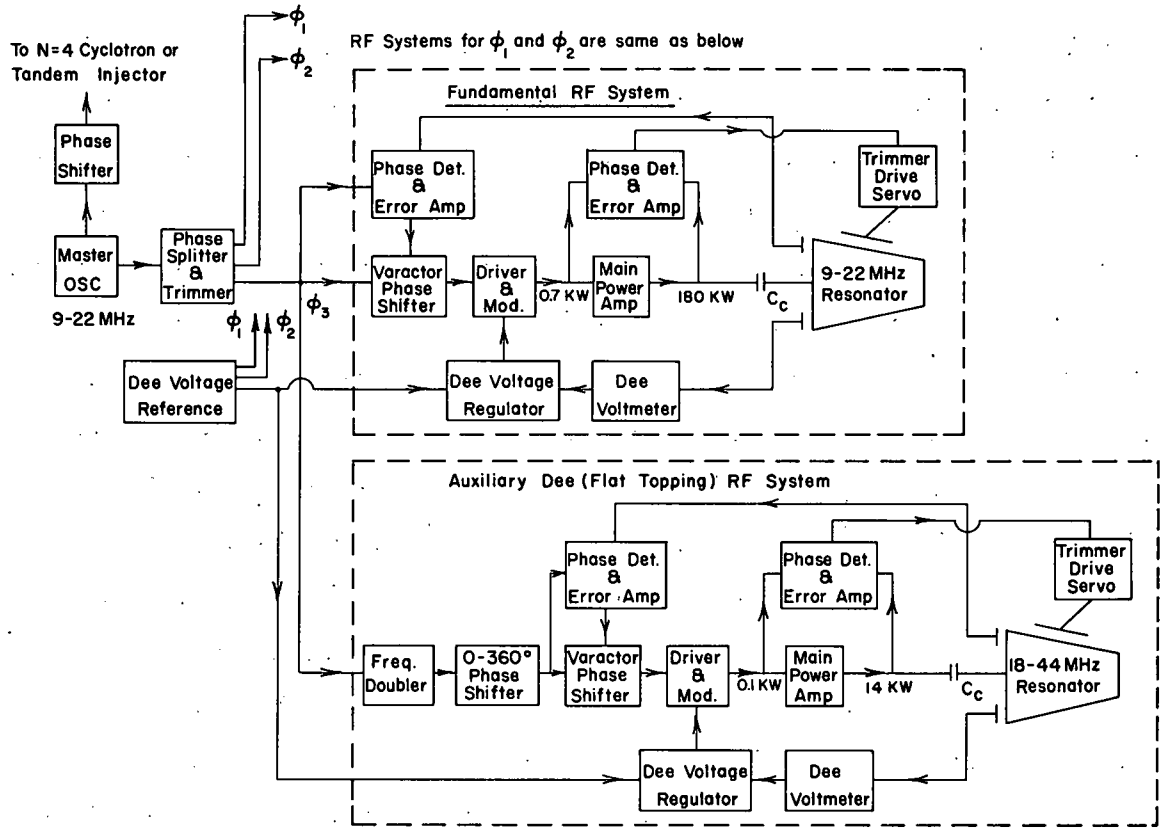

Fig. II. B-11. Block diagram of the rf generator system.

(direct-type frequency synthesizer[1]) capable of providing a stability in frequency of 1 in 10^8, phase stability to 0.018° rms, and a signal-amplitude stability of about 4 in 10^5 throughout the operating range (9—22 MHz). These stabilities are comfortably better than the bare requirements for successful operation.

The oscillator signal is coupled into a wide-band (1 octave) passive phase splitter,[2] from which the 3-phase rf voltage signals are obtained. Each of these voltages is amplified by an identical amplifier chain, and is then capacitively coupled into the dee resonator. Each chain contains two amplifiers, the first of which functions as both a low-level amplifier (0.7 kW output) and a modulator (dee-voltage

[1] Fluke Model 644A or equivalent.

[2] Merrimac Research and Development, Inc., 41 Fairfield Place, West Caldwell, New Jersey.

regulator loop); the second is the main power amplifier. The latter contains one amplification stage which uses an RCA A2872A tetrode, capable of delivering 250 kW of rf power. It is conservatively operated even at the maximum calculated (9 MHz) rf power level of 180 kW.

The calculated total power dissipation for each main dee, including copper losses, beam loading, and efficiency of power conversion, is 300 kW at 9 MHz—i. e., a total (3 dees) power-line load of about 900 kW. This has been calculated on the assumption of a 250-kV dee-to-ground voltage; and it is quite possible that upon completion of model studies and further orbit calculations, this requirement will be reduced to about 600 kW. At 21 MHz, this load decreases to 350 kW. For a large cyclotron, these power requirements are surprisingly small. This can be attributed to the use of the 3-dee system, the half-wave ($\lambda/2$) resonator design instead of $\lambda/4$, and the low dee-to-ground capacitance (large vertical dee-to-ground distances) that is inherent in an open-sector cyclotron.

For electrical and mechanical simplicity, each of the three final amplifier tetrodes is located at the outer radius of the accelerator chamber with its output capacitively coupled to the dee resonator. This placement eliminates the need for both a tuned, high-power, matching network and a transmission line.

Each dee system has three feedback loops: (a) to control the resonant frequency of the structure, (b) to stabilize the amplitude of the voltage, and (c) to control the relative phase of its voltage with respect to the other dee voltages.

To obtain maximum voltage on a dee with minimum expenditure of power, the resonant frequency of the complete dee structure must be identical with the oscillator frequency. The control to bring this about operates through the phase detector, which senses the phase shift between grid and plate voltages of the power-amplifier tube (RCA A2872A). The error signal, amplified by the error amplifier, causes mechanical motion of the resonator tuner plates. This is a servo-loop

with slow response, but serves to correct for small mechanical variations in the resonator, such as those arising from thermal effects.

Conventional circuit techniques serve to stabilize the amplitude of the dee voltage. The voltage on each dee is sampled by four pickup capacitors,[3] two located above the dee and two below. Each signal is rectified, and the sum is compared with a reference voltage; to a first approximation, the resultant voltage is independent of changes in the dee position. The error signal, amplified by the dee voltage regulator, will modulate the grid bias of the low-level power amplifier. To aid in achieving an amplitude stability of 1 in 10^4, it is planned that the ripple voltage of the main-amplifier power supply be less than 0.5% and that the amplifier filaments be heated by direct current.

Good energy resolution in the output ion beam requires accurate control of the relative phases between dee voltages. The dee-phase regulator loop will provide phase stability for the most stringent operating conditions. When no energy flat-topping is used, an energy spread $\Delta E/E$ of 1 in 10^3 requires a phase stability of 2.5°; for $\Delta E/E = 1/10^4$, the required phase stability is about 0.25°. With flat-topping, the phase stability of the fundamental voltages is much less important, but the phase between the main and auxiliary voltages must be controlled; $\Delta E/E = 1/10^3$ requires 1.6° stability, while $\Delta E/E = 1/10^4$ requires control to 0.16°.

For harmonic operation with the 3-phase system, phase relations are programmed as follows: For h = 3, 6, 9, · · ·, the dees are operated in phase; for h = 1, 4, 7, · · ·, the dee voltages are in the 3-phase (120°) orientation, rotating in the direction of ion motion; for h = 2, 5, 8, · · ·, the direction of rotation of the voltage vectors is opposite to that of ion motion.

The energy gain per revolution is a function of dee voltage, ion charge, transit time, the value of h, and the sector width. Even with

[3] W. Ramler and G. Parker, The Argonne 60-Inch Cyclotron, Argonne National Laboratory Report ANL-5907, pp. 13—14 (1959).

fixed voltage, the energy gain varies with the h mode. Thus, if V is the voltage between dee and ground and Z is the charge state of the ion, then the approximate energy gain per turn is 4.2 VZ for h = 3, increases to 5.8 VZ for h = 6, and gradually decreases to 2.8 VZ for h = 10; 6 VZ is the maximum attainable.

To ensure that each ion has almost the same acceleration per revolution, the energy gain per turn is "flat-topped" by applying a lower voltage on auxiliary dees that operate at twice the frequency of the main rf system. The combination, with suitably controlled relative voltages and phases, can (within limits) provide almost the same acceleration for any ion in the injected bunch—regardless of its phase. The circuitry and control for the auxiliary dees are similar to those of the main set (shown in Fig. II. B-11), but it operates at a lower power.

Each dee system, main and auxiliary, is designed to resonate in the half-wave ($\lambda/2$) mode. The resonant coaxial system consists of an inner conductor (a "dee") operating inside the outer conductors formed by "liners" lining the magnet pole and vacuum chamber and the cylindrical resonator tanks. The dee is made up of two parts: the "dee head" which forms the accelerating gaps and the "dee stem" which extends vertically from the dee head into the resonator tank.

In plan view, the shape of a main dee head is trapezoidal, almost $11\frac{1}{2}$ ft long radially and almost 8 ft wide at the large end. It has a vertical gap height of $2\frac{1}{4}$ in. Structurally, it will consist of a framework of longitudinal stringers and transverse ribs to which will be brazed a high-conductivity copper skin $\frac{1}{8}$ in. thick. The skin will be water cooled to prevent thermal distortion due to resistive heating.

The stem of the main dee is a 15-in.-diameter copper tube. It is surrounded by the resonator tank, 35-in. inside diameter, made of copper-clad mild steel, the steel serving as the wall of the vacuum chamber. Two resonators (i.e., tuning stubs) are required for each dee head and extend above and below the dee heads. These form a $\lambda/2$ resonator and add mechanical rigidity to the entire structure.

(A plan view is shown in Fig. II. B-8 and a cross section in Fig. II. B-12.) The height of each resonator tank is almost 8 ft, referenced to the midplane of the cyclotron. The flat-topping structure is smaller and its maximum vertical extension is 6 ft on each side of the midplane.

A frequency range of 9—22 MHz is required for the resonant frequency of the main dee system and a range of 18—44 MHz for the auxiliary dee structure. On a main dee, this frequency variation is achieved in two steps by use of a combination of large capacitive tuning panels facing the upper and lower surfaces of the dee head and an annular short between the dee stem and resonator tank. With the short closed at a position about 27 in. from the dee head, tuner movement will vary the frequency from 13.8 to 22 MHz. With the short open, the length of the resonator is increased and the tuner variation yields a 9—14-MHz range. With an auxiliary dee, the frequency will probably be varied by the combined effect of a moving short and tuners.

Even though it has been stated that the auxiliary dees will be located in the open sectors, considerable thought must still be given to the problem of determining the relative merits of this arrangement and one in which an auxiliary dee "nests" within a main dee. At this time, we prefer to have the two dees mechanically independent because of the lessened mechanical and electrical complexity.

The final choice of the configuration of the dee structure will determine the design of the particle-injection system. The system described in Sec. II. B8 assumes that the dees are nested and that the injection path is through one of the unused valleys. If the main and auxiliary dees are independent, however, all of the valleys are occupied, and the injection transport line might have to be carried over or under the magnet or rf structure. In this case, the details of the injection system would be different, but the basic approach outlined in Sec. II. B8 is still applicable.

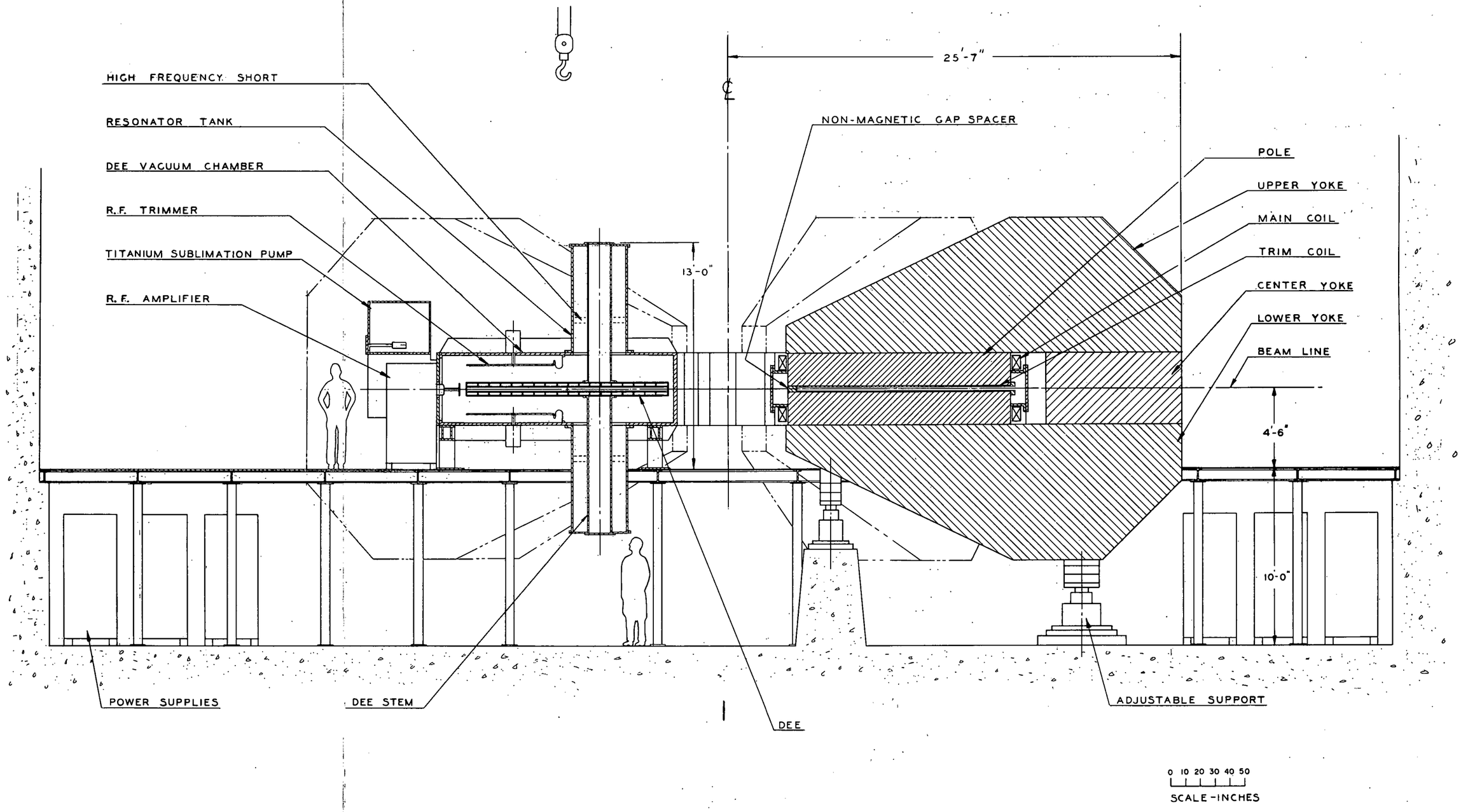

Fig. II. B-12. Sectional view of magnet, rf feedthroughs, and accelerating dee structures in the N = 6 machine.

c. Summary of RF Parameters of the N = 6 Cyclotron

(i) Main dees, number	3
Resonance mode	$\lambda/2$
Azimuthal width	30°
Maximum voltage	250 kV
Frequency range	(a) 22—13.8 MHz
	(b) 14—9 MHz
Frequency tuning	Tuners and short (open or closed)
Maximum total power (60 Hz)	900 kW
(ii) Auxiliary dees, number	3
Resonance mode	$\lambda/2$
Location	Probably mechanically separated from the main dees
Azimuthal width	15°
Maximum voltage	80 kV
Frequency range	44—18 MHz
Frequency tuning	Tuners and movable short
Maximum total power (60 Hz)	~100 kW
(iii) Dee voltage regulation	Design aim, 1 in 10^4
(iv) RF phase control	Design aim, 0.16°

7. Vacuum

In this section we examine both the degree of heavy-ion beam attenuation due to inelastic collisions of ions with residual gas molecules and the vacuum hardware necessary to provide operating pressure low enough to minimize such losses.

a. Beam Attenuation

Producing beams of highly charged and energetic ions (e.g., I^{25+} and U^{38+}) with adequate intensities requires that these beams pass through the MTC with minimum attenuation. Ions are lost as a result of their inelastic collisions with residual gas molecules in the several vacuum chambers of the accelerator. The gain or loss of one or more electrons in an inelastic encounter changes the charge state of the ion, which then is no longer in phase with the radio-frequency accelerating voltage and will be deflected to the wall and lost. Because the cross sections for electron capture or loss are often large, and because the ion trajectories in the cyclotron are long, the cyclotron's transmission efficiency (the fraction of ions in the initial beam that traverse the entire machine) may be critically affected by the vacuum attained.[1] Hence the great importance of the vacuum-system design.

The transmission efficiency can be calculated from the path length in the accelerator, the residual-gas concentration, and the cross sections for capture and loss of an electron. To simplify the calculation, the residual gas is assumed to be air, even though the vapor in a vacuum-tight machine would consist mostly of hydrogen, water, carbon monoxide, and hydrocarbons; the charge-exchange cross sections are roughly the same for all these gases except H_2. Estimated weighted average cross sections for the sum of capture and loss of electrons by U^{38+} and I^{25+} are 18×10^{-17} and 2×10^{-17}

---

[1] S. Wexler, Transmission of Highly Charged MeV-Xe and Kr Ions Through Proposed Argonne HIVEC, informal report, Argonne National Laboratory, Argonne, Illinois, June 1966.

cm^2/molecule, respectively.[2] The cross sections used are for collisions in which a single electron is transferred; multiple transfer will occur with lower cross sections.[3]

With these cross sections, the calculated particle transmission through the cyclotron for an average operating pressure of 1×10^{-7} Torr is 82% for U^{38+} and 98% for I^{25+}. In the beam transport system from the tandem to the cyclotron, vacuum requirements are somewhat less stringent, namely 3×10^{-7} Torr for almost 100% particle transmission. Since ion velocities are greater in the high-energy beam-transport system beyond the cyclotron, the pressure in this region need not be less than 10^{-6} Torr.

For light ions, the vacuum requirements throughout the system are very much less rigorous—approximately 10^{-6} Torr.

b. Vacuum System

For the heavy ions to be produced in the MTC, cyclotron transmissions exceeding 80% require that the gas pressure be $\lesssim 1 \times 10^{-7}$ Torr. Such a pressure is less than has been commonly used in cyclotrons designed for light and medium-heavy ion beams. Nevertheless, vacuum technology has been so developed as to make routine operation at 10^{-7} Torr a realistic goal. Further, the open-sector design of the cyclotron mitigates the vacuum problems of the ordinary cyclotron in two very important respects. First, the ion source of the MTC is not in the cyclotron, which is therefore free from this source of heavy gas load. Indeed, the gas load is solely that due to outgassing from the surfaces of the system and the inevitable minute in-leaks. The second advantage is that large pumping conductances are achievable, since each open sector can accommodate a pumping manifold for the gap in the adjacent magnet sectors. Such freedom permits the attachment of

[2] H. D. Betz and C. Schmelzer, Charge Exchange Cross Sections of Fast Heavy Ions (Institut f. Angew. Physik der Univ. Heidelberg, 1967), UNILAC Ber. Nr. 1-67.

[3] See for example, B. Franzke, N. Angert, A. Møller, and Ch. Schmelzer, Phys. Letters 25A, 769 (1967).

pumps close to the acceleration region, with a resulting efficient utilization of pumping speed. In the vacuum system design, the volume of each gap is pumped from both sides, the pumping speed within the gap being limited only by the gap conductance.

(i) Gas load. The total volume of the cyclotron vacuum chamber is 71×10^3 liters; its gas load is largely due to outgassing (Table II-B-II).

TABLE II-B-II. Outgassing load.

	Surface area (m^2)	Outgassing rates (Torr liter m^{-2} sec^{-1})
Copper	460	1.5×10^{-5}
Stainless steel	285	1×10^{-5}
Mild steel	80	2.1×10^{-5}

The listed outgassing rates are reasonable values attainable with moderate care in construction and handling.[4-7] The computed total gas load of the system is 2.2×10^{-2} Torr-liter/sec; this includes a very conservatively estimated in-leak rate and gasket-outgassing load of 1×10^{-2} Torr-liter/sec.

(ii) Pumps and instrumentation. Only when heavy-ion beams are being used is it required that the pressure be as low as 10^{-7} Torr. When light ions are accelerated, the vacuum specifications

[4] N. T. M. Dennis and T. A. Heppell, Vacuum System Design (Chapman and Hall, Ltd., London, 1968).

[5] E. Hoyt, SLAC Report TN-64-5 (1964).

[6] H. Diels and R. Jaeckel, Leybold Vacuum Handbook (Pergamon Press, New York, 1966).

[7] N. Milleron, Lawrence Radiation Laboratory Report UCRL-1729 (1967).

may be considerably relaxed. To take care of the two levels of vacuum requirement, the pumping system is planned to operate in a dual mode—achieved through the use of three 35-in. oil diffusion pumps and three titanium sublimation pumps and liquid-nitrogen-cooled cryopanels. The diffusion pumps with baffle-valve combinations by themselves provide a net pumping speed of 75 000 liter/sec and an operating vacuum of about $2-3 \times 10^{-6}$ Torr. To achieve the 10^{-7} Torr operation, the sublimation pumps will be required to add an additional pumping speed of 140 000 liter/sec. It is estimated that the titanium sublimation rate will be 0.75 g/hr and the operating time per charge of titanium will be about 3000 hr. Use of the sublimation pumps will be necessary only when heavy ions are accelerated.

The three diffusion pumps will be backed by a commonly-used 1600-cfm Roots blower pump, in turn backed by a 500-cfm fore-pump. Compared to the use of one mechanical pump per diffusion pump, this design provides a more economical arrangement, and also yields lower fore-pressures, as well as a faster recovery from gas bursts occurring in the acceleration chamber.

Figure II·B-13 is a schematic diagram of the vacuum system.

Instrumentation for the entire system will include a read-out device (with an automatic range-changing mechanism) and a parallel servo-loop to control the sublimation rate of each of the titanium pumps. Vacuum protection and isolation valves will be provided, along with a display map that will function as a control point for the pumps, valves, and the readout of system data.

(iii) Improved vacuum. Present-day experience indicates that the 10^{-7} Torr pressure will be attainable through the use of Viton O rings, extensive use of minimum outgassing material (stainless steel), careful surface treatment, and preliminary baking. Should future experiments or calculations on the charge-exchange cross sections indicate the necessity for reducing the operating pressure below 10^{-7} Torr, such

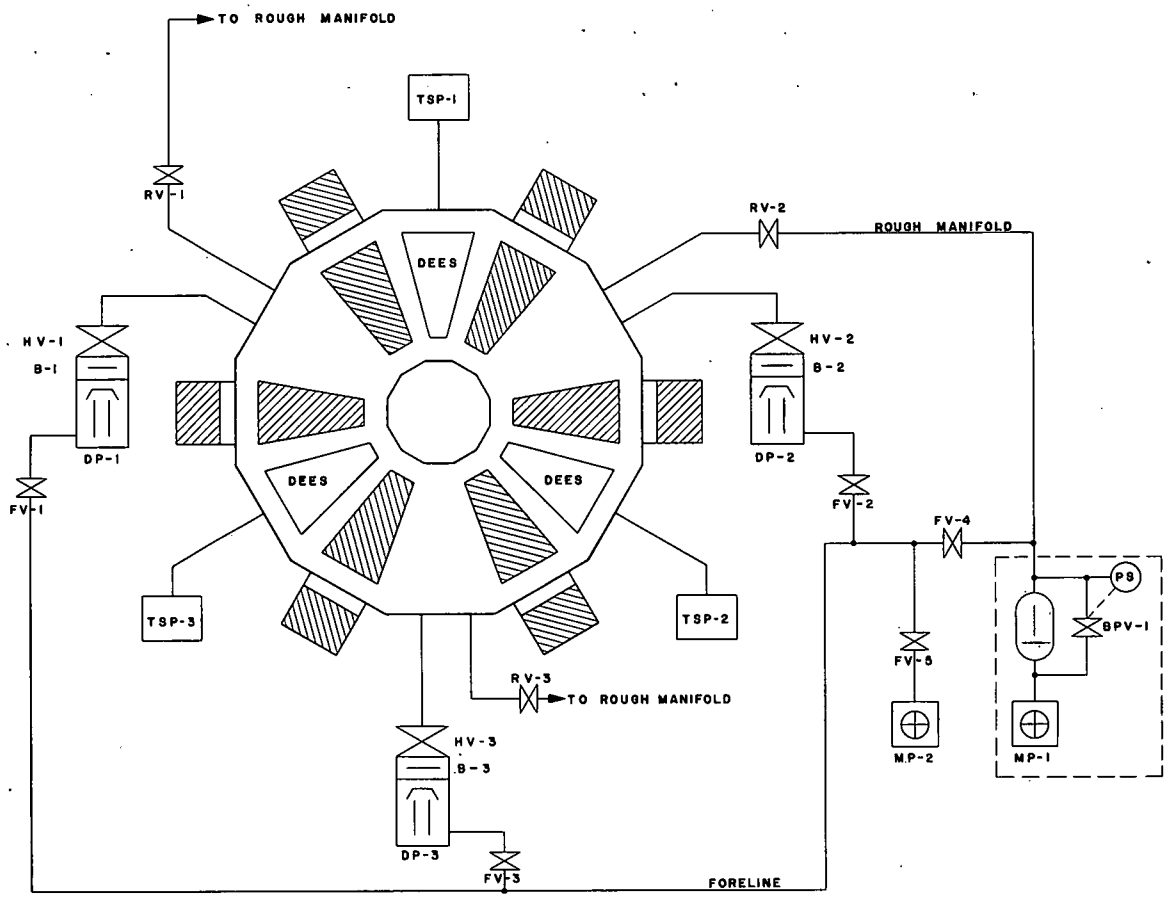

Fig. II·B-13. Block diagram showing the pumping and valving of the vacuum system. Tank pressure = 1×10^{-7} Torr, tank volume = 71 000 liters. Internal surface areas: copper 460 m^2, stainless steel 285 m^2, mild steel 82 m^2. The pumping equipment is as follows:

DP-1, 2, 3:	Oil diffusion pump, 35-in.
B-1, 2, 3:	Baffle, cryogenic, 35-in.
HV-1, 2, 3:	Valve, Hivac, 90°, 35-in.
FV-1, 2, 3:	Valve, foreline, 6-in.
FV-4:	Valve, main foreline, 8-in.
FV-5:	Valve, holding pump, 3-in.
TSP-1, 2, 3:	Titanium sublimation pump with cryopanels
RV-1, 2, 3:	Valve, rough, 6-in.
BPV-1:	By-pass valve: 6-in.
MP-1:	Fore-rough pump, 1600/500 cfm blower
MP-2:	Holding pump, 100 cfm

can be achieved through: (a) greatly reducing in-leakage through use of double O rings plus pumpout of intermediate space, (b) pre-baking of O rings, (c) increased use of welded joints, (d) use of additional liquid-nitrogen cryopanels or additional sublimation pumps in the drift sections, and (e) built-in provisions for supplying heat for degassing internal surfaces.

c. Vacuum Chambers

The system of vacuum chambers that encloses the magnet pole gaps and the dees in an envelope to be pumped down to 10^{-7} Torr must (a) facilitate original assembly of all components of the cyclotron, (b) allow access for maintenance or modification with a minimum of disassembly, (c) allow for small motions of the individual magnets when these are being initially aligned or subsequently realigned, and (d) present a low gas load to the system.

As presently conceived, the complete vacuum-chamber assembly contains three types of chamber segments: pole chambers, dee chambers, and open (drift) chambers. These are shown in plan view in Fig. II·B-13. The pole and dee chambers have been shown in vertical section in Fig. II·B-11 and the drift chamber is shown in section in Fig. II·B-14.

(i) Pole chamber. The poles are an integral part of the pole chamber, thus taking advantage of the strength and rigidity of the pole and yoke in resisting magnetic forces and atmospheric pressure. Trapezoidal nonmagnetic stainless steel plates will be welded to the poles about 8 in. from the pole face. Around the periphery of these horizontal plates, vertical flanges will be welded which mate with the adjacent chambers and with covers on the inner and outer ends. These plates are located so that the main magnet coils (conventional or cryogenic) are outside the vacuum envelope, thus greatly reducing the pumping requirements.

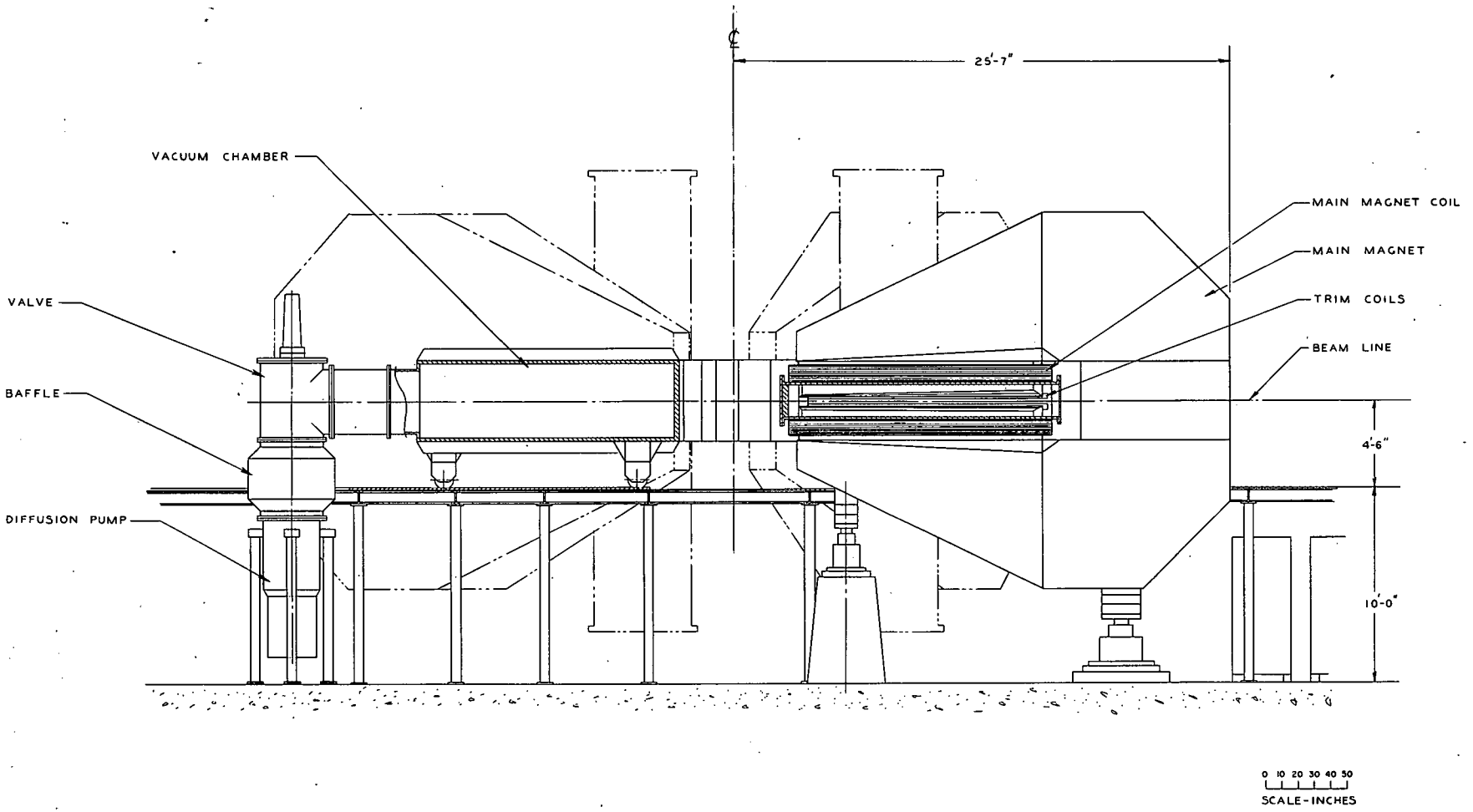

Fig. II. B-14. Sectional view of the drift section of the vacuum chamber and its associated pumping system.

At the four corners of the trapezoid, vertical corner posts will be inserted between the top and bottom plates. These removable corner posts will utilize the novel three-surface O-ring seal used on the Philips AVF cyclotron,[8] and later (with modifications) on the Harwell[9] and Texas A & M[10] variable-energy cyclotrons. The side cover plates of the chamber will be attached to these corner posts.

(ii) Dee chambers. Each complete dee structure assembly will be located in a wedge-shaped chamber. These chambers must not only resist the forces due to atmospheric pressure, but must also provide a mounting for the resonator tanks and a rigid support for the dees.

Another major design requirement is that of a sealing arrangement which will allow the position of a main magnet to be adjusted in any of its six degrees of freedom, and yet allow it to be sealed to the stationary adjacent chambers. One such design involves the use of large rectangular picture-frame flanges on the two radial sides of the chamber. These flanges would be attached to the chamber with a V-shaped flexible stainless steel element, much like a single convolution of a welded bellows. The bellows would accommodate adjustments required for an adjacent magnet in roll or yaw, a slight amount of pitch, and in radial or tangential translations. Vertical and radial translations are also allowed through enlarged clearance holes around the flange screws. The weight of the loose flange would be supported on several pins extending from fixed supports on the chamber into loose-fitting holes in the movable flange. Screws or a mechanism hold the flanges in a retracted position during assembly, or when major magnet adjustments are made.

---

[8] N. F. Verster, H. L. Hagedoorn, J. Zwanenburg, A. J. J. Franken, and J. Geel, "Some Design Features of the Philips AVF Prototype," Nucl. Instr. Methods 88, 18 (1962).

[9] J. D. Lawson, The Harwell Variable Energy Cyclotron, NIRL/R/85 (1965).

[10] W. A. McFarlin and D. J. Goerz, Jr., "Unique Features of the Texas A & M Variable Energy Cyclotron," in Proceedings of the 1966 International Isochronous Cyclotron Conference, Gatlinburg, Tennessee.

The titanium sublimation pumps are located on the outer radius of the dee chamber, with ducts to the chamber straddling the rf amplifier housing. The pump chamber is lined with liquid-nitrogen-cooled cryo-panels upon which the evaporated titanium condenses, providing the dual pumping action of gettering and cryosorption.

(iii) Drift chambers. The drift chambers are located in the three spaces (between magnets) that do not contain dees. These are very similar in construction to the dee chambers. The injection beam line will enter through one chamber, and the extracted beam will exit through another. A 35-in. oil diffusion pump with its valve-baffle combination will be connected via a nonmagnetic duct to the rear of each chamber. This placement removes these magnetic components from the vicinity of the main guide field and eliminates the necessity for providing nonmagnetic pumps and associated hardware.

For operational convenience, these chambers are mounted on wheels, so that they may be rolled radially outwards to provide open access to the magnet gap and trim coils for maintenance or later internal modifications.

Since these chambers are free of dees, liners, or other internal structures, they may also be used for inserting beam probes and other diagnostic equipment.

d. Beam-Transport System

The vacuum requirements for the beam-transport system are modest, but must not be overlooked. For the injection side of the main cyclotron, a vacuum of 3×10^{-7} Torr limits charge-exchange losses to a few percent or less (almost 100% transmission). For the final beam-transport paths, a vacuum of about 5×10^{-6} Torr suffices.

The pumping on the injection side will be by turbo-molecular pumps. Experience at ANL has demonstrated the ability of such equipment to achieve 10^{-7} Torr in beam tubes. With reasonable care in both

design and construction techniques, such a vacuum is not difficult to maintain. The less stringent requirements for the remainder of the system will be achieved with internally-baffled oil diffusion pumps.

8. Injection into and Extraction from the N = 6 Cyclotron

a. Injection

After entering the main cyclotron vault the beam transport line from the N = 4 injector cyclotron will consist of (in order of traversal) two conventional sector magnets bending in opposite directions with a reversing quadrupole set between them, followed by a sector magnet, a current-sheet septum magnet, and an electrostatic deflector which is mounted in the gap of one of the magnets of the large cyclotron, as seen in Fig. II·D-2. This system can be adjusted to give isochronous injection of light ions.

When the TU is used as the injector, the first three elements are inoperative. The remaining system is almost isochronous, as discussed in Sec. II·D, but not completely so. For a beam with a radial divergence which seems reasonable to expect from the stripped tandem beam, the path difference for the most widely divergent rays is calculated to be 0.1 cm. In the case of a slow uranium ion, this corresponds to a time spread of approximately 0.1 nsec. This is to be compared with an injection pulse width of 0.5 nsec in the most stringent case, so this value is quite tolerable.

In preliminary estimates of the electric field $\mathcal{E}$ needed to deflect the incident particles, the magnetic field B is assumed to be constant in the neighborhood of the deflected path. Then the radius of curvature due to the combined field is

$$\rho' = \frac{\rho}{1 + (\mathcal{E}/300\ B\beta)} ,$$

where ρ is the radius in the field B (kG) only, $\mathcal{E}$ is in kV/cm, and $\beta = v/c$ is the particle velocity relative to the speed of light.

For the proposed injection system, the greatest value of $B\beta$ encountered is 2.26, the value for protons with an ultimate energy of 350 MeV. For $\mathcal{E}$ = 100 kV/cm, we find $\rho' = 0.87\ \rho$ for these

particles—the most difficult ones to deflect; and a scale drawing shows that this radius will leave adequate room for insertion of the septum magnet.

The septum magnet and the conventional magnets that form the rest of the injection chain must have fields and radii of curvature suitable for the injected ion of greatest rigidity—namely for U^{238}, for which the required value of $B\rho$ would be as large as 290 kG-in. The limited open space at the center of the N = 6 machine and the need for the injected beam to enter through a valley that is unencumbered by a dee (if the auxiliary dees lie inside the main dees) require that the bending radii of these magnets be no more than about 16 in., and hence their maximum fields must be ~18 kG. This is not excessive, since the gap heights can be very small.

It may be found impractical to nest the auxiliary dees (needed for flat-topping) inside the main dees. If so, the auxiliary and main dees will occupy all six valleys and the injection transport line will be carried over or under the N = 6 magnet or dee structure.

b. Position of the Second Stripper

When the beam from the TU tandem is to be used directly, it is switched into the selected target room by a 90° deflecting magnet. For heavy ions (which, after only one stripping, are in relatively low charge states), the required deflecting field would be unreasonably high; for example, 96-MeV U^{5+} ions from the TU would have the prohibitive rigidity of 1713 kG-in. Thus the second stripper must be placed upstream from the deflecting magnet.

But when the TU is used as an injector for the N = 6 cyclotron, the second stripping must be delayed as long as possible. Stripping will introduce a spread in energy; and if a long path were to follow (e.g., the 100-ft interval between TU and cyclotron), then the ion bunch would grow in length and in time duration. Consequently it would spread

in phase at the dee-gap traversals and its energy homogeneity at extraction would be degraded. We plan, therefore, to place the second stripper close to the focal point of one of the quadrupole triplets near the periphery of the N = 6 machine, prior to passage through any of the injection magnets. The angular scattering in the foil will then be small compared to the divergence of the beam as a whole.

Calculations show that quadrupoles of reasonable length and field gradient can control the beam after it has been stripped only by the gas stripper in the TU terminal.

Downstream from the second stripper, unwanted charge states will be rejected in the first of the magnets used for injection into the N = 6 cyclotron.

c. Extraction

In a purely isochronous field, the current filament in each of the two final orbits for 350-MeV protons will be 4 mm in diameter so the two distributions will just be in contact. The orbit separation to enable the beam to clear the septum of an electrostatic deflector can be obtained either by controlled use of the $\nu_x = \frac{3}{2}$ resonance or by trimming the magnetic field to be uniform for the last 20 turns.

If it proves feasible to nest the auxiliary dees inside the main dees, the deflector can be a single structure that lies in an otherwise unoccupied valley. On the other hand, if each of the auxiliary and main dees occupies a valley, then the deflector will be in two parts, one before and one following an auxiliary dee.

Matrix calculations show that the separation between the deflected path and the last equilibrium orbit will be large enough that the fields of the next two magnets traversed after the deflection can be trimmed to make them uniform rather than isochronous. For the last third of the second magnet, the field will be greatly reduced by a

compensated channel. The separation and divergence in the next valley will then be large enough that a bending magnet can steer the beam completely away from the cyclotron.

9. Injector Cyclotron: N = 4, $\theta = 35^{\circ}$

The main six-sector cyclotron will be served by two alternative injectors: the tandem Van de Graaff for heavy ions, and a small cyclotron for light and perhaps intermediate particles. (When the cyclotron injector is used, the tandem will be available for independent experiments.)

Two possibilities for the small injector cyclotron have been considered. The first, a standard device with azimuthally varying field (AVF), uses either a centrally located source or an external source with axial injection through a hole in one of the yokes and poles. The second is an open-sector machine into which ions are fed from an auxiliary pre-injector. Although the decision is not yet final, at present we favor the second alternative for the same reasons that led to the choice of an open-sector machine for the main cyclotron: since particles are injected at a substantial energy, the problems of space charge are reduced; the input and output beams can be of good quality; focusing forces are present in full strength from the start; there is no raw projectile gas to impair the vacuum; and there is adequate space for the dees.

Calculation of the oscillation frequencies ν_x and ν_z show that an N = 4, $\theta = 35^{\circ}$ design is entirely satisfactory for the energy range that must be covered; no resonances at all will be encountered. To permit acceleration of medium-mass particles (when the TU is being used alone on other tasks), the output momentum must be about 285 kG-in. Since the final radius has been fixed at 19.3 in., the maximum field in the magnet sectors will be 14.8 kG.

The choice of the input energy to the injector cyclotron is not easily made at this stage of the design. Factors to be considered and weighed include the final energy homogeneity, the duration of a beam pulse and the amount of charge in it, the deleterious effects of space charge at low energy, the accessibility of the ion source, the

permissible degradation of yield at the lowest energies, and the cost of the pre-injector. At present, our choice is a 3-MV pre-injector because of the space-charge effect on short pulses.

Assume that energy flat-topping is not used in either cyclotron, that the magnetic-field stability is $\Delta B/B = 10^{-5}$, and that the energy spread for 350-MeV protons is to be $\Delta E/E = 10^{-3}$. Then

$$\frac{\Delta E}{E} = \frac{\pi^2}{2}\left(K\frac{|\Delta B|}{B} + DF\right)^2,$$

where K is the number of turns (350 in this case) and the duty factor is defined as DF = (pulse duration)/(rf period) = τf. At f = 20 MHz, this means that the pulse length is τ = 0.55 nsec. If flat-topping is used (as expected), such short pulses would not be required for good energy resolution, but the accelerator system should nevertheless be able to provide short pulses for use in fast-timing experiments.

If the pulse is to be short (say 0.5 nsec) and the average output current 10 μA, then the peak current in the klystron buncher in the pre-injector must be very high—about 5 mA if losses of current during the acceleration process are taken into account. Although this is well within the capability of bunchers and ion sources, the effect of space charge on such a pulse may be important at low energies. For example, at 200 keV a 5-mA beam 1 cm in diameter and 0.55 nsec in duration will double its diameter in a distance of about 1.3 m, at 500 keV in 2.5 m, and at 3 MeV in about 10 m.

Ideally, therefore, the pre-injector should give protons (destined for 350 MeV) such a high energy that space-charge effects would still be negligible when the injection energy is reduced to the value needed for protons of only 50 MeV at the output of the N = 6 cyclotron. Practical considerations of cost must sober such aspirations, and it is doubtful if ions of very low final energy will be in demand for a majority of the operating time. At the present, we favor a 3-MV Van de Graaff or Dynamitron as the pre-injector, recognizing that the ion source will not

be readily accessible and that a specially elongated terminal may be needed to contain a klystron buncher capable of providing pulse times shorter than 0.5 nsec.

Given this choice of input energy to the small N = 4 cyclotron, the energy gain per nucleon as a function of final Z/A for the N = 4 and N = 6 machines is as shown in Fig. II·B-15 when the N = 6 cyclotron is fully excited to Bρ = 1160 kG-in. at its output. It is seen that the energy amplification factor of the injector is about 4.5, while for the larger machine it ranges from 25 for the lightest ion to 16 for the heaviest. The overall amplification of both accelerators is 117 for protons but is down to 78 for C^{4+}.

The amplification factor permits a rapid evaluation of the required voltage of the pre-injector when the output energy of the N = 6 cyclotron is lowered. Thus for a final proton energy of 50 MeV, the pre-injector must deliver 430-keV ions. Space charge will then not be

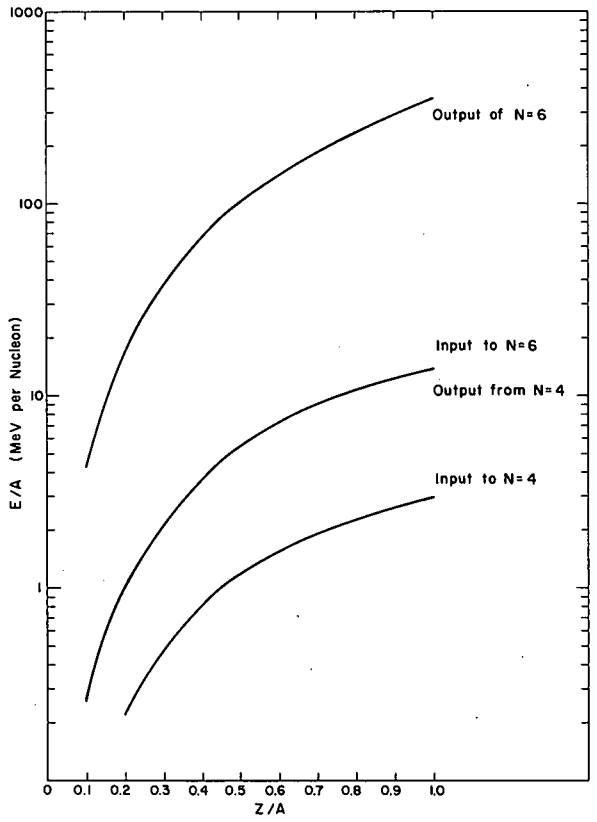

Fig. II.B-15. The output and input energies of the N = 4, $\theta = 35^{\circ}$ injector and the N = 6, $\theta = 20^{\circ}$ main cyclotron as functions of the charge-to-mass ratio in the larger machine, which is assumed to be fully excited to Bρ = 1160 kG-in. at its final radius.

negligible and in all likelihood the output current will be less than 10 μA when short pulses are required.

Some users will want extremely short pulses while others will want long ones, and sometimes a more intense beam will be welcome without regard to homogeneity of energy. In this case, the pulse length (and hence the duty factor) can be increased; this raises the energy spread but allows the peak current to be lowered, so that space charge becomes less potent and the average output current will rise.

Energy flat-topping increases the duty factor without raising the energy spread; as shown earlier, a 10% duty factor can be contemplated. This lowers the buncher's peak current from 5 mA to 0.375 mA, thus drastically reducing space charge. For this reason, auxiliary dees to permit flat-topping are attractive in the N = 4 machine as well as in the large one.

Both cyclotrons will operate at the same harmonic number h, this being the ratio of the dee frequency to the rotation frequency. As a result, each machine will have h bunches of ions uniformly distributed around one turn. Therefore it is necessary for the final orbit in the small cyclotron and the initial orbit in the large one to have the same length.

The injector cyclotron will have four straight sectors of 35° angular width. The magnets are 6 ft long and weigh 18 tons each. The central region of the array has an inner diameter of 3 ft and an outer diameter of 15 ft.

The gap height is 2 in., and the maximum field strength is 17.7 kG. Maximum power to excite the main and trim coils will be 66 kW.

There are two dees, each of 40° angular width. The frequency range is 9 – 22 MHz. Flat-topping will require a pair of auxiliary dees nested inside the main pair. (If the mechanical and electrical difficulties of such an arrangement turn out to be too severe, the beam-transport line from the pre-injector can be routed over the

magnets so as to leave clear two valleys in which the auxiliary dees can be mounted.) Tuning of both sets will be by movable shorts and trimmer capacitors. The maximum voltage is 100 kV for the main dees and 33 kV for the auxiliary dees. Total rf power for both sets is 150 kW.

Vacuum pumps will produce a pressure of $2-3 \times 10^{-6}$ Torr.

The beam is injected and ejected by procedures similar to those used with the larger cyclotron.

II. C. EXPERIMENTAL BUILDING

1. Introduction

Several major considerations strongly influence the configuration of the building. The accelerators described in Secs. II·A and II·B must be able to operate together as a single system, but must also be able to operate independently with a minimum of interference between them. The particle beams must be fed into a number of experimental areas suitable for a wide range of experiments and designed to accommodate simultaneous experiments with each major accelerator used separately as well as in combination. Since it is expected that there will be considerable demand on the experimental facilities by a large number of scientists (many of whom will be at Argonne for only a brief period prior to each experimental run), it is important to facilitate the setup of an experiment while a previous experiment is in progress. There must be adequate provision for operating and maintaining the accelerators, convenient laboratory and counting areas for the experiments, accommodation for the operating staff and supporting personnel, and a limited amount of office space for members of groups actively engaged in an experiment. All of this space for personnel must be adequately shielded from radiation

and arranged so that no desirable future extensions of beam lines or other facilities are rendered impossible.

2. Radiation Shielding

The primary purpose of this section is to present the proposed plan for the building. However, since radiation shielding is a major consideration in designing the building, this question will be discussed first.

a. Shielding Calculations

It is clear that the major problem in shielding is the radiation produced by the high-energy light ions from the large cyclotron, with light ions accelerated in the tandem and injector cyclotron being next in importance. Since the heavy-ion beams are confined to rather low energies per nucleon, they present a much less difficult problem. Thus the heaviest bulk shielding will be required for the cyclotron. We have therefore calculated the radiation dose rates which will be expected outside the shielding walls as a result of the neutron flux produced by protons of energies up to 350 MeV.

When high-energy protons are brought to rest in a thick target, a considerable fraction of them undergo reactions with the nuclei of the target material. The neutrons produced in the course of these reactions belong to two distinct spectral distributions. The evaporation neutrons are of low energy (less than 10 MeV) and are isotropic in angular distribution. The cascade neutrons have energies extending continuously to a maximum almost as high as the energy of the incident proton, and the angular distribution tends to be peaked forward (in the direction of the incident protons). Bertini[1] has made Monte-Carlo calculations of the spectra of both evaporation and cascade neutrons resulting from reactions at proton energies from 50 to 400 MeV in steps of 50 MeV. These results are averaged over four angular ranges, $0-30^{\circ}$, $30-60^{\circ}$, $60-90^{\circ}$, and $90-180^{\circ}$.

---

[1] Hugo W. Bertini, Phys. Rev. 131, 1801 (1963).

Alsmiller et al.[2] have fitted Bertini's spectra with a least-squares method and have obtained the coefficients used in our calculations.

In our preliminary calculations based on these coefficients, we have used the computer program SHIELD,[3] which computes the number of neutrons penetrating shield material on the assumption that they have been generated by inelastic reactions of protons at the incident energy E_{inc}. But since the proton energy is steadily degraded in a thick target, successive neutrons are in fact produced in progressively less energetic collisions—so this calculated value must be rather higher than the correct one. To obtain a more accurate number, we have used a modified method which first computes a neutron spectrum that corresponds more closely to that produced by the protons as they slow down.

The first step in the calculation of the neutron spectrum produced in a thick target was to divide the energy of the incident protons into 50-MeV segments. Next the total neutron spectrum per inelastic collision was calculated for each segment by use of the coefficients of Alsmiller et al.[2] The resulting spectrum for each segment was then normalized by multiplying it by the probability that a proton would have an inelastic collision while in that energy segment, these probabilities being obtained from the tabulation of Janni et al.[4] The sum of the contributions from the different segments then gave the total neutron spectrum (evaporation plus cascade). Figure II·C-1 shows the results of such a calculation for 350-MeV protons. This method gives a closer approximation to the true neutron spectrum than does a calculation in which the neutrons are assumed to be produced by protons of the full incident energy; in particular, the fraction of high-energy neutrons is distinctly less.

---

[2] R. G. Alsmiller, Jr., M. Leimdorfer, and J. Barish, Oak Ridge National Laboratory Report ORNL-4046.

[3] P. P. Singh (private communication).

[4] Joseph F. Janni, Air Force Weapons Laboratory Technical Report TR-65-150.

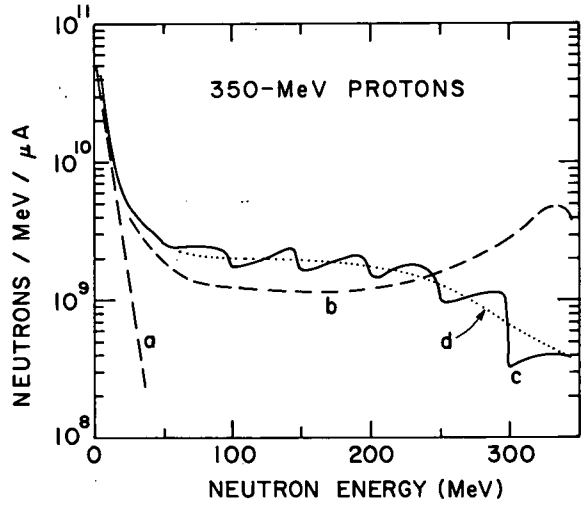

Fig. II.C-1. Spectra of neutrons produced by 350-MeV protons. (a) Evaporation and (b) cascade spectra produced in inelastic collisions of 350-MeV protons on Cu. (c) Approximation to the total neutron spectrum produced by 350-MeV protons slowing down in a Cu target; it consists of a weighted sum of spectra of types (a) and (b) calculated for proton energies at 50-MeV intervals. The breaks in the curve correspond to these intervals. (d) Smooth curve drawn through (c). Curves (a) and (b) are normalized to the same number of inelastic collisions as (c).

To convert these neutron spectra from the target into dose rates outside the shield walls, we have made use of a calculation by Alsmiller et al.,[5] who obtained the spectra produced in shield walls by monoenergetic incident neutrons of 50, 100, 200, 300, and 400 MeV. Reference 5 also presents the neutron dose equivalent as a function of depth in the shield for these same monoenergetic incident neutrons, this figure being obtained by applying known flux-to-dose conversion factors to the spectra. These data have been used in converting the total neutron spectra discussed above into dose equivalent. By means of a least-squares fit to the data of Ref. 5, the dose equivalent for any incident neutron energy at any depth (up to 1400 g/cm^2) could be obtained.

Finally, the total neutron dose rate D (rem/sec) was obtained by multiplying each neutron energy (in 1-MeV intervals) by its appropriate equivalent and summing, i.e.,

$$D(E_p,t) = \sum_{E_p=25}^{E_{inc}} \left\{ \sum_{\epsilon=1}^{E_p} \left[F(\epsilon)\cdot d_{\epsilon,t} \right] \right\},$$

[5] R. G. Alsmiller, Jr., F. R. Mynatt, T. Barish, and W. W. Engle, Jr., Oak Ridge National Laboratory Report ORNL-TM-2554.

where the first summation is over the energy segments of the incident proton energy, the second is over the individual neutron spectra, d is the dose equivalent, ϵ is the neutron energy, and t is the shield thickness. We have written a computer program[6] to evaluate $D(E_p, t)$ and have used it to calculate dose rates for proton energies from 25 to 350 MeV. Figures II·C-2 show the results outside a concrete shield wall for the cases of 50- and 350-MeV protons incident on a copper target. Not only are the neutrons at the higher energy much more penetrating, but they are also more strongly peaked in the forward direction.

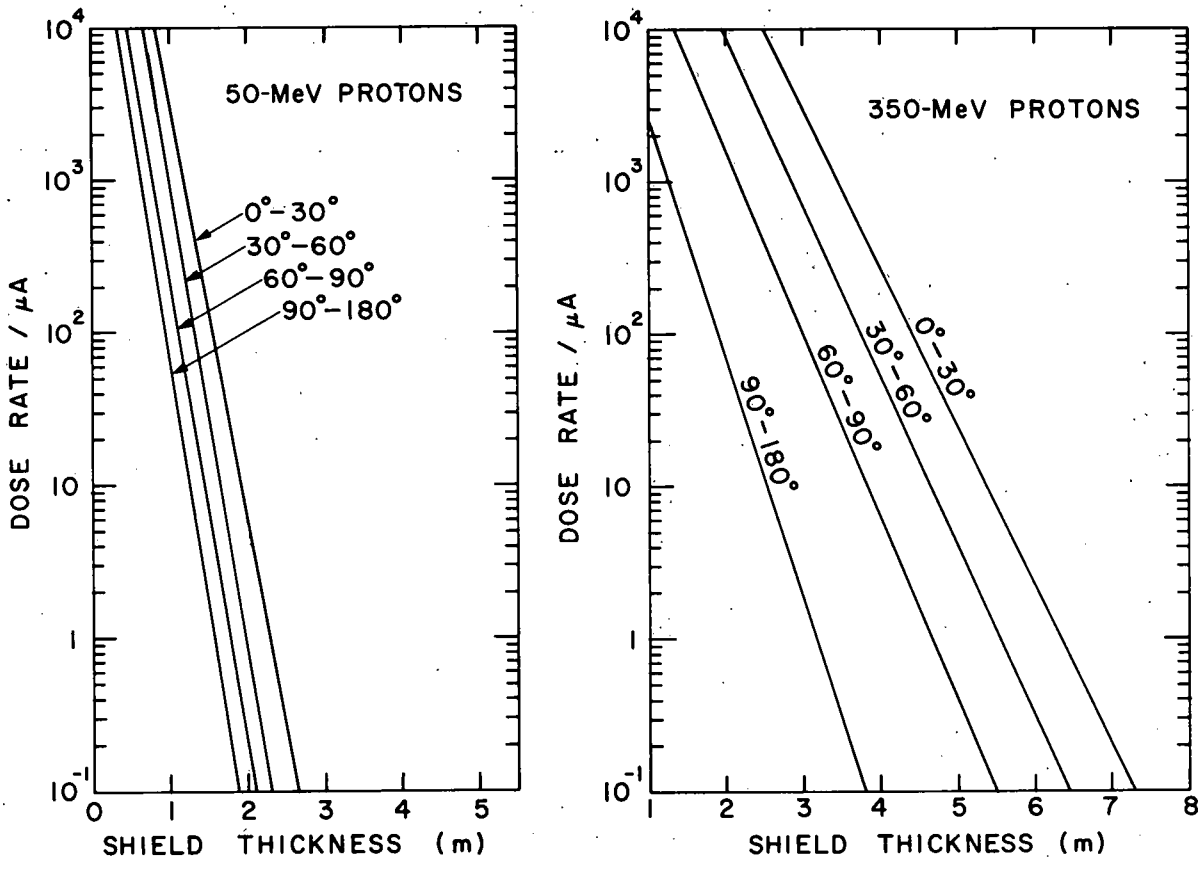

Fig. II·C-2. Dose rate from neutrons penetrating a concrete shield wall when a Cu target is bombarded by 50-MeV protons (left) and by 350-MeV protons (right). The unit on the dose-rate scale is the standard tolerance level (2.5 mrem/hr).

[6] R. H. Siemssen, J. W. Tippie, R. W. Rapids, and T. H. Braid (unpublished).

II·C-3 shows the angular-distribution effect more clearly, and Fig. II·C-4 shows how the radiation dose coming through a not-very-thick shield wall depends on the incident energy E_{inc} of the protons. This makes it clear how the required shielding thicknesses depend on the maximum energy of the cyclotron, but it should be noted from Fig. II·C-2 (right) that even at the highest energies, 1 m of concrete attenuates the dose rate by a factor of ten.

Direct radiation is not the only danger from an accelerator. Skyshine—neutrons escaping through the roof and being reflected back from the atmosphere—can be very important. Unfortunately there

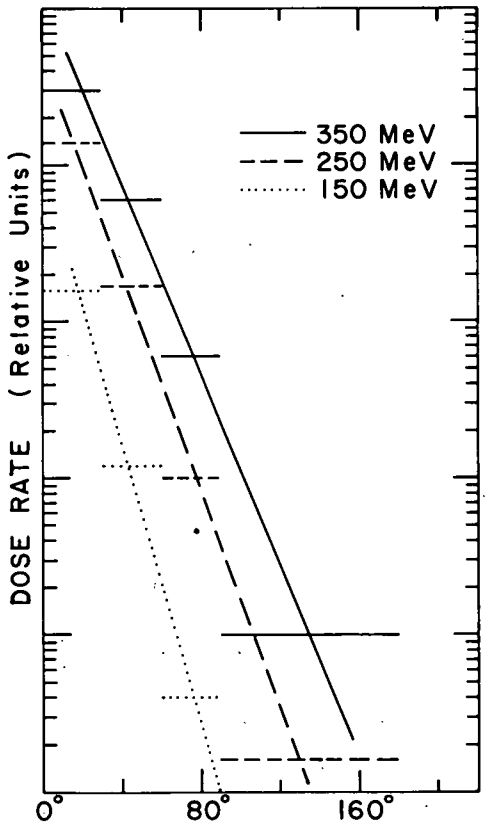

Fig. II·C-3. Angular distribution of radiation from neutrons (produced by protons on a Cu target) penetrating a 3-m concrete shield wall.

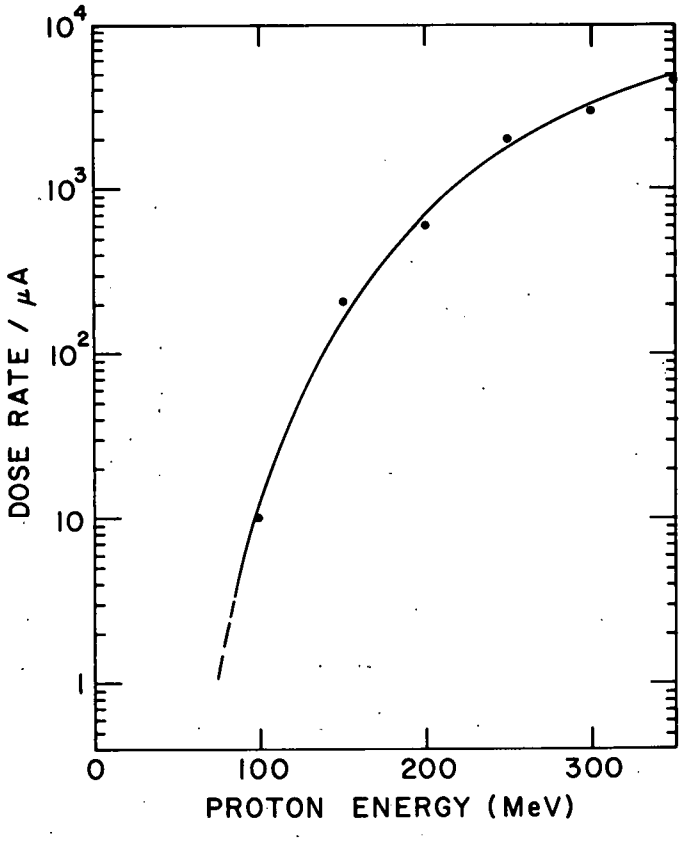

Fig. II·C-4. Radiation level (at 30° to a proton beam on a Cu target) due to neutrons penetrating a 3-m concrete shield as a function of proton energy.

is no agreement on the method of calculating skyshine. There is some indication that the skyshine calculated with the formula due to Lindenbaum[7] is too high, but we have used it in our calculations since these higher values give some assurance that the roof thickness of the cyclotron vault will be adequate by conservative standards. According to this formula, the skyshine flux ϕ_{ss} is

$$\phi_{ss} = 4.7 \times 10^{5} \frac{e^{-r/830}}{r} \cdot q,$$

where r is the distance in feet and q is the effective source strength. We have estimated q from the 60—90° flux in the calculation previously described. Assuming this to fall on the roof, we have used the spectra in Ref. 5 to find how many neutrons in the energy range 0.1—40 MeV will penetrate a roof of a given thickness. (It is believed that neutrons in the range from a few MeV to a few tens of MeV are primarily responsible for skyshine at short distances.) This value has been used for q in the above formula; with 1 μA of 350-MeV protons and a roof thickness of 2 m of concrete, ϕ_{ss} is comfortably less than 10 neutrons/cm^2 per sec—even within 50 ft of the source. Since skyshine neutrons are predominantly low in energy, the tolerance level in any case is presumably higher than this.

b. General Shielding Considerations

As is readily seen from Fig. II·C-3, very considerable thicknesses of material are necessary to reduce radiation to tolerance levels in the worst case (e.g., in the case of the 0—30° cone of neutrons produced by 10 μA of 350-MeV protons). It would be very difficult and cumbrous to shield all parts of the cyclotron, target areas, and beam lines against such a neutron flux. But fortunately this is not necessary; the strong

[7] S. T. Lindenbaum, Ann. Rev. Nucl. Sci. 11, 213 (1961).

forward peaking of the radiation can be exploited by arranging to keep personnel away from areas immediately downstream from heavily bombarded surfaces. The intensity in regions $60-90^{\circ}$ from the beam direction is less than or about a hundredth of that at $0-30^{\circ}$. Distance can be a major factor in as large a building complex as the present one inevitably must be, and time is also an important consideration since the cyclotron will spend only a fraction of the time accelerating protons to maximum energies at maximum current. Also, higher radiation levels can be tolerated in certain areas of very occasional and limited access.

Because a very clean beam of small emittance will be injected into the cyclotron, it may be reasonable to assume that the particles will all be very cleanly accelerated, that very few if any will be spilled in the cyclotron vault, and that there will be almost no spillage in the beam-transport system except at definite points known in advance. If this is indeed the case, then it may suffice to provide only relatively limited general shielding, supplemented by local shielding at key points. No such extreme view was adopted in designing the building proposed here—partly because the assumption must remain doubtful until justified by experience with this type of cyclotron, and partly because it leaves insufficient allowance for error and for equipment failure during operation. Since we expect very steady use of the facilities by many people, we feel that we cannot afford either the risks of minimal shielding or the inconvenience that might arise if the optimism proved to be unjustified.

We have adopted the view that the permanently-occupied parts of the building should have bulk shielding which allows permanent occupation during normal operation of the cyclotron at full energy. For this purpose we have assumed a 10-μA beam of protons at 350 MeV, with 1 μA lost in the vault—mainly at extraction. Should the total beam be increased, or more lost in the vault (e.g., because of a continuous

bombardment of a target in the vault at full current), or should there be a catastrophic loss of beam at some other point in the cyclotron ring, it will be possible to use supplementary local shielding. In the areas not occupied permanently (e.g., in experimental and beam-transit areas), similar remarks apply except that the reliance on local shielding is proportionately larger.

The shielding required for the lower-energy machines has been calculated by the same methods, but these estimates have been supplemented by the information available from the many years of Argonne experience with the operation of accelerators in the same general energy range.

3. The Building Plan

a. General

The proposed building plan is shown in Fig. II·C-5. The axis of the tandem points directly at the central area of the cyclotron. This placement is dictated by the basic requirement that the tandem beam with the ions in a low charge state must go to the cyclotron injection magnets via an isochronous path. The tandem beam can be diverted into either of two experimental areas by the appropriate 90° analyzing magnet. The first area (A) can be reached by beams from the tandem only, while the second (C) can also be reached by beams from the cyclotron. The beam from the cyclotron can be brought out directly into a third area (D) with a minimum of bending magnets, as well as into the room in common with the tandem. These three experimental areas are located on one side of the line from tandem to cyclotron so that the general beam direction is away from the rest of the structure. The injector cyclotron is located in a vault near one corner of the main cyclotron vault, and the pre-injector is in a room beside it. All the occupied areas are arranged down the other side of the main structure from the beam-line areas. In particular, the

control rooms and the experimenters' data rooms are located in the corner between the tandem and the cyclotron vault, and a group of chemistry laboratories are placed at the other end of the complex.

Figure II·C-6 shows a plan of the basement area. Most of this area will be taken up with the mechanical equipment necessary to a building of this size and with the power supplies and pumps for the accelerators. The U-shaped tunnel is to provide communication between the experimental areas on the one side and the people and facilities on the other.

Figure II·C-7 shows a suitable location for the MTC in relationship to the other related facilities in the research area at Argonne.

Some parts of the building will now be discussed in greater detail.

b. Tandem Vault

The dimensions of the tandem vault are set by the manufacturer's specifications. The large tank is to be assembled and tested outside the building and then moved inside. The tank will rest on four pillars which will rest on footings on solid ground. There will be a basement the full length of the building, of which the middle part will be occupied by the "under-belly" of the tank which hangs through the floor. The rest of the basement will accommodate equipment and power supplies and the piping and wiring necessary to the operation of the accelerator. Gas-storage tanks may be placed in this basement or may alternatively be placed outside at the low-energy end. The area at the high-energy end will accommodate a 90° magnetic analyzer, quadrupoles, beam steering, etc. At the low-energy end there is space for additional ion sources. This end of the building is deliberately left very open so that if it is ever desired to make additions of special ion sources (e.g., for polarized beams) there will be space to do so. A heavy shield wall down one side of the vault protects operators and experimenters.

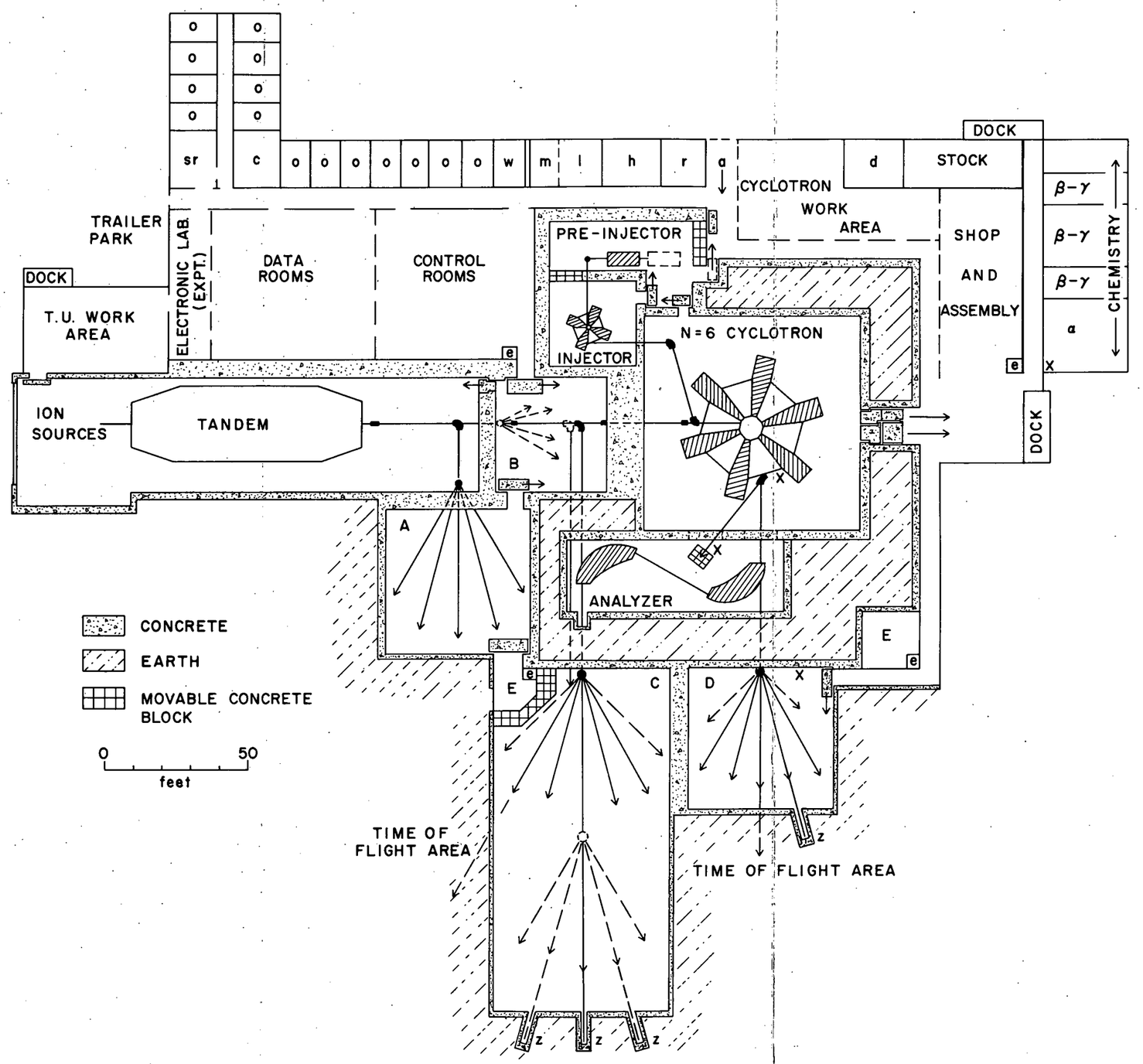

Fig. II. C-5. The plan of the building. The directions of particle beams are indicated; some alternative beams, or beam directions, available to particles of less than the maximum rigidity are shown by dashed lines. The important beam-bending and switching magnets are shown (not necessarily to exact scale) but many minor components (e.g., quadrupoles) are omitted. Alternative positions of components are shown dashed. The experimental areas A, B, C, D, and E are referred to in the text. Non-fixed shield walls in C are not shown. Other areas are: a—access route for heavy components to injector area, c—conference room, d—drafting room, e—elevator positions, h—target and radioactive components laboratory, ℓ—locker room, m—men, o—office space, r—radiation safety, sr—secretary-reception, w—women, x—rabbit stations, and z—shielded beam dumps.

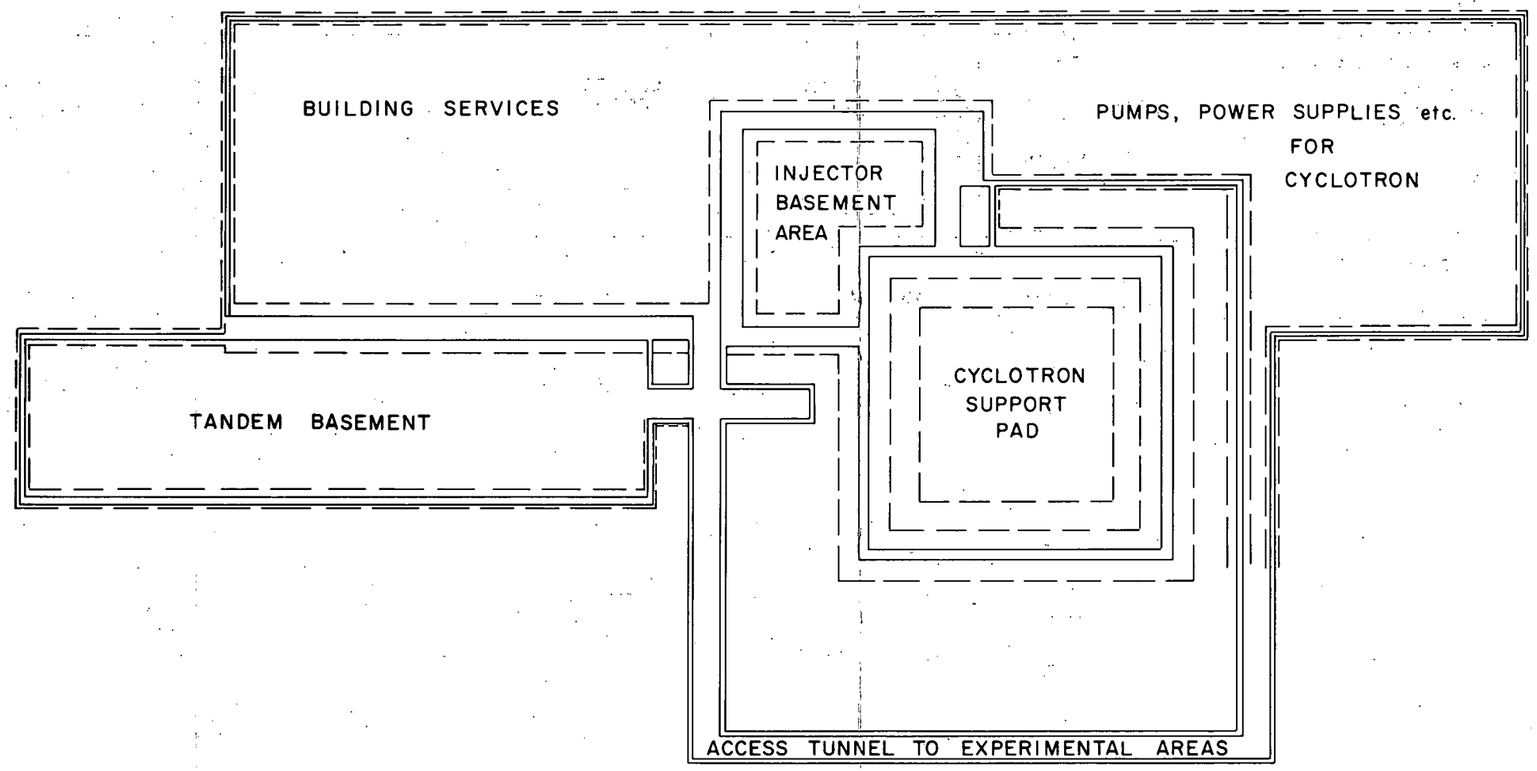

Fig. II.C-6. Plan of the basement areas. The dotted lines indicate foundations for major walls and heavy components such as the cyclotron. The U-shaped tunnel connects the experimental areas with the basement of the control and service building, giving access for services, signal cables for experiments, and experimenters.

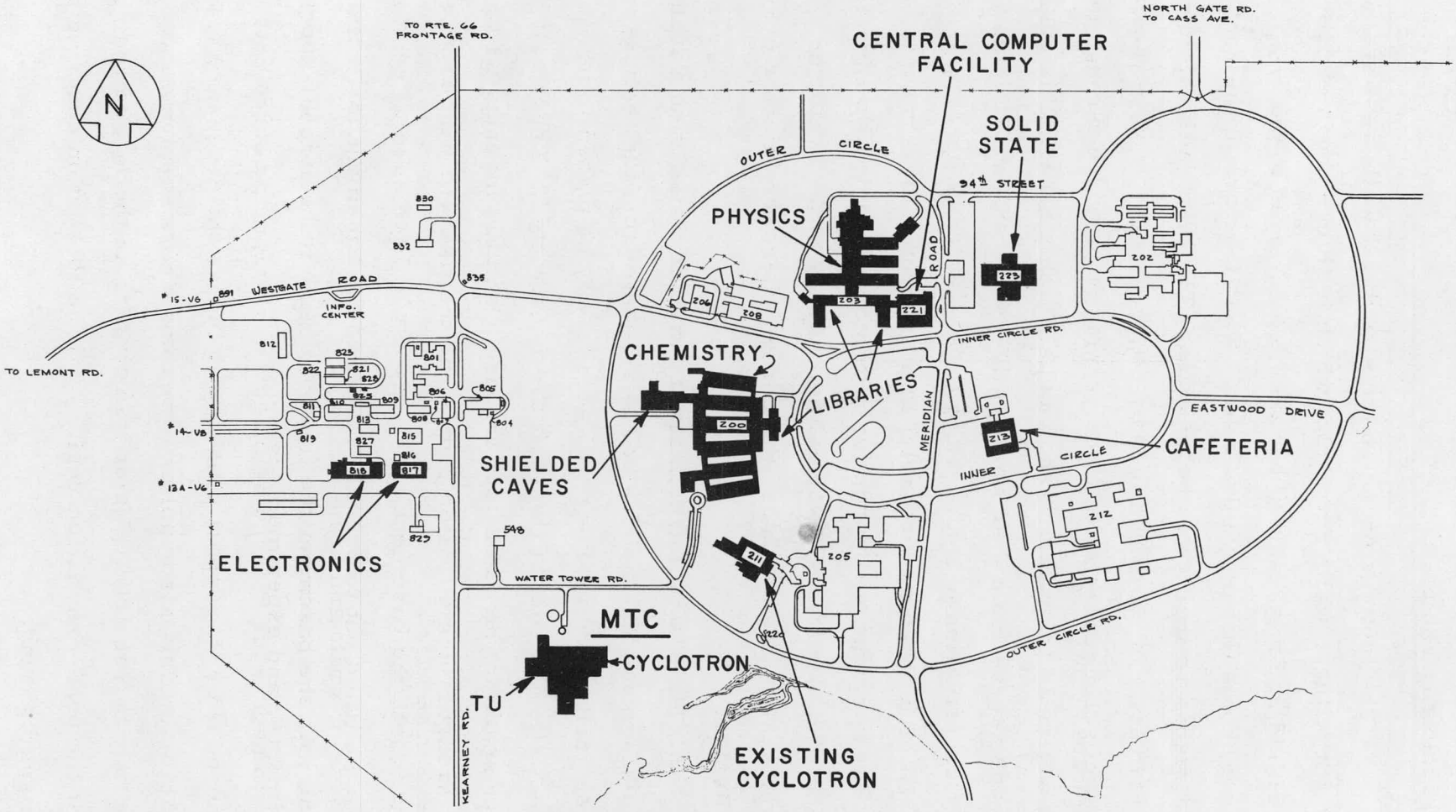

Fig. II·C-7. The proposed location of the MTC in relation to the other buildings and services of interest to experimenters.

c. Main-Cyclotron Vault

The footings on which the structural walls rest are heavy enough to carry these walls and a roof which is thick enough to provide adequate shielding for skyshine, but are also designed to carry a much thicker roof should that prove desirable. The structure of the roof itself is designed so that it can be added to. The thick bulk shielding consists primarily of earth confined by concrete walls to save the cost and weight of solid concrete. A wide opening is provided through the shielding wall near the machine shop and assembly area. This opening is to provide access for major work on the cyclotron, in particular during the construction period. While the cyclotron is operating, this opening will be blocked by (probably) four concrete blocks mounted on wheels. These blocks will normally be removed only to allow installation or removal of major items. Normal fast access to the cyclotron will be through the system of doors near the corner where the injector cyclotron is situated.

The six cyclotron magnets will sit on jacks on a foundation pad at the basement level. This pad is separate from the footings supporting the vault. The magnets will necessarily be placed in position before the walls and roof of the vault are constructed. There will be a large open space in the main floor through which the magnets will project and through which diffusion pumps and the like will hang from the vacuum tank into the basement. This floor will have several sections which may be lifted out to provide access to the basement for installing equipment. At other places, the floor will have to be strong enough that heavy equipment (such as bending magnets, shielding, source pots, etc.) can be moved over it; support pillars will ensure the necessary load-bearing ability. This also applies to regions where supplementary local shielding may be required. Major items, such as the large bending magnet at the beam-extraction region, will be located on concrete piers based on solid ground.

The floor dimensions allow a clearance of at least 12 ft around the cyclotron, to allow room to pull the dees out radially.

d. Injector Vault

The injector area contains the N = 4 cyclotron and a low-energy dc positive-terminal pre-injector. The cyclotron portion will be a rectangular vault rather similar to the one just described but smaller. A relatively light shield wall is provided between the vaults for the two cyclotrons since the N = 6 cyclotron will be accelerating only heavy ions when the injector cyclotron itself is not running. A similar consideration applies to the shielding required between the injector cyclotron and pre-injector, and consequently a considerable part of the shield between the cyclotron and the pre-injector area (and also the short wall at the entrance to the area) will consist of blocks which will not be placed in position until after construction is complete and which will be removed for major repairs. The pre-injector area has extra space to allow for possible future additions such as a polarized-ion source.

e. Analyzer Vault

The analyzer vault contains the analyzing magnets for the high-energy cyclotron beam. Access is from the cyclotron vault through openings in the interior structural wall. The magnets, on installation, will be brought through the cyclotron vault. Part of this area might also be used as a beam dump or high-intensity bombardment facility.

f. Operation and Maintenance

The control rooms for all the accelerators and beam transport are located near the high-energy end of the tandem, and form part of a large area which also contains the experimental data room. There is room for a computer to be used in running the accelerators, to record

conditions, and numerous other tasks. There is a work area for technicians near the ion-source end of the tandem and a similar area near the entrance to the cyclotrons. There is a machine shop for 2—4 men, and also an area for the assembly of major components, a drafting room, a stock room, space for radiation-safety personnel and for the handling of radioactive components, and office space for the operating staff and typists.

g. Experimental Beam Areas

A total of four areas may be used for experiments with the particle beams.

The first—the room (A in Fig. II·C-5) reached by the tandem beam only—is rather similar to the experimental area which has been found satisfactory at the existing Argonne tandem. There will be five beam lines providing an energy-analyzed beam. The whole area is shielded by concrete and earth and a concrete roof so that it can be occupied at all times when the beam is not actually directed into it.

A second area (B) available for experiments with the tandem beam alone lies between the tandem and the cyclotron, and is partly a beam "switchyard." The non-analyzed beam is available here for experiments that do not require the highest energy resolution—for example, activation measurements or in-beam optical spectroscopy.

The third area (D) is accessible only to the direct non-analyzed beam from the cyclotron. It is the same size as the main tandem-only area, will likewise have five beam lines, and is intended also to be available (for setting up experiments or the like) at any time when the beam is not actually in it. It has been thought of as the area in which much of the heavy-ion work will be done. High-energy light ions will also be available but then some local shielding may become necessary.

The fourth room (C) can receive energy-analyzed beams from either the tandem or the cyclotron. It is much larger than the

other areas and has been thought of as the area where most of the light-ion and high-resolution heavy-ion experiments will be done. The lower part of the walls are concrete and the upper part is a fairly light metal structure. A heavy crane travels in this upper part and will be used to place concrete blocks to form interior shielding walls with beams placed above to form a roof on individual areas. The amount of shielding for any area will obviously depend on the type and energy of the particle being used there. When heavy ions are being used, it should ordinarily be easy to arrange that the rest of the room be habitable. In the case of high-energy protons, this will not be true for "downstream" areas because of the forward peaking of the neutrons already discussed, but may well be possible for "upstream" areas. The extent to which this is possible depends on the cleanliness with which the beam is transported; probably in practice we shall depend on a combination of reasonable quantities of shielding block and radiation monitors to turn the beam off quickly should the radiation level rise above the permissible level.

For the reasons mentioned above, the high-energy light particles will be directed towards the end of the building and in the direction away from the third experimental area. (The relatively light shielding wall between the two areas is planned for the less potent particles.)

All three areas have earth piled against their outside walls to provide the final shielding of the surrounding area. Beam dumps will be provided at a number of places by setting pipes into this embankment. Figure II. C-7 shows that the surrounding area is quite empty; this minimizes the shielding problem and leaves considerable distances available for time-of-flight experiments.

Two small areas (E) are provided for local experimental electronic areas close to the beam areas, for equipment which cannot be placed in the central data room, or for the convenience of experimenters in setting up.

Access to these areas is obtained via the service tunnel shown in Fig. II·C-6; elevators are placed at several points. They can also be reached directly from the main floor, but this access is to some extent restricted according to beam conditions.

h. Experimental Facilities

The main data room is next to the accelerator control room and will be connected to all the experimental areas and local counting rooms, both with cables for electronic signals and also with an intercommunication system and closed-circuit television. Space will be allowed for an on-line computer to be used in conjunction with experiments.

Immediately adjacent to the data room and to the tandem work area is an electronics and general-purpose laboratory for the use of experimenters. At the other end of the building, where samples can be taken immediately after bombardment, is a block of chemistry laboratories. A fast "rabbit" connects these laboratories, tunnel D, and the cyclotron vault area with the shielded caves in the Chemistry Building. Near the data room is an area where trailers may be parked and hooked to the building data link. More details of available hardware are given in the next section. A number of offices near the data room are intended for use by visitors to Argonne while at the MTC for an experiment. It is not intended that there should be any permanently assigned office space for experimentalists in this building; longer term visitors will have accommodations elsewhere, presumably in the Physics and Chemistry Buildings.

Figure II·C-7 shows the other major facilities which will be near the MTC and of value to people doing experiments there—in particular the central computer building, libraries, and the buildings housing the Physics, Chemistry, and Electronics Division.

II. D. BEAM HANDLING AND EXPERIMENTAL EQUIPMENT

1. Beam Transport

a. General

The particle beams in the system of accelerators cover a wide range of magnetic rigidity, given by

$$B\rho \propto (ME/z^2)^{1/2},$$

where M is the particle mass in amu, E its kinetic energy, and z its charge. The quantity (ME/z^2), the product of mass and energy divided by the square of the ion charge, is a convenient figure of merit for the bending power of a magnet. The rigidity of 15-MeV protons from the N = 4 cyclotron is $B\rho$ = 5.62 kG-m; for 32-MeV protons from the tandem, $B\rho$ = 8.2 kG-m; and for 350-MeV protons from the N = 6 cyclotron $B\rho$ = 29.5 kG-m. The rigidity of a heavy ion depends on its mass and, even more strongly, on its charge. For a U^{238} ion in a 7+ charge state emerging from the tandem with an energy of 128 MeV, $B\rho$ = 35.9 kG-m, distinctly more than the value for the most energetic particles from the cyclotron. (For heavy ions from the cyclotron, the value of $B\rho$ is as given above for protons.) However, if this ion is stripped to charge state 34+, then the value drops to 7.25 kG-m. This effect of the charge of the heavy ions strongly influences the arrangements made for handling such beams, since impractically large magnets would be

required in order to bend them appreciably in the low-charge state. Therefore a gas or foil stripper must be used before any point at which the beam is to be bent. Since, for reasons discussed in Sec. II. A 5, a foil stripper must be used before injection into the cyclotron; and since it must be used as close to the injection point as possible (to avoid too large a time spread in the pulse as a result of the spread in velocity inevitably introduced by a foil) the beam must travel from the tandem vault to the cyclotron vault in its low-charge state (and therefore without being appreciably bent) until after the foil stripper.

At other points where the beam is to be directed off this straight line and where it is not so important to have the highest charge state, a gas stripper can be used. Having less effective thickness, it will introduce less energy straggling. However, it will introduce a gas leak into the beam tube. The importance of a low vacuum in the beam lines carrying the heavy ions has been emphasized in Sec. II. B7d. Therefore, for each such gas stripper it will be necessary to provide additional high-quality differential pumping.

We have used the program TRANSPORT, based on one reported by Brown[1] to trace the beam through important parts of the system.

b. Beams from the Tandem

To put a light-ion beam in experimental room A (Fig. II. C-5), the system of magnetic elements required is completely conventional. A quadrupole doublet at the high-energy end of the tandem is used to focus the beam to a sharp image on the object slit of a 90^{o} magnetic analyzer. This is a flat-field magnet ($n = 0$), with $ME/z^2 = 140$, which produces a double focus at the symmetrically-placed image slit. Signals derived from the jaws of this slit are used to stabilize the tandem

[1] Karl L. Brown, SLAC-75 (1967).

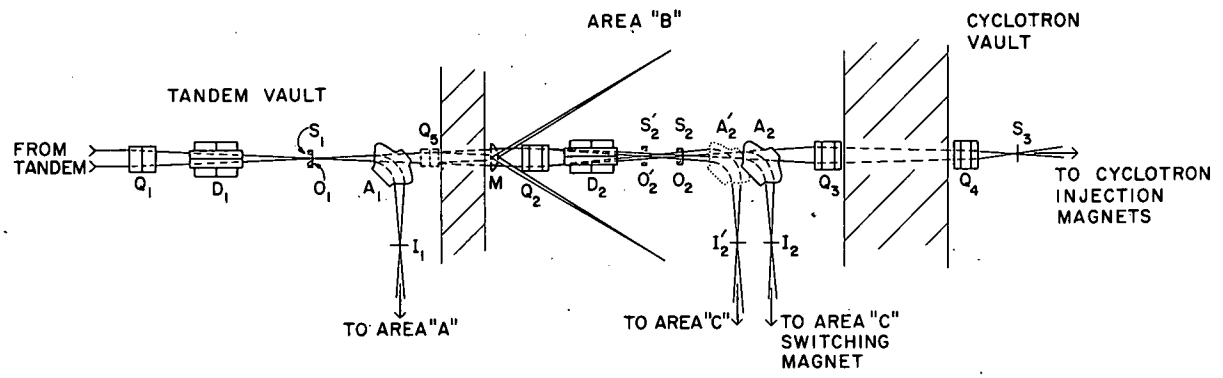

Fig. II. D-1. Beam-transport system to enable the tandem beam to be fed into different areas. The beam is conducted into area A by means of the quadrupole set Q_1 and the analyzer A_1 (with object and image slits O_1 and I_1). In the case of heavy ions, the gas stripper S_1 must also be used. A beam is put into the switching magnet in area C by using Q_1, Q_2, and A_2; S_1 is not used but S_2 is used for heavy ions. A_2 can be moved to the position A_2' to feed a parallel line going into area C without passing through the main switching magnet. Quadrupoles Q_1, Q_2, Q_3, and Q_4 focus the beam onto the foil stripper S_3 for injection into the cyclotron. Beams may be made available in area B by using Q_5 and M in conjunction with the gas stripper S_1. The beam is steered by means of electrostatic deflectors D_1 and D_2.

in the customary fashion. The beam then passes through a switching magnet which is capable of bending it through $\pm 30^\circ$. This allows five beam lines (spaced 15° apart) in the experimental area, each with a quadrupole doublet to focus the beam onto the target.

For heavy ions a gas stripper will have to be used downstream from the tandem. This means that only a part of the beam can be analyzed. The gas stripper is placed at the object point of the doubly focusing magnet to minimize losses due to scattering of the ions by the gas. For uranium ions, the quadrupole doublet used to focus the beam on the object slit will have to be run at a field strength which is high but still reasonable.

The beam is directed into experimental room C by means of a second 90° magnet situated in room B (Figs. II. C-5 and II. D-1).

A second quadrupole in conjunction with that already mentioned focuses a suitable image on the object slit, at which there is a second gas stripper. This 90° analyzing magnet will be able to send an analyzed beam into the switching magnet in area C (which can also be fed by the cyclotron) or, by moving along its rails to a position slightly closer to the tandem, it can send the beam into a parallel beam line entering area C without going through the main switching magnet. This will enable a tandem beam to be fed into one corner of room C while a beam from the cyclotron is being fed into some other part.

The 90° analyzing magnets are, of course, non-isochronous[2] since the rays that travel round the outside of the bend have to travel farther than those that travel round the inside of the bend. Hence the duration of an originally short pulse of particles is spread out, and this might be of importance in some coincidence and time-of-flight experiments involving use of a bunched beam. The effect is probably not large enough to be important for the lightest particles; but for slow-moving heavy ions, the time spread could be intolerable. The time spread in the 90° magnet can be compensated by another bend in the same direction, and the second bend need not be as great as 90°, provided that the beam is more widely spread in the radial direction.[2] A quadrupole set is required in any case to transport the beam from the second analyzing magnet to the switching magnet in area C; this quadrupole can be adjusted to spread the beam out in the horizontal direction just enough that on being deflected by 30° in the switching magnet it is again isochronous, and in that condition can be refocused onto a target. The total distance from the tandem bunching system is in this case large enough to allow the buncher to work with full effectiveness.

The nonanalyzed tandem beam can be used in room B for experiments not requiring the highest energy resolution. For the heavy ions, the direct beam line to this room is the only one in which the full

---

[2] H. Naylor, K. H. Purser, and P. H. Rose, IEEE Trans. Nucl. Sci. NS-12 (No. 3), 306 (1965).

intensity of the heavy-ion beam is available. To provide other beam lines in this area, it will again be necessary to make use of the stripper at the object point of the first analyzer, and to refocus the beam through a switching magnet by means of a quadrupole set.

For injection into the cyclotron, a third quadrupole set in the direct line carries the (low-charge) beam into the cyclotron vault.

c. Injection into the N = 6 Cyclotron

The beam from the TU must be stripped into its high-charge state before passing through any of the inflection magnets, and this is done in a foil stripper. The radial divergence of the beam will be somewhat poorer after the foil, but the emittance of the tandem beam is so much better than that required that this should present no problem. For perfect injection, the beam should be brought to a double focus (ideally a "waist") in the center of an open sector. At this waist, the half-width in the radial direction should be $x \leq 3$ mm and the half-angle of divergence should be $x' \leq 3$ mrad. This has to be achieved subject to a number of physical constraints, as can be seen from Fig. II. D-2. There is only a limited amount of space for placement of the magnets; and as the beam passes into the center region, it must not pass through either an electric field between dees or a magnetic field. The question has been discussed in Sec. II. B8a, where it is shown that with the aid of an electrostatic field a beam traversing the region of the first pole tip of the cyclotron can be bent into the correct direction. The magnet system in Fig. II. D-2 is an example of a suitable method for transferring the beam from the foil stripper to the first pole tip so that the injection conditions are met. For uranium ions with $B\rho = 285$ kG-m, the field in those magnets in which no electric field is superimposed must be 18 kG. The beam emerging from the stripper is focused to a crossover in an open sector, then deflected through 75° (magnet B) and brought to a sharp focus on a set of slits. The beam is dispersed in momentum at this point, and the particular charge state desired for injection will

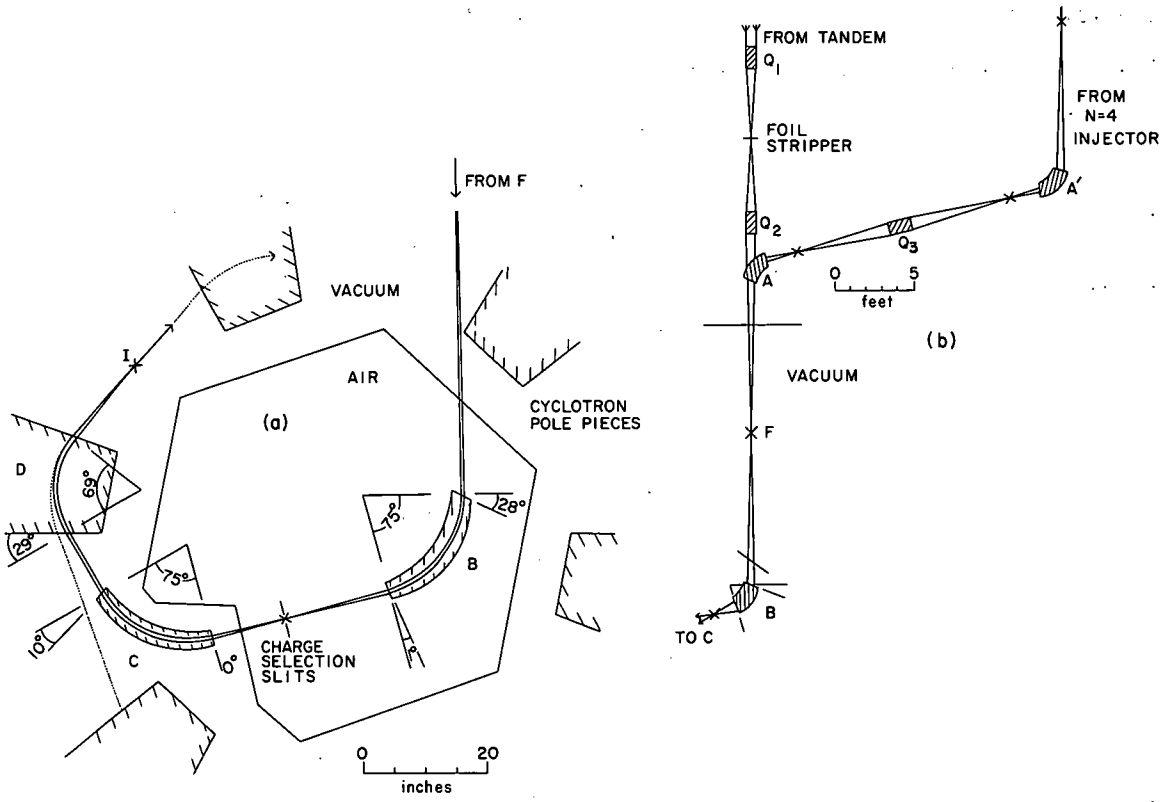

Fig. II. D-2. Injection into the N = 6 cyclotron. (a) The arrangement in the central region of the cyclotron. The dotted line indicates the orbit into which the particles must be injected. In the region of pole piece D, the beam is bent by a combination of a magnetic and an electrostatic field. (b) The arrangements to bring beams into the central region from the tandem and from the N = 4 cyclotron. The symbol × represents a double focus.

be selected there. A further bend of 75° in septum magnet C brings the beam within about 7 in. of the first complete orbit. It travels almost parallel to this orbit until it reaches the first pole tip D of the cyclotron, where the combined force of the magnetic and electric field bend it by just over 69° and it is brought to a double focus in the center of the straight section.

In its passage through the open sector, the beam misses a pole tip by about 2 in. The angle through which it is bent by magnet B, or the distance between magnets B and C, can be adjusted to give greater clearance. Similarly the distance between C and D can be lengthened a little to give rather more clearance between septum magnet C

and the position of the first orbit. Such changes can be made within a limited range, and have a slight effect on the angle at which the incoming beam traverses the open sector and on the positions of the foci. The injection of the ion beam is almost, though not quite, isochronous; the extreme variation in path length is 0.1 cm, corresponding to about 0.1 nsec for uranium ions, which is acceptable. The beam has the characteristics $x = 0.2$ cm, $x' = 1.7$ mrad at the "injection point" in the straight section; this is better than the minimum requirement.

To inject light ions from the N = 4 cyclotron, two additional magnets such as A and A' (Figs. II.C-5 and II.D-2) are needed to bend the beam into the correct angle to pass through the open sector as described above. Since the part of the system already described is virtually isochronous, the combination A and A' must be isochronous also. This can be arranged by using a quadrupole set between them to reverse the image. The requirements on isochronism of the total system from the N = 4 machine to the N = 6 machine are not, in any case, so stringent because of the much higher velocity of the light ions.

Injection from the pre-injector into the N = 4 cyclotron is basically the same problem on a smaller scale and need not be discussed in detail.

Electrostatic deflectors in the tandem vault will steer the beam from the tandem to the cyclotron and may be supplemented, if necessary, by a second set along the path between the two accelerators.

d. Analyzer for the Extracted Beams from the N = 6 Cyclotron

After passing through the electrostatic deflector of the cyclotron, the beam forms a waist (4 mm wide in the radial direction) in the center of a straight section. It then passes through a pole section in a region where the field is flat (n = 0), and through another straight section, and part of another pole section before passing into a magnetically shielded channel. (Fig. II.D-3). It then emerges into a straight section where it travels at almost 20° to the last complete orbit. In the center

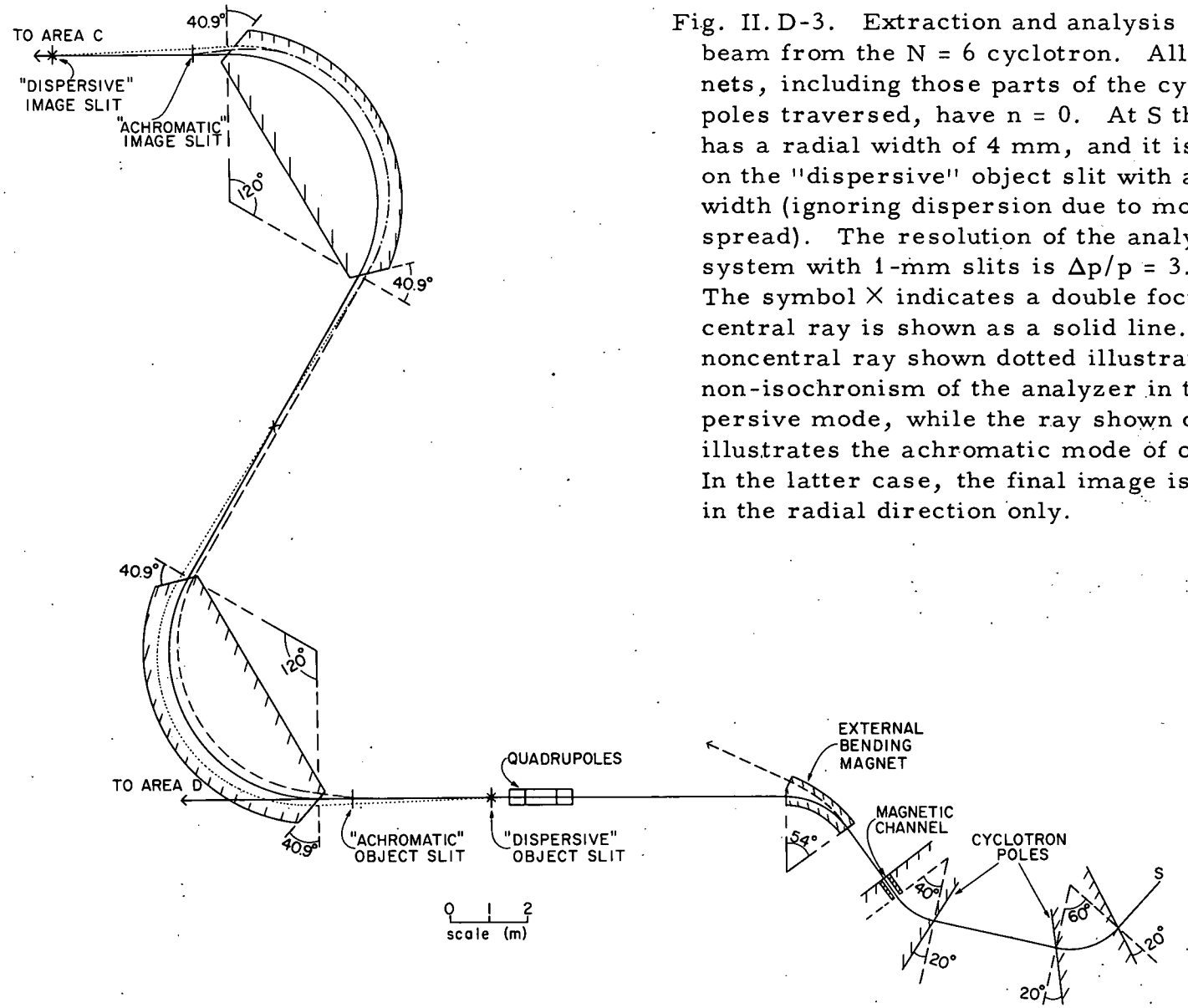

Fig. II. D-3. Extraction and analysis of the beam from the N = 6 cyclotron. All magnets, including those parts of the cyclotron poles traversed, have n = 0. At S the beam has a radial width of 4 mm, and it is imaged on the "dispersive" object slit with a 1-mm width (ignoring dispersion due to momentum spread). The resolution of the analyzer system with 1-mm slits is $\Delta p/p = 3.3 \times 10^{-5}$. The symbol × indicates a double focus. The central ray is shown as a solid line. The noncentral ray shown dotted illustrates the non-isochronism of the analyzer in the dispersive mode, while the ray shown dashed illustrates the achromatic mode of operation. In the latter case, the final image is focused in the radial direction only.

of this section it is separated from that orbit by almost 34 in. At this point it enters a magnet which deflects it by 54° and directs it into a quadrupole set which focuses it into the beam line leading to the analyzer area and experimental area D.

The energy spread of the accelerated beam is expected to be $\leq 0.1\%$, depending on the effectiveness of the energy flat-topping. To ensure that a spread as small as 0.006% (20 keV at 350 MeV) can be obtained, magnetic analysis is being provided. We have chosen to have two flat-field magnets (n = 0) bending the beam 120° in opposite directions, with a focus between them. Such a system is double focusing provided that the edges of the magnet are at an angle of 40.9°.[3] The magnets have a radius of curvature of 12.4 ft; a slit width of 1 mm will give a momentum resolution width $\Delta p/p = 3.3 \times 10^{-5}$, which corresponds to 20 keV for 350-MeV protons. (A different possibility for the analyzer magnets would be two 120°, n = 0.5 magnets of the same radius of curvature; but these would take up more floor space and are presumably more difficult and expensive to make in such a large size. They would, however, have the advantage of being also double-focusing when used in the achromatic mode.[3]

The beam is diverging as it emerges from the bending magnet immediately after extraction and must be focused on the entrance slit of the analyzer by means of quadrupoles. In order to lose as little beam as possible in the analysis, the image should be only 1 mm wide (the source inside the cyclotron is almost 4 mm wide) and this can be achieved for the most energetic particles by means of a quadrupole triplet using very reasonable fields.

The beam before extraction has some radial dispersion due to the range of momentum contained in it; and as it is brought out through the n=0 regions of the poles, this radial dispersion is increased. Since the 54° bend of the extraction magnet is in the opposite direction

[3] J. J. Livingood, The Optics of Dipole Magnets (Academic Press Inc., New York, 1969).

to that of the cyclotron, the dispersion is reduced but it is not reversed since no image is formed by this magnet. On the other hand, the image formed by the quadrupole is reversed, and the dispersion is also so that it is in the proper direction to add to the dispersion of the first analyzer magnet. However, the cyclotron contributes very little to the dispersion of the total system because the quadrupole must introduce demagnification to match the beam to the 1-mm object slit of the analyzer.

The beam path has been calculated from the straight section in the cyclotron to the double focus at the output of the analyzer. The resolution of the total system with a 1-mm image slit is $\Delta p/p = 3.3 \times 10^{-5}$ to first order.

For many purposes, of course, such extreme energy resolution will not be required and more beam with poorer resolution can easily be obtained by opening up the slits. Indeed, the whole beam can be transmitted by opening them up completely. For a 0.1% spread in the extracted momentum, this would result in an image approximately 3 cm wide, and it would probably be better to operate the pair of analyzer magnets in an achromatic mode. In this case the quadrupoles would have to be readjusted to form an image on a set of slits placed at the "focal length" so that the beam becomes "parallel" between the two magnets and is then refocused by the second.[3] Unfortunately the system will not then be double focusing. This is not a serious effect, however, and it can be remedied by additional quadrupoles.

In the dispersive mode, the analyzers are not isochronous since there is an image between them. The total range in path length amounts to 9.5 cm, which corresponds to less than 0.5 nsec for a 350-MeV proton and about 2 nsec for a heavy ion with an energy of 10 MeV/nucleon. An additional amount, <0.5 cm, is introduced by the magnets during beam extraction. The latter is unavoidable, but the former can be reduced by limiting or reducing the radial divergence of the beam, depending somewhat on whether the highest energy resolution

is required at the same time as the shortest pulse. Of course compensation can be introduced by a subsequent magnet, as discussed in Sec. II. D1b. In the achromatic mode the system is isochronous; the unavoidable spread in arrival time of the unanalyzed beam (the result of a 0.1% spread in momentum) is about half of the corresponding values just given for the dispersive mode.

Slit systems for high-energy protons have not been worked out in detail. Quite possibly they will be fairly thin and will operate by degrading the energy of the unwanted particles so that they can be cleaned out by a subsequent magnet.

e. Cyclotron Beams

The beam that the analyzer, either dispersed or achromatic, transports into area C is distributed by a powerful switching magnet, capable of bending the most energetic particles through $\pm 30^{\circ}$. Of course less rigid particles can be bent to greater angles. A number of beam lines will be equipped with suitable quadrupoles. Beam lines parallel to the long dimension of the room will need several quadrupoles distributed along them to enable particles (presumably energetic protons) to pass through several different potential experimental stations and on to a beam dump. Provision will be made for placing a second switching magnet half-way along the area to give extra beam lines.

When the analyzer magnets are not actuated, the nonanalyzed beam passes directly into area D, where it is distributed by a switching magnet similar to that in area C. As in area A, there will be five beam lines at 15° intervals. It is not necessary to bend the beam quite as far as 54° in extracting it from the cyclotron. If it is bent about 30°, it will just miss the nearest yoke and can be taken into the analyzer area. This is a convenient place for intense chemistry bombardments. The beam could be taken on into experimental area C if necessary, and this line could be looked on as an alternative to the analyzer as a transport mechanism to this area.

The whole area to the south of the MTC is open and available for long time-of-flight paths. The direct beam through area D would be most useful for this purpose unless high energy resolution was required. Provision will be made for running time-of-flight tubes through the concrete-and-earth shielding at several strategic locations.

f. Control Computer

The proposal includes a small computer to be used in the operation of the accelerators. A data interface will link it to many of the recording and control instruments. It is obvious that such a computer can very readily record an enormous amount of data on running conditions, can reproduce these as a guide on later occasions, and can take action during a run if this should be required. (For example, faulty beam transport and consequent high radiation levels could cause the computer to give warning or shut off the beam.) This is perhaps the most elementary level of use. The next level might be for the operators to direct it to calculate correct operating conditions as need arises. Lastly, the computer could be programmed to make operating decisions on the basis of information it receives from the monitoring instruments and to adjust magnet currents, rf frequencies, etc. to optimize conditions. This matter has not been worked out, but we believe that such a computer would be able to take over part of the operation of the accelerators. For this reason, all of the controls will be arranged to be adaptable for digital reading and operation, and we intend to have beam-position monitors that are adaptable to such interfacing.

g. Multiple Use of Beam

In the case of high-energy light particles, we believe that it may well be possible to have more than one experiment operating simultaneously—one after another along the same beam line.

In the case of the heavy ions, it may be possible to have a number of users of the same beam after it has been stripped to a high charge state. The main user will select his beam by means of a magnet, and those charge states not selected will be bent either more or less (the value of $B\rho$ will vary in steps of roughly 3%) and might be usable in another experiment. The most obvious possibility is the production of radioisotopes by bombardment of targets placed in the image plane of a 90° analyzer. It is also clear that a switching magnet could be used to spread a number of differently charged beams in an experimental area (e.g., area B). The extent to which this idea can be used depends on how many experiments can make use of the less intense fractions of a beam without disturbing a major user who is accepting the most intense fraction. If the demand were great enough to justify it, it would be possible to arrange always to have some part of the unused beam available in area B whenever the tandem beam was directed into area A or C. However, no details have been worked out.

Similar possibilities for multiple use exist with the beam from the cyclotron, except that there the magnet systems are usually able to handle the beams without further stripping and fractionating, so that there is not necessarily a part that is normally unused.

Another possibility, which applies to the tandem used alone, is that of accelerating two different ion species at the same time—e.g., protons and uranium ions. This could only be done, of course, if no charge selection were done in the terminal (i.e., dc operation of the tandem alone), so several charge states would be accelerated and the heavy-ion beam would be complex. For some purposes (e.g., bombardment to produce radioisotopes), this complexity might not matter; the light ions could be peeled off with the 90° analyzer while the heavy ions, being little deflected, could be available in area B. This possibility has also not been worked out in detail.

2. Experimental Equipment

In this discussion of experimental equipment to be used with the MTC, there is no intention of making an exhaustive list of all the apparatus that may ultimately be installed, but rather to indicate those items that will be provided at the start of operation.

The plans are based on the assumption that when the MTC comes into use, the experiments at the existing 60-in. cyclotron at Argonne will be transferred to the new accelerator. An immediate consequence of this will be that a number of pieces of apparatus can then be moved to the MTC. Among these is a split-pole (Enge) magnetic spectrograph[4] (Fig. II. D-4) which can bend particles with ME/z^2 up to about 95 amu-MeV, and can achieve an energy resolution $E/\Delta E = 2000$. This instrument will be very useful with the tandem beams; and with the energetic heavy-ion beam from the cyclotron it may be applicable to examination of (highly stripped) heavy products. (Its magnetic field is not powerful enough for energetic light-ion beams or for the light products from bombardment by energetic heavy ions.) It would be mounted either in the tandem-only room A or in the adjacent section of the large experimental area C where it could be reached by a beam from either machine independently.

There is also a precision 60-in. scattering chamber,[5] shown in Fig. II. D-5, which has been in use at the cyclotron for many years. This instrument can be used to measure angular distributions in elastic scattering and nuclear reactions with a high degree of accuracy. Its large dimensions also make it suitable for measuring the time-of-flight of heavy ions.

---

[4] J. E. Spencer and H. A. Enge, Nucl. Instr. Methods 49, 181 (1967).

[5] J. L. Yntema and H. W. Ostrander, Nucl. Instr. Methods 16, 69 (1962).

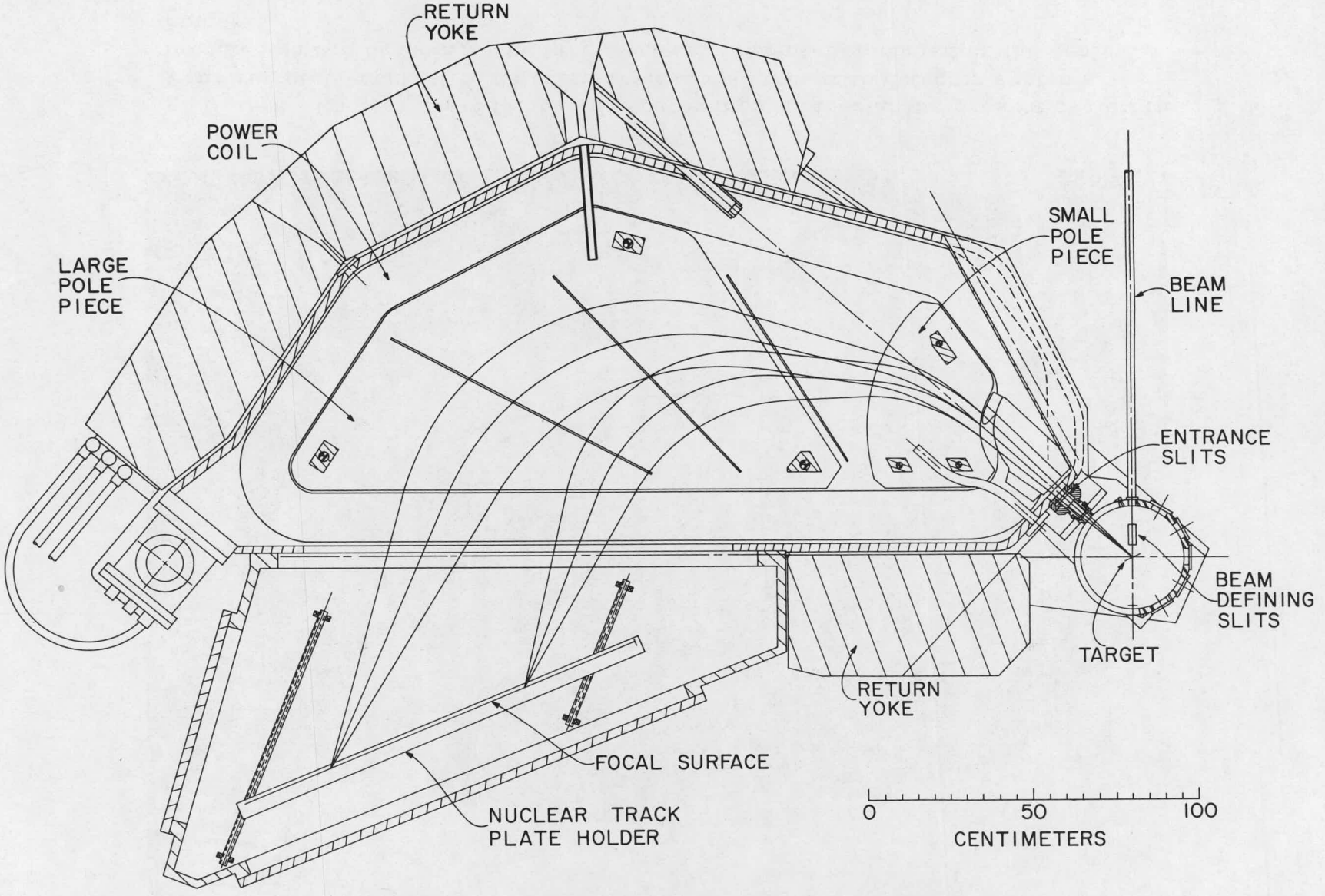

Fig. II. D-4. The split-pole magnetic spectrograph.

Fig. II. D-5. Photograph of the 60-in. scattering chamber at the present cyclotron. Four remotely-controlled detector arms are shown, with detector systems mounted on two of them. The target wheel is normally mounted on the central spindle.

There are two 18-in.-diameter scattering chambers[6] (Fig. II. D-6) which are used at present in a variety of experiments, including the scattering and reactions of charged particles, charged-particle-induced fission, and charged-particle—γ-ray coincidence measurements. These scattering chambers are designed for maximum flexibility (including portability) and for easy interchangability of components, so that they can be adapted to quite different experiments and can be used by several groups of experimenters. These will accommodate experiments on the tandem and with any of the heavy-ion beams.

A number of magnets and quadrupoles are used in the experimental areas of the present cyclotron. These include two switching magnets and the magnet used to bend the beam into the spectrograph. These will also be available for the MTC experimental areas.

A substantial amount of electronic equipment is in current use by three groups of experimenters, much of it very up-to-date. This includes several multichannel analyzers and the associated linear and fast-coincidence circuits.

A data link to the Sigma-7 computer in the Chemistry Division is at present being installed at the cyclotron. This can also be moved to the data room of the MTC and will provide some direct on-line computing capacity for experiments.

In addition to the equipment definitely available from the cyclotron, some equipment in use at the existing tandem will also be moved to the MTC though it is impossible to specify this in advance. The possibilities include another 18-in. scattering chamber, a 28-in. chamber and, with rather more difficulty in transportation, a large γ-ray coincidence goniometer which in its present location is computer controlled. Of course there are also smaller components such as Ge(Li) γ-ray counters and electronic units which are easily taken where they are needed.

[6] J. T. Heinrich and T. H. Braid, unpublished; J. T. Heinrich, Nucl. Instr. Methods 31, 337 (1964).

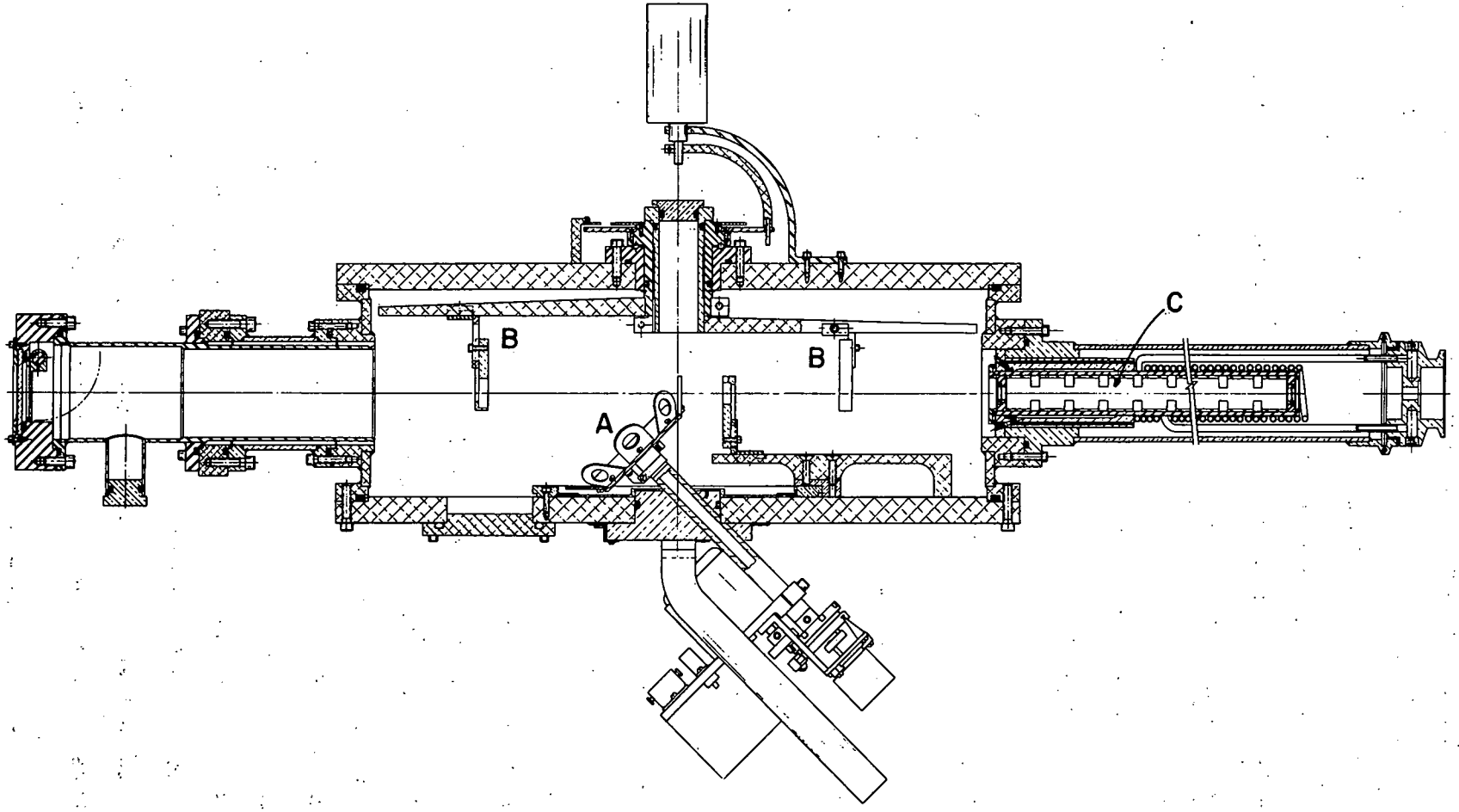

Fig. II. D-6. An 18-in. -diameter scattering chamber. A—target changer, B—counter arm, C—collimator.

It is to be expected that some groups of outside users will wish to establish some items of equipment in the experimental areas; but even without this, the apparatus mentioned would enable a healthy program to be carried on with all types of particles accelerated by the tandem, and also with both heavy ions (all energies) and the less energetic light ions from the cyclotron. For the more energetic light ions, conventional scattering chambers will presumably not be used in any case; for many experiments we shall have ad hoc arrangements of vacuum pipe for flight paths of scattered particles or even flight paths in the open air with spark-chamber or multi-wire proportional counters as detectors, as is customary in high-energy physics experiments. (We already have a group acquiring experience on these latter devices.)

For chemistry experiments, the proposal includes five laboratories for radioactive work—convenient to the area in which sources will be prepared. It is assumed that one of these will be a "cold" room for target preparation, one will be an alpha laboratory, and that three will be used for β-γ work at various levels of intensity. The furniture for these laboratories includes glove boxes, radiochemistry hoods, radioactivity hoods, fume hoods, sinks, benches, chemical storage cabinets, etc. and should completely equip them for radioactive experiments.

It has already been mentioned (Sec. II. E) that the proposal includes a fast rabbit to enable sources to be transferred rapidly from one area to another in the MTC and from there to the shielded cave facility in the Chemistry Building.

II. E. ARGONNE FACILITIES DIRECTLY RELATED TO MTC EXPERIMENTS

The kinds of experiments planned for the MTC can be considerably extended through the use of facilities already built and staffed at Argonne. It is planned that a number of the general-type facilities will be made available to users of the new accelerator. The specialized facilities, mostly elaborate and unique experimental setups, are at present involved in experimental programs; but the responsible experimenters are planning to take advantage of the unusual experimental opportunities provided by the MTC.

1. Hot Laboratory for High Activities

The $ 4.3 million hot laboratories in M wing of the Argonne Chemistry Building will play a crucial role in the effective use of the MTC, since irradiated targets will often be too radioactive to be handled in ordinary radiochemical laboratories. These existing laboratories will provide a number of heavily-shielded well-equipped caves and a trained technical staff to operate them. Sophisticated master-slave manipulators allow many physical and chemical operations to be done on the target while it is observed through large windows that absorb the radiation. Since many radioactive species of interest are expected to be short lived, the usefulness of this facility to accelerator experiments will be considerably enhanced by a pneumatic rabbit to be installed between the accelerator building and M wing. Hot targets can then be transferred in times well under a minute.

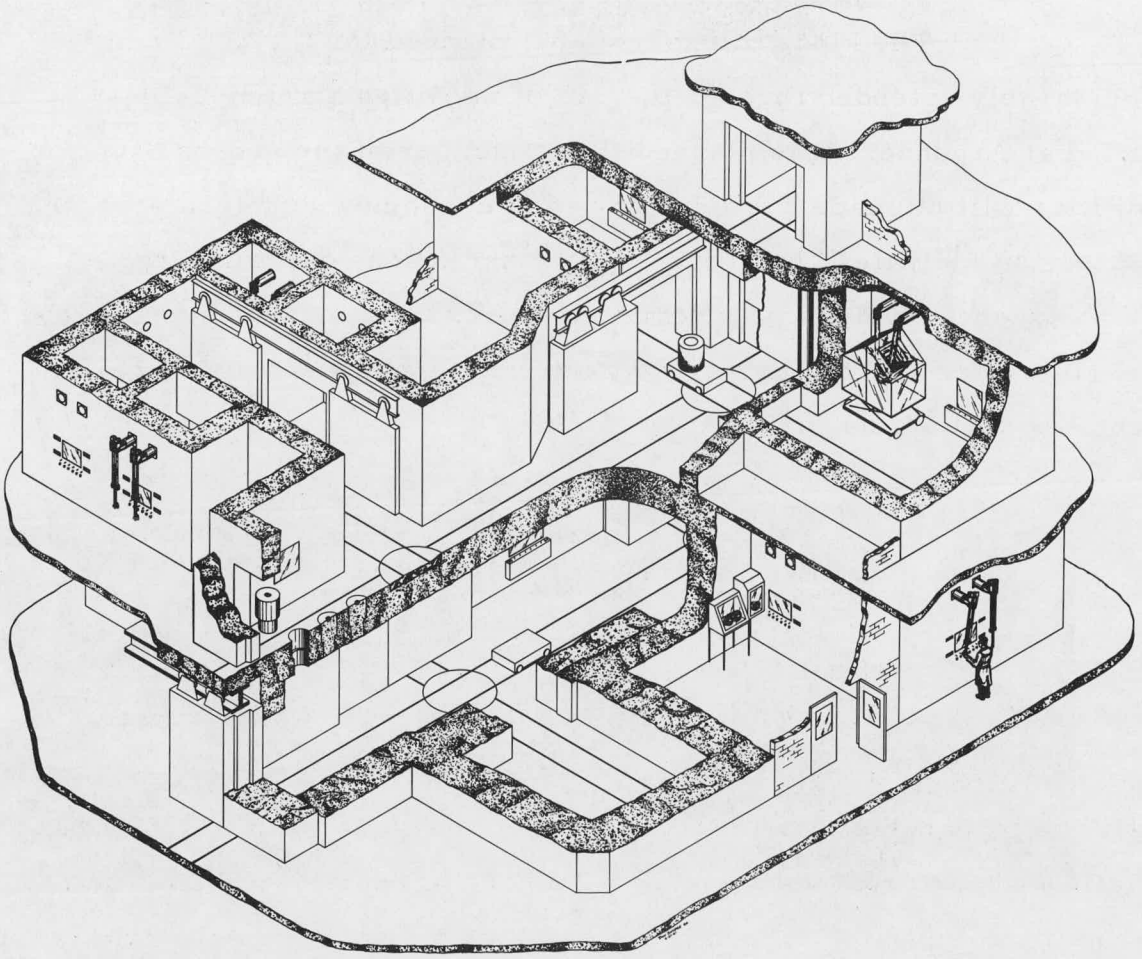

Fig. II. E-1. Three-dimensional view of the cave facility.

A variety of cells are available in the hot-lab facility (Fig. II. E-1); their radiation shielding capabilities range from 30 to 10^6 Ci of 1-MeV gamma activity. In addition, within some cells there are many relatively thin barriers designed to minimize the possible spread of alpha activity. Among hot laboratories, these cells are unique in that they are designed to shield against high neutron levels as well as high gamma-radiation levels. When samples with large amounts of heavy elements such as Cf^{252} are handled, spontaneous-fission neutrons may be even more hazardous than the gamma radiation.

The hot laboratories may be used quite efficiently. For example, the cell complex was designed so that all of the cells are independent. Hence, one experimenter may work in a particular cell

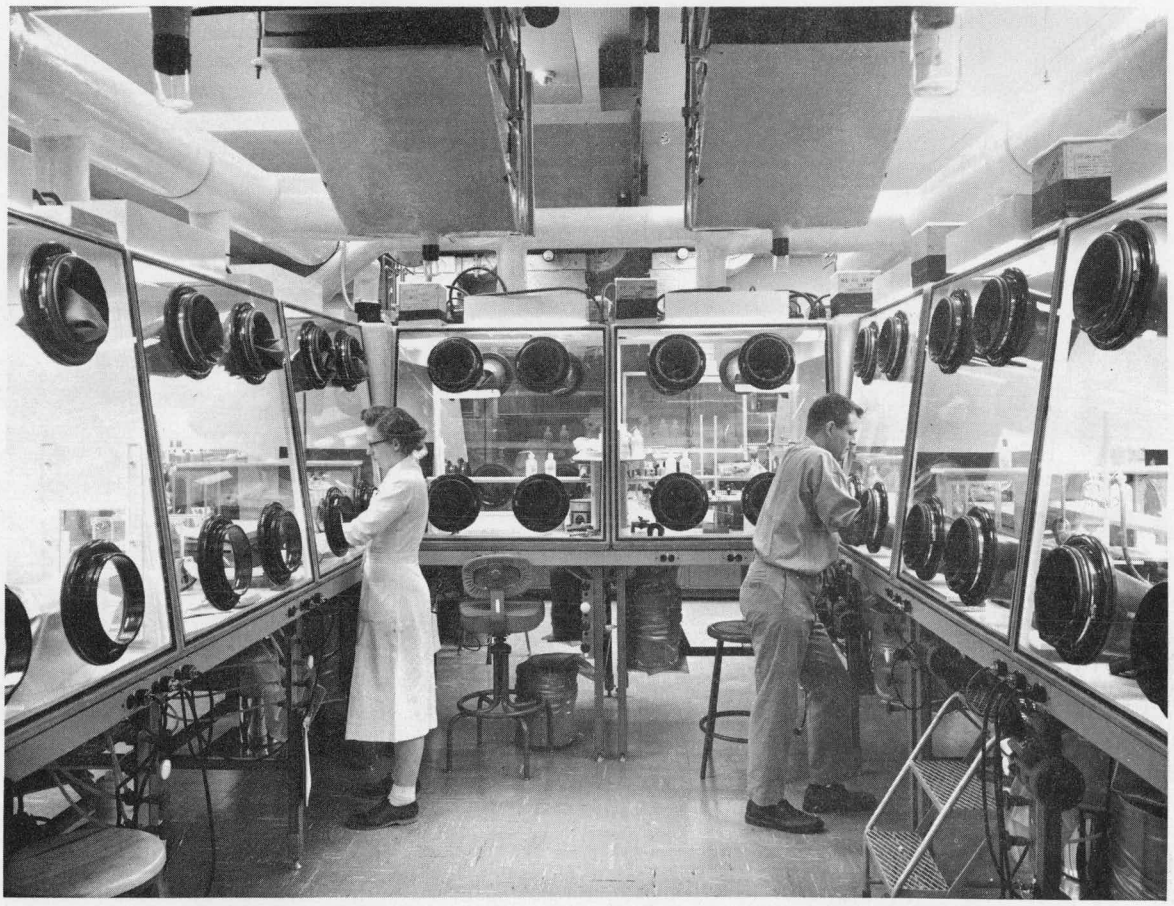

Fig. II. E-2. Typical alpha-activity laboratory with glove-box lines.

while another experimenter is setting up in a neighboring cell. Elaborate storage and waste-handling facilities allow rapid throughput of high-level activities. Further, for experiments involving a high risk of cell contamination, five of the cells are unusually large so that they are capable of holding within-cell containment boxes. These boxes minimize cell contamination, so that a new experiment can be installed almost immediately after another has been finished. Because cleanup time is minimal, with prior arrangements an experimenter can usually schedule the use of a cell.

For handling highly alpha-active and/or spontaneously fissioning transuranic targets, a ventilated glove box (Fig. II. E-2) is more convenient if the beta and gamma levels permit. Here, too, the use of a glove box in the M-wing facility can be scheduled by experimenters.

2. Isotope Separator

In the same wing as the caves and the alpha glove boxes is the isotope separator (Fig. II. E-3), which may be used for the preparation of thin targets or for the separation of reaction products after bombardment. Since its installation, the separator has been used to prepare hundreds of targets for use in the Van de Graaff accelerator and cyclotron at Argonne as well as for use in accelerators at many universities.

A particular virtue is its relatively high resolution. In a single pass, the enrichment is about 100 times that of the Oak Ridge Calutrons, so that a target with isotopic purity exceeding 99% is readily obtained.

The isotope separator is also useful in preparing targets for which separation per se is not required but for which target material is to be deposited on a thin and fragile supporting foil. By retarding the

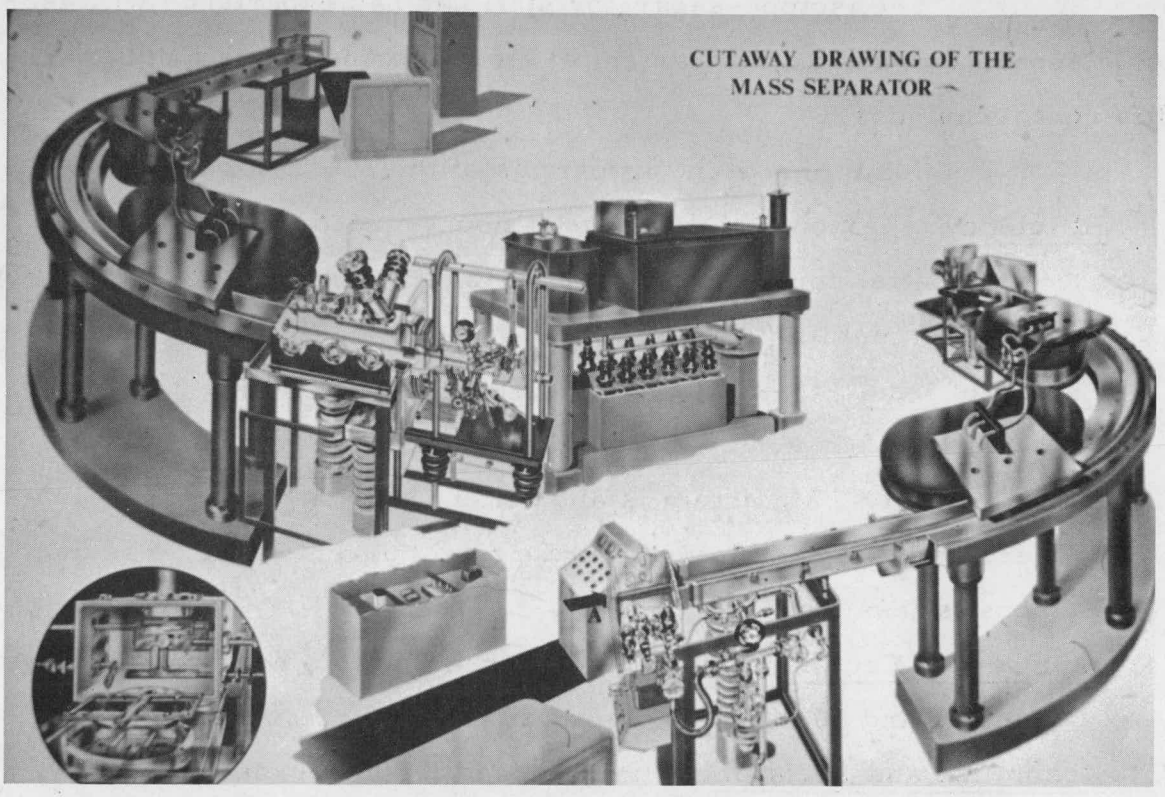

Fig. II. E-3. Cutaway view of the isotope separator.

ion beam so the particles have little energy at the collector, densities up to 1 mg/cm^2 have been built up on 50-μg/cm^2 carbon films. This collection process deposits valuable material more efficiently than does evaporating separated material onto a foil.

The separator has been designed to handle quite radioactive sources. It has been used to separate curie levels of both beta and alpha emitters, levels frequently attained in freshly bombarded targets. With the rabbit facility terminating in the same building, reaction products of quite short half-lives can be handled. In a number of cases, it has taken less than 5 min to separate the desired product from a target brought to the separator.

The isotope separator has also been used to directly form very thin radioactive sources for α or β spectrometry. The beam-retarding capability serves to keep the radioactivity from burying itself in the foil.

The isotope-separator staff has had experience with isotopic separations for a wide variety of elements and with a number of different techniques.

Some important properties of the separator are:

(1) Efficiency = [Amount collected]/[Amount placed into source]. 5% or better for most elements. Exceptions: Mo, Ta, W (~1%), platinum metals (< 0.1%).

(2) Energy of Ions. 15—70 keV (typically 50 keV). With a retarded beam: 0—5 keV.

(3) Beam Intensity. Maximum is about 100 μA for a single mass number, with the restriction that the total current in all mass numbers is less than 250 μA.

(4) Enrichment Factor. Typically 1000 relative to a neighboring mass number and 30 000 for a separation of two mass units.

(5) Beam Size and Location. Minimum width about 1 mm; height variable from 3 to 50 mm. The beam can be oscillated to spread material over a larger area.

(6) Separation. (1680 mm)/A for masses A and A + 1.

(7) Penetration into Target. At full energy, typically about 10 $\mu g/cm^2$.

(8) Saturation Concentration. About 5 $\mu g/cm^2$ in an aluminum target.

3. On-Line Computer Facility

An on-line computer system is an essential feature of a modern accelerator. Although the field of computer technology is advancing so rapidly that it is difficult to anticipate developments five years in the future, for the initial experiments at the MTC we tentatively plan to make use of the excess capacity of the central multi-programmed real-time computer facility now being developed for the Chemistry Division. In this facility, based on a Sigma 7, a single central computer will be used to service a number of experiments in the Chemistry Building and at the present cyclotron. Each experiment feeds data directly to the central computer and obtains partial analysis in real time; final analysis occurs at the end of the experiment.

The Operating System (executive control program and various processors) has been designed and implemented at Argonne. This system provides a multi-programming environment for a large number (limited only by memory size) of concurrent memory-resident programs, each associated with a particular experiment. Electronic interfaces link the remote experiments and the computer. Data rates up to 10^5 characters/sec are obtainable over coaxial cable at distances up to 2000 ft. The proposed sites of the MTC are well within this distance from the computer site.

Under current plans, the central computer facility will use only about 20% of its input/output bandwidth when in full use and the central processing unit (CPU) is expected to have about 40% of its computational capability unused. The excess capacity would be used for monitoring several accelerator experiments in real time. Providing a continuously updated display of a 512×512 two-parameter experiment

would require about 20% of the CPU capacity and 33% of a single "random-access disk" bandwidth (2 disks are planned).

While it is difficult to accurately predict the future usage of the computer system, both as to the expected number of simultaneous uses and their requirements, it is certain that the system could readily provide simultaneous real-time services for some experiments at the MTC during the initial stages of its operation.

4. Argonne Tandem Van de Graaff Facility

Because a tandem Van de Graaff is an integral part of the MTC, the existing Argonne tandem and its supporting facilities constitute an invaluable asset for the effective use of the proposed new system.

The existing accelerator, a model FN tandem converted from an EN, is capable of operating at 8.5—8.75 MV and of delivering high-resolution beams of a variety of types from protons to argon ions. The beam is magnetically analyzed and then steered into either of two areas; in each, one of five beam lines is activated with a beam-switching magnet (Fig. II. E-4). In the experimental areas are several scattering chambers, a broad-range magnetic spectrograph, a split-pole magnetic spectrograph, and a gamma-gamma angular-correlation device.

The FN tandem provides a facility that will be of great value in developing and operating the MTC. Many important questions regarding strippers, charge-state selection, and even ion-source development will need to be tested on the FN. In addition, when the proposed facility is in operation, the FN tandem will be used to develop some experiments and experimental systems.

Perhaps the most important contribution from the FN to the MTC is that the latter can take over and continue a highly developed and effective experimental program at the former. In particular, the

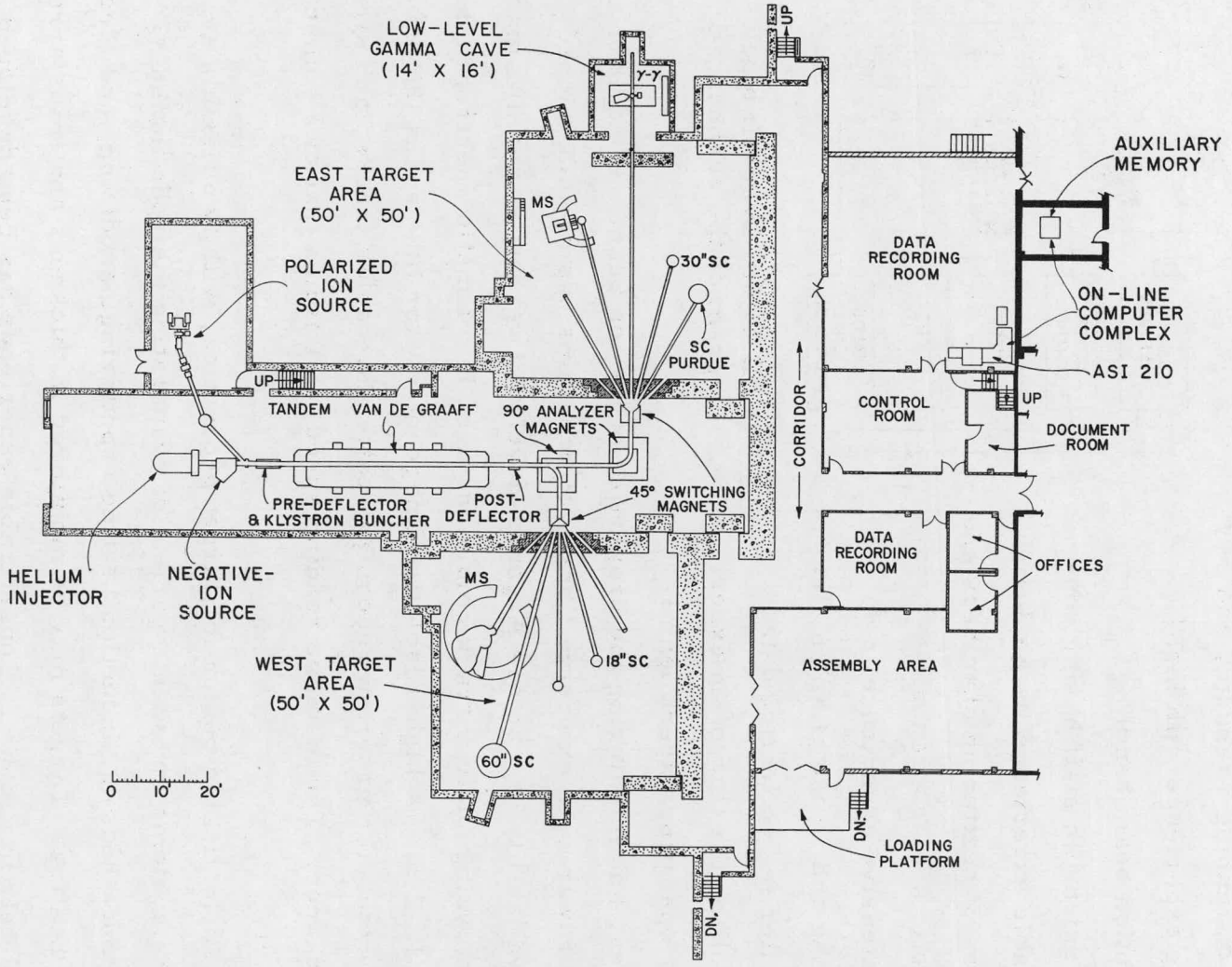

Fig. II. E-4. A plan view of the present tandem Van de Graaff accelerator and its experimental facilities.

advantages to the MTC program include:

(1) A staff familiar with the problems of running a tandem, and having experience with high-resolution beam handling.

(2) A scientific staff having considerable experience in the design and use of scattering chambers and magnetic spectrographs.

(3) Extensive experience in data-handling and in use of an on-line computer for collecting data, controlling the flow of an experiment, operating experimental devices, and monitoring the properties of the ion beam. In addition to the hardware, an extensive library of programs has been developed.

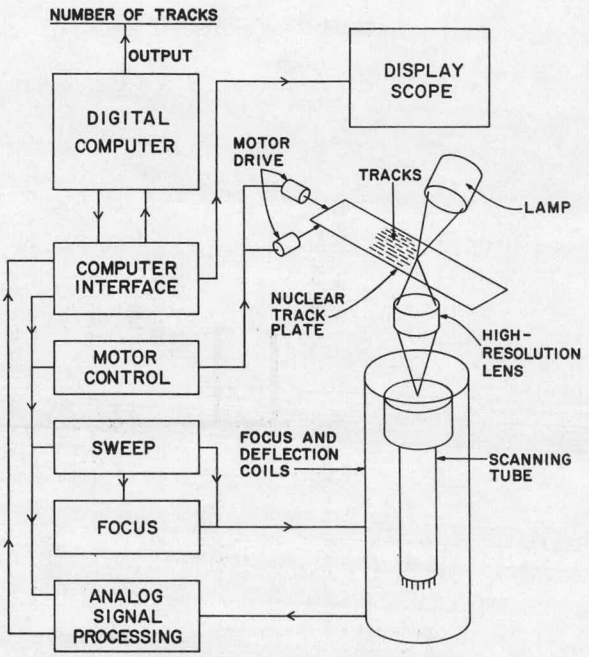

Fig. II. E-5. Over-all block diagram of the scanner

(4) Availability of a unique Argonne-developed versatile scanning machine[1] for analyzing nuclear track emulsions used in magnetic spectrographs (Fig. II. E-5). A high-resolution image-dissector tube scans the emulsion and a computer program recognizes patterns, counts tracks, and directs the scanner. The machine reading speed is 50 times that of a human scanner.

(5) A sophisticated center for target production, with two flexible evaporating systems and with a variety of evaporating methods including resistance heating, induction heating, sputtering, anodizing, and electron-beam heating. Targets may be monitored in thickness and transferred completely in vacuum. Considerable experience has been developed

---

[1] J. R. Erskine and R. H. Vonderohe, "Automatic Counting of Tracks in Nuclear Emulsions," Conference on Computer Systems in Experimental Nuclear Physics, Skytop, Pennsylvania, 3-6 March 1969, paper IV. B1.

for evaporating targets of exotic materials. The Metallurgy Division has developed facilities and experience for producing very thin self-supporting foils as thin as 250 $\mu g/cm^2$.

(6) Elaborate facilities for preparing, installing, and using highly radioactive heavy-element targets with minimal contamination or health hazard. (For example, 0.5 Ci of Cm^{244} has been used with no spread of contamination.)

(7) Experience with making and using polarized-ion sources.

5. Facility for Making Monocrystalline Metal Foils

Because of channeling effects, ionization processes in monocrystalline foils differ from those in ordinary polycrystalline foils. In particular, the crystalline channels tend to concentrate the ions into beams with little angular spread. This improved emittance may be of importance in a foil stripper. Monocrystalline foils as thin as 8×10^{-5} in. have been prepared by etching and electropolishing; and monocrystalline foils 5000 Å (2×10^{-5} in.) thick have been made by epitaxial growth through vacuum deposition.[2]

6. High-Resolution, High-Transmission Double Beta Spectrometer

Testing of theoretical fine structure in the (A, Z) region to be made accessible by the MTC, particularly in regions of predicted quasi-stability, depends heavily upon a detailed elucidation of level schemes and level properties. On the basis of estimated production

[2] M. Kaminsky, in ANL Physics Division Annual Review, April 1967—March 1968 (Argonne National Laboratory, Argonne, Illinois, 1968), Report No. ANL-7481, p. 152; Argonne National Laboratory Physical Research Program Budget, Fiscal Years 1969, 1970, and 1971, p. 237; ANL Physics Division Annual Review, April 1968—March 1969 (Argonne National Laboratory, Argonne, Illinois, 1969), to be published.

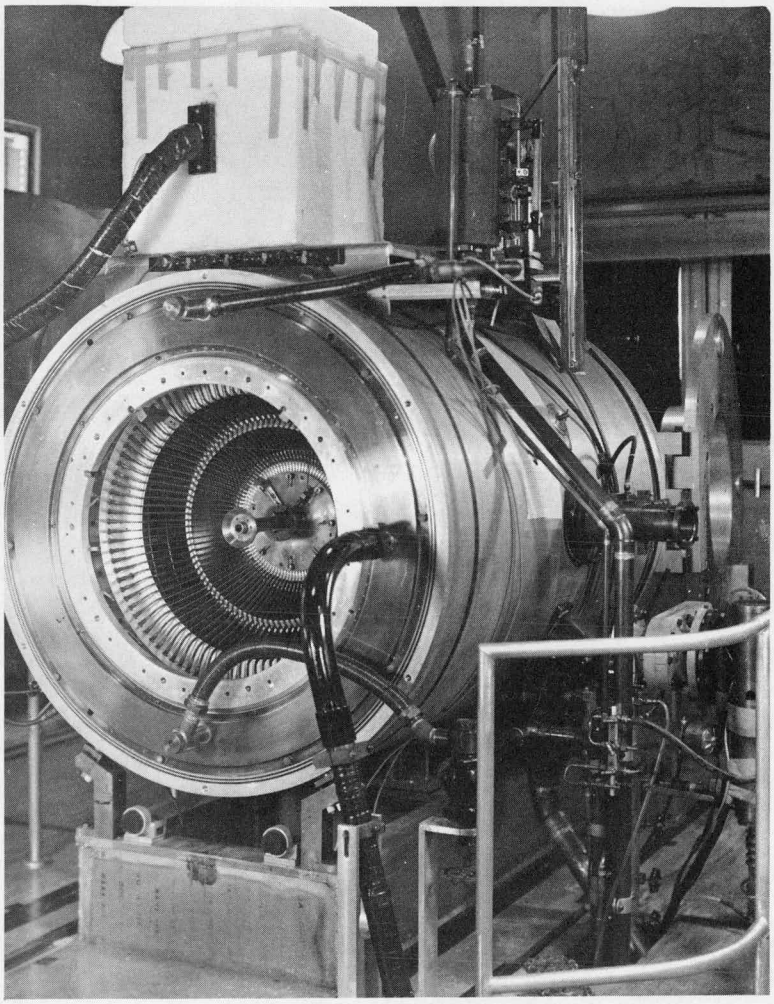

Fig. II. E-6. Dual, sliced-orange β spectrometer.

cross sections, it appears that a significant number of nuclides can be made in the nanocurie intensity range with lifetimes exceeding a few minutes. With the unique ability of the Argonne toroidal double beta spectrometer (Fig. II. E-6) to give very high transmission without sacrifice of its high resolution, it should be possible to conduct such investigations even on such small samples, with efficiencies comparable to those of solid-state detectors and with relative advantages in resolution and precision.

Measurement of de-excitation energies through examination of conversion electrons has several advantages over gamma-spectroscopic measurements aimed at the same result. These include the specific identification of atomic number, and the precision

measurement of electron-atom binding energies. The latter are of interest in calculating many quantities of importance for atomic theory in the trans-californium range, even including some outer-shell effects. Since the beta spectrometer is situated not far from the terminus of the pneumatic rabbit connecting the accelerator to M wing, it should be possible to measure nuclides with quite short half-lives.

Table II. E-I presents sample sets of the relevant operating parameters for the electron spectrometer, in comparison with those of the Chalk River double-focusing electron spectrometer (the best of numerous existing high-resolution precision instruments of this type).

TABLE II. E-I. Comparison between the operating parameters of the ANL toroidal electron spectrometer and the Chalk River double-focusing one.

ANL toroidal spectrometer		Chalk River
Single	Tandem	spectrometer
T = 18; R = 0.4	T = 16; R = 0.3	T = 1.0; R = 1.0
T = 9; R = 0.1	T = 12; R = 0.1	T = 0.3; R = 0.1
T = 0.9; R = 0.06	T = 4; R = 0.05	T = 0.1; R = 0.01

T = transmission (% of 4π).

R = resolution width (full width of a line at half maximum; %).

From this comparison one finds, for example, a 40-fold advantage in transmission for the ANL instrument, at a resolution (0.1%) typically used and generally adequate in such studies.

The instrument contains two spectrometers, back-to-back, in one vacuum envelope. They may be used in tandem to increase resolution with no appreciable loss in transmission or may be adjusted independently to allow measurement of coincidences between betas and conversion electrons or coincidences between conversion electrons and conversion electrons.

7. High-Resolution, High-Sensitivity Mass Spectrometer

Mass spectrometry can detect and identify a nuclear species whose half-life is too long for detection by counting radioactive decay products. The Argonne 100-in. mass spectrometer (Fig. II. E-7), in addition to having very high resolution, is also capable of high-sensitivity isotopic analysis of very small amounts of an element, such as those produced by cyclotron charged-particle reactions. In general, the sensitivity ranges from 10^{-17} g for Type A elements having ionization properties similar to the transuranic elements to 10^{-13} g for Type B elements difficult to ionize, such as Hg and Au.

If we consider the sensitivity limit for counting methods to be 1 disintegration per hour, the spectrometer is more sensitive for analyzing radioactive nuclides when the half-life exceeds one year for Type A elements or 10^{4} years for Type B elements. For cases in which the counting limit is 1 d/min, the use of the spectrometer is even more favorable (as seen in Fig. II. E-8). Examples where

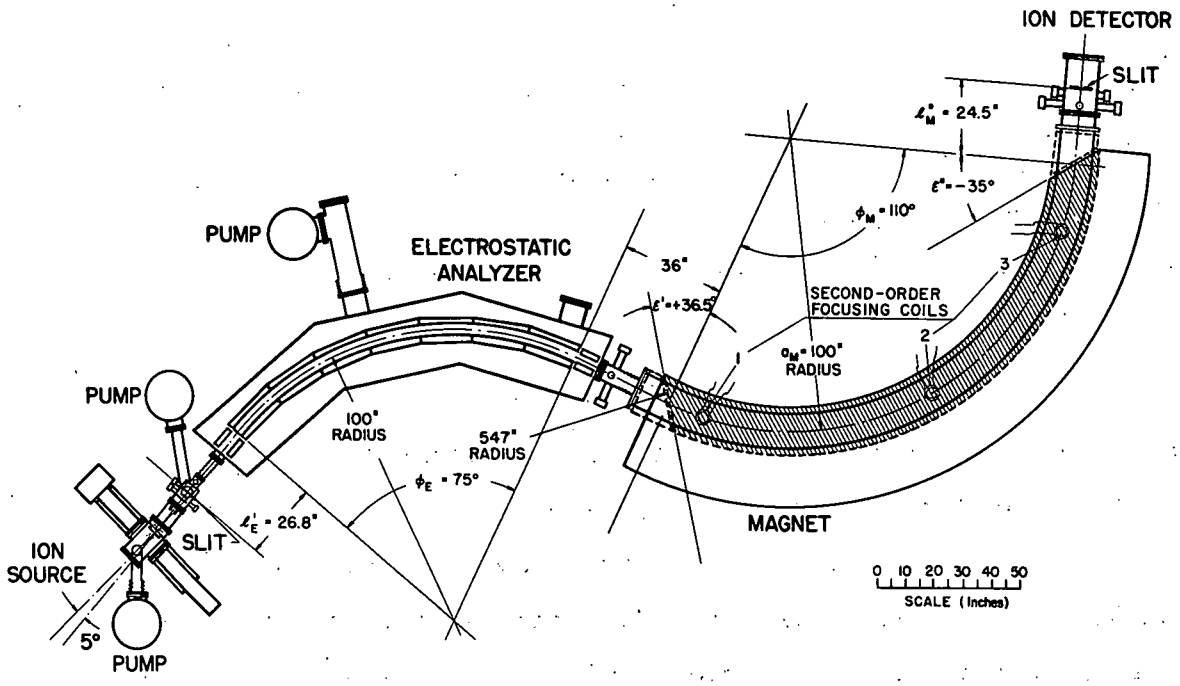

Fig. II. E-7. Plan view of the Argonne 100-in. -radius double-focusing mass spectrometer.

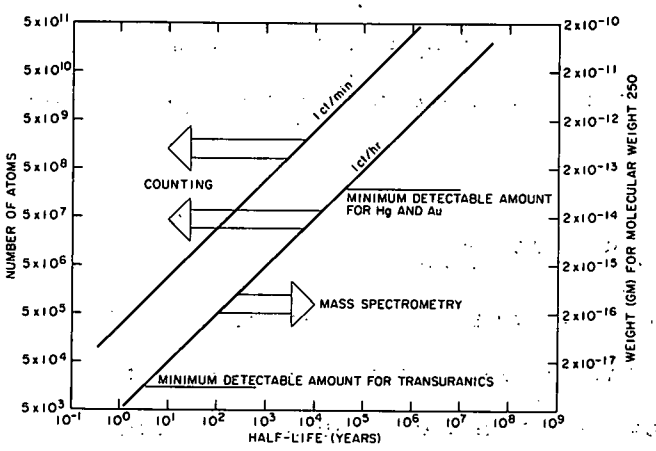

Fig. II. E-8. Sensitivity of mass spectrometry as compared with counting methods for detecting small amounts of radioactive nuclides. For very small amounts, the mass spectrometer is competitive at moderately short half-lives, particularly where counter backgrounds limit the useful counting rates.

mass-spectrometric detection has been used to discover long-lived nuclides and isomeric species produced by cyclotron bombardment are Pb^{202} and Pb^{205} [3], Bk^{248} [4], and Au^{198} [5].

The counting-preferred range of Fig. II. E-8 is calculated on the assumption that the radioactive emissions are readily detectable. Where the desired radiations are difficult to detect (as when they have very low energy or are obscured by other radiations) the use of mass spectrometry is even more favored—i. e., the boundary indicated in Fig. II. E-8 is moved to the left. Examples of such cases are found in the discovery of Cf^{251} (Ref. 6) and of Cm^{246} and Cm^{247} (Ref. 7).

The spectrometer has been used for and is capable of analyzing almost any of the elements. In view of the difficulty to be

---

[3] J. R. Huizenga and C. M. Stevens, "New Long-Lived Isotopes of Lead," Phys. Rev. 96, 548-550 (1954).

[4] J. Milsted, A. M. Friedman, and C. M. Stevens, "The Alpha Half-Life of Berkelium-247; A New Long-Lived Isomer of Berkelium-248," Nucl. Phys. 71, 299 (1965).

[5] Based on preliminary results of an experiment in progress.

[6] H. Diamond, L. B. Magnusson, J. F. Mech, C. M. Stevens, A. M. Friedman, M. H. Studier, P. R. Fields, and J. R. Huizenga, "Identification of Californium Isotopes 249, 250, 251, and 252 from Pile-Irradiated Plutonium," Phys. Rev. 94, 1083-1084 (1954).

[7] C. M. Stevens, M. H. Studier, P. R. Fields, J. F. Mech, P. A. Sellers, A. M. Friedman, H. Diamond, and J. R. Huizenga, "Curium Isotopes 246 and 247 from Pile-Irradiated Plutonium," Phys. Rev. 94, 974 (1954).

expected in identifying elements in the mass range around A = 298, this instrument may be very important in demonstrating their production.

8. Alpha Spectrometer

Investigation of decay schemes of alpha emitters in the regions of quasi-stability complements measurements made by beta spectrometry. On the basis of known systematics, the odd-A isotopes are expected to be the longer-lived nuclides and may be the only ones whose half-lives are long enough for extensive examination. The high-resolution measurements necessary for unscrambling the expected complex spectra are best carried out with a magnetic spectrograph. The resolution of solid-state detectors has not proved to be adequate.

This instrument, nearing completion, uses an array of solid-state detectors, which makes possible: (1) rejection of energy-degraded background alphas (by setting a pulse-height requirement), (2) simultaneous multichannel data collection over a range of about 120 keV, and (3) coincidence measurement with a γ-ray or electron detector at the source.

Basic instrumental resolution (without effects of source and detector widths) is $\Delta E/E \approx 0.05\%$ if ΔE is the half-width at half-maximum and $\sim 0.10\%$ if ΔE is the half-width at 1/10 maximum—both at a transmission of 0.13%.

II. F. SUMMARY OF PERFORMANCE CHARACTERISTICS

In this section the characteristics of the beams provided by the MTC system in its several modes of operation are summarized in one place. Unless otherwise stated, these results are given on the assumption that the system is operated under conservative "standard" conditions in which the terminal voltage of the tandem is 16 MV, a gas stripper is used in the terminal, a foil stripper is used between the tandem and the cyclotron, the cyclotron magnet has normal copper coils, and the ion-source currents are within the range of present technology.

There are a number of possible technical developments that could serve to increase the maximum energies and beam currents of the MTC well beyond those obtainable under the standard conditions specified above. For instance, if it becomes possible to use a foil stripper rather than a gas stripper in a terminal, heavy ions would be more highly stripped (as discussed in Sec. II. A4) and the maximum energies obtainable would increase markedly. Similarly, it may turn out that the TU tandem will operate up to the design voltage of 20 MV on the terminal (rather than only to the guaranteed 16 MV), and this would also increase the maximum energy. And again, the use of superconducting coils in the cyclotron would allow it to operate with higher fields and hence give higher maximum energies. As to beam currents, improvements in ion-source technology may well yield heavy-ion beam intensities substantially greater than the estimates given in this report. None of these improvements necessarily require a major expenditure of money, but rather they depend on technical developments that are not clearly feasible at this time.

Polarized hydrogen beams should present no serious difficulty for either the TU or the cyclotron. Within the five-year period before the MTC can be put into service, it seems likely that sources of polarized

ions—both positive and negative—will have developed sufficiently that microamperes of beam will be feasible. Even now, polarized negative hydrogen beam currents > 0.2 μA have been obtained at the University of Wisconsin and 0.6 μA at Los Alamos.

1. The TU Tandem Van de Graaff

The beam injected into the tandem consists of singly-charged negative ions which are then accelerated to the terminal voltage V (up to at least 16 MV), stripped of electrons to a charge state q, and accelerated to ground potential as positive ions. They then have an energy $E \approx V(1 + q)$. For ions heavier than boron, the most probable value is $q \approx 6$ when $V = 16$ MV; ions in higher and lower charge states are also produced, but with lower intensity. This aspect of electron stripping is treated in more detail in Sec. II.A5.

The output currents of the tandem will be limited either by the ion source or by the current-carrying capacity of the TU (60 μA of time-averaged current both for the incident negative beam and for the positive ions accelerated from the terminal).

The energy resolution width of the particle beams from the TU tandem will be a few parts in 10^4. The beam will be dc unless pulsing is required, in which case a time-resolution width of about 1 nsec will be readily achievable.

The characteristics of hydrogen and helium beams are summarized in Tables II.F—I and II.F—II. Here and in Table II.F—III, dc operation of the tandem is assumed.

The beam currents expected from the tandem for some heavy ions are given in Table II.F—III. Except for U^{238}, the indicated currents are within the range of present source technology. For the uranium beam, it has been assumed that a source output of 50 μA of UF_5^- ions will be attainable by the time the MTC is in operation. This expectation is reasonable and is supported by reports on ion sources used in the Manhattan Project, where it was found that UF_n^- beams were

TABLE II·F-I. Characteristics of hydrogen beams from the TU tandem and from the cyclotron.

	Energy range p (MeV)	Energy range d (MeV)	Beam current (10^{12} particles/sec)
TU tandem	6—32 (40)[a]	6—32 (40)[a]	180
Cyclotron	50—350	30—200	50

[a]Maximum energy calculated for a 20-MV terminal voltage.

TABLE II·F-II. Characteristics of helium beams from the TU tandem and from the cyclotron.

	Energy range He^3 (MeV)	Energy range He^4 (MeV)	Beam current (10^{12} particles/sec)
TU tandem	6—48 (60)[a]	6—48 (60)[a]	36
Cyclotron	48—510	48—400	10

[a]Maximum energy calculated for a 20-MV terminal voltage.

TABLE II·F—III. Maximum beam currents of heavy ions (10^{12} particles/sec).

Ion species	O^{16}	F^{19}	Cl^{35}	Br^{79}	I^{127}	U^{238}
TU tandem	50	40	40	40	40	30
Cyclotron	10	10	7	1.5[a]	1[a]	0.7[a]

[a]These currents are not limited by the current-carrying capacity of the TU. See text for further explanation.

comparable in intensity to the most intense positive beams.[1] Even though there has heretofore been no major incentive for developing negative uranium beams, a current of 5 μA has already been reported from a diode source. The maximum energies of heavy ions accelerated by the tandem under various sets of assumptions are given in Table II·F-IV. The selection of ions does not imply that these are the only species that could be accelerated (as discussed in Sec. II.A).

2. Cyclotron

The energy resolution width of the cyclotron beam is expected to be $\Delta E/E < 10^{-3}$. An analyzing system included in this proposal will reduce the width to $\Delta E/E \approx 10^{-4}$, but this improvement may involve some loss of beam intensity.

The time characteristics of the cyclotron are tied rather closely to the energy resolution. To achieve an energy resolution $\Delta E/E \approx 10^{-3}$ in the cyclotron itself, a duty cycle of 0.7% is required when there is no flat-topping of the rf voltage on the dees; flat-topping allows the duty-cycle to be about 10%.

The characteristics of hydrogen and helium beams provided by the cyclotron are summarized in Tables II·F-I and II·F-II. For these light ions, the energy range covered does not depend on whether the tandem or the small cyclotron is used as an injector.

Even when used with its small cyclotron injector, the main cyclotron will have some capabilities for accelerating heavy ions. For example, it could accelerate C^{4+} to about 500 MeV and O^{4+} to about 400 MeV.

3. The Tandem-Cyclotron System

The beam intensities for representative heavy ions accelerated by the tandem-cyclotron system are given in Table II·F-III, where

---

[1] A. Guthrie and R. K. Wakerling, Characteristics of Electrical Discharges in Magnetic Fields (McGraw-Hill Book Co., Inc., New York, 1969), p. 156.

one sees that some of the intensities given are limited by the currents available from present ion sources. With the expected improvements in ion-source techniques, by the time the system comes into operation beam intensities will probably be limited by the current-carrying capacity of the tandem accelerator tubes, in which case the beam intensities for Br, I, and U will be about three times those listed in the last line of Table II·F-III.

The energy resolution and timing characteristics of the tandem-cyclotron system will be the same as those described above for the cyclotron alone.

For U^{238}, the charge distribution after the second stripping is so broad that the yield decreases rather slowly with increasing energy so that, if the maximum beam intensity is not required, the energy range achievable may be considerably extended. This effect is illustrated in Fig. II·F-1 for U^{238} and Fig. II·F-2 shows a similar though smaller effect for I^{127}.

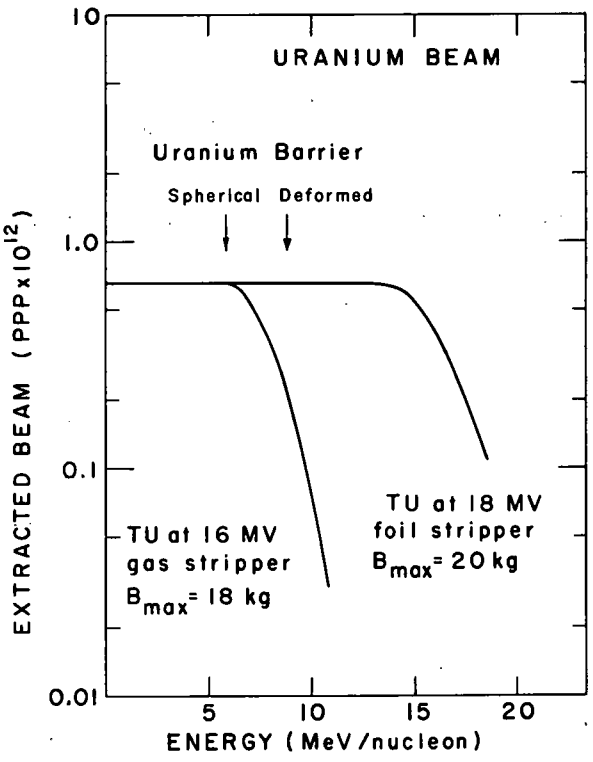

Fig. II·F-1. Plot of current vs energy for U^{238} ions.

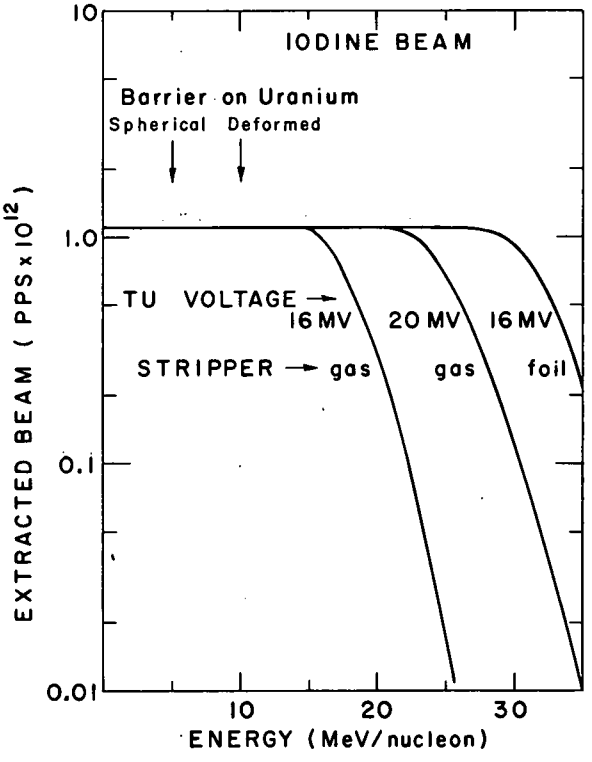

Fig. II·F-2. Plot of current vs energy for I^{127} ions.

Usable heavy-ion beams of still higher energy would result if any of the various possible technical developments mentioned at the beginning of this section do in fact materialize. Table II. F-IV shows the maximum energies that would result from various developments of this kind, and the curves on the right in Fig. II. F-1 and II. F-2 show the energy dependence of the intensity that would be obtained if the hoped-for developments turn out to be feasible.

TABLE II·F-IV. Maximum energies (MeV/A) of heavy-ion beams from the TU tandem and from the tandem-cyclotron system under various conditions.

	TU Tandem				TU + Cyclotron			
TU terminal voltage	16	16	16	20	16	16	16	20
TU terminal stripper	gas	gas	foil	gas	gas	gas	foil	gas
Beam intensity	$\frac{1}{2}$ Max	$\frac{1}{10}$ Max	$\frac{1}{2}$ Max	$\frac{1}{2}$ Max	$\frac{1}{2}$ Max	$\frac{1}{10}$ Max	$\frac{1}{2}$ Max	$\frac{1}{2}$ Max
Ion species								
O^{16}	7.0	8.0	7.0	8.8	100[a]			
F^{19}	6.7	7.6	6.7	8.4	81[a]			
Cl^{35}	4.1	4.6	5.0	5.7	75	84	94	
Br^{79}	1.8	2.0	2.6	2.5	31	35	46	44
I^{127}	1.1	1.3	1.9	1.6	19	21	32	27
U^{238}	0.5	0.65	0.86	0.65	8.6	9.7	10.8	9.3 17[b]

[a] 12 MV on TU terminal.

[b] 18 MV on TU terminal, foil stripper, superconducting coil system for maximum field of 20 kG in cyclotron.

II.G. COMPARISON OF ALTERNATIVES

1. Cost Assumptions
2. Performance vs Size of Accelerator System
3. Selection of the Tandem
4. Maximum Proton Energy

A project as large and complex as the MTC has so many variables that several alternative approaches to the technical problems need to be considered. In this section we attempt to put such considerations on a qualitative basis, always assuming that the primary design objective is an accelerator system with a genuine capability for the production of superheavy elements by means of heavy-ion reactions and, within this framework, the best possible light-ion capability.

The tandem-cyclotron combination was chosen as the basic concept for our system because it can satisfy a very wide range of research needs and also support a large volume of research. Alternative concepts were considered and rejected; the superconducting linac is believed to be at too early a stage of development, and the heavy-ion linac would not support a broad enough research program.

1. Cost Assumptions

Construction cost is a primary variable in the consideration of alternative combinations of tandems and cyclotrons. The cost estimates on most of the cyclotrons considered in this section are thought to be quite reliable, because they are based on rather detailed studies of both 4-sector and 6-sector machines. As is discussed later, there is some

problem in specifying the cost of the smaller tandems for the required high-current performance. The costs given in the tables and the figure are under the assumption that the MP tandem would be modified to provide the special features proposed for the TU* and that the cost of the modified, installed MP system would be $2.4 million more than the list price, as it is for the TU (including escalation). The other costs of the system—building and beam handling—depend greatly on one's assumptions about the nature of the research program for which the system is intended. Our estimates were made under the assumption that each accelerator system considered would be used in much the same way as is planned for the MTC—that is, as an intensively-used regional facility for a research program that is consistent with the capabilities of the accelerator. All cost estimates include the same percentage for cost escalation and contingencies.

2. Performance vs Size of Accelerator System

Since a tandem-cyclotron system may be formed by various combinations of tandems and cyclotrons, one needs to consider what accelerators are required to satisfy the needs of the research program. In this proposal we assume that the accelerator system should be able to accelerate heavy-ion beams of reasonable intensity up to energies of 8 or 10 MeV per nucleon so as to maximize the probability of producing and detecting the predicted superheavy elements. This objective is achieved in our design by using the largest tandem available and a relatively large cyclotron. But what might have been achieved with smaller accelerators? A partial answer to this question is given in Table II. G-I, where the heavy-ion performance of several combinations of tandems and cyclotrons are compared. Here one sees that the systems

*The TU tandem referred to throughout is an XTU model modified in the way discussed in Sec. II. A.

TABLE II. G-I. Comparison of energies of U^{238} ions for several accelerator systems. The initial ion is assumed to be UF_5^-. Energies would be somewhat higher for U^- ions.

Accelerator system	Beam intensity	Charge state		Cyclotron energy (MeV/nucleon)		Cost ($10^6)	
		Terminal stripping	Second stripping	Input	Output	Accelerators	Facility
Injector (8 MV) + FN tandem (7.5 MV) + Indiana cyclotron	Max.	5+	21+	0.20	1.9		
	½ Max.	7+	24+	0.27	2.5		
MP tandem (10 MV) + Indiana cyclotron	Max.	4+	21+	0.20	1.9	11.3	19.0
	½ Max.	6+	25+	0.28	2.7		
TU tandem (16 MV) + Indiana cyclotron	Max.	5+	28+	0.39	3.3	12.4	20.5
	½ Max.	7+	33+	0.52	4.5		
MP tandem (10 MV) + MTC cyclotron	Max.	4+	21+	0.20	3.2	14.3	23.0
	½ Max.	6+	25+	0.28	4.6		
MTC system	Max.	5+	30+	0.39	6.3	15.4	24.4
	½ Max.	7+	34+	0.52	8.6		

that involve smaller accelerators give energies that are probably too small for efficient production of superheavy elements, which (as discussed in Secs. I and V. A) may require energies well above the Coulomb barrier for interactions between two very heavy nuclei. Moreover, the beam currents obtainable from the TU are expected to be substantially larger than is obtainable from the smaller tandems, especially the FN. Thus, the MTC is seen to have a much greater heavy-ion research potential than the other systems considered in Table II. G-I, and it also gives much higher energies for light ions than the first three systems in the table. This potential is gained at a relatively small increase in the total cost of the facility.

3. Selection of the Tandem

In a tandem-cyclotron accelerator system, a given maximum energy of a heavy-ion species can be achieved by various combinations of tandems and cyclotrons; obviously, the smaller the tandem, the larger must be the cyclotron. But how does the total cost of the system, for a fixed performance, depend on the size of the tandem? In an attempt to answer this question, let us compare accelerator systems based on the four available models of tandems—the EN, FN, MP, and TU. Some of the basic information for this comparison is given in Table II. G-II for the acceleration of uranium ions. Here we list terminal voltage in the tandem, the ion energy after acceleration through the tandem, and the charge state after the accelerated ion passes through a foil stripper. This energy and charge state determine the energy gain and the size of the cyclotron required to produce ion beams with a given final energy.

The design of the cyclotron depends greatly on the priorities in the research program for which the machine is intended. Here we present the cost information under the three sets of assumptions about

TABLE II. G-II. Properties of U ions from various tandems. The initial ion is U^-. The terminal stripper is assumed to be a gas and the final stripper a foil. The energy gain for the cyclotron is the gain required to give the same final energy as the MTC.

	Tandem model			
	TU	MP	FN	EN
Tandem terminal voltage (MV)	16	10	7.5	5.0
$\bar{q}$ after terminal stripper	5.3	4.0	3.4	2.6
Energy after tandem (MeV)	100.6	50.2	32.8	18.0
$\bar{q}$ after final stripper	29.3	21.2	17.1	12.4
Cyclotron energy gain required	16	32	51	90
Tandem list price ($\$10^6$)	4.5	3.2	1.5	0.8

the cyclotron outlined below; for each set, the tandem-cyclotron system is designed to have the same final energy for heavy ions as the MTC.

Approach A: Use a direct extension of the MTC design: magnet-sector angle $\theta = 20^\circ$, sector number N = 6, constant inner radius, variable outer radius, maximum proton energy $E_p = 360$ MeV. The energy can increase beyond this value with increasing outer radius if the serious $\nu_z = 1$ resonance at $E_p \approx 360$ MeV can be crossed, but the cost estimates do not allow for this increase.

Approach B: Omit all light-ion capability: N = 4, $\theta = 60^\circ$.

Approach C: Starting with the MTC cyclotron, allow θ to increase as the maximum charge q of incident heavy ions decreases with decreasing tandem size; ignore resonance problems.

Thus far in this comparison only the energy of the ion beam has been mentioned. However, the beam current is also an important variable. Consider first a current that is low enough to be easily obtainable with any of the four types of tandems—say, 0.01 μA of accelerated current from the tandem. Then the cost of the tandem is approximately the list price (given in Table II. G-II) of the conventional

machines, without any major costs for the features considered necessary for good heavy-ion capability. Moreover, a foil stripper could be used in the terminal and the resulting high charge would allow the cyclotron to be much smaller than would be required if a gas stripper were used. However, a design that depends on having a low current of heavy ions is not an acceptable solution, since such a system would have very limited capacity for heavy-element production.

The requirement of high currents of heavy ions places severe demands on the tandem, since it must be modified to provide the various special features outlined in Sec. II.A. These features are most easily and cheaply provided in the TU, since it was explicitly designed for heavy-ion acceleration. For the sake of discussion, we may assume that these features could also be provided in the MP, although at a greater cost because of the problems in obtaining a satisfactory vacuum and because of the limitations on space and power in the terminal. When we come to the EN and FN models, these limitations are much more severe and it may not be feasible to develop a high-current capability with present technology.

The estimated costs of the tandem-cyclotron systems corresponding to the three design approaches outlined above are given in Fig. II.G-1. Here the arrows on the points for systems involving EN and FN tandems reflect the fact that only a lower limit on cost can be set, because of the difficulty of obtaining a high current of heavy ions from these tandems. The figure shows that the estimated cost is at a minimum for the TU tandem for all three design approaches, although there is not much difference between the costs for the MP- and TU-based systems under some assumptions. The accelerator systems based on the EN and FN models are not competitive, since with them one does not know how to achieve high currents of heavy ions.

The data in Fig. II.G-1 and the above discussion indicate that the choice between an MP and a TU depends on factors other than the cost involved in satisfying the energy requirements for heavy ions.

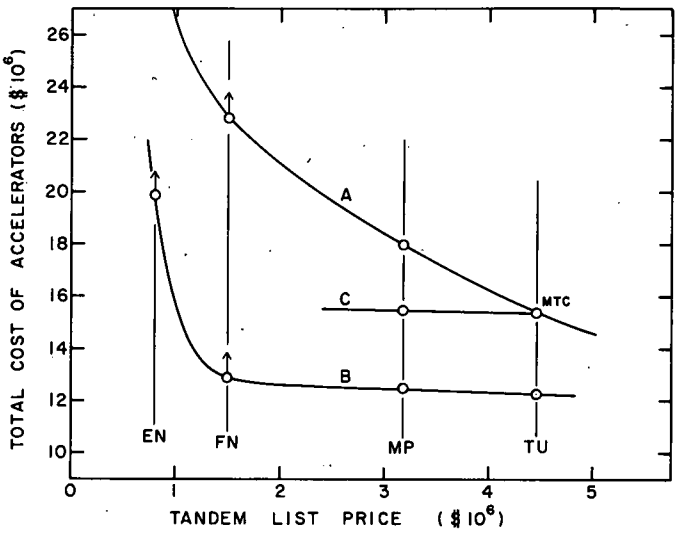

Fig. II. G-1. Total cost of tandem-cyclotron accelerator systems for various models of tandems. The labels A, B, and C on the curves refer to the three different approaches to cyclotron design outlined in the text.

If accelerating protons to energies greater than 350 MeV is considered to be more important than heavy-ion capability, then the MP tandem might be the best choice. However, for our system, in which heavy-ion acceleration is given highest priority, the TU tandem is clearly better, (a) because the TU used as an injector will probably deliver much more beam current than is obtainable from an MP and (b) because the TU by itself is a much more useful accelerator than the MP.

4. Maximum Proton Energy

The basic configuration of the proposed accelerator system and the approximate sizes of the individual components were determined by the heavy-ion requirements. Nevertheless, one still has some freedom to adjust the characteristics of the cyclotron for proton acceleration. Our first decision in this regard was that the cyclotron should not have a high enough energy for the research at the MTC to have an appreciable overlap with that planned for the Los Alamos Meson Factory. On the other hand, it was considered to be highly desirable for the maximum energy to be well above the meson threshold (290 MeV) provided that this requirement for protons does not increase the cost of the

TABLE II. G-III. Comparison of savings obtained by eliminating the ability to accelerate various projectiles. System 1 is the proposed MTC. System 2 is similar to the MTC but uses a 4-sector cyclotron and does not accelerate protons. System 3 is similar to the MTC but uses a 4-sector cyclotron and has no light-ion capability. System 4 is an MTC cyclotron with a maximum energy of 350 MeV for protons and no heavy-ion capability.

Accelerator System	Cost ($\$10^6$)	
	Accelerators	Facility
1. MTC	15.4	24.4
2. MTC without protons	14.1	22.0
3. MTC without light ions	12.4	19.4
4. Light ions only	8.6	16.0

cyclotron substantially. These conditions lead to the selection of $E_p \approx 350$ MeV as an optimum upper limit.

The extent to which the dual (cost and performance) requirements on the proposed cyclotron are satisfied is best appreciated by comparing various alternatives. This is done in Table II. G-III, where the construction cost of the proposed MTC is compared with the cost of several systems with more limited research capabilities. In this table the cost of the facility is calculated under the assumption that the building is designed to make use of the full research capability of the several systems considered. The comparison shows that the saving achieved by eliminating proton acceleration altogether is relatively small. Substantial savings are made only by eliminating either the light-ion or the heavy-ion capabilities altogether, a saving gained by a sacrifice of half of the research capability of the system. Note that the combined costs of two independent systems to provide the research capability of the MTC would be about $\$11$ million more than the proposed system.

Although the energy range of the MTC was deliberately chosen to be lower than the range in which the Meson Factory is expected to operate most of the time, there is some overlap in the ranges in which the two machines can operate, namely, about 200—350 MeV. Thus, one may ask whether the proton capability of the MTC is of any interest, in view of the much higher current available from the Meson Factory. There are two aspects of the answer to this question. First, the MTC is not inferior to the Meson Factory for all experiments; indeed, whenever a beam with good energy resolution is required, the MTC will be competitive. Second, interest in experiments to be done with the 200—350 MeV protons is great and many of the experiments involve careful coincidence and double-scattering measurements that require a great deal of beam time. Thus, there is a genuine need for additional research capacity in the energy range for which the MTC is planned. The availability of the MTC will enable the Meson Factory to be used more effectively by removing some of the need for it to operate at low energies, where its multiple-use capabilities are greatly reduced.

III. ARGONNE STAFF AND SERVICES

A strong justification for the construction of the MTC at Argonne is that much of the research for which it is intended is a natural extension of major research programs now in progress at the Laboratory. As a result, a large staff that is well qualified to make effective use of the MTC has already been assembled. This section gives a brief description of the several groups of Argonne staff members who will be most directly involved in the construction, operation, or use of the MTC.

Two important pieces of information are missing from this description of staff members. First, no list of publications is given, since a listing of this kind covering a period of several years would be a small volume in itself—some 250 pages for a ten-year period. Publication lists for relevant research are given in each annual Physical Research Program Budget under the sections labeled "Heavy Element

Chemistry and Nuclear Chemistry" and "Low Energy Nuclear Physics." The same information on the physics research is also given in the Physics Division Annual Reviews, namely reports ANL-6720 (1963), ANL-6879 (1964), ANL-7081 (1965), ANL-7246 (1966), ANL-7354 (1967), and ANL-7481 (1968). These lists include about 40 journal papers annually in nuclear chemistry and about 70 annually in areas of nuclear and atomic physics that would benefit directly from the MTC. A considerably larger number of titles of oral papers are also listed.

A second omission is a description of the very large group of scientists scattered throughout the Laboratory whose work would benefit from the unusual radioactive sources and radiation effects produced by ion beams from the MTC. Many of these are involved in various aspects of the materials sciences.

The section closes with an outline of general services available at Argonne to provide essential backup for research at a major accelerator. The facilities and services more directly related to the particular needs of research at the MTC were described in Sec. II. E.

1. Accelerator Design

The Accelerator Design Group of the Chemistry Division has developed the conceptual design of the proposed cyclotron and it is intended that they will form the core of the group that takes on the primary responsibility for the design, construction, and assembly of the machine. The present group consisting of 10 staff members has competence in accelerator theory, rf and electronic engineering, systems control, magnetics, mechanical design, and vacuum and ion-source technology. The group has been well prepared for this work on the MTC system by its recent involvement in the design of two other isochronous cyclotrons—the HIVEC and the conversion of the 60-in. cyclotron into a variable-energy machine. Also, for many years these staff members and their

technical assistants have had the broadening experience of being responsible for the operation and development of several different kinds of machines. These include a 60-in. cyclotron, an electron Van de Graaff, a high-current electron linac, and a Cockcroft-Walton, each of which has been developed into a machine of exceptional usefulness for research.

The large group of accelerator technologists involved in the development and operation of the ZGS will be an additional source of technical skill and knowledge during all phases of the proposed project. This support has already been of crucial importance for two major aspects of the MTC design—the calculation of orbit stability and the consideration of superconducting magnets for the cyclotron.

The staff members of the cyclotron design group and their areas of competence are listed below. The members of the Physics Division who are experienced in the technology of electrostatic accelerators are listed in Sec. III.3a.

W. J. Ramler, Illinois Institute of Technology, M.S., 1952.
General accelerator technology.

R. Benaroya, Case Institute of Technology, M.S., 1950.
Magnets and superconductors.

J. Aron, Fenn College, B.S., 1955.
Vacuum and control technology.

O. D. Despe, Northwestern University, M.S., 1961.
Power supplies and regulators.

K. W. Johnson, Thornton Junior College, Pre-Engineering (2 yr.), 1948.
RF engineering and fast electronics.

T. K. Khoe, Technische Hogeschool Delft, Ph.D., 1960.
Accelerator theory.

J. J. Livingood, Princeton University, Ph.D., 1929.
General accelerator technology.

G. S. Mavrogenes, Northwestern University, B.S., 1955.
RF engineering and linac design.

J. M. Nixon, Rice Institute, B.S., 1948.
Mechanical design.

G. W. Parker, Cony High School, Diploma, 1929.
Mechanical design.

W. Wesolowski, University of Illinois, B.S., 1967.
Computer programming and measurements of magnetic field.

2. Nuclear Chemistry

a. Properties of Heavy Elements; Nuclear Fission; Other Heavy-Element Nuclear Reactions

The Heavy-Element Group of the Chemistry Division has a long history of productive work since Argonne's inception. Members of this group have been involved in the discovery of new elements in the transuranic region, and have made important studies on at least half of the known transuranium isotopes. The major activity of this group will be transferred to the MTC. Since the best methods for attempting to make new elements are not known, considerable attention will be paid to studying the mechanisms of pertinent nuclear reactions, such as heavy-cluster transfer reactions or "cold nucleus" reactions (Sec. V.A1d).

Because clarifying the nature of fission is basic both to understanding the structure of heavy nuclei and to the atomic energy program, our nuclear chemistry groups have long been deeply involved in the study of the fission process. These groups plan to shift most of their activity to the MTC, investigating heavy-ion fission and fission at high excitation energies. The study of fission with heavy ions takes on added importance in the light of the fact that such fission now appears to be the most promising nuclear reaction for making superheavy elements and will be the best source for the creation of heavy neutron-rich radioactive nuclides.

Scientists engaged in high-resolution nuclear spectroscopy of the heavy-element nuclides at the 60-in. cyclotron and the FN tandem accelerator will shift their major activities to the MTC.

Eleven staff members are involved in these activities; the number of temporary staff scientists varies from 2 to 7. There is a comparable supporting group of scientific assistants and technicians. The long-term staff members now involved in these programs and their present research interests are as follows.

Paul R. Fields, University of Chicago, B.S., 1941.
Properties of heavy elements and nuclear reactions.

Irshad Ahmad, University of California, Ph.D., 1966.
Decay schemes and nuclear reactions.

Raymond F. Barnes, University of Illinois, B.S., 1950.
Production and properties of heavy elements and their isotopes.

Herbert Diamond, University of Chicago, B.S., 1948.
Nuclear properties of the heavy elements, decay schemes, and atomic-beam studies of the actinide elements.

John Milsted, Bristol University, Ph.D., 1940.
Nuclear properties of the heavy elements and alpha decay measurements.

Ruth K. Sjoblom, Northwestern University, B.S., 1946.
Production and properties of the heavy-element nuclides.

Arnold M. Friedman, Washington University, Ph.D., 1953.
Nuclear spectrometry using nuclear reactions.

Lawrence E. Glendenin, Massachusetts Institute of Technology, Ph.D., 1948. Radiochemical and physical studies of fission.

Kevin F. Flynn, Illinois Institute of Technology, M.S., 1953.
Radiochemical and physical studies of fission.

James E. Gindler, University of Illinois, Ph.D., 1954.
Nuclear fission, spallation, and isomeric ratios.

John P. Unik, University of California, Ph.D., 1960.
Nuclear fission properties by use of charged-particle nuclear reactions.

b. Heavy-Element Chemistry and Other Nuclear Chemistry

Members of the Chemistry Division have been very productive in examining the chemistry of the actinide elements through studies of solution chemistry, dry chemistry, physical chemistry, crystal structure, and electronic structures. Although these scientists will continue to be interested in the actinides, they intend to shift much of their activity to examining the chemistry of those superheavy elements for which the formation cross sections and half-lives are sufficiently great. Some fast chemical techniques have been developed, and it is intended to develop new ones capable of giving useful chemical information even for half-lives as short as a few seconds.

Several groups are engaged in the study of level schemes and level properties in radioactive decay through the use of beta and alpha spectroscopy. Though interests now center in the traditional regions of the nuclear chart, the production of sufficient amounts of activity will allow much of the work to be shifted to the study of superheavy nuclei or other new isotopes—especially those far from stability.

Present theoretical investigations of the nuclear structure of actinide isotopes will extend naturally into theoretical studies in the superheavy region when the experimentalists provide some basic data.

The nuclear chemists engaged in high-energy experiments at the 12-BeV Zero-Gradient Synchrotron (ZGS) intend to use the MTC as a means of getting information over a broader range of energies to aid in interpreting their observations. Proton reaction studies at intermediate energies (to 350 MeV) will be correlated with the high-energy ZGS results. In an important calibration measurement, highly-charged very-heavy ions of known energy will be used to study ionization defects in solid-state detectors. With such a calibration, these detectors can be applied in accurate measurement of fragment energies from superheavy fission as well as ordinary fission.

Sixteen staff members are involved in these activities; the number of temporary staff scientists varies from 4 to 9. There is a comparable supporting group of scientific assistants and technicians. The long-term staff members now involved in these programs and their present research interests are as follows.

Sherman M. Fried, University of Chicago, Ph. D., 1942.
Inorganic chemistry of the heavy elements.

William T. Carnall, University of Wisconsin, Ph. D., 1954.
Spectroscopic studies of the lanthanide and actinide elements; physical chemistry of the actinides.

Donald Cohen, Purdue University, Ph. D., 1950.
Inorganic chemistry of the actinide elements.

Elizabeth G. Sherry, Ball State University, B. S., 1947.
X-ray studies of lanthanide and actinide compounds.

Melvin S. Freedman, University of Chicago, Ph. D., 1942.
Beta-ray spectrum shape analysis; atomic and chemical effects on electron spectra.

Fred T. Porter, Washington University, Ph. D., 1953.
Beta-ray spectrometry.

Frank Wagner, Jr., University of Chicago, M.S., 1950.
Beta-ray spectrometry.

Arthur H. Jaffey, University of Chicago, Ph. D., 1941.
Alpha-ray spectrometry.

Niels J. Hansen, University of Wisconsin, M.S., 1954.
Alpha spectrometry and solid-state detectors.

Dale J. Henderson, Elmhurst College, B.S., 1951.
Alpha- and gamma-ray spectrometry.

Ellis P. Steinberg, University of Chicago, Ph. D., 1947.
Study of high-energy proton-induced reactions.

Sheldon B. Kaufman, University of Chicago, Ph. D., 1953.
Study of high-energy proton-induced reactions.

Andrew F. Stehney, University of Chicago, Ph. D., 1950.
Study of high-energy proton-induced reactions.

Bruce D. Wilkins, University of California, Ph. D., 1962.
Study of high-energy proton-induced reactions.

Richard R. Chasman, University of California, Ph. D., 1958.
Theoretical nuclear-chemistry studies.

Paul A. Benioff, University of California, Ph. D., 1959.
Theoretical studies of nuclear reactions at high energy.

c. Other Nuclear Scientists

The 100-in. mass spectrometer (Sec. II. E7) has been used for detecting small amounts of isotopes over the whole periodic table. It has been particularly useful in the study of actinide isotopes, and is expected to be very important in investigating nuclides formed in the superheavy region.

The isotope separator (Sec. II. E2) is capable of efficient separation of isotopes of most elements and will be important in allowing the examination of individual superheavy nuclides, as well as for target preparation.

The talents of nuclear chemists experienced in developing efficient separation methods will be invaluable in aiding the development of rapid separations in the superheavy region.

The central multi-programmed real-time computer facility being developed by the Chemistry Division (Sec. II. E3) is capable of being used for on-line operation of some of the MTC experiments. Staff presently engaged in devising suitable programs for Chemistry Division activities can develop some of the on-line programs for the MTC.

Twelve staff members are involved in these activities, with a comparable supporting group of scientific assistants and technicians. The long-term staff members now involved in these programs and their present research interests are as follows.

Donald C. Stewart, University of California, Ph. D., 1950.
Administration of analytical-chemistry and hot-laboratory functions of the division.

Louis J. Basile, St. Louis University, Ph. D., 1952.
Preparation and characterization of rare-earth and actinide-element organo-complexes.

E. Philip Horwitz, University of Illinois, Ph. D., 1957.
Chemical separation methods for heavy-element research.

John P. Hughes, St. Louis University, M. S., 1950.
Fission-product yield studies correlated with other parameters involved with highly irradiated reactor fuels.

James H. Patterson, Iowa State University, Ph. D., 1950.
Development of alpha-scattering techniques for the analysis of surfaces, with particular reference to remote analysis of extra-terrestrial objects.

Morris A. Wahlgren, University of Michigan, Ph. D., 1961.
Group leader for analytical radiochemistry; specialist in activation techniques.

Charles M. Stevens, University of Minnesota, B. A., 1942.
Isotope cosmology and nuclear chemistry using 100-in. mass spectrometer.

C. Harry Youngquist, Illinois Institute of Technology, B. S., 1957.
Mechanical design and shielding problems for hot-laboratory operations.

Jerome L. Lerner, University of Chicago, M.S., 1950.
Application of mass separator to nuclear and chemical problems.

Paul P. Day, Illinois Institute of Technology, M.S., 1955.
Nuclear spectroscopist with principal responsibility for design and implementation of the Sigma-7 Real-Time Computer Facility.

Conrad E. Thalmayer, University of Chicago, M.S., 1958.
Physical chemist presently designing and writing applications programs to provide real-time computer service (Sigma 7) for a cryogenic NMR and a low-temperature laboratory.

Kurt A. Kaiser, University of Minnesota, M.S., 1961.
Mass spectroscopist presently designing and writing applications programs to provide real-time computer service (Sigma 7) for neutron diffractometry. Implementation of a molecular-orbital computation facility on Sigma-7.

d. Temporary Appointments in Chemistry

In recent years the Laboratory has learned from experience that a research staff that consists of scientists with both long-term and temporary appointments is optimum for a vital research program. Thus, we assume that future temporary appointees (especially at the postdoctoral level) will play an important role in research at the MTC.

The temporary appointments in the area of nuclear chemistry during the period 1 January 1960—June 1969 are summarized in Table III-I and the universities from which these temporary appointees originated are given in Table III-II. Others who have been involved in the nuclear-chemistry program by way of consultant and guest-agreement appointments are listed in Table III-III.

TABLE III-I. Summary of the numbers of temporary appointments in nuclear chemistry and in the combined areas of nuclear and atomic physics. The temporary appointees in nuclear chemistry were associated with about 27 nuclear chemists on the regular staff in the Chemistry Division. Those in nuclear and atomic physics were associated with about 45 regular staff members in the Physics Division. All of these chemists and at least 70% of the physicists on the regular staff are expected to be seriously involved in some aspect of research with the MTC.

Type of Appointment	Jan. 1960—June 1969 Nuclear Chemistry	July 1962—June 1969 Nuclear & Atomic Physics
Long-term		
Postdoctoral	24	42
Visiting Scientist (Faculty)	16	17
Thesis Student		
ANL	4	6
AMU	4	9
Co-op Student	3	85
*ACM Professor	1	8
No-Pay Appointee	2	8
Short-term		
Faculty		
Visiting Scientist	24	97
*OCUC-CEA-AMU	7	3
No-Pay Appointee	5	29
Graduate Student		
ANL	9	21
*AMU	2	5
Undergraduate		
ANL	50	158
*ACM-CEA-CSUI-SSTP	28	77

*Refers to educational programs sponsored in part by NSF and DNET. Office of College and University Cooperation (OCUC) and its successor Center for Educational Affairs (CEA), Associated Midwest Universities (AMU) most of whom have joined Argonne Universities Association (AUA), Associated Colleges of the Midwest (ACM), Central States Universities, Incorporated, (CSUI) Summer Student Training Program (SSTP).

TABLE III-II. Summary of the universities from which temporary appointees[a] in nuclear chemistry originated. The period of time covered is January 1960 to June 1969.

Institution (address)	Long-term appointments			Short-term appointments	
	Postdoctoral Appointees	Visiting Scientists	Graduate Students	Faculty	Students
Alabama, University of (Huntsville, Alabama)				1	
Albion College (Albion, Michigan)					2 (1*)
Andrews University (Berrien Springs, Michigan)				1	
Arkansas, University of (Fayetteville, Arkansas)					1
Beloit College (Beloit, Wisconsin)					3 (2*)
Boston University (Boston, Massachusetts)					1
Bridgewater College (Bridgewater, Virginia)					1*
Bradley University (Peoria, Illinois)					2
California, University of (Berkeley, California)	5				1
Calvin College (Grand Rapids, Michigan)				3	
Carleton College (Northfield, Minnesota)		1††		2	3 (1*)
Chicago, The University of (Chicago, Illinois)	1		1		1
Christian Brothers College (Memphis, Tennessee)					2
Coe College (Cedar Rapids, Iowa)					1*
Colgate University (Hamilton, New York)					2
Colorado State University (Fort Collins, Colorado)			1		
Columbia University (New York, New York)	1				
Cornell University (Ithaca, New York)					1*
Detroit, University of (Detroit, Michigan)			1‡		
Eastern Kentucky State College (Richmond, Kentucky)					1
Geneva College (Beaver Falls, Pennsylvania)					1
Georgia Institute of Technology (Atlanta, Georgia)				1	
Grinnell College (Grinnell, Iowa)					3 (2*)

TABLE III-II. (Cont'd.)

Institution (address)	Long-term appointments			Short-term appointments	
	Postdoctoral Appointees	Visiting Scientists	Graduate Students	Faculty	Students
Hartwick College (Oneonta, New York)					1*
Harvard University (Cambridge, Massachusetts)				2 (1†)	2
Holy Cross College (Worcester, Massachusetts)				1	
Illinois, University of (Urbana, Illinois, and Chicago Circle Campus)			1	2 (1**)	7 (1*) (1**)
Illinois Institute of Technology (Chicago, Illinois)				1	
Johns Hopkins University (Baltimore, Maryland)	1				
Kansas State University (Manhattan, Kansas)			1**	1**	
Knox College (Galesburg, Illinois)					4 (1*)
Lawrence College (University) (Appleton, Wisconsin)					1*
Lewis College (Lockport, Illinois)				1	
Manchester College (North Manchester, Indiana)					2
Marquette University (Milwaukee, Wisconsin)				1	
Massachusetts Institute of Technology (Cambridge, Massachusetts)	1				
Michigan College of Mining & Technology (Houghton, Michigan)					1
Michigan Technical University (Houghton, Michigan)			2**		
Michigan, University of (Ann Arbor, Michigan)		1		3 (1**)	1
Missouri School of Mines and Metals (Rolla, Missouri)			1‡		
Monmouth College (Monmouth, Illinois)					1*
Morris Brown College (Atlanta, Georgia)					1*
Mundelein College (Chicago, Illinois)					2 (1*)
Nebraska State College (Kearney, Nebraska)					1
Northern Illinois University (DeKalb, Illinois)				1**	

TABLE III-II. (Cont'd.)

Institution (address)	Long-term appointments			Short-term appointments	
	Postdoctoral Appointees	Visiting Scientists	Graduate Students	Faculty	Students
Northwestern University (Evanston, Illinois)			1‡	2	3
Notre Dame, University of (Notre Dame, Indiana)					1
Oberlin College (Oberlin, Ohio)					1
Oklahoma State University (Stillwater, Oklahoma)				2**	
Oklahoma, University of (Norman, Oklahoma)				1	
Oregon State University (Corvallis, Oregon)				1	
Pennsylvania, University of (Philadelphia, Pennsylvania)					1
Princeton University (Princeton, New Jersey)					1*
Purdue University (Lafayette, Indiana)					2
Rosary College (River Forest, Illinois)					1**
St. Augustine College (Raleigh, North Carolina)					1
St. John's University (Collegeville, Minnesota)					2 (1*)
St. Joseph's College (Rensselaer, Indiana)					2
St. Olaf College (Northfield, Minnesota)					2 (1*)
St. Procopius College (Lisle, Illinois)			1**		1*
St. Xavier College (Chicago, Illinois)					1*
Sienna Heights College (Adrian, Michigan)					1
South Dakota, University of (Vermillion, South Dakota)					1
Southern Illinois University (Carbondale, Illinois)					1**
Taylor University (Upland, Indiana)					2
Tougaloo College (Tougaloo, Mississippi)					1
Upper Iowa University (Fayette, Iowa)					3
Valparaiso University (Valparaiso, Indiana)					1

TABLE III-II. (Cont'd.)

Institution (address)	Long-term appointments			Short-term appointments	
	Postdoctoral Appointees	Visiting Scientists	Graduate Students	Faculty	Students
Villa Madonna College (Covington, Kentucky)				1	
Wabash College (Crawfordsville, Indiana)					1
Washington, University of (Seattle, Washington)	1				1
Washington University (St. Louis, Missouri)	1				
Wayne State University (Detroit, Michigan)	1				
Western College for Women (Oxford, Ohio)					1*
Western Michigan University (Kalamazoo, Michigan)					1
Western Reserve University (Cleveland, Ohio)	1		1		
Wheaton College (Wheaton, Illinois)	1			3	2 (1*) (1**)
Wilmington College (Wilmington, Ohio)					1
Wisconsin State University (River Falls, Wisconsin)					1
Xavier University (New Orleans, Louisiana)					1*
Neighborhood Youth Corps (Chicago, Illinois)					1
Foreign Appointments					
Argentina					
AEC		1			
Austria					
Vienna, University of		2			
Belgium					
AEC		1			
Canada					
McMaster University	1				
Denmark					
Institute for Theoretical Physics		1			
England					
Harwell (UKAEA)		1			
King's College, University of Durham	1				
Nottingham University	2				
France					
Faculty of Sciences, Paris	1				

TABLE III-II. (Cont'd.)

Institution (address)	Long-term appointments: Postdoctoral Appointees	Long-term appointments: Visiting Scientists	Long-term appointments: Graduate Students	Short-term appointments: Faculty	Short-term appointments: Students
Germany					
Hamburg, University of		1			
Institute of Inorganic Chemistry, Univ. of Munich	1				
Technische Hochschule, Munich	3				
India					
AEC				2	
Israel					
AEC				2 (1**)	
Weizmann Institute of Science		1			
Italy					
National Commission for Nuclear Research, Rome	1				
Japan					
Osaka University		1††			
South Africa					
AEC				1**	
Sweden					
Nobel Institute for Physics, Stockholm		2			
Switzerland					
CERN, Geneva		1			
Cyanamid Research Institute		1			
Eidg. Institute for Reaktor Forschung		1			

[a]The reference marks designating the types of appointments have the following meanings.

* ACM, CEA, CSUI, SSTP
** OCUC, CEA, AMU
† No-Pay Appointee
†† ACM Professor
‡ Co-op Student

TABLE III-III. Summary of consultant and guest-agreement appointments in the area of nuclear chemistry during the period January 1960—June 1969. Those marked with an asterisk have active appointments as of June 1969.

Affiliation	Participant	Type of appointment	
		Consultant	Guest
University of Arkansas	Robert Clark		x
	R. Ganapathy		x
	Marvin W. Rowe		x
	Richard Strother		x
Calvin College	Roger Griffioen	x	
Carleton College	*Eiler Henrickson	x	
	*Richard Ramette	x	
University of Chicago	Gordon Goles		x
Harvard University	William Sabine		x
Holy Cross University	*Ram Sarup	x	
University of Illinois	Peter Axel	x	
	Carol Stearns		x
	*Lester Winsberg	x	
Kansas State University	*Chander Bhalla	x	
	*Robert Leachman		x
University of Kentucky	William D. Ehmann	x	
Marquette University	Richard Fink		x
University of Maryland	*James Griffin	x	
	*Victor Viola	x	
Michigan State University	*William C. McHarris	x	
The University of Michigan	Philip LaFleur		x
Northwestern University	*Arthur Freeman	x	
	Ernest D. Klema	x	
Oregon State University	*W. Loveland	x	
Purdue University	Zbigniew W. Grabowski		x
	R. S. Raghavan		x
University of Rochester	Aziz Behkami		x
	*John Huizenga	x	
Washington University, St. Louis	Herbert Potratz	x	
University of Washington	*Robert Vandenbosch	x	
Western Michigan University	*Katheryn Rajnak	x	
University of Wisconsin	Larry Haskin	x	
Argonne National Laboratory[a]	*Lucy Person	x	
University of Chicago[a]	*Stanka Jovanovic	x	
Field Museum	*Edward Olsen		x
Nuclear Diodes, Inc.	Hans Fiedler	x	
University of Rochester[a]	Esther S. Segel	x	
St. James Hospital	*David Dennen		x

[a]Formerly.

3. Nuclear and Atomic Physics

a. Charged-Particle Physics

The large and vigorous program in Charged-Particle Physics now based on the FN tandem and the 60-in. cyclotron will be transferred to the MTC to the extent that running time is available. Thus, the strength of the present program is good evidence that the future facility will be used effectively in physics research.

The group of experimental physicists involved in the present program consists of 16 regular and about 5 temporary Ph. D. - level staff members, and some graduate students; in addition, there is an approximately equal number of technicians and junior staff members with developed skills. A notable characteristic of the physicists in this group is the great breadth of their research interests, which encompass almost all aspects of nuclear-physics research with charged particles as well as experience in other areas such as neutron physics and the Mössbauer effect. This diversity of scientific competence and the technical know-how gained in the regular use of three accelerators (the FN tandem, the 60-in. cyclotron, and the Dynamitron) make the group exceptionally well qualified to use the MTC with skill and imagination.

The regular (long-term appointment) staff members now involved in the Charged Particle Physics program and their major research interests at this time are as follows.

Thomas H. Braid, Edinburgh University, Ph. D., 1950.
Elastic scattering, transfer reactions, delayed-proton emitters, optical-model studies, nuclear apparatus, multi-wire proportional-counter development for position-sensitive detection.

John R. Erskine, University of Notre Dame, Ph. D., 1960.
Nuclear reactions, structure of deformed nuclei, transfer reactions in actinide nuclei, magnetic spectrographs, automatic scanning of nuclear emulsions.

Donald S. Gemmell, Australian National University, Ph. D., 1960.
Channeling of charged particles in crystals, particle-gamma correlation studies, on-line computer development, proton-capture inverse giant resonances.

David C. Hess, University of Chicago, Ph. D., 1949.
Polarized-ion-source development, ion-source and beam-optics technology.

Robert E. Holland, University of Iowa, Ph. D., 1950.
Lifetimes of nuclear energy levels, Coulomb excitation, shape isomers, particle-gamma correlation studies.

Frank J. Lynch, University of Chicago, B. S., 1944.
Fast-timing technology, lifetimes of nuclear energy levels, properties of scintillators.

Luise Meyer-Schützmeister, Technical University of Berlin, Ph. D., 1943.
Giant dipole resonance, two-nucleon transfer reactions, isospin violation in medium nuclei, Doppler-shift studies, gamma-ray decay of analog states.

F. Paul Mooring, University of Wisconsin, Ph. D., 1951.
Electrostatic-accelerator technology, neutron cross sections, ion-source development.

George C. Morrison, Glasgow University, Ph. D., 1957.
Analog states, heavy-ion reactions, alpha-particle transfer reactions, Li-ion source development, isospin-forbidden resonances, reaction mechanisms in transfer reactions.

John P. Schiffer, Yale University, Ph. D., 1954.
Transfer reactions, nuclear structure near closed shells, charge-exchange reactions and anti-analog states, Coulomb energies and nuclear radii, coherent states in two-particle and four-particle transfer.

Ralph E. Segel, Johns Hopkins University, Ph. D., 1955.
Giant dipole resonances, tests of conservation laws, lifetimes of nuclear states, Doppler-shift measurements, inelastic scattering on light nuclei.

Rolf H. Siemssen, University of Hamburg, Ph. D., 1963.
Heavy-ion scattering and reactions, transfer reactions on light nuclei, elastic scattering and optical-model investigations, tests of parity conservation in strong interactions.

Dieter von Ehrenstein, University of Heidelberg, Ph. D., 1960.
Polarized-ion-source development, transfer reaction studies.

Jack R. Wallace, College of Wooster, B. A., 1942.
Van de Graaff accelerator operation and improvement.

Jan L. Yntema, Free University of Amsterdam, Ph. D., 1952.
Direct reactions, energy levels of medium-weight nuclei, elastic and inelastic scattering, DWBA and optical-model investigations, automation of nuclear apparatus.

Benjamin Zeidman, Washington University, Ph. D., 1957.
Transfer reactions in medium-weight nuclei, heavy fragments in nuclear reactions, design of magnetic spectrographs, reaction mechanisms.

b. Other Experimental Physics

Although the impact of the MTC will be most direct for the Charged Particle Physics program, virtually all of the present program of the Physics Division will be greatly strengthened by the availability of the new machine. In particular, all research that makes use of radioactive radiation sources will benefit. This applies especially to β- and γ-ray spectroscopy and to various studies that make use of the Mössbauer effect as a research technique. Other research such as atomic-beam experiments will study the atomic characteristics of the new isotopes produced. The energetic beams of heavy ions available from the new machine provide a natural and exciting extension of work now in progress on the interaction of light ions with monocrystals.

It is expected that the new accelerator will have the beneficial effect of drawing together the interests of nuclear physicists and atomic physicists at Argonne, because so many of the technical problems associated with the acceleration of heavy ions involve problems that are of fundamental interest to atomic physics and these problems need to be understood to develop a good system for nuclear physics.

The regular (long-term appointment) staff members in the Physics Division who will make use of radioactive isotopes produced by the new accelerator or use the accelerator itself for atomic-physics experiments are listed below. This list does not include many staff members now involved in the Neutron Physics program, whose work will benefit from the results of closely-related experiments with charged particles from the MTC. Also, it does not include the names of the very large number of scientists in other divisions at Argonne whose work will be strengthened by the unusual radiation sources that will be produced by the MTC.

Joseph Berkowitz, Harvard University, Ph. D., 1955.
Ionization phenomena in gases, mass spectroscopy.

Herbert H. Bolotin, Indiana University, Ph. D., 1955.
Gamma-ray spectroscopy of radioactive sources, Coulomb excitation, neutron-capture gamma rays.

S. Bradley Burson, University of Illinois, Ph. D., 1946.
Gamma-ray spectroscopy of radioactive sources, internal conversion, neutron-capture gamma rays.

William J. Childs, University of Michigan, Ph. D., 1956.
Atomic beams.

William A. Chupka, University of Chicago, Ph. D., 1951.
Ionization phenomena in gases, mass spectroscopy.

Alexander J. Elwyn, Washington University, Ph. D., 1956.
Double fission barrier, (d,n) reactions, neutron-induced reactions, intermediate structure.

Leonard S. Goodman, University of Chicago, Ph. D., 1952.
Atomic beams.

Manfred S. Kaminsky, University of Marburg, Ph. D., 1957.
Channeling of ions in crystals, atomic and ionic impact phenomena at metal surfaces, vacuum technology, mass spectroscopy.

Richard S. Preston, Yale University, Ph. D., 1954.
Mössbauer effect applied to studies in metallurgical physics.

Gilbert J. Perlow, University of Chicago, Ph. D., 1940.
Mössbauer effect applied to studies in chemical, solid-state, nuclear, and biological physics.

Stanley L. Ruby, Columbia University, B. A., 1947.
Mössbauer effect applied to studies in chemical, solid-state, and nuclear physics.

Robert K. Smither, Yale University, Ph. D., 1958.
Nuclear energy levels, neutron-capture gamma rays.

c. Nuclear Theory

An important justification for the construction of the proposed facility at Argonne is the presence of an outstanding group of nuclear theorists to help guide the research program. This group has been responsible for many of the important advances in the nuclear shell model, starting with its initial formulation at Argonne by Maria

Mayer. More recently, strength has also developed in the areas of nuclear matter, statistical theory of nuclear energy levels, reaction mechanisms, and advanced computational techniques. All of these areas are directly relevant to the kinds of physics that will be done with the MTC.

The group of theorists consists of 11 regular (long-term) staff members, about 3 temporary members, and several graduate students. The regular staff members and their current research interests are listed below.

Arnold R. Bodmer, Manchester University, Ph. D., 1953.
Hypernuclei, three-body problem.

Fritz Coester, University of Zurich, Ph. D., 1944.
Nuclear matter, scattering theory, basic theoretical physics.

Stanley Cohen, Cornell University, Ph. D., 1955.
Advanced computational methods, nuclear shell model.

Benjamin D. Day, Cornell University, Ph. D., 1963.
Nuclear matter, nuclear reaction-matrix calculations.

Hans Ekstein, University of Berlin, Ph. D., 1934.
Fundamentals of quantum mechanics, scattering theory.

Dieter Kurath, University of Chicago, Ph. D., 1951.
Structure of light nuclei, electromagnetic transitions.

Robert D. Lawson, Stanford University, Ph. D., 1953.
Nuclear structure, many-body problem.

Malcolm H. Macfarlane, University of Rochester, Ph. D., 1959.
Nuclear many-body theory, direct nuclear reactions.

Peter A. Moldauer, University of Michigan, Ph. D., 1956.
Nuclear reaction mechanisms, statistical theory of nuclear reactions, neutron cross sections.

James E. Monahan, St. Louis University, Ph. D., 1953.
Nuclear reaction theory, statistical methods, neutron-induced reactions.

Murray Peshkin, Cornell University, Ph. D., 1951.
Utilization of basic symmetry properties, magnetic flux quantization in superconductors.

Norbert Rosenzweig, Cornell University, Ph. D., 1951.
Statistical theory of nuclear energy levels, time-reversal invariance.

d. Temporary Appointments in Physics

Temporary appointees at the postdoctoral level are expected to make an important contribution to the physics research program at the MTC, as they do in the research at the present accelerators at Argonne. The past and present temporary appointments in the Physics Division in the areas of atomic and nuclear physics are summarized above in Table III-I. The universities from which these temporary appointees originated are not given, but the range of institutions is similar to that shown in Table III-II for nuclear chemistry.

An important class of temporary appointments that is not included in Table III-I is the large number of university faculty members and students who in recent years have made use of the FN tandem for their own research or for research in collaboration with Argonne staff members. These faculty members are listed in Table III-IV.

4. Supporting Services

The extent and quality of supporting services can be crucial to the adequate exploitation of a major facility such as MTC, particularly for a scientist not based at the facility and having only a limited amount of time to respond to exigencies. In this respect, Argonne can offer outstanding capacities in shop work, electronics support, computation, procurement of materials, handling of large quantities of radioactivity, and the multiplicity of arts and skills attendant upon 5000 technical people assembled on one site. Many of these services will be of great value to outside users of the MTC.

Shops. Machine, glass-blowing, carpentry, optical, and plastic shops are available on site. There are over 320 craftsmen, 90 engineers and draftsmen, and 70 supporting personnel available in

TABLE III.IV. Outside users of the present Argonne tandem since it went into operation in mid-1962. The names given are investigators at the postdoctoral level. The numbers of graduate students involved are also given.

1. Columbia University
   J. M. Miller

2. DePaul University
   M. Stautberg

3. Indiana University
   R. D. Bent
   W. W. Eidson
   J. J. Kroepfl
   D. S. Plummer
   P. P. Singh
   + 15 students

4. University of Iowa
   R. R. Carlson
   R. T. Carpenter
   + 7 students

5. Kansas State University
   J. C. Legg
   + 1 student

6. University of Kansas
   R. S. Cox
   R. W. West
   + 1 student

7. University of Minnesota
   R. R. Johnson
   J. Lilley
   W. R. Phillips

8. State University of New York at Stony Brook
   L. L. Lee, Jr.

9. Northwestern University
   E. D. Klema

10. Notre Dame University
    E. H. Berkowitz
    C. P. Browne
    A. A. Rollefson
    + 9 students

11. Purdue University and Case-Western Reserve University
    R. P. Scharenberg
    J. W. Tippie
    + 6 students

12. University of Rochester
    W. P. Alford
    D. Cline
    H. E. Gove
    + 3 students

13. University of Texas
    C. F. Moore

14. Western Michigan University
    E. Bernstein
    G. Hardie
    R. E. Shamu
    + 1 student

15. University of Wisconsin
    L. Haskins

16. Yale University
    C. K. Bockelman
    + 3 students

17. Brookhaven National Laboratory
    K. Jones

the Central Shops Division. Since commercial suppliers are used whenever possible, the Laboratory shops are bent toward "state of the art" projects requiring extraordinary tolerances, rapid response, new techniques, unusual or hazardous materials, or close collaboration between scientists and shops.

The shops have been uniquely successful in the manufacture of superconducting magnets, Kel-F and epoxy plastic products, and high-precision sheet-metal work. Some of the shops can cope with radioactive materials.

Electronics. An Electronics Division of 80 technical employees works in instrument development, circuit design, circuit and system applications, feasibility studies, and commercial equipment application. There are specialized groups for fabrication and maintenance, nano-second circuitry, radiation transducers, data handling, and analytical machines. The division maintains a test-equipment facility containing expensive electronic equipment that is not likely to be used frequently. This equipment is available on short-term loan.

Analytical Chemistry. The analytical chemistry section (over 30 technical people) has well-developed capabilities in optical spectrography, mass spectrometry, radiochemistry, neutron activation, gas analyses, crystallography, polarography, atomic absorption, and wet chemical techniques. Target preparations and analyses of contamination have aided the use of the Tandem Van de Graaff and the 60-in. cyclotron.

Computation Center. The Applied Mathematics Division operates a major computation center that provides service to the whole Laboratory. Currently the center contains a CDC-3600 and an IBM-360 computer complex with an extensive array of peripheral devices, supplemental memories, and coordinating computers. This system can now be conveniently entered via remote stations where printouts and other outputs may be obtained. Turnaround time for small jobs may be less than an hour.

In addition, there are numerous lesser computers and shared-time capabilities that are subject to direct control by the scientist. More than 80 employees operate, maintain, and program the machines. Typical applications are pattern recognition in nuclear emulsions and in human fingerprints, calculation of molecular orbitals, and fitting of gamma-ray spectra.

Radiation Safety. The Industrial Hygiene and Safety Division provides equipment and personnel to help the scientist in his responsibility for maintaining safety in his work. Inexperienced scientists can be well served by the many monitoring instruments and by IHS representatives who, in general, have had long experience with the problems of radioactivity, neutrons, and hazardous chemicals. Bioassay and environmental monitoring groups measure low-level activity of personnel, of the effluent wastes, and of the wildlife and streams in the surrounding area.

Radioactive-Waste Disposal. A specialized, trained crew from the Reclamation Department (26 employees) moves in on any spills, using frogmen suits and air-packs where necessary. More routinely, they quickly decontaminate experimental facilities to make them ready for the next user. They process radioactive wastes and change the air filters that remove radioactive particles from the effluent air.

Special Materials. Personnel in the Special Materials Division meet the legal (and safety) requirements for the transportation of radioactive materials and for maintaining inventory controls of fissionable materials.

Libraries. The Library system has about 100 000 books, 200 000 reports, and 1800 different journals. There is a staff of 41, including individuals with some capacity to translate Russian and German. The Library is open at all hours, and is staffed during the day. The library in the Chemistry Building, which would provide service to users of the MTC, is now being enlarged.

IV. UNIVERSITY PARTICIPATION

The Midwest Tandem-Cyclotron accelerator complex is to be a regional facility for advanced research by nuclear physicists and nuclear chemists. It is therefore important to determine the extent to which the proposed facility and its performance specifications would satisfy the research needs of the Midwest community. To determine these needs, an ad hoc committee was appointed by the president of the Argonne Universities Association. The committee met numerous times with the Argonne group responsible for the conceptual design of the proposed system and contacted individually most of the potential users in the area. On the basis of the response to these contacts, the committee recommended that AUA should strongly support the construction of the MTC; the Report* of the committee is appended to this section. Thus, while the conceptual design of the accelerators has been carried out by the design group at Argonne, the performance specifications have been influenced by feedback to the Argonne staff from potential users in the AUA universities.

A number of AUA universities have been pioneers in nuclear research. As long as 25 years ago cyclotrons were in operation at Michigan, Indiana, Illinois, Washington, Ohio State, and Chicago, and Van de Graaff accelerators at Wisconsin, Minnesota, Notre Dame, and Iowa. One of the earliest betatrons was built at Illinois, the first race-track type synchrotron at Michigan, the first reactor at Chicago, and the first proton linac used extensively in research at Minnesota. Physicists at Ohio State University developed the first tandem accelerator and the concept of the sector-focused cyclotron--the two types of accelerators used in the MTC. Current research programs and

*Several items contained in the Report, such as the description of the facility and the collection of letters from prospective users, have been left out of the appended copy.

achievements would take more space than is appropriate here. This strong tradition, with its accumulated know-how and experience, and the continuing vigorous activity in nuclear science represent a research capability that ensures the optimum use of the proposed facility.

The potential outside users of the MTC number approximately 150 staff members (of which 12 are nuclear chemists), some 80 current postdoctorals (16 in nuclear chemistry), and something over 400 graduate students (including approximately 60 in nuclear chemistry) from 29 universities. A list of staff members and institutions is given in Appendix IV-2 at the end of this section. While these numbers are necessarily inexact, they do reflect the considerable interest of a large number of active researchers.

University groups would use the MTC much as they use their own facilities—in other words, both faculty members and graduate students would participate in the research. The mechanism for participation by outside users has yet to be worked out in detail, but it is expected to be similar to that used at the Zero-Gradient Synchrotron. The day-to-day operation would be handled by the staff at Argonne, while questions of policy and the scheduling of running time would be settled by a group representing all users.

The large number of potential outside users and their enthusiastic response to the proposal (including the listing of ideas for experiments) suggest that the facility will not be able to satisfy the total demand for running time. Thus, much of the research now carried out at university laboratories will continue there and will presumably encompass preliminary experiments in preparation for running time at the MTC. These might range from testing detectors and equipment to carrying out complementary experiments at lower energies. While the extent to which such preliminary experiments could be done would depend on the facilities available at the home laboratory, it is clear that considerable work would often be required before going on line at the MTC. The development of new types of equipment (such as detectors,

ion sources, and high-resolution spectrometers) could and should be done in university laboratories as well as at Argonne.

It has been suggested that, since the university staff will be closely involved in the development and use of the MTC facility, this involvement might be enhanced by the mechanism of temporary appointments at Argonne for university staff members. Such appointments might be coordinated with the temporary appointment of members of the ANL research staff to university positions. Such exchange would be attractive to some and healthy both for the universities and Argonne.

Funding for groups participating in experiments at MTC would presumably come from the sources presently supporting their effort, and would cover travel and living expenses while at MTC in addition to the normal in-laboratory support and specialized equipment peculiar to the needs of each group. Participating individuals or groups presumably would not pay for running time. Some technical assistance, laboratory supplies, and other simple basic items of equipment may also be made available, although the extent of such support cannot be specified at this time. Funds for such items would be part of the operating budget of MTC.

APPENDIX IV·1. Report of the ad hoc Committee for a Heavy Particle Accelerator

A medium-energy accelerator capable of accelerating a great variety of ions, from hydrogen to uranium, has been proposed by the Argonne National Laboratory. An information meeting, organized by ANL and attended by thirty-six representatives from Universities and twenty-eight from Argonne, was held at O'Hare Airport on January 11, 1969. On February 10, 1969 the President of the Argonne Universities Association appointed an ad hoc committee to determine the need for such an accelerator facility as felt by the AUA chemistry and physics community and to determine the extent to which the proposed ANL

facility would satisfy this need. The following is the report of that committee.

The committee met some four times with representatives of Argonne National Laboratory, including one meeting held jointly with representatives of the AEC Division of Research. The meetings permitted the committee to keep abreast of Argonne's thinking about the proposed facility as well as to feed back to the technical staff of Argonne some of the thinking of the midwest community.

In brief, the proposed $24M facility contains two separate accelerator systems which could be used together or independently in various modes of operation to provide intense, variable energy beams of light and heavy ions with high resolution in energy. This system would be particularly well suited for nuclear structure work, the production of new isotopes and elements, and for the study of complex nuclear reactions. The building would provide for laboratories, experimental areas, shops and offices.

In determining the need for such a facility as felt by the AUA community a first sampling of opinion was obtained by contacting by phone most of the representatives of AUA Universities that attended the January 11 information meeting. Because their response suggested genuine interest and support for the proposal, it was concluded it would be appropriate to document the degree of support among essentially the entire AUA community of nuclear physicists and chemists, and at the same time to determine the performance requirements as viewed by these potential users. A letter, dated March 12, a copy of which is attached, was mailed to 145 individuals (12 nuclear chemists and 133 nuclear physicists) in 30 universities. Responses in the form of both individual letters and group letters were received from 10 chemists and 110 physicists (including 10 not on the mailing list) representing 26 universities. The committee was gratified by this large response and as a result believes it has an excellent measure of the interest and support for the proposal.

In general the performance characteristics as presently proposed have been arrived at by the Argonne technical group with the benefit of discussions with the committee, and reflect the consensus view of the majority of potential users. There was little diversity of opinion about the performance requirements among the potential users, although one group would have the upper proton energy near 500 MeV so that more intense meson beams would be produced, and several among those interested in light ions expressed strong interest in having higher resolution capabilities than originally proposed. As a result of such feedback, the maximum proton energy has been raised to 350 MeV and the higher resolution capability is now included in the design. With three conditional exceptions, personnel from each of the responding universities would plan to use the facility. The number expressing interest in using beams of heavy ions was essentially equal to the number with interest in using light ones. Some expressed concern of the effect of funding the new facility on existing support.

The committee concludes that there is overwhelming enthusiasm and support for the proposal and that the specifications as presently stated will meet the research needs foreseen by the great majority of working nuclear physicists and chemists in the midwest. The committee believes it is particularly significant that those with experience as outside users of Argonne's facilities are enthusiastic about the cooperation and help they have received at Argonne.

Many of the interesting problems at the forefront of nuclear physics and chemistry require for their elucidation both higher energy and higher precision measurements. The committee believes this proposed facility would provide the next logical step in the development of the necessary experimental apparatus to attack these problems. It believes it is a most important step, and one that

should be initiated at the earliest possible time to ensure the continued logical development in these fields. It therefore recommends to the committee for Physical Sciences and Mathematics and through them to the Board of Trustees of AUA that full support and backing be given ANL in their attempt to obtain this regional facility.

Because of the regional character of the facility, the committee suggests that an AUA interim committee be formed promptly to consult with Argonne personnel on the design of the facilities and on the preparation of the formal proposal.

In summary, your committee is convinced of the need for, the interest in, and the support for the proposed ANL-AUA facility and hopes very much that the AUA Board of Trustees will believe it to be a sufficiently important venture for the future of nuclear physics and chemistry to give it its full endorsement and encouragement.

Respectfully submitted,

R. R. Carlson - University of Iowa
J. W. Cobble - Purdue University
L. Winsberg - University of Illinois, Chicago Circle
W. C. Parkinson (Chairman) - University of Michigan

APPENDIX IV-2. University Scientists Interested in the Possibility of Doing Research at the MTC Facility

Carnegie-Mellon University
- P. Barnes
- A. A. Caretto, Jr.
- T. P. Kohman

Case-Western Reserve
- P. Bevington
- B. Robinson
- R. E. Shrader
- H. B. Willard

Illinois Institute of Technology
- E. L. Sprenkel-Segel

Indiana University
- B. M. Bardin
- R. D. Bent
- D. W. Devins
- L. M. Langer
- D. W. Miller
- M. E. Rickey
- M. B. Sampson
- P. P. Singh

Iowa State University
R. G. Barnes
B. C. Cook
E. N. Hatch
D. W. Martin, Jr.
R. C. Morrison
W. L. Talbert, Jr.
A. B. Tucker
A. F. Voight

Kansas State University
C. L. Cocke, Jr.
B. Curnutte
J. S. Eck
L. D. Ellsworth
D. Fontenla
R. B. Leachman
J. C. Legg
J. R. Macdonald
G. C. Seaman
T. A. Tunolillo

Michigan State University
A. I. Galonsky
R. K. Jolly
W. H. Kelly
W. C. McHarris

Northwestern University
R. E. Segel*
K. K. Seth

Ohio State University
R. G Arns
S. L. Blatt
T. R. Donoghue
H. J. Hausman
P. S. Jastram
W. D. Ploughe

Ohio University
J. L. Adams
C. E. Brient
R. W. Finlay
R. D. Koshel
R. O. Lane
D. S. Onley

Pennsylvania State University
E. Bleuler
R. Graetzer
W. A. Lochstet
T. T. Thwaites

Purdue University
J. W. Cobble
P. J. Daly
Z. W. Grabowski
O. E. Johnson
R. G. Kerr
N. T. Porile
F. A. Rickey
R. P. Scharenberg
R. M. Steffen

St. Louis University
M. Taylor
A. H. Weber

University of Arizona
S. Bashkin
W. S. Bickel

University of Chicago
J. P. Schiffer*
N. Sugarman
A. L. Turkevich

University of Cincinnati
W. F. Stubbins

University of Illinois
P. Axel
M. K. Brussel

(Chicago Circle Campus)
L. Winsberg

University of Iowa
B. C. Carlson
R. T. Carpenter
E. Norbeck
N. W. Waggoner

*Joint appointment at Argonne.

University of Kansas
- D. B. Beard
- R. W. Krone
- H. M. Kuan
- F. W. Prosser, Jr.

University of Michigan
- J. Bardwick, III
- W. S. Gray
- H. C. Griffin
- J. Janecke
- W. C. Parkinson
- R. M. Polichar
- R. S. Tickle

University of Minnesota
- J. M. Blair
- J. Broadhurst
- R. E. Brown
- D. Dehnhard
- G. W. Greenlees
- N. M. Hintz
- R. K. Hobbie
- J. S. Lilley
- C. H. Poppe

University of Missouri
- D. E. Troutner

University of Notre Dame
- E. D. Berners
- C. P. Browne
- P. R. Chagnon
- S. E. Darden
- E. G. Funk, Jr.
- E. R. Marshalek
- J. W. Mihelich
- W. Miller
- C. J. Mullen
- A. A. Rollefson
- P. E. Shanley

University of Pittsburgh
- B. L. Cohen
- W. W. Daehnick
- J. N. McGruer
- J. X. Saladin
- R. L. Wolke

University of Texas
- T. I. Bonner
- W. R. Coker
- E. L. Hudspeth
- P. Lieb
- R. N. Little
- C. F. Moore
- I. L. Morgan
- P. Richard
- P. J. Riley
- C. E. Watson
- S. A. A. Zaidi

University of Wisconsin
- H. H. Barschall
- R. R. Borchers
- W. Haeberli
- H. T. Richards

Washington University
- J. C. Hafele
- P. L. Reeder
- J. B. Reynolds
- F. B. Shull

Wayne State University
- G. B. Beard
- M. G. Stewart

Western Michigan University
- E. Bernstein
- G. E. Bradley
- G. Hardie
- L. D. Opplinger
- R. E. Shamu

V. EXPERIMENTAL PROGRAM

The present section on proposed research on the MTC is the work of many individual scientists, both at Argonne and at AUA universities. The writing of the section was coordinated by P. R. Fields and J. P. Schiffer with considerable assistance from M. H. Macfarlane and J. E. Monahan. Other Argonne staff members who contributed are R. C. Bearse, J. R. Erskine, A. Friedman, S. Fried, M. Freedman, J. Gindler, R. E. Holland, A. Jaffey, M. Kaminsky, D. Kurath, R. Lawson, J. V. Maher, L. Meyer, G. C. Morrison, A. Richter, S. L. Ruby, R. E. Segel, R. H. Siemssen, W. K. Sinclair, J. L. Yntema, and B. Zeidman. Universities whose staff members have contributed directly to parts of this section or have proposed experiments that have been incorporated include Carnegie-Mellon University, Indiana University, Kansas State University, Michigan State University, Purdue University, St. Louis University, State University of Iowa, Washington University, and the Universities of Arizona, Chicago, Illinois (Chicago Circle), Illinois (Urbana), Michigan, Minnesota, Pittsburgh, Texas, and Wisconsin.

V.A. SUPERHEAVY ELEMENTS

High-flux reactors, so successful in producing the transplutonium elements, cannot produce elements beyond fermium (Z = 100). Indeed, the synthesis of elements 102—104 was accomplished by heavy-ion bombardments of heavy-element targets. In this section, possible methods of producing the superheavy elements with heavy-ion bombardments are considered and the predicted nuclear and chemical properties of the transactinide elements are summarized.

Theoretical calculations which predict that the next closed proton shells will occur at Z = 114 and possibly 126 and that the next closed neutron shell will be at 184 are discussed and intercompared. Calculations also indicate that nuclides in the region of double-closed-shell nuclei (island of stability) are expected to have relatively long spontaneous-fission and alpha-decay half-lives as a result of increased nuclear stability.

An examination of possible nuclear reactions to produce new elements in or near the island of stability indicates that only the less desirable, short-lived nuclides are produced in the conventional type of heavy-ion nuclear reactions in which a new element results after a few nucleons evaporate from the compound nucleus. Several unusual types of transfer reactions are suggested that may produce the neutron-rich isotopes of the superheavy elements. The most promising approach, however, appears to be the use of very heavy ions ($Z \approx 53—92$) to induce fission of uranium or some heavier element. The yield of the longer-lived superheavy elements is expected to be several orders of magnitude greater for the fission approach than for the other reactions mentioned earlier. Furthermore, the fission yield distribution is very broad; hence a large number of isotopes of many elements in and near the island of stability would be formed simultaneously.

Because of Coulomb distortion of the heavy-ion projectile and of the target nucleus and because of the need for increased excitation energy of the compound nucleus to produce favorable yields of superheavy elements, a minimum of 9—10 MeV/nucleon will be needed for the bombarding projectile.

A brief discussion of the chemistry of the transactinide elements, inferred from their position in the periodic table, is given in the last part of this section. A new transition series of elements is expected to start at element 104 and to be completed at element 110. A superactinide series of elements is expected to begin with element 121 and to be finished with element 153. Some rapid separation techniques are proposed based on predicted physical and chemical properties.

With its outstanding ability to produce intense beams of very heavy ions at a high energy per nucleon, the MTC offers exciting opportunities for research in the field of new-element production.

V.A1. Production of New Elements

a. Introduction

The chemical elements are the building blocks of the universe and a knowledge of their properties is essential for understanding the material world around us. In an effort to systematize our knowledge about the elements, Mendeleev arranged the known elements into the periodic table, emphasizing the periodic recurrence of similar chemical properties with increasing atomic weight. Later, quantum theory provided a basis for understanding the periodicity on the basis of electronic structure.

After the discovery of radioactivity, intensive efforts were made to understand the nuclear properties of the elements. It was in conjunction with the latter effort that many new synthetic elements were produced in the laboratory. Some of the isotopes of artificially-formed elements play an important role in the atomic energy field. If we wish to continue increasing our understanding of atomic and nuclear structure and the ultimate stability of atoms and nuclei, it is important that we continue our efforts in producing even heavier elements in order to extend the periodic table as far as possible.

Certainly one of the most exciting areas of research that we would want to explore with the proposed accelerator is the production of new elements. This would include trying to produce elements just beyond the end of the known periodic table as well as looking for super-heavy elements in regions of increased nuclear stability.

Argonne has had a strong tradition and wide experience in this area of research—dating from the Metallurgical Laboratory, founded in 1942, to the present time. A large number of transuranium nuclides were first isolated and identified at Argonne, and the Heavy Element Chemistry Group contributed significantly to the knowledge of the nuclear properties of approximately one-half of all the known

transuranium isotopes. This group was the co-discoverer of two new elements, einsteinium (element 99) and fermium (element 100), and did some of the early experimental work on the heavy-ion nuclear reaction which led to the production of element 102. The presently accepted systematic correlation of spontaneous fission half-life with the mass of a nuclide was first noted at this laboratory; the experimental results leading to it were developed at Argonne and elsewhere. An experienced staff having the technical know-how in this area of research has been built up over a number of years and will be invaluable in an effective search for new elements.

The known elements extend through element 104 and possibly element 105. Those beyond uranium and through fermium (element 100) are best prepared in high-flux reactors. From our knowledge of heavy-element buildup, based upon 20 years of experience, it appears that elements beyond fermium will not be formed in high-flux reactors. The buildup terminates at Fm^{258}, an isotope that apparently decays by spontaneous fission with a half-life less than 1 sec. At one time it was expected that thermonuclear explosions might be effective in making the neutron-rich isotopes through element 106. However, we have participated in many such shots over a 15-year period and, particularly in the light of our failures to detect masses beyond 257 in the most recent tests, we doubt that this path will be effective in producing elements beyond Z = 100.

The source of elements beyond 100 has been and seems likely to continue to be accelerator irradiations. Elements 102, 103, and 104 have been produced by heavy-ion bombardments of heavy-element targets. Isotopes of element 102 were prepared by carbon-ion irradiations of curium,[1] nitrogen ions on americium,[2] oxygen ions on

---

[1] A. Ghiorso, T. Sikkeland, J. R. Walton, and G. T. Seaborg, Phys. Rev. Letters 1, 18 (1958).

[2] B. A. Zager, M. B. Miller, V. L. Mikheev, S. M. Polikanov, A. M. Sukhov, G. N. Flerov, and L. P. Chelnokov, At. Energ. (USSR) 20, 230 (1966) [English transl.: Soviet J. At. Energy 20, 264 (1966)].

plutonium,[3] and neon bombardments of uranium[4]; isotopes of element 103 were formed by irradiations of californium with boron ions[5] and americium with oxygen ions[6]; element-104 isotopes have been produced by irradiating plutonium with neon ions,[7] einsteinium with boron ions,[8] and californium with carbon ions.[8] These irradiations were carried out either in heavy-ion cyclotrons or heavy-ion linear accelerators. Both types of accelerators have produced heavy-ion beams through neon in intensities sufficient to produce new elements; but because of low cross sections, beyond neon the beam intensities have been too low for the production of new heavy elements.

Within the capabilities of present heavy-ion accelerators, the best approach to the production of new elements appears to be the irradiation of the heaviest available target material with the lightest heavy-ion consistent with the atomic number to be produced. As the atomic number of new heavier elements increases, difficulties in producing them by this technique will increase very rapidly because of the scarcity of very heavy target elements, rapidly decreasing cross section

---

[3] G. N. Flerov, S. M. Polikanov, V. L. Mikheev, V. I. Ilyushchenka, V. F. Kushniruk, M. B. Miller, A. M. Sukhov, and V. A. Shchegolev, Yadern. Fiz. 5, 1186 (1967) [English transl.: Soviet J. Nucl. Phys. 5, 848 (1951)].

[4] E. D. Donets, V. A. Shchegolev, and V. A. Ermakov, At. Energ. (USSR) 16, 195 (1964) [English transl.: Soviet J. At. Energy 16, 233 (1964)].

[5] A. Ghiorso, T. Sikkeland, A. E. Larsh, and R. M. Latimer, Phys. Rev. Letters 6, 473 (1961).

[6] E. D. Donets, V. A. Shchegolev, and V. A. Ermakov, At. Energ. (USSR) 19, 109 (1965) [English transl.: Soviet J. At. Energy 19, 995 (1965)].

[7] G. N. Flerov, Yu. Ts. Oganesyan, Yu. V. Lobanov, V. I. Kuznetsov, V. A. Druin, V. P. Perelygin, K. A. Gavrilov, S. P. Tretiakova, and V. M. Plotko, At. Energ. (USSR) 17, 310 (1964) [English transl.: Soviet J. At. Energy 17, 1046 (1964)]; Phys. Letters 13, 73 (1964).

[8] G. T. Seaborg, Ann. Rev. Nucl. Sci. 18, 68 (1968).

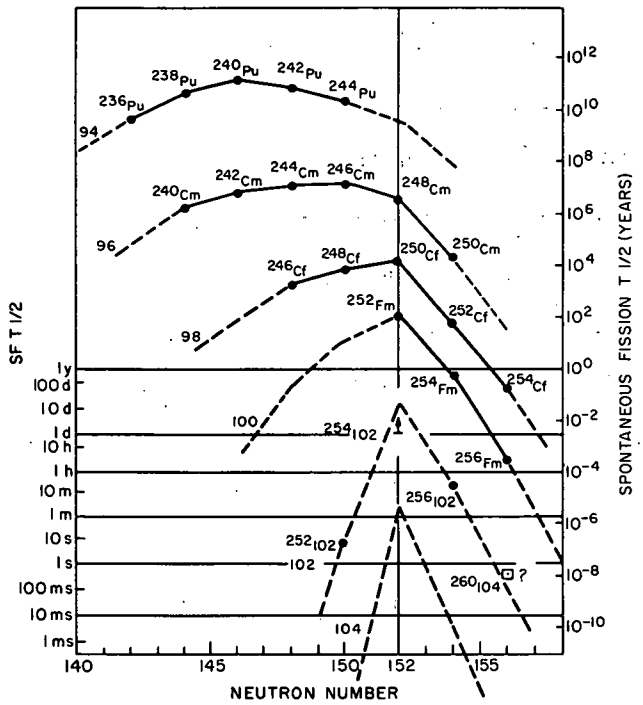

Fig. V.A1-1. Plot of partial spontaneous-fission half-life vs neutron number for even-even nuclides.

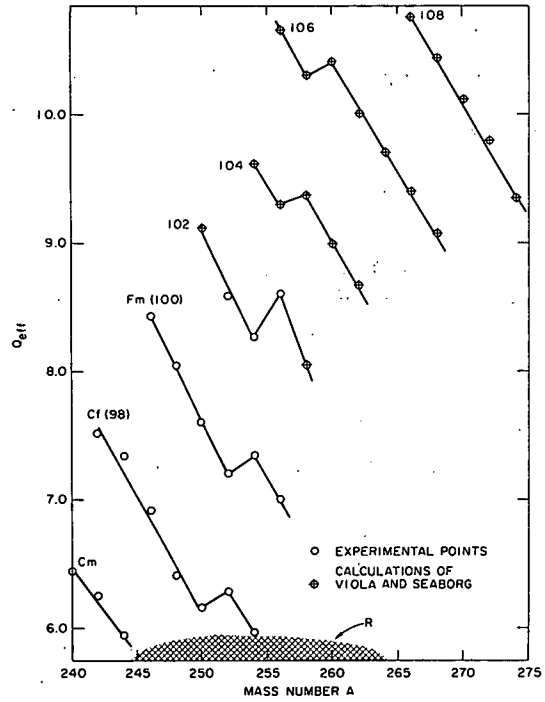

Fig. V.A1-2. Plot of alpha disintegration energy as a function of mass number for even-even isotopes of elements 96—108. The approximate mass region obtainable with present accelerators is indicated by the shaded area R.

as heavier ions are used, and the decreasing alpha and spontaneous-fission half-lives of the neutron-deficient isotopes produced in such reactions. Figure V.A1-1 summarizes the present data on spontaneous fission; Fig. V.A1-2 summarizes the alpha disintegration energies of

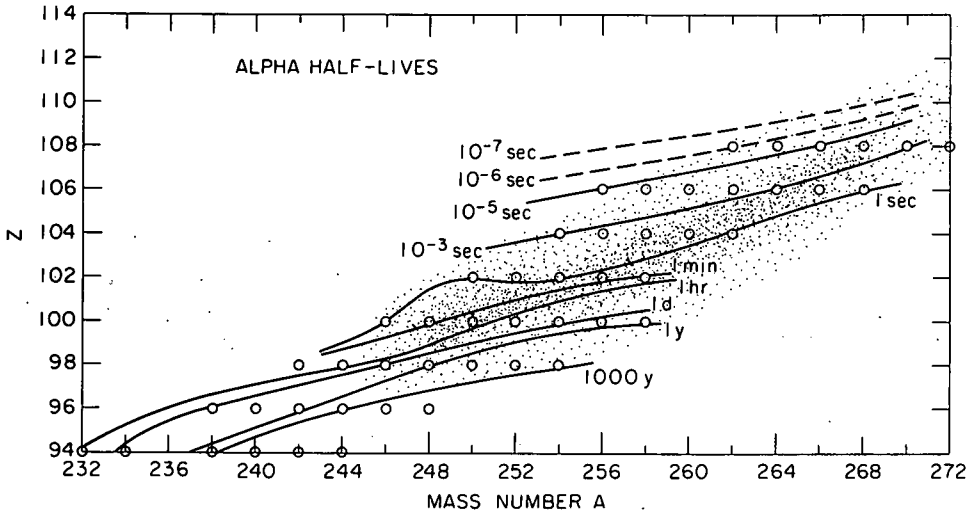

Fig. V.A1-3. The alpha half-lives of isotopes of elements 98—108 that can be formed with present accelerators. Circles represent nuclides that can be produced by irradiating very-heavy-element targets (Z = 94—99) with heavy-ion projectiles through Ne^{20}. The density of the shaded area is proportional to the probability of both forming and observing the isotopes, taking into consideration the limitations set by the alpha half-lives.

the very heavy even-even nuclides and the expected alpha energies of isotopes just beyond the known elements. The alpha disintegration energies of odd-Z isotopes lie between those of the neighboring even-Z elements. The expected alpha half-lives (based on the alpha-decay energies shown in Fig. V.A1-2) are illustrated in Fig. V.A1-3. The regions marked in Figs. V.A1-2 and V.A1-3 show the mass range for elements 102—108 which can be formed by heavy-ion bombardments in presently available accelerators.

b. Closed Neutron and Proton Shells in the Superheavy Region

A number of very interesting theoretical calculations have been reported recently concerning the location of the next closed proton shell beyond 82 protons and the next neutron shell beyond the 126-neutron shell. Early extrapolations as to the next closed proton shell were strongly influenced by the analogy between the closed neutron

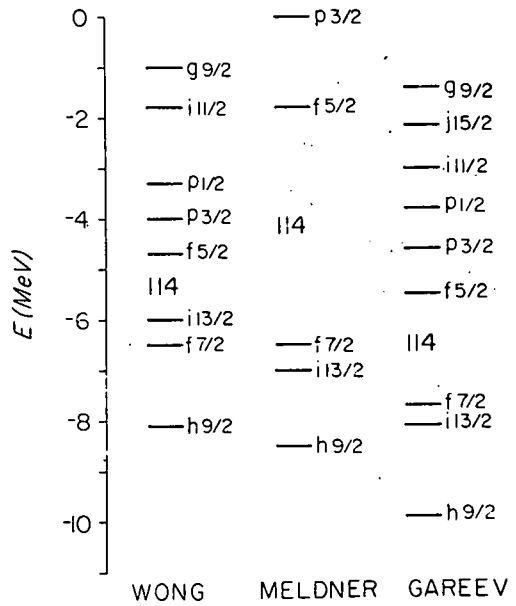

Fig. V.A1-4. Predicted level spacings for protons, showing the shell closure at 114 protons. Based on calculations given in Refs. 10, 11, and 12.

and proton shells in the lighter nuclides, so they generally predicted that the next closed proton shell would be at Z = 126. However, more recent calculations by many different theorists[9—14] both at Argonne and elsewhere agree that the next closed proton shell will be at 114, but there is some disagreement as to whether 126 will also be a closed proton shell.

Figure V.A1-4 shows the predicted proton level spacing for spherical nuclei in the mass region 290—300 as calculated by three different theorists using different approaches. Thus, Meldner[10] used

---

[9] A. Friedman, in International Symposium on Nuclear Structure, Dubna, USSR, 4-11 July 1968, Contributions (Joint Institute for Nuclear Research, Dubna, 1968), Dubna publication D-3893, p. 61.

[10] H. Meldner, Arkiv Fysik 36, 593 (1966).

[11] A. Sobiczewski, F. A. Gareev, and B. N. Kalinkin, Phys. Letters 22, 500 (1966).

[12] C. Y. Wong, Phys. Letters 21, 688 (1966).

[13] S. G. Nilsson, J. R. Nix, A. Sobiczewski, Z. Szymanski, S. Wycech, C. Gustafson, and P. Möller, Nucl. Phys. A115, 545 (1968).

[14] E. Rost, Phys. Letters 26B, 184 (1968).

a nonlocal potential of the Van Vleck type; his approach leads to the right mass defect for the total nucleus and also correctly accounts for the energy levels of the tightly-bound protons observed in (e,e'p) scattering measurements. His calculation predicts a closed shell at 114 protons with a 4—6-MeV energy gap between the $f_{5/2}$ and $f_{7/2}$ levels, the gap distance depending upon the strength of the spin-orbit interaction used in the calculations. The energy gap at 126 protons (the gap between the $3p_{3/2}$ and $1i_{11/2}$ levels) is much smaller—of the order of 2 MeV.

Gareev[11] and Wong[12] both used a local Woods-Saxon potential in their calculations. This approach reproduces the observed spin sequences and equilibrium deformations, but does not account for the energy levels of the tightly bound protons observed in the high-energy electron-scattering experiments nor does it yield the correct mass defect, i.e., total binding energy. Although they used somewhat different values of the parameters (the depth and radius of the proton potential, the surface diffuseness, and the spin-orbit coupling constant), Gareev and Wong predict a closed proton shell at 114. However, while Wong's calculations predict a shell at 126 protons, Gareev's sequence of levels shows no energy gap at 126.

The results of more recent calculations by Nilsson[13] and Rost[14] are shown in Fig. V.A1-5. Both calculations involve local potentials. Rost used a Woods-Saxon potential and carefully selected his parameters to reproduce the proton levels recently measured in Bi^{209}. He also obtained closed shells at 114 and 126 protons, but the $f_{5/2}$-$f_{7/2}$ energy gap is about 1.6 MeV. Nilsson used a harmonic-oscillator model for his calculations, and determined his parameters in the deformed region of the rare-earth and actinide nuclides with the condition that these parameters reproduce the right separation and sequence of levels for closed-shell nuclei. Nilsson's calculations show a closed proton shell at 114 with a level gap slightly more than 2.5 MeV.

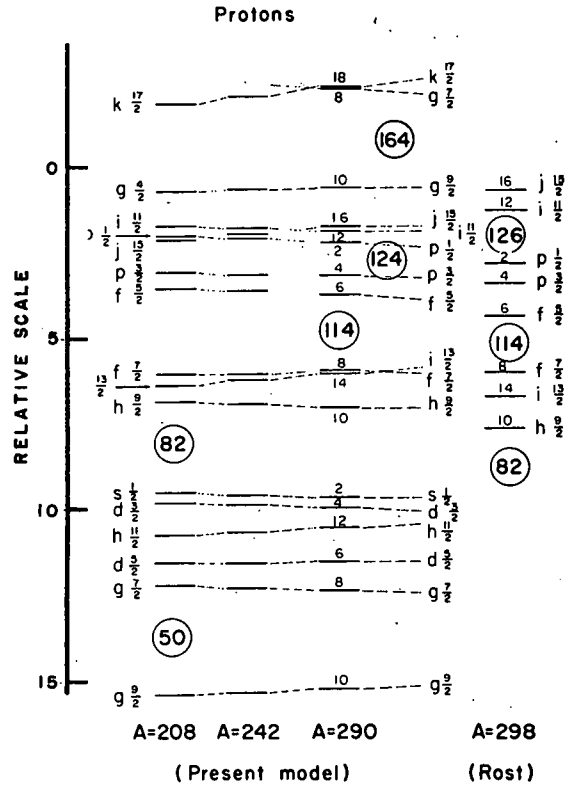

Fig. V.A1-5. Predicted level spacings for protons, showing shell closures at 114, 126, and 164. Based on calculations given in Refs. 13 and 14. The ordinate is in MeV.

As for the neutron levels in the superheavy region, Figs. V.A1-6 and V.A1-7 show the results of the theoretical calculations by the same five authors that reported the proton-level calculations. There is a unanimity of opinion that there will be a closed neutron shell at 184 neutrons. Meldner, and Rost also show energy gaps in the neutron levels at 164, and Nilsson shows a gap at 170 neutrons. The neutron gap energies vary from about 2 to 4 MeV.

It is very encouraging that so many different approaches—using not only different models, but also a range of parameter values—still come to virtually the same conclusions. On the basis of the above calculations, 114^{298} and 126^{310} (and perhaps with somewhat less likelihood, 114^{278} and 126^{290}) are expected to be doubly-closed-shell nuclides with stabilization energies estimated variously from about 8.5 down to 3 MeV.

It should be noted that the stabilizing influence of a closed shell extends over a range of neutron and proton numbers. Such behavior is known to occur in the vicinity of the closed shells at 126, 82, etc.

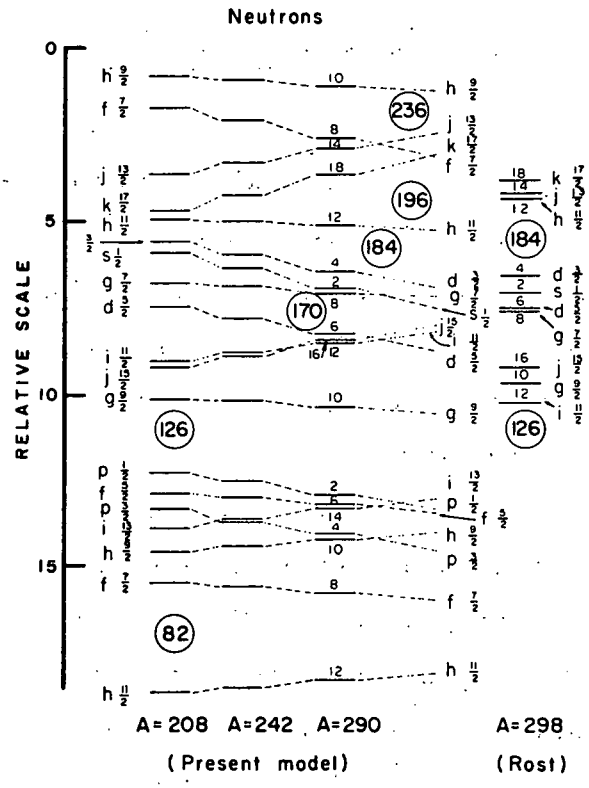

Fig. V.A1-6. Predicted level spacings for neutrons, showing shell closures at 170, 184, and 196 neutrons. Based on calculations given in Refs. 13 and 14. The ordinate is in MeV.

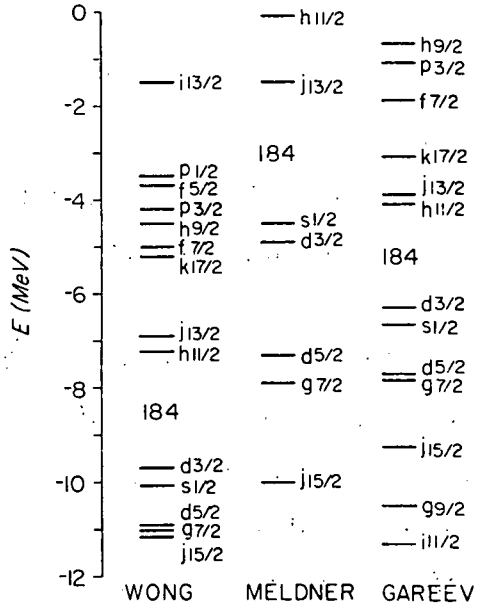

Fig. V.A1-7. Predicted level spacings for neutrons, showing a shell closure at 184 neutrons. Based on calculations given in Refs. 10, 11, and 12.

Thus, an entire region of increased nuclear stability is expected in the general area of Z = 114 and N = 184. Seaborg refers to this large region as the "island of stability."

c. Alpha and Spontaneous-Fission Half-Lives of Superheavy Elements

Accepting the possibility of stable doubly-closed-shell superheavy nuclei, what would the expected alpha and spontaneous-fission half-lives be in these regions? These are the truly limiting half-lives as far as detection of new elements is concerned, since these half-lives can be much less than 10^{-9} sec, whereas the half-lives for beta and electron-capture decay do not become much shorter than 0.1—0.01 sec.

Let us examine the theoretical predictions for the spontaneous-fission half-lives of the superheavy nuclides in the region of doubly-closed shells. This mode of decay is one of the important limiting factors in the ability to form and identify the lighter isotopes of the heaviest known elements.

For nuclides in the region near Z = 114, the fissionability parameter

$$X = \frac{Z^2/A}{(Z^2/A)_{\text{limiting}}} = \frac{Z^2/A}{50.18}$$

is normally about 0.9; and one would expect the liquid-drop fission barrier to be about 0.9 MeV, and the corresponding spontaneous-fission half-life to be $\sim 10^{-15}$ sec. For element 126, $X \approx 1.0$ and the nucleus would fission almost immediately after formation—i.e., in about 10^{-22} sec. However, shell effects can have a pronounced influence on the height of the fission barrier and can change the predicted spontaneous fission half-lives drastically. Stabilization of the superheavy nuclei by shell effects has been calculated by a number of theoreticians and their results are again very encouraging.

In their semi-empirical extension of the liquid-drop model, Meyers and Swiatecki[15] determined the Z^2/A dependence of spontaneous-fission half-life by correcting for deviation in the actual mass of a

[15] W. D. Myers and W. J. Swiatecki, Nucl. Phys. 81, 1 (1966).

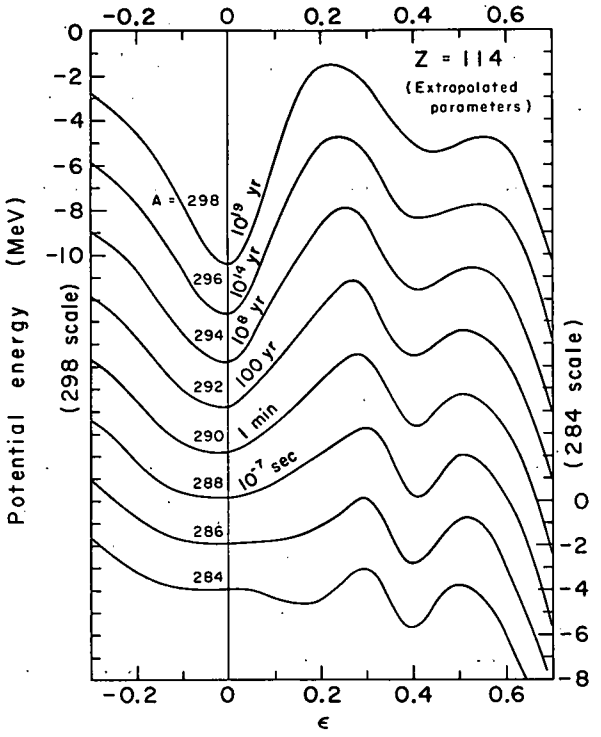

Fig. V.A1-8. Plot of potential energy barriers, showing degree of stability against decay by spontaneous fission for nuclei with Z = 114 and A = 284—298. The energy scale is arbitrarily displaced 3 MeV between successive values of A. The abscissa ϵ is a parameter related to nuclear deformation. (From Ref. 8.)

nucleus from a liquid-drop reference mass. This model was used to calculate fission barriers and spontaneous-fission half-lives as a function of Z and A. The calculations predicted long spontaneous-fission half-lives for nuclides in the region of the doubly-closed shells.

A more sophisticated approach was used by Nilsson and co-workers[13] to calculate the spontaneous fission half-lives to be expected for the superheavy nuclides. Their approach and results are presented here in somewhat greater detail. Their calculations involved computing the total-potential-energy surfaces as a function of Y_{20} (quadrupole) and Y_{40} (hexadecapole) distortions, considering single-neutron and single-proton states and taking into account the pairing force of these nucleons and the addition of the Coulomb energy. Figure V.A1-8 shows the variation of spontaneous-fission half-life for different isotopes of element 114 and illustrates the fact that shell effects extend over a range of neutron numbers. Table V.A1-I lists the expected spontaneous-fission half-lives for isotopes of the even-A elements from 114—124. Again the results agree with the principle that the proton shell effect extends over a range of atomic numbers.

TABLE V.A1-I. Spontaneous-fission half-lives (years) for various isotopes with Z = 114—124. (From Ref. 13.)

N	Z = 114	116	118	120	122	124
188						2×10^{-9}
186					4×10^{-6}	2×10^{-8}
184	2×10^{19}			9×10^{0}	2×10^{-5}	1×10^{-7}
182	2×10^{14}	8×10^{8}	5×10^{2}	2×10^{-5}	1×10^{-8}	1×10^{-10}
180	3×10^{8}	6×10^{2}	2×10^{-7}	5×10^{-11}	1×10^{-12}	
178	1×10^{2}	2×10^{-5}	1×10^{-11}			
176	7×10^{-6}	2×10^{-11}				
174	5×10^{-15}					

It should be noted that in the region of the known nuclides, the odd-A or odd-Z isotopes usually have much longer spontaneous-fission half-lives than their even-Z or even-A neighbors. Hence the values shown in Fig. V.A1-8 and in Table V.A1-I should represent lower limits to spontaneous-fission half-lives for superheavy nuclides in this region of mass and charge.

Figure V.A1-9 shows the alpha energies derived from

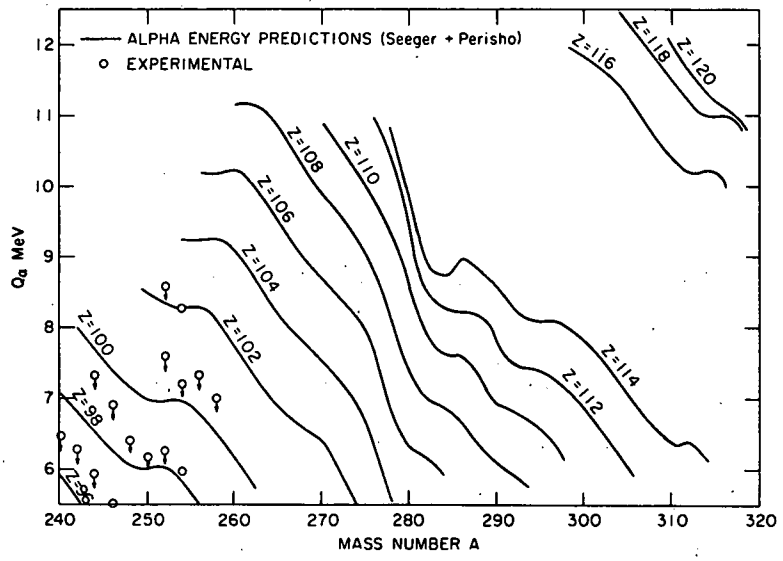

Fig. V.A1-9. Plot of alpha disintegration energy as a function of mass number for even-even isotopes of elements 96—120. The curves are based on the mass formula given in Ref. 16. Circles represent experimental data; arrows indicate the appropriate Z curve.

the mass formula of Seeger and Perisho.[16] This formula is based on the liquid-drop model with shell corrections derived from the Nilsson model, but the Y_{40} distortion is neglected. Calculations using this formula show a closed proton shell at Z = 114. Figure V.A1-10 shows the modes of decay expected in the region of double-closed-shell nuclides, with the beta-stable isotopes clearly marked and the alpha half-lives calculated from the alpha energies given in Fig. V.A1-9. The alpha half-lives were calculated by use of Preston's equations,[17] in which only the nuclear radius is a variable. This approach agrees fairly well with the half-lives calculated by the more empirical method of Viola and Seaborg.[18]

Several odd-proton odd-neutron isotopes, predicted to decay by either electron capture or beta-particle emission, would have high-spin isomers whose half-lives for these modes of decay would be much longer than those of their low-spin isomers and which would be primarily alpha-particle emitters. Examples of such nuclides are 109^{284}, 111^{288}, and 113^{296}. These isotopes would also be expected to have much longer spontaneous-fission half-lives than their even-even neighbors.

d. Nuclear Reactions to Produce Superheavy Elements

In order to reach the desired superheavy nuclei in the island of stability, a new heavy-ion accelerator, such as is being proposed here, is necessary. The heavy-ion accelcrators in existence cannot develop a useful beam of projectiles above Ar (Z = 18). At present, the best yield of elements above Z = 100 is obtained by irradiating

---

[16] P. A. Seeger and R. C. Perisho, Los Alamos Scientific Laboratory Report LA-3751 (1967).

[17] M. A. Preston, Phys. Rev. 71, 865 (1947).

[18] V. E. Viola and G. T. Seaborg, J. Inorg. Nucl. Chem. 28, 741 (1966).

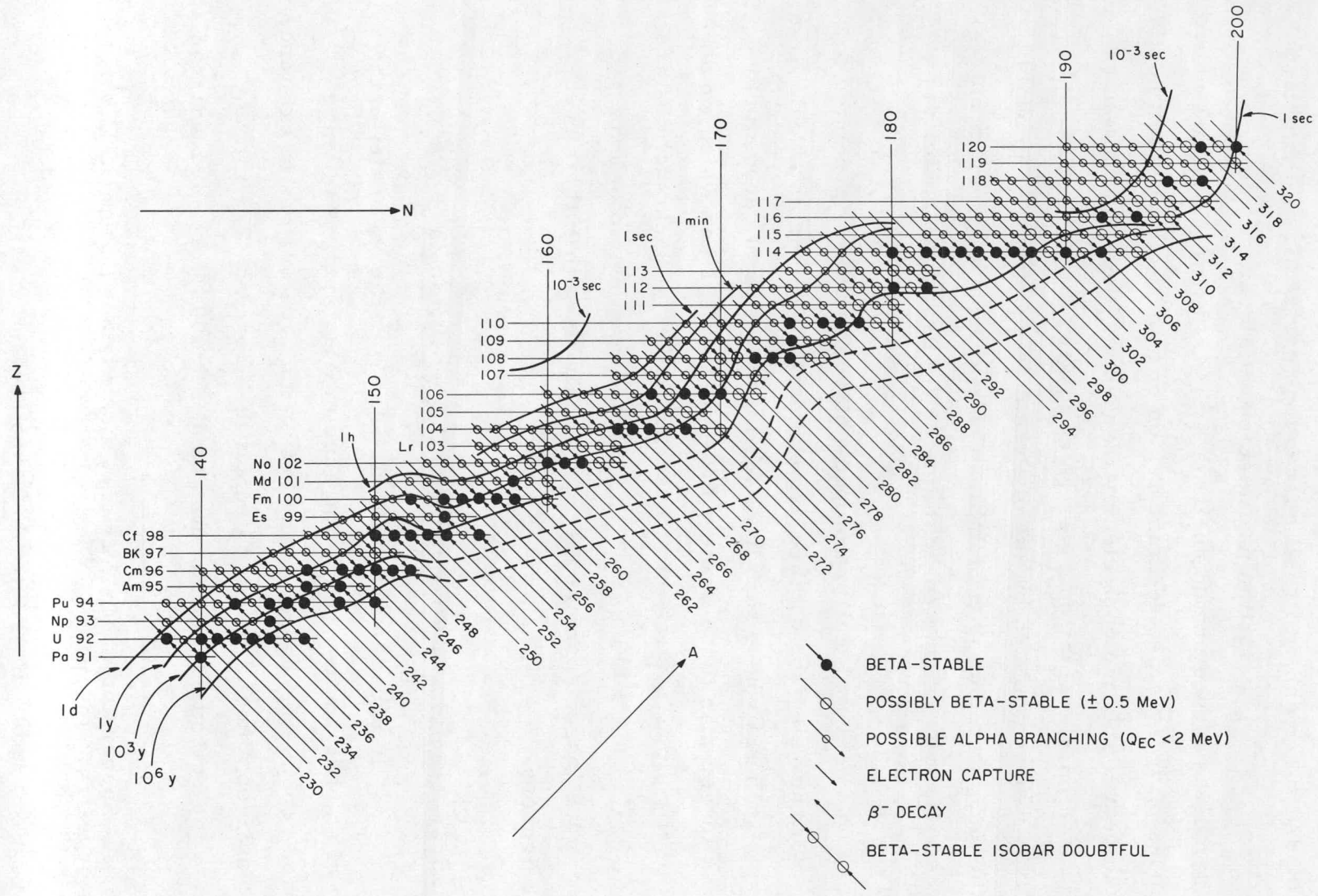

Fig. V.A1-10. Predicted alpha half-lives for the superheavy nuclides in or near regions of beta stability. (See Fig. V.A1-8 and Table V.A1-I for predicted spontaneous-fission half-lives.)

the heaviest available target with ions lighter than neon (Z = 10). As the mass of projectiles is increased, the cross section for producing a given heavy element drops off rapidly as a result of fission competition. Thus, the neutron-deficient isotopes that can be produced with existing accelerators fall short of the island of stability. However, the following considerations indicate that if much heavier ions with adequate energy are used, they will be able to form the superheavy nuclides in the region of increased nuclear stability.

i. Cold-nucleus reactions (inverse fission). It has been suggested by many different groups of scientists that perhaps the yield of new elements could be vastly improved, particularly among the superheavy elements, through the use of the so-called "cold nucleus" reactions (also called "inverse fission"). In these, the compound nucleus is formed with low excitation energy. The target and projectile are of comparable mass, so that target and projectile nuclei lie in a region of high particle binding energy and produce heavy elements lying in a region of lower binding energy. Such reactions are endothermic and, at least in principle, the excitation energy of the compound nucleus should be controllable by regulating the kinetic energy of the bombarding projectile. For example, Table V.A1-II shows the expected excitation of various element-106 compound nuclei for different combinations of targets and projectiles. The table lists the nuclear reaction being considered, the Q of the reaction as calculated from Cameron's mass table,[19] the Coulomb barrier calculated for undistorted nuclei, and the excitation energy of the compound nucleus. It indicates that projectiles in the region of atomic number 28 (nickel) or greater can form compound nuclei with excitation energies less than zero. The excitation energies of these reactions, in principle, can then be controlled by the amount of kinetic energy imparted to the projectile. By limiting the excitation

[19] A. G. W. Cameron and R. M. Elkin, "Role of the Symmetry Energy in Atomic Mass Formulas," Goddard Institute for Space Studies, New York.

TABLE V.A1-II. Typical nuclear reactions to produce element 106.

Nuclear reaction	Q of reaction (MeV)	Barrier height (MeV)	Minimum excitation energy (MeV)
$_{100}Fm^{257} + {}_{6}C^{13} \rightarrow 106^{270}$	-34.8	76.3	+37.4
$_{88}Ra^{226} + {}_{18}Ar^{40} \rightarrow 106^{266}$	-125.7	185	+31
$_{78}Pt^{198} + {}_{28}Ni^{64} \rightarrow 106^{262}$	-214	246	-28
$_{70}Yb^{176} + {}_{36}Kr^{86} \rightarrow 106^{262}$	-244	279	-57
$_{52}Te^{130} + {}_{54}Xe^{136} \rightarrow 106^{266}$	-288	305	-135

energy, fission competition could perhaps be suppressed and large compound-nucleus cross sections could result.

Table V.A1-III illustrates some types of nuclear reactions that might be used to produce nuclides near or in the region of the island of stability. Reaction 1 was attempted at the Lawrence Radiation Laboratory, Berkeley, but no positive results were observed. $_{22}Ti^{50}$ was accelerated at Dubna and Reaction 2 was attempted, also without any positive results. Both of these nuclear reactions would yield nuclei fairly far from the closed neutron shell at N = 184 and the spontaneous-fission half-lives are estimated to be much less than a nanosecond, which would make the products unobservable. Reactions 3 and 4 are illustrative of nuclear reactions in which neutron-rich isotopes are employed to give isotopes of element 114 with more neutrons than in Reactions 1 and 2. According to Fig. V.A1-10 this product lies in the region of nuclides that are readily detectable. Reactions 5 and 6 are of the "cold nucleus" type, but produce isotopes of element 114 which probably have too short a spontaneous fission half-life to allow detection. It is fairly obvious that a neutron-rich isotope of element 114 near mass 298 is difficult to produce with conventional reactions (exemplified by

TABLE V.A1-III. Possible heavy-ion reactions leading to element 114.

1.	$_{96}Cm^{248} + {}_{18}Ar^{40}$	$\rightarrow 114^{284} + 4n$
2.	$_{92}U^{238} + {}_{22}Ti^{50}$	$\rightarrow 114^{284} + 4n$
3.	$_{94}Pu^{244} + {}_{20}Ca^{48}$	$\rightarrow 114^{290} + 2n$
4.	$_{96}Cm^{248} + {}_{20}Ca^{48}$	$\rightarrow 114^{290} + 2n + {}_{2}He^{4}$
5.	$_{50}Sn^{124} + {}_{64}Gd^{160}$	$\rightarrow 114^{284}$
6.	$_{54}Xe^{136} + {}_{60}Nd^{150}$	$\rightarrow 114^{286}$
7.	$_{64}Gd^{160} + {}_{70}Yb^{176}$	$\rightarrow 114^{298} + 20p + 18n$
8.	$_{48}Cd^{116} + {}_{92}U^{238}$	$\rightarrow 114^{298} + {}_{26}Fe^{56}$
9.	$_{64}Gd^{160} + {}_{92}U^{238}$	$\rightarrow 114^{298} + {}_{42}Mo^{98} + 2n$
10.	$_{92}U^{238} + {}_{92}U^{238}$	$\rightarrow 114^{298} + {}_{70}Yb^{174} + 4n$

the first six in Table V.A1-III. Perhaps unusual transfer reactions such as Reactions 7 and 8 might yield neutron-rich isotopes of element 114 in or near the island of stability, although they may prove to have too small a cross section. Currently, reactions such as 9 and 10 appear to offer the most hope for getting the desired very-neutron-rich isotopes near element 114. Reactions 9 and 10 are in essence fission reactions, in which the superheavy elements occur as fission products.

It should be emphasized that the nuclear reactions in Table V.A1-III represent only selected kinds of interactions between complex nuclei; other possibilities exist as well. Reactions 9 and 10 deserve a little more discussion, since they may well represent the kind of reaction that will succeed in yielding the desired superheavy

nuclei. Furthermore, these reactions will produce many different isotopes over a range of atomic number Z and mass number A.

ii. Heavy-ion-induced fission. On the basis of recent heavy-ion studies, it appears that very-heavy-ion-induced fission of the elements available is the most favorable approach to producing the elements in the "island of stability." Extrapolating from heavy-ion-induced fission with lighter projectiles, calculations indicate that the superheavy elements will fall in the high-mass tail of the single-peak fission-yield curve. The width of the fission-yield curve increases with increasing mass and energy of the bombarding projectile, thus raising the yield of the superheavy elements. To produce the necessary compound nuclei that lead to the desired fission products will require projectiles with atomic numbers 50—92 and having energies of approximately 8—10 MeV/nucleon.

Karamian[20] has shown that in heavy-ion-induced fission the width of the mass distribution of fission products increases rapidly with the Z^2/A of the compound nucleus. Figure V.A1-11 shows the fission yield curves for neon and argon irradiations of uranium, and the predicted curve for uranium irradiated with krypton. The curves indicate that possibly new elements and the neutron-rich isotopes of the very heavy elements would result from the krypton-induced fission of uranium. The use of $_{96}Cm^{248}$ instead of $_{92}U^{238}$ as a target would increase the probability of forming even heavier fission products. If this trend were to continue when such heavy ions as $_{54}Xe^{136}$, $_{64}Gd^{160}$, or $_{92}U^{238}$ are used as the projectiles, then nuclei in the region of Z = 114 with masses about 300 would result. These, of course, are the desired superheavy nuclei in the region of increased stability.

---

[20] S. A. Karamian, F. Normuratov, Yu. Ts. Oganesyan, Yu. E. Penionzhkevich, B. T. Pustyl'nik, and G. N. Flerov, Joint Institute for Nuclear Research, Dubna, 1968, preprint P7-3732 [ANL translation 747].

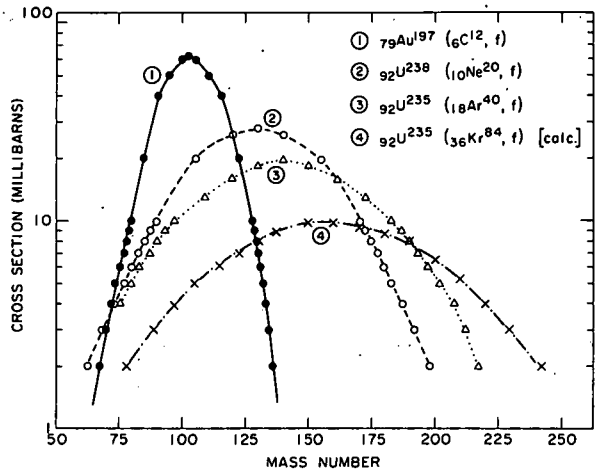

Fig. V.A1-11. Mass distribution of fission fragments produced by heavy-ion-induced fission of targets listed in the figure. (From Ref. 20.)

Recent calculations by Karamian and Oganesyan[21] of the yields of elements 110 and 114, given in Table V.A1-IV, indicate very favorable formation cross sections through the fission-type nuclear reaction. These estimated cross sections are orders of magnitude larger than the expected cross sections for the production of these elements by nuclear reactions of types 1 — 8 listed in Table V.A1-III. Some of the arguments underlying the calculations that led to the values given in Table V.A1-IV are the following. (1) The formation of very heavy compound nuclei are possible. This is justified on the dynamics of fission and compound-nucleus formation. (2) The ratio Γ_f/Γ_n of super-heavy nuclei with closed shells (in the neighborhood of Z = 114) is small, as calculated by Sikkeland.[22] Hence, they will not have a high probability of being lost by secondary fission. (3) Coulomb-induced fission is negligible, as estimated from the work of Wilets et al.[23] (4) The mass and charge distribution of fission products can be extrapolated from the measured values in Ne- and Ar-induced fission of uranium to the unknown values for Xe- and U-induced fission of uranium.

[21] S. A. Karamian and Yu. Ts. Oganesyan, Joint Institute for Nuclear Research, Dubna, 1969, preprint P7-4339 [ANL translation 745].

[22] T. Sikkeland, Arkiv Fysik 36, 539 (1966).

[23] L. Wilets, E. Guth, and J. S. Tenn, Phys. Rev. 156, 1349 (1967).

TABLE V.A1-IV. Parameters and results from the in the reactions U(U,f) and U(Xe,f). (From Ref. 21.)

	Total excitation energy of the compound nucleus (MeV)	Parameter of the width of mass distribution[a] σ_A^2	Charge dispersion σ_Z^2
$U^{238}(Xe^{136},f)$	50	3500	2.5
	100	3800	2.7
$U^{238}(U^{238},f)$	50	4100	3.5
	100	4500	3.7

[a]The standard deviation of the fission-product distribution is $\sigma_A/\sqrt{2}$ and is ~43 for a Xe projectile and ~46 for a U projectile. Since the fission yield drops only to 13% of the peak value at ±2 standard deviations, the fission products within a range about 180 mu wide have comparable yields.

The cross sections calculated in Table V.A1-IV may be underestimated as a result of the neglect of two possible effects: (1) The fission-yield curves may not be smoothly varying functions of A and Z as predicted, but rather may be sensitive to shell structure, so that the yield in the region of the doubly-closed-shell nuclide 114^{298} could be enhanced. (2) Calculations show that about 90% of the total cross section goes into direct interactions, whereas the yields quoted in Table V.A1-IV are based on the remaining 10% that goes into compound-nucleus formation followed by fission. It is quite possible that 110^{294} and 114^{298} could result from the direct interaction of projectile and target, thus increasing the over-all formation cross section.

The projectile energy required to overcome the conventionally-calculated Coulomb barrier between a uranium target and

calculation of production cross sections of the nuclei 110^{294} and 114^{298}

Number of neutrons evaporated from the reaction product	Most probable mass of the reaction product after the evaporation of neutrons		Production cross section (cm^2)	
	Z = 110	Z = 114	110^{294}	114^{298}
4	288	299	0.7×10^{-30}	3×10^{-30}
7	285	296	0.3×10^{-30}	8×10^{-30}
5	288	300	6×10^{-30}	1.5×10^{-29}
9	284	296	0.4×10^{-30}	3.5×10^{-29}

uranium projectile to form a compound nucleus in the laboratory system is 6.3 MeV per nucleon. This energy, calculated on the basis of the naive model of spherical nuclei, is undoubtedly too low. As a result of Coulomb (polarizing) distortions of the target and projectile, the Coulomb barrier may be approximately 30% higher[24,25]; this implies that about 8.2 MeV/nucleon would be required for the uranium projectile to form a compound nucleus with a uranium target. A lighter ion such as $_{54}Xe^{136}$ or $_{53}I^{127}$ would require 7.3 MeV/nucleon, after correcting for Coulomb distortion, to form a compound nucleus with uranium. Using extrapolations discussed in Ref. 20, one finds that the Q of the reaction to form a compound nucleus between a uranium target and a uranium or xenon projectile is actually negative, so an energy greater

[24] R. Beringer, Phys. Rev. Letters 18, 1006 (1967).

[25] C. Y. Wong, Phys. Letters 26B, 120 (1968).

than 8.2 or 7.3 MeV/nucleon will be needed. Since the fission yield is relatively small in the region of element 114 and depends on the excitation of the compound nucleus formed by uranium with either uranium or xenon projectiles, an additional 10% increase in the energy of the incoming projectile might be desirable. It would also be very desirable to have available another 2—3 MeV/nucleon in order to see where a decrease in the yield of 114^{298} occurs. The decrease could then be related to the onset of fission in the double-closed-shell fission-product nuclide and may be the only way of measuring Γ_f/Γ_n for "stiff" nuclei in the superheavy elements. The variable energy of the proposed accelerator would be a valuable feature in such a study. Thus it appears that any proposed accelerator should produce uranium ions with about 9—11 MeV/nucleon and ions in the region of xenon with about 8.5—10.5 MeV/nucleon. These energies are well within the capabilities of our proposed accelerator. It would be unrealistic to expect accelerators that cannot reach at least the lower range (~9 MeV/nucleon) of these energies to produce elements in the "island of stability" by the fission technique.

If the fission type of reaction is successful, then the formation of a large number of new elements—even beyond 114—will be possible, as well as the synthesis of many new neutron-rich nuclides.

For elements above 114, synthesis by ordinary heavy-ion reactions is more favorable because the neutron/proton ratio required is lower, and nuclear reactions using available combinations of projectiles and targets are more plentiful than in the Z = 114 region. For example, the synthesis of 126^{310}, a possible doubly-closed-shell nuclide, might be accomplished by the reactions

$$_{36}Kr^{80} + {}_{90}Th^{230} \rightarrow 126^{310},$$

$$_{35}Br^{79} + {}_{91}Pa^{231} \rightarrow 126^{310},$$

etc.

Similarly, the preparation of element 118 might be accomplished by

$$_{20}Ca^{48} + {}_{98}Cf^{252} \rightarrow 118^{296} + 4n.$$

The number of possible combinations is very large but will not be listed here.

Another consideration, mentioned earlier in this discussion, is a possible closed shell of neutrons at N = 164. Should this neutron number give sufficient added stability to some of the superheavy elements, then the synthesis of nuclei having 164 neutrons would be much easier than that of nuclei in the vicinity of the 184-neutron shell. Only experimental results can provide the necessary data for proving the existence of nuclear stability in the vicinity of the proposed closed neutron and proton shells.

e. Electronic Structure of Superheavy Elements

From the foregoing discussion it appears that the use of fission-type reactions is a promising technique for producing the superheavy elements in the "island of stability." This approach would produce a fairly large number of new elements, some of which are calculated to have long alpha and spontaneous-fission half-lives. Thus, to identify the nuclides produced, it will be necessary to chemically separate each element from a wide distribution of other elements, and then to identify the atomic number of the new species. To predict the chemical behavior of the superheavy elements, and thus provide the necessary clues to devise separation procedures, requires a consideration of the probable position of the new elements in the periodic table.

The positions of the elements in the periodic table depend on their electronic structure. An excellent discussion of this problem has been given by Seaborg[8] and only the essential points are mentioned here. The expected locations of the new elements in the periodic table,

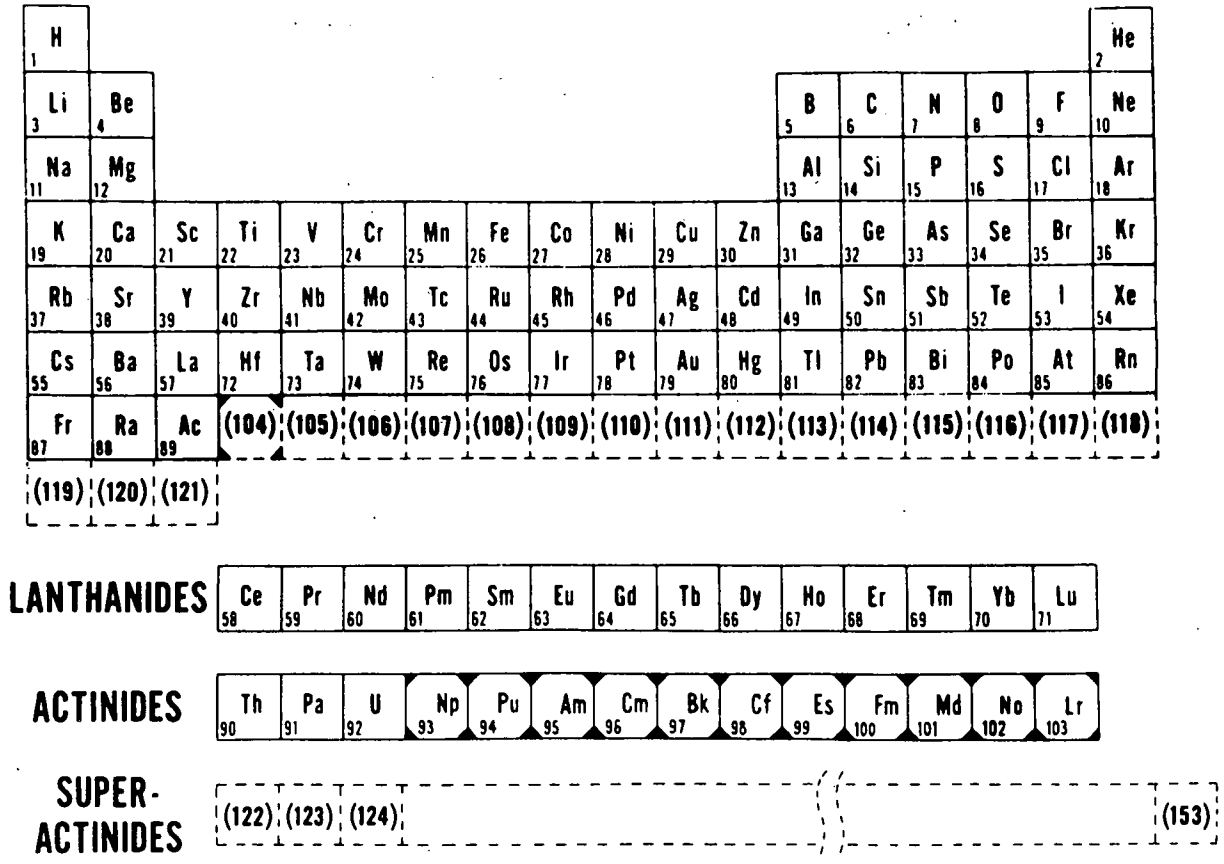

Fig. V.A1-12. Periodic table showing predicted location of elements 104—153. (Adapted from Ref. 8.)

as predicted by Seaborg, are shown in Fig. V.A1-12. This chart is based on various Hartree-Fock-type calculations made by several groups at the Los Alamos Scientific Laboratory. Theory indicates that elements 104—112 are formed by filling the 6d subshell with electrons; their chemical properties should then resemble the series of elements from hafnium (Z = 72) to mercury (Z = 80). This analysis also predicts elements 113—118 will result from the filling of the 7p subshell, elements 119 and 120 result from filling the 8s subshell, and element 120 should begin to fill the 7d subshell. As is evident from Fig. V.A1-12, the elements 104—120 occupy the usual positions in the periodic table and should resemble their homologs in the various periodic groups.

The exact electronic structures of the elements above 121 are somewhat uncertain because there are four electronic subshells

available with very close energies, so the sequence in which these levels are filled is difficult to determine. These levels are 7d, 6f, 5g, and 8p. The best estimates indicate that some electrons will add initially to the 7d, 8p, and 6f subshells and then the 5g subshell will be sequentially filled. Following the filling of the 5g inner shell, the 6f subshell will be completed and the new super-actinide series (containing 32 elements) will be completed with element 153.

The chemistry of elements above 121 is likewise difficult to predict because the various electronic configurations are close in energy and the valence states of these elements are uncertain. However, for the elements below 121, one should be able to develop chemical separations based on the known chemistry of their lighter homologs and various extrapolation techniques used to predict the systematic change in chemical properties with increased mass in a given periodic group. Thus, the preparation of the superheavy elements presents the exciting prospect of exploring the chemistry of a whole new group of elements and of probing the electronic structure of the atoms in this new region of the periodic table.

f. Detection of Superheavy Elements

A variety of techniques will be required to isolate and identify the new elements. The detection of elements formed in compound-nucleus reactions will be considerably eased by the large recoil energy of the product nucleus. In the case of "cold nucleus" type reactions, the recoil energy could be in the neighborhood of 300 MeV. This is equivalent to a velocity of $\sim 2 \times 10^9$ cm/sec for a medium-weight target and projectile. Thus, a nuclear product could travel ~ 2 cm from the target in 10^{-9} sec and then be available for detection by solid-state detectors. This behavior makes it possible to detect half-lives as short as 10^{-9} sec in searching for new elements and isotopes. Nuclides with half-lives of a few microseconds could be identified and studied by

moving-belt or moving-wheel techniques. Isotopes with shorter half-lives ($\sim 10^{-7}$ sec) could be examined by on-line mass spectrometers designed for this special purpose. If the fission-type reaction proves to be the best approach to producing new elements in the "island of stability," as predicted by some calculations, then chemical separation will be required. Since many of the nuclides in this region are expected to have long half-lives, it should be feasible to detect these elements not only by their emitted radiations, but also with the very sensitive Argonne 100-in. mass spectrometer described in Sec. II. E7.

On the basis of estimations of production cross sections, it appears that the isotopes of several elements with half-lives exceeding a few minutes will be made in amounts of the order of 10^{-9} curie. It should be possible to study these nuclides with the very high-transmission, high-resolution Argonne toroidal double beta spectrometer. This machine has an efficiency comparable to that of solid-state detectors, but is superior in resolution and precision. Additional advantages over gamma spectroscopy are that electron spectroscopy allows identification of atomic number and precision measurement of electron binding energies, even for outer shells.

* * *

The search for new elements and isotopes will be conducted with the tandem Van de Graaff for the lighter range of heavy ions and the full accelerator (Van de Graaff injecting into the variable-energy cyclotron) to provide the high-energy, very-heavy ions. The specialized equipment necessary to prepare the very radioactive targets and to process irradiated targets have been described in Secs. II. E1 and 2.

We are confident that the proposed accelerator will produce many exciting discoveries in very-heavy-element research.

VA.2. Chemistry of the Trans-Actinide Elements

With only a few or even thousands of atoms available, a discussion of chemical methods of identifying elements and elucidating their chemical properties must necessarily be limited to generalities. When the specific properties of the element in question are unknown, the position in the periodic table provides one of the few clues upon which to base experiments.

It may be difficult to accurately predict the properties of elements beyond the present limit of element 104. In many previous discoveries of unknown elements, the periodic table proved its usefulness because the element could be "bracketed" by known elements above, below, and to the right and left. Judgment and insight guided by the regularities of the table, have led to remarkably accurate predictions of the properties of the (then unknown) missing elements. Even when elements were not "bracketed," as was the case for elements beyond uranium, accurate forecasts of chemical properties were possible once it was realized that the transuranium elements formed a new "rare earth" or "actinide" series. It is, of course, well known now that the actinides form a series with a regular progression of properties varying in a more or less monotonic manner with certain specific prominences in oxidation states superimposed at specific intervals. This felicitous state of affairs can hardly be expected to continue in the trans-actinides and a resumption of the periodic aspects in the Mendeleeff sense is to be expected. The chemist will find it necessary to extrapolate, not interpolate, the properties of the element of interest and to do it in a manner that allows a great deal of leeway.

Nevertheless, some general statements can be made. A report from the USSR[1] states that, even with a few atoms, element-104 chloride appears to exhibit vapor pressures consistent with being a

[1] I. Zvara et al., At. Energ. (USSR) 21, 83 (1966) [English transl.: Soviet J. At. Energy 21, 709 (1966)].

homologue of zirconium and hafnium; indeed it followed along with these chlorides when present in masses of their vapors. If this observation is correct, it would suggest that these kinds of experiments should be extended to heavier elements. For example: the atoms of element 105 ought to be carried along in the vapor of TaF_5 or in F_2, element 106 should volatilize as a hexafluoride with WF_6 at room temperature, element 107 should form a volatile oxide at slightly elevated temperatures with oxygen or Re_2O_7, and at about 100°C element 108 should also from a volatile tetraoxide with oxygen or carry along with OsO_4. In each of these cases, the "chemistry" distinguishes one element from the others. These experiments can be extended and amplified further to characterize the chemistry of a trans-actinide, but in the absence of other information do not prove the identities.

If, in the case of the vapor-carrying experiments, concommitant mass determinations can be made, an important piece of confirmatory or suggestive evidence is obtained. This may, of course, be a formidable technical problem. Final identification of an element may depend on the genetic relationship with known nuclides through radioactive transformations. If new elements can be made at the level of a few tens of thousands of atoms, mass spectrometry can be used to determine the mass number of the isotopes produced in the experiments.

Elements 104—110 should be members of a transition series of elements in which the 6d subshell is being filled with electrons. As in the case of the lighter transition elements, elements 104—110 should form chloride complexes that adsorb on anion exchange resins and extract into certain types of substituted amine solvents.

In the group of elements Z = 111—118, one expects to find many members of this period to be fairly volatile, especially elements 112, 114, 116, 117, and 118. Element 118 is expected to be a noble gas and should have distinctive properties. Since most of the elements in this group are expected to have several valence states, the chemistry of different oxidation states could be used to aid in separating and isolating them.

Investigating the chemistry of trans-actinides in solution requires that it be possible to obtain the elements in the form of nuclides having a half-life of a few seconds or longer. It is probably unrealistic to form and identify pure compounds on this scale, except perhaps by mass spectrometry. Co-precipitation experiments, particularly with putative isomorphous compounds, can provide a certain amount of chemical information. Solvent extraction procedures have been so developed in recent years that proper selection of solvent and extraction conditions can be very suggestive as to the oxidation state of elements. The same may be said of ion-exchange procedures. Electromigration and electrolytic or chemical oxidation or reduction in various media also can provide chemical information and can be made fairly rapid.

While the foregoing descriptions are not specific, it may be said that many of the methods have already been used in one form or another in the search for new elements. To apply any of these techniques it is, of course, necessary to tailor the experiment very carefully to expose the chemistry of the element in question.

As an example of a possible type of separation procedure, let us consider an experiment designed to rapidly isolate some of the elements from the group Z = 112—116 formed as fission products during the bombardment of a uranium target with uranium projectiles. Since the fission fragments will recoil out of the uranium target with fairly high energy (many hundreds of MeV), their energy will have to be reduced by collisions in a gas stream to prevent them from embedding themselves on striking the collector plate—a carbon plate heated to approximately 400—500°C. In this temperature range, elements 112, 114, 116, and 117 are expected to distill away from the carbon plate, whereas elements 113 and 115 may evaporate to a small extent. Almost all of the lighter elements will remain in the carbon plate. The evaporated atoms will be entrained in the gas stream, transported through an orifice to increase the gas velocity, and then deposited on a cool metal plate. Solid-state detectors could then record the alpha energies, spontaneous fissions,

K x-ray emission (to establish atomic numbers), and half-lives of the isotopes of shorter half-life (down to the range of 0.01 sec). The isotopes of longer half-life could then be studied by further chemical separations of the elements, a study of their radiations, and possibly their half-lives; and this may then be followed by mass-spectrometric measurements of the mass numbers. Additional rapid separations could be made, such as distilling element 114 from the second foil (it is expected to have a low boiling point). Of course, the exact conditions to produce optimum yields of the various elements will require experimental determination.

A specific chemical separation for element 113, for example, is suggested by its expected similarity to thallium. Element 113 is expected to form an oxidized trivalent ion in solution which can be extracted rapidly into ether from a hydrochloric acid solution. The oxidized element 113 can then be reduced to the univalent state and be reextracted back into an aqueous acidic phase, leaving many of the contaminating elements in the ether phase. Predictable differences between the ease of oxidation or reduction of thallium and element 113 could possibly be used to aid in establishing the identity of the separated new element; such evidence would be combined with that derived from its radioactive decay properties and K x-ray emission, the latter being characteristic of atomic number.

Such experiments illustrate the kind of rapid physical and chemical separation that can be devised on the basis of the expected location of the elements in the periodic table and their predicted properties.

V.B. OTHER RESEARCH WITH HEAVY-ION BEAMS

The variety of ions that can be accelerated and the range of energies that would be available at the proposed accelerator complex make possible an almost embarrassingly large number of unique and interesting measurements. In addition to the possible production of entirely new elements, promising areas of investigation include a variety of interrelated studies of the basic interactions between and among nucleons—investigations that are essential to any future progress in nuclear physics.

The purpose of this section is to present a brief review of a few areas of investigation that are feasible with energetic heavy-ion beams but not with existing accelerators and that, according to our

present understanding of nuclear interactions, seem most relevant to progress in nuclear research. These include studies of the dynamics of heavy-ion reactions, which are of considerable interest in their own right and must be understood before a systematic attempt to produce new heavy elements can be made. Interesting possibilities for the production and study of entirely novel light and medium-weight isotopes also are discussed. These studies will become possibly only with the availability of a range of energetic ions such as is envisioned with the proposed accelerator. The heavy-ion beams would also be useful in the direct investigation of problems in atomic physics, solid-state physics, and in biological and medical research and would have some possible applications to semiconductor and transistor technology.

No explicit attempt has been made to relate these studies to practical problems in such fields as biology, environmental research, medicine, and industrial technology since it seems impossible to speculate realistically about physical phenomena that are almost totally unexplored. It does seem obvious, however, that the probability of socially-advantageous contributions from scientific research tends to decrease as the parameters of the physical phenomenon investigated stray further from those of our immediate environment. Thus the "practical applications" that may be expected from research at the proposed installation have a much greater potential than does research carried out at various existing and proposed higher-energy accelerators.

V. B1. Simple Modes of Nuclear Excitation

The scientific justification of the proposed accelerator has as its essence the following three-stage argument. (1) Nuclear-structure physics continues to uncover entirely new and unexpected aspects of nuclear behavior. Two recent discoveries—those of isobaric-analog states and of shape isomers—establish the truth of this statement. Thus nuclear physics is not a matter of filling in the details of a long-established framework but is rather a subject that continues to evolve in new and unpredictable directions. (2) Qualitatively new discoveries in nuclear physics have invariably been at the outset experimental discoveries. Thus the future of nuclear physics demands experimental facilities qualitatively different from those available in the past. (3) The proposed MTC accelerator is indeed qualitatively different from what is now available; furthermore, as we now argue in more detail, it is qualitatively different in a fashion calculated to reveal new aspects of nuclear behavior. Its essential advantages, of course, are its high and variable energy, its ability to accelerate very heavy ions, its precision, and its flexibility in the type of particle accelerated.

Nuclear physics progresses by the identification and study of simple modes of excitation of the nucleus. This is necessarily so because the nucleus is a many-body system of exactly the wrong size; it has far too many degrees of freedom for solution of its full Schrödinger equation, but far too few for a statistical treatment. It is therefore necessary to identify phenomena that involve as few of the degrees of freedom of the nucleus as possible. Such simple modes of excitation are then examined in detail; the essential degrees of freedom are identified and a suitable phenomenological model is constructed. This model in its first and simplest form is a blatant caricature wherein the nucleus is capable of the sort of excitation under consideration and of nothing else. The next step is to extend the model to include other aspects of nuclear dynamics; finally the parameters of this extended model are related to the constituent

nucleons of the nucleus and to their interactions. But the first and crucial step in this development is the experimental discovery of simple modes of excitation.

Many such nuclear excitations are known. The classic example is the E1 giant resonance observed in photonuclear reactions—a dipole vibration ($J = 1^-$, $T = 1$) of the nucleus wherein the proton mass-center oscillates about the neutron mass-center. The simplest and most basic nuclear excitation is the single-particle excitation; the fact that the width of a low-lying single-particle state is at most a few MeV is the foundation of the nuclear shell model. The rotational excitations of deformed nuclei are perhaps the most conspicuous fact in all of nuclear systematics. Near-harmonic vibrations other than E1 are also well known—the low-lying quadrupole (2^+, $T = 0$) and octopole (3^-, $T = 0$) vibrations and the M1 (1^+, $T = 1$) excitation observed in inelastic electron scattering.

More recently pairing vibrations (0^+, $T = 1$) wherein two correlated nucleons are transferred to or from the nucleus, have been identified and studied. In like fashion, reactions such as (d, Li^6) or (Li^7, t) reveal 'α-particle states' wherein correlated groups of four nucleons (with $J = 0^+$, $T = 0$) are added or removed. Finally, recent work on fission has led to the discovery of shape isomers—low-lying states of heavy nuclei that seem to have shapes distorted far beyond what had previously been regarded as normal.

Much work remains to be done on the already-known nuclear excitations, on their relation to each other, and on their mutual interactions. Of even greater significance is the clear fact that nuclear physics continues to uncover entirely new sorts of nuclear excitation. The shape isomers are a striking recent example; their discovery has already brought the study of fission into close contact with the mainstream of nuclear physics and their full impact has yet to be felt. We know almost nothing about the monopole excitations associated with nuclear density fluctuations—a subject of enormous importance to any many-body description of nuclear properties. The study of simple excitations involving the transfer of correlated groups

of many nucleons is still in its infancy; the use of heavy-ion beams in such experiments may reveal not only new regions of stable nuclei but also nuclei in states qualitatively different from those now known. We have little idea about what happens when very large amounts of angular momentum are transferred to the nucleus.

The situation is thus one in which the new sorts of experiment possible with the proposed accelerator cannot fail to change our ideas about nuclei. The known nuclear excitations are those that involve low excitation energy, low angular momentum, small equilibrium deformations, and the transfer of very few nucleons. The light- and heavy-ion beams of the proposed accelerator will remove every one of the restrictions mentioned. In so doing it will ensure, as no other sort of accelerator could, that nuclear physics continues to develop in new and unexpected directions.

V. B2. Electromagnetic Transitions

The study of electromagnetic transitions has been the backbone of nuclear spectroscopy. It has provided a wealth of information not only on the spins and parities of nuclear states but also on transition probabilities. Many nuclear models can be traced to attempts to explain data of this kind. The new accelerator will contribute in many ways to the study of electromagnetic transitions. The range of heavy ions available will greatly extend the techniques of Coulomb excitation and Doppler-shift lifetime measurements. Also, the property that heavy-ion reactions selectively populate very-high-spin states is likely to lead to many new experiments and experimental fields. These areas of investigation are discussed in the following subsections.

a. Coulomb Excitation

The availability of intense beams of energetic heavy projectiles can be used to great advantage in Coulomb-excitation studies of excited nuclear states. The results of these investigations can provide a wealth of valuable new information that could be expected to contribute a great deal to the understanding of salient nuclear problems. One of the striking attributes of the proposed accelerator in connection with Coulomb excitation is that there is no constraint on the energy imposed by the accelerator. In Coulomb excitation one usually wants a high bombarding energy to get a good yield, yet remain slightly below the Coulomb barrier to avoid competing reactions. Such an energy cannot be obtained for heavier projectiles with existing accelerators, the present facility removes any such constraints on experiments.

In order to illustrate the usefulness of heavy ions for Coulomb excitation, it is instructive to plot the expected thick-target yield from E2 Coulomb excitation as a function of the nuclear charge Z_1 of projectiles incident on a U^{238} target. In the calculations, the reduced transition rate B(E2) was taken equal to the single-particle

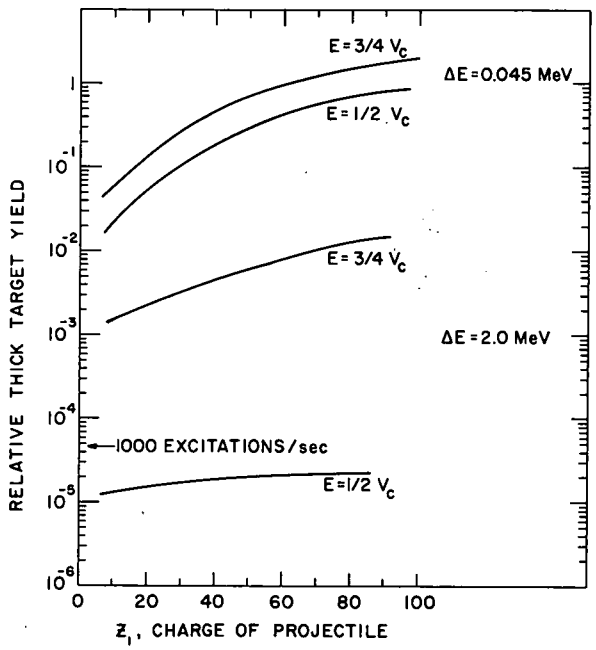

Fig. V.B2-1. Calculated thick-target yield from E2 Coulomb excitation of the 0.045- and 2.0-MeV levels in U^{238} as a function of the projectile charge Z_1. For each of these levels, the yield is calculated for ions whose laboratory energy corresponds to a center-of-mass energy equal to first 0.5 V_C and then 0.75 V_C, where V_C is the Coulomb barrier $V_C = Z_1 Z_2 e^2/R$ with $R = 1.26(A_1^{1/3} + A_2^{1/3})$ fm. The arrow marks the ordinate that represents 1000 excitations/sec for 10^{12} particles/sec incident on the target.

estimate and the bombarding energy was adjusted so that the initial kinetic energy in the center-of-mass system was either 0.5 or 0.75 of the Coulomb barrier V_c. With the energy at 0.5 V_c, the yield increases with the projectile charge Z_1 for all levels up to 2 MeV, as shown in Fig. V.B2-1; but for level energies above this, increasing Z_1 does not lead to an increase in yield. For ions incident with energy 0.75 V_c, however, the yield increases with Z_1 for levels with energies up to 5 MeV. The behavior of the yield for E3 Coulomb excitation is similar to that discussed above for E2 excitation. In an actual experiment with a U^{238} target, one would expect multiple excitation of the ground-state rotational band and, for heavy projectiles, excitation of the projectile also. In this regard, Pb^{208} appears to be the best heavy projectile if one wishes to avoid complications due to excitation in the projectile.

Odd-parity collective vibrations of lowest energy in even-even nuclei are known to be of the octopole type. The collective nature of these states would imply that the transition probabilities for single E3 Coulomb excitation would be appreciably in excess of single-particle estimates. Few of these octopole vibrational states have lent themselves

to previous study by Coulomb excitation because of the low cross section. The enhanced transition probabilities expected for these states, coupled with the great advantage gained in the use of heavy-ion projectiles, could permit detailed and systematic studies of these vibrational states by means of E3 Coulomb excitation.

Although single E2 excitation is greatly favored by the use of heavy projectiles, the usual enhanced nature of these transitions normally allows adequate study of single E2 excitations of low-lying excited states by means of intense beams of light ions. However, when multiple E2 Coulomb excitation is considered, the advantage in the use of heavy ions becomes enormous since the relative excitation probabilities that favor the use of heavy projectiles apply to every step of the multiple process. Furthermore, the use of more intense beams of light projectiles cannot begin to compensate for the enormous factors by which heavy projectiles are favored in these multiple processes. The normally enhanced nature of E2 excitations, combined with the use of heavy projectiles will allow extremely-high-spin members of ground-state rotational bands in heavy nuclei (spins as high as 24^+ to 28^+) to be populated by multiple Coulomb excitation; and their subsequent sequential γ-ray decay to lower members of these bands, as well as to members of other rotational and vibrational bands, could be studied in detail with high-resolution Ge(Li) detectors of large volume. Determinations of the excitation probabilities and characteristic decay modes of these states, coupled with precisely measured intraband energy spacings, can shed new light on the nature of the nuclear rotation. For example, even low-spin members of rotational bands have been found to display intraband energy spacings that systematically deviate from predictions of the strong-coupling model. These departures have already been noted for members of ground-state rotational bands with spins as low as 6^+ and 8^+. A very interesting interpretation of these deviations is that they result from possible progressive variations in the nuclear moment of inertia in the higher-spin members of these bands. It would be of

great interest to be able to study these effects in much-higher-spin members of these bands. Multiple E2 Coulomb excitation with energetic heavy projectiles will allow such studies to be made.

The determination of the E2 matrix elements of beta and gamma vibrational states is of great value in the classification of these states. The exact nature of the nuclear collective couplings giving rise to many of the vibrational states is not well understood. Heretofore, experimental restrictions on the higher states have limited the studies to the lowest members of these vibrational bands. Since these vibrational excitations are usually strongly enhanced over single-particle estimates, the use of heavy projectiles in multiple Coulomb excitation can provide a practical mechanism for the population of high-spin members of the rotational bands built upon these vibrational states and permit detailed studies of their properties.

Some evidence of the onset of collective rotations in highly excited states of spherical nuclei has recently been reported. These states demand further study in order to systematically characterize their nature. Multiple Coulomb excitation by use of heavy projectiles can provide a very powerful tool with which to examine states of this type in many more nuclei, and information derived from such studies should contribute greatly to our present meager understanding of their character.

Coulomb excitation has also been used at several laboratories to measure the static quadrupole moments of 2^+ first excited states of nuclei. This is done by making use of the "reorientation effect," which is a second-order effect in Coulomb excitation and can be important when the first-order probability for Coulomb excitation is high. Measurements of this kind have been carried out at Argonne by a group from Purdue University.[1] Their technique differed somewhat from the usual in that the scattered ions from Coulomb excitation were detected in

[1] G. Schilling, R. P. Scharenberg, and J. W. Tippie, Phys. Rev. Letters 19, 318 (1967).

coincidence with the de-excitation gamma rays. The shape of this differential Coulomb-excitation cross section can give conclusive evidence for the presence of the reorientation effect.

The reorientation effect can be regarded as a multiple Coulomb-excitation process in which the second Coulomb excitation corresponds to a transition between the magnetic sublevels of the excited state and depends on the static quadrupole moment of this state. Other possible second-order processes leading to the state of interest involve excitation of higher energy levels. These effects introduce an uncertainty in interpretation of the observed deviation from the predictions of first-order theory of the Coulomb excitation process. This uncertainty can be reduced by performing the experiment at low bombarding energy.

An example of the Purdue group's measurements is their work[1] on the first excited state of Cd^{114}. They observed the angular distribution of scattered O^{16} ions in coincidence with de-excitation gamma rays from the first excited state. The value they obtained for the static electric quadrupole moment of the 0.558-MeV excited state of Cd^{114} was

$$Q = (-0.64 \pm 0.19) \times 10^{-24} \text{ cm}^2 .$$

This value, which is in agreement with other values obtained by measuring the Coulomb-excitation cross section for various projectiles, is in striking contrast to the vanishingly small quadrupole moment predicted by the pure vibrational model.

Recent calculations of Kumar and Baranger[2] consider a strong interaction of rotation and vibration by means of large-amplitude nonharmonic vibrations about a nonzero equilibrium deformation. They are able to calculate an excitation spectrum similar to that of the vibrational model as well as a large static quadrupole moment for the first 2^+ excited state.

---

[2] K. Kumar and M. Baranger, Nucl. Phys. A122, 273 (1968).

These kinds of experiments appear to be a very promising approach to the study of nuclear deformations. The step required to make them feasible is the development of energetic ion beams with a mass range from about A = 40 to A = 120. For a given velocity in the center-of-mass system, the magnitude of the reorientation effect is directly proportional to the mass of the exciting ion. Thus laboratory energies between 1.5 and 5 MeV/nucleon are required. The availability of these beams would allow nuclear shapes to be determined precisely without the uncertainties of interpretation inherent in more traditional methods. For the first time the calibrated electric field gradients available to physicists would be large enough to produce observable effects.

b. Lifetimes of Excited Nuclear States

The measurement of lifetimes or level widths furnishes detailed knowledge about nuclear structure. In order for this knowledge to be useful, one must have additional information such as the energy of the decaying level and its spin and parity. In combination with these parameters, knowledge of the lifetime offers an opportunity for sensitive comparisons between the predictions of various nuclear models and experimental data. Development of the high-resolution Ge(Li) detector, combined with improvements in electronics and other techniques, have greatly increased the number of transitions that can be studied.

The availability of a high-energy heavy-ion accelerator would offer a number of advantages in lifetime studies. (1) A great variety of proton-rich nuclei with many strongly-populated gamma-emitting levels become available for lifetime measurements. (2) Heavy-ion bombardment can transfer large amounts of angular momentum and can thus form high-spin states that have not been seen and studied before. (3) Large translational momenta are transferred to the gamma-emitting nucleus; and the resulting velocity not only produces large Doppler shifts in the gamma-ray energies but also allows the nucleus to travel a long distance before the gamma is emitted.

In a recent survey Schwarzschild and Warburton[1] give the ranges of lifetimes that can be measured by different experimental techniques. Their summary curve is given in Fig. V.B2-2. Nearly all these methods will profit by the heavy-ion accelerator via advantages (1) and (2) listed above; but the transfer of translational momentum is of special interest for those based on the observation of the Doppler shift. In the following, the three techniques most likely to be useful will be discussed with some illustrative examples.

i. The attenuated Doppler shift. This method has been used extensively in the measurement of lifetimes; it has become especially useful since the advent of Ge(Li) detectors. The technique is to study the

[1] A. Z. Schwarzschild and E. K. Warburton, Ann. Rev. Nucl. Sci. 18, 265 (1968).

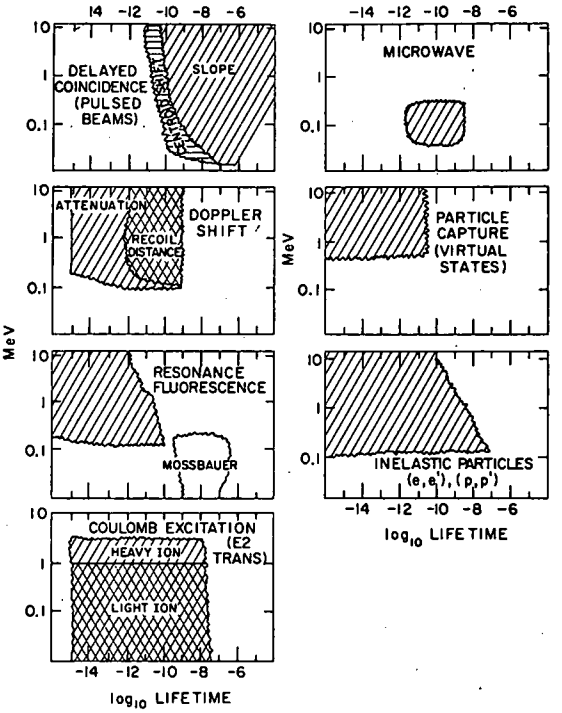

Fig. V.B2-2. Schematic diagram showing the ranges of lifetime and γ-ray energy to which different experimental techniques are applicable. The boundaries are somewhat indefinite and are to be taken as historical indications of the past use of the methods—not as their absolute limits. (From Schwarzschild and Warburton, Ref. 1.)

energy shifts of gammas while the gamma-emitting recoil nuclei are being slowed down in various media. If the lifetime of the gamma-emitting state is of the order of the slowing-down time, the gamma-ray energies will be spread out. The distribution of gamma-ray energies reflects the varying Doppler shifts during the slowing-down process of the recoil nucleus. This distribution can be calculated as a function of the lifetime since the slowing-down process is understood reasonably well.[2] Since different materials have different slowing-down times, a rather broad range of lifetimes can be measured with this attenuation method.

Some early measurements in this area were made at Argonne.[3] Other experiments with NaI crystals were carried out at Argonne[4] and Indiana[5] in the Midwest and at a number of laboratories

[2] A. E. Blaugrund, Nucl. Phys. 88, 501 (1966).

[3] R. Krone, A. Everett, and S. S. Hanna, Bull. Am. Phys. Soc. 1, 329 (1956).

[4] C. M. Class, P. P. Singh, and S. S. Hanna, Bull. Am. Phys. Soc. 8, 358 (1963).

[5] S. W. Robinson and R. D. Bent, Phys. Rev. 168, 1266 (1968).

elsewhere. More recent work with Ge(Li) detectors has again been carried out at Argonne,[6] Iowa,[7] and in several other laboratories. The potential usefulness of this technique with the proposed accelerator is enormous because of the large recoils that can be obtained.

ii. The recoil-distance method. This is another technique making use of the Doppler shift. Such experiments have been carried out in many forms[8]; a typical recent arrangement is shown in Fig. V.B2-3. This technique is useful for lifetimes somewhat longer than the ones measured in the Doppler attenuation method. The lifetime of a γ-emitting state is deduced by observing the number of gamma rays emitted in flight and comparing this with the number emitted in the stopping material (the two can be distinguished by their different Doppler shifts) as a function of the separation D between target and plunger. The high recoil velocities and large Doppler shifts will be very advantageous in these measurements.

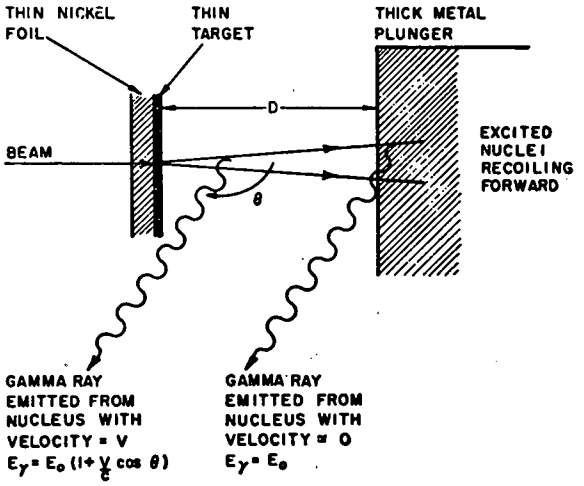

Fig. V.B2-3. Recoil-distance method of measuring lifetimes of excited states. (From Schwarzschild and Warburton, Ref. 1.)

---

[6] S. I. Baker and R. E. Segel, Phys. Rev. 170, 1046 (1968).

[7] M. J. Throop, Phys. Rev. 179, 1011 (1969).

[8] S. Devons, H. G. Hereward, and G. R. Lindsey, Nature 164, 586 (1949).

iii. Electronic techniques with pulsed beams from accelerators. Argonne is prominent among the laboratories using these methods. The techniques developed here include improvements in timing with NaI(Tl) scintillators, the development of a fixed-fraction discriminator which is particularly useful for pulse-shape discrimination of neutrons from gamma rays, and the development of new and faster organic scintillators.[9] Electronic techniques have been used to measure the lifetimes of several M2 transitions in nuclei near mass 40.[10] The fact that these transitions, which in terms of the shell model can be described as $d_{3/2} \rightarrow f_{7/2}$ transitions, turn out to be several hundred times slower than the single-particle speed has been explained theoretically.[11]

All these techniques could be used to great advantage with the proposed MTC and will undoubtedly contribute much valuable information on electromagnetic transition matrix elements.

---

[9] F. J. Lynch, IEEE Trans. Nucl. Sci. NS-13, 140 (1966); NS-15, 102 (1968).

[10] R. E. Holland, F. J. Lynch, and K.-E. Nysten, Phys. Rev. Letters 13, 241 (1964).

[11] D. Kurath and R. D. Lawson, Phys. Rev. 161, 915 (1967).

c. Highly-Aligned Nuclei: the (HI, xnγ) Reaction

Recent experiments at Berkeley,[1—6] using heavy ions from the HILAC, have demonstrated the feasibility of investigating the level schemes and decay characteristics of a large range of neutron-deficient nuclei. These experiments make use of the A(HI, xn)B reaction in which the bombarding energy of the heavy ion HI is used to control x, the number of neutrons boiled off the initial compound nucleus and therefore to determine the final nucleus B that is most strongly populated. The compound nucleus is formed predominantly in a very-high-spin state with the spin oriented in the plane perpendicular to the beam direction.

The compound nucleus will decay by emitting neutrons of low angular momenta which will not change the spin orientation appreciably. After the neutron decays bring the excitation energy of the compound nucleus below the neutron threshold, the decay will continue by gamma emission. The nucleus then will usually be near the yrast level (the excitation energy at which the lowest state of given spin occurs) and will preserve its high degree of alignment throughout the γ cascade. The angular distribution of the gamma rays should reflect this alignment and, in a rotational nucleus, the decays will tend to be channeled into the ground-state rotational band. This special form of alignment makes

---

[1] R. M. Diamond, F. S. Stephens, W. H. Kelley, and D. Ward, Phys. Rev. Letters 22, 546 (1969).

[2] J. O. Newton, F. S. Stephens, R. M. Diamond, K. Kotajima, and E. Matthias, Nucl. Phys. A95, 357 (1967).

[3] J. E. Clarkson, R. M. Diamond, F. S. Stephens, and I. Perlman, Nucl. Phys. A93, 272 (1967).

[4] J. Burde, R. M. Diamond, F. S. Stephens, Nucl. Phys. A92, 306 (1969).

[5] F. S. Stephens, N. L. Lark, and R. M. Diamond, Nucl. Phys. 63, 82 (1969).

[6] F. S. Stephens, N. L. Lark, and R. M. Diamond, Phys. Rev. Letters 12, 225 (1964).

possible a number of experiments of great value in unraveling the complex gamma spectra resulting from the (HI,xn) reaction.

i. The measurement of the angular distribution of the emitted gamma rays (or conversion electrons) relative to the beam direction can, in many cases, identify the multipolarity of the transition.

ii. By combining angular-distribution measurements with a lifetime measurement in which the angular distribution of both the Doppler-shifted and unshifted component of the gamma spectrum are measured separately, it should be possible to measure the relaxation of this spin alignment as a function of time and excitation energy. This may allow one to study extranuclear relaxation effects in addition to the reduction of alignment intrinsic to the chain of gamma decays.

iii. The high beam currents and high energy per nucleon will make it possible to perform γ-γ angular-correlation measurements on these highly-aligned nuclei. This type of triple correlation should allow one to determine the spins of initial and/or final states in many cases in which the simple angular distributions relative to the ion beam are insensitive to them. It should also give some information on the multipole admixture of the transitions.

iv. Many of the above experiments can also be carried out on conversion electrons. In some cases the angular distribution of conversion electrons carries information in addition to that obtained from gamma-ray correlations. In particular, E1 and M1 transitions can be distinguished in this way and thereby give information on the relative parities of the levels.

v. Recent results on fission isomers and intermediate structure in neutron-induced fission resonance widths suggest the existence of a shape isomer which can be accounted for by a second minimum in potential energy at large deformations.[7] States within this second minimum seem to mix only very slightly with the "normal"

[7] G. T. Seaborg, Ann. Rev. Nucl. Sci. 18, 54 (1968).

states of usual deformation and are produced by light projectiles with very small cross sections. With reactions of the type discussed here, one may perhaps expect that the cascade is as likely to wind up in the rotational band of the second minimum as in the normal rotational band. Since this second minimum is thought to have $\beta \approx 0.7$, the 0^+-2^+ spacing in the rotational band of a heavy nucleus would be $\sim$10 keV and the transition would proceed almost entirely by internal conversion.

With the wide variety of projectiles and energies available from the MTC, it will be possible to make the same compound nucleus by use of different projectiles and to study in detail such processes as the neutron evaporation mechanism of a highly excited system, level densities of high-spin states at high excitation energies, and competition between neutron emission and such processes as fission or the emission of a proton, alpha, or heavier cluster.

In addition to the usual gamma-ray spectroscopy, one would excite rotational bands to much higher spin states than is now possible with the HILAC and learn a great deal about the microscopic description of nuclear rotations. It will be interesting, for instance, to see whether the predicted breakdown in the pairing correlations between protons will be observed in such data.

It is clear that the value of heavy-ion-induced reactions will be great because they can produce nuclei with a high degree of alignment in high-spin states and thus allow a number of studies to be made. Undoubtedly there will be many new ways in which this unique feature will be exploited; such simplicities are rare in nuclear reactions, and when they exist they inevitably lead to many new and interesting discoveries which cannot be anticipated.

V. B3. Scattering and Reactions of Heavy Ions

The study of the mechanisms of heavy ion nuclear reactions will be of great importance in helping to decide the most promising approach toward producing new elements. If the results of such studies are to be more than empirical, it will require a comprehensive attack in which we seek a basic understanding of the interaction of complex nuclei with each other. Such experiments may well be of crucial importance to our understanding of nuclear structure.

A considerable beginning to the investigation of heavy ion scattering and reactions has been made, but of necessity has been limited to the lighter projectiles (those with $Z \leq 10$). When it is realized that virtually all of the elements in the periodic table will be available as projectiles with the proposed new accelerator, and that their highest energies will be sufficient to surmount the Coulomb barrier of even the heaviest targets, the wealth of possible new information can be appreciated.

a. Elastic Scattering

In the last decade the elastic scattering of heavy ions has generated considerable interest. Qualitatively new and striking phenomena have been showing up ever since Bromley et al.[1] suggested quasi-molecular states as an explanation of the resonances seen in the $C^{12} + C^{12}$ elastic scattering.

To date only a limited amount of data on heavy-ion scattering exists. Scattering studies with tandem accelerators have generally been restricted to light targets and projectiles ($A \leq 40$). Measurements on the HILAC accelerators cover selected nuclei of the whole mass range, but for experimental reasons have been limited to forward angles

[1] D. A. Bromley, J. A. Kuehner, and E. Almquist, Phys. Rev. Letters 4, 365 (1960).

($\theta \leq 50^{\circ}$). Angular distributions on light nuclei show a diffraction-like pattern, whereas the scattering data from the heavier nuclei exhibit a relatively smooth dropoff from Rutherford scattering beyond the breakoff angle—the angle at which the classical impact parameter is equal to the effective radius of the target. Beyond this breakoff angle the projectile begins to experience the effect of nuclear forces, and the differential cross section drops off rapidly from the Rutherford prediction. Recent measurements at Argonne as well as at other places suggest that interesting gross structure in the differential cross sections will be observed whenever the elastic cross section is between a hundredth and a thousandth of that for pure Rutherford scattering, i.e., whenever the energy of the incident ion is well above the Coulomb barrier.

Following the observation of very pronounced and regular gross structure (Fig. V.B3-1) in the $O^{16} + O^{16}$ elastic scattering,[2] there has been considerable theoretical interest[3—5] in the heavy-ion—nucleus potential and its relation to the properties of nuclear matter. In particular, it has been suggested that the heavy-ion—nucleus potential is of the molecular (Lenard-Jones) type with a soft repulsive core; and an attempt has been made to derive the nuclear compressibility from a fit to heavy-ion scattering data. Although there is still no conclusive evidence for these molecular-type potentials in heavy-ion scattering, and these theories most probably have to be viewed as gross oversimplifications, nevertheless they are of considerable interest and may well serve as a starting point for a deeper understanding of the heavy-ion—nucleus interaction. Molecular-type phenomena will most probably

[2] R. H. Siemssen, J. V. Maher, A. Weidinger, and D. A. Bromley, Phys. Rev. Letters 19, 369 (1967); J. V. Maher, M. W. Sachs, R. H. Siemssen, A. Weidinger, and D. A. Bromley (to be published).

[3] B. Block and F. B. Malik, Phys. Rev. Letters 19, 239 (1967).

[4] K. A. Brueckner, J. R. Buchler, and M. M. Kelly, Phys. Rev. 173, 944 (1968).

[5] W. Scheid, R. Ligensa, and W. Greiner, Phys. Rev. Letters 21, 1479 (1968).

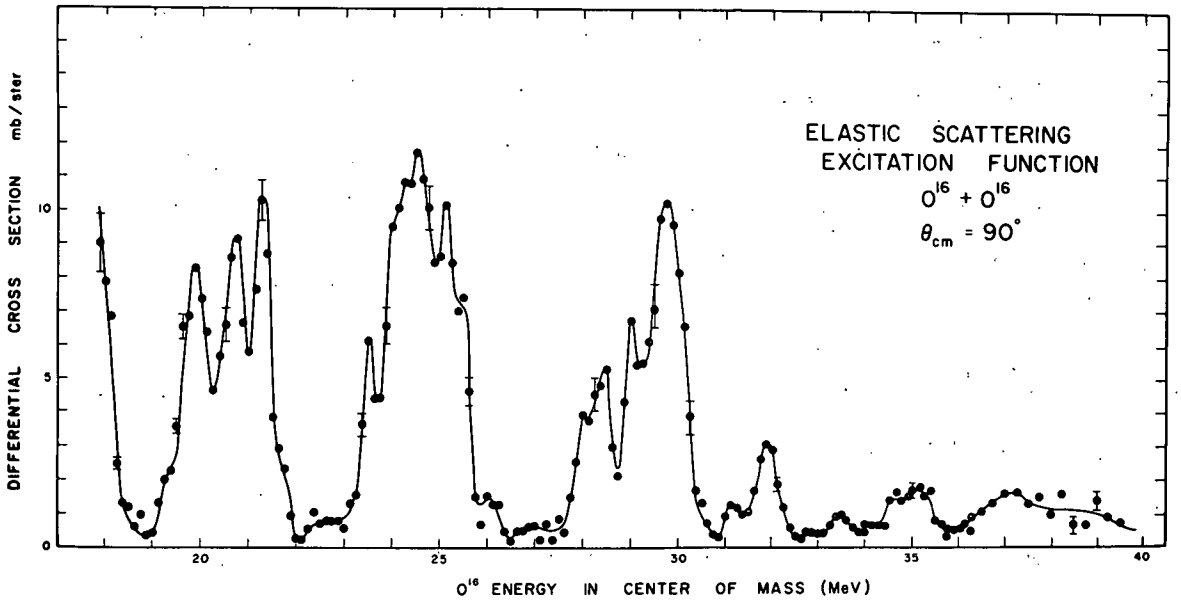

Fig. V. B3-1. Excitation function of the elastic $O^{16} + O^{16}$ scattering at 90°. (From Ref. 2.)

manifest themselves in the scattering of particles of approximately equal weight, whereas average potentials will probably be best studied with interacting systems in which the target is very much heavier than the projectile.

Potentials derived from the scattering of complex particles are highly ambiguous. These ambiguities are particularly serious for heavy ions because their short de Broglie wavelength and their strong absorption result in a series of discrete values of the potential strengths which fit an observed angular distribution equally well and which are spaced only a few MeV apart. The investigation of the $O^{16} + O^{16}$ system[2] shows that some of these ambiguities might be resolved if the energy dependence of the scattering were studied. The study of heavy-ion elastic-scattering excitation functions is also important if compound elastic scattering cannot be neglected since, by fitting to the gross structure in the excitation functions, it is possible to filter out the direct (potential scattering) component of the data.

A program of scattering of some of the lighter of the heavy ions has been started at Argonne. The extension of these measurements

to higher energies and heavier targets, as well as to a wider range of heavy projectiles, is of considerable importance to our better understanding of this very basic phenomenon. Such a program would be possible with the proposed accelerator since it would make possible the scattering of almost any ion from any nucleus at energies that are well above the Coulomb barrier.

b. Inelastic Scattering

Heavy ions are strongly-absorbed projectiles. Thus inelastic scattering of heavy ions is best described through the deformed optical model[6] rather than through the microscopic shell-model theory of inelastic scattering. In the framework of the deformed optical model, the interaction does not depend (to first order) on the projectiles involved. Thus the spectroscopic amplitudes for excitation of the target by different projectiles are expected to be the same. For the few cases of heavy-ion inelastic scattering that have been studied, this indeed has been found to be the case within approximately 20%. Deviations in the spectroscopic amplitudes would indicate differences in the effective potentials seen by the different projectiles and may contain important information about the polarizability of the target nucleus.

In addition to giving new spectroscopic information, heavy-ion inelastic scattering is also of great importance in its own right. The better localization of heavy ions and the large momentum transfer associated with heavy-ion inelastic scattering make this process a fine probe to sample the surface; inelastic scattering may resolve the ambiguities in the elastic-scattering optical potential; and mutual excitations of both target and projectile are possible. This last process[7]

---

[6] R. H. Bassel, G. R. Satchler, R. M. Drisko, and E. Rost, Phys. Rev. 128, 2693 (1962).

[7] G. T. Garvey, A. M. Smith, and J. C. Hiebert, Phys. Rev. 130, 2397 (1963).

permits a study of the reaction mechanism of multiple excitations in the special case in which both nuclei involved undergo only a single excitation—in contrast to the more general case in which the multiple excitation can occur in the same nucleus.

The proposed accelerator will greatly extend our knowledge of inelastic scattering by virtue of both the variety of projectiles and the range of energies of the heavy-ion beams available. In addition, the energy precision of these beams may for the first time permit strongly-deformed rotational nuclei to be studied with a variety of projectiles.

c. Transfer Reactions

With few exceptions, presently available heavy-ion transfer-reaction data are poor both in energy resolution and in counting statistics. In very few cases are individual final nuclear states resolved. The general difficulties in particle identification, counting statistics, and limitations in the number of angles measured create severe ambiguities in the shapes and absolute values of the angular distributions.

The theoretical interpretation of transfer reactions is in a rudimentary state, at least partly because of the lack of experimental results against which to test the theoretical approaches. Breit[8] and his collaborators have successfully interpreted transfer reactions below the Coulomb barrier in terms of a tunneling mechanism, according to which the cores of the heavy ions follow undisturbed Coulomb trajectories. Above the Coulomb barrier several approaches (some three-body[9,10] and other "effective" two-body[11,12]) have been proposed. More recently,

[8] G. Breit and M. E. Ebel, Phys. Rev. 103, 679 (1956); 104, 1030 (1956).

[9] K. R. Greider, Phys. Rev. 133, B1483 (1964); 136, B420 (1964).

[10] A. Dar, Phys. Rev. 139, B1193 (1965).

[11] W. E. Frohn and R. H. Venter, Ann. Phys. (N. Y.) 24, 243 (1963); 27, 135 (1964).

[12] V. M. Strutinski, in Proceedings of the Third Conference on Reactions Between Complex Nuclei, edited by A. Ghiorso, R. M. Diamond, and H. E. Conzett (University of California Press, Berkeley, 1963), p. 246.

finite-range DWBA calculations have been applied by various authors. All have qualitatively reproduced some of the available data, probably because many of the general characteristics of the heavy-ion angular distributions are determined by low partial waves being strongly absorbed and high partial waves following approximate Coulomb trajectories.

Much as transfer reactions with light ions have proved their usefulness as a spectroscopic tool, it can be hoped that future developments in the study of heavy-ion-transfer reactions also will contribute significantly to the understanding of nuclear structure. The proposed accelerator will be the first one capable of overcoming the present experimental difficulties. With it, transfer reactions can be studied over wide ranges of energy and angle with (1) sufficient energy to use counter-telescope or time-of-flight techniques, unhampered by the high specific energy loss of the heavy ions, (2) sufficient energy resolution to resolve final states, and (3) high beam flux to permit excellent counting statistics.

It is most likely that the initial spectroscopic studies with transfer reactions will concentrate on reactions induced by relatively light ions—i.e., 1p-shell and possibly 1d2s-shell projectiles with which fairly light clusters (Li, Be, C) are transferred. For these studies the optimum bombarding energies will be a few tens of MeV above the Coulomb barrier, i.e., in a range between 5 and 10 MeV/nucleon. This energy is well below the projected maximum energy of the proposed accelerator and, in fact, many of these studies would be done with the TU tandem alone. It also seems fairly certain that for the study of one- and two-nucleon transfers, one will not rely on heavy-ion reactions except those transferring a pair of protons. However, much of the initial work will probably deal with few-nucleon transfers in order to understand the reaction mechanisms involved. These processes can readily be compared with the analogous reactions induced by light ions.

Three additional obviously promising areas of heavy-ion spectroscopy center on the possibilities of testing for clustering on the nuclear surface, of forming high-angular-momentum states, and of reaching new exotic nuclides off the stability curve. With the alpha-transfer reactions (Li^7,t) and (Li^6,d), very interesting results were obtained recently at the University of Pennsylvania.[13] They find that these reactions on targets ranging from C^{12} to Si^{28} select out particular final states, presumably ones with alpha-particle-like correlations — in much the same way that the two-nucleon-transfer reactions (p,t) and (t,p) select out final states with pairing correlations. For heavier target nuclei, recent Argonne work on (O^{16}, C^{12}) reactions shows interesting α-transfer effects. There is some evidence for reduced α-transfer cross sections, with the possibility that the reaction is inhibited when the transferred protons and neutrons populate different shells in the heavy nucleus.[14] Further interest will center upon the energy dependence of the average values of cluster-transfer cross sections and deviations from these. Table V. B3-I lists average data[15] on various transferred clusters for reactions in the neighborhood of the Coulomb barrier. An investigation of the systematics of these cross sections at various energies could provide information on average nuclear correlations. Deviations of individual reactions might then be interpreted in terms of the spectroscopy of the relevant nuclides.

High angular momentum and highly deformed states are of spectroscopic interest for many reasons. For example, high members of rotational bands, the highly deformed states associated with the "second minimum" in the fission potential, and rotational bands built on highly excited states whose deformation is vastly different from the

[13] R. Middleton, B. Rosner, D. J. Pullen, and L. Polski, Phys. Rev. Letters 20, 118 (1968).

[14] V. V. Volkov, G. F. Gridner, G. N. Zorin, and L. P. Chelnokov, Nucl. Phys. A126, 1 (1969).

[15] D. A. Bromley, in Proceedings of the Summer Study Group, Brookhaven National Laboratory, 1965, p. 1045.

TABLE V.B3-I. Average cross sections for the transfer of various clusters for reactions in the neighborhood of the Coulomb barrier.

Transferred cluster	Mean total cross section (millibarns)
Single neutron	5
Two neutrons	0.05
Three neutrons	0.005
Single proton	2
Deuteron	0.25
Alpha	~0.5
Two protons	~0.1
Charge exchange	0.001

ground state of the nuclide are all of current interest. The few attempts to explain such states spectroscopically have been largely restricted to special cases of the compound nucleus.[16] It is hoped that not only compound-nucleus reactions but also transfers of large clusters, as in (Si^{28}, C^{12}) reactions, will allow the above types of states to be studied extensively at the proposed facility.

In another class of experiments, it is possible to use the Barshay-Temmer theorem[17] to investigate isospin purity by means of transfer reactions with heavy ions. If a T=0 nucleus is incident upon a target and the reaction products are directly related by means of the isospin operators, then the angular distributions of the two reaction products are identical if isospin is conserved. While a few experiments of this class have already been performed,[18] a number of interesting

[16] H. E. Gove, Ref. 15, p. 337.

[17] S. Barshay and G. M. Temmer, Phys. Rev. Letters 12, 728 (1964).

[18] H. T. Fortune, A. Richter, and B. Zeidman, in Proceedings of the Second Conference on Nuclear Isospin, Pacific Grove, California, 1969; W. von Oertzen et al., Phys. Letters 28B, 482 (1969).

possibilities remain to be investigated. If the reaction mechanism can be shown to conserve isospin, then the isospin purity of the initial or final nuclei may be determined.

Finally, the heavy-ion-transfer reaction allows the study of nuclei otherwise unattainable with light projectiles. For example, $T_z = 0$ nuclei well into the 1f-2p shell can be studied through the bombardment of Ca^{40} with heavy ions—e.g., $Ca^{40}(Mg^{24},O^{16})Cr^{48}$ and $Ca^{40}(Si^{28},O^{16})Fe^{52}$. Similar studies can also be carried out in other regions of the table of nuclides (as explained in Sec. V.B5), including both neutron-rich and neutron-deficient regions. For example, in neutron-deficient regions the (heavy ion, 2p) reaction "would provide unique possibilities for investigating the shape of the potential barrier around the nucleus, and the below-barrier interaction of paired protons, as well as nuclear phenomena related to those observed for superconductivity."[19] The studies described above represent the best available approach to extend the regions of known nuclides, and thus to provide new testing grounds for current nuclear models.

d. Grazing Collisions; Bulk Effects of Nuclear Matter

Heavy-ion-induced reactions at high energies may provide unique information on some gross properties of nuclear matter: compressibilities, surface tension, and viscosity as well as the deformability of nuclei. Information about the energy-vs-density curve of nuclear matter—particularly for densities substantially above the interior densities of heavy nuclei, and also for a wide range of the ratio of neutron density to proton density—would provide a much more comprehensive test of the generally accepted Brueckner-Bethe-Goldstone theory of nuclear matter than is now available. A very promising candidate for use in the study of these effects is the grazing collision, first identified by Kaufmann and Wolfgang[20] for light nuclei.

[19] V. I. Goldanskii, Ann. Rev. Nucl. Sci. 16, 1 (1966).

[20] R. Kaufmann and R. Wolfgang, Phys. Rev. 121, 192 (1961).

In such a collision, the colliding particles are thought to penetrate the Coulomb barrier in a grazing trajectory. In the model of Kaufmann and Wolfgang the two drops of nuclear matter are drawn together by the bond formed between projectile and target, while the projectile will tend to continue its motion tangentially along the surface of the target. Because of friction there will be local heating at the point of contact; and this, together with the centrifugal force, will eventually lead to a breaking of the bond between the drops. The local heating also leads to a boiling off of nucleons or clusters of nucleons as well as to an exchange of particles between projectile and target. The signature of the grazing collision is found in the angular distributions of the heavy reaction products, which are peaked in either the forward or backward angular range (in contrast to the symmetrical distribution in the compound process) and in the statistical population of final states (in contrast to the selective population in the direct reaction).

Predictions concerning such reactions are difficult to make since what little is known is restricted to very few projectiles and target elements. In addition, the measurements to date have been based mainly on activation methods, and thus have not allowed resolution of individual final states. When high-energy heavy projectiles are produced in the proposed accelerator, it should be possible to examine the transfer of unusual fragments as a function of angular momentum, projectile charge and mass, and the total energy of the bombarding particle. This study might reveal possible reactions for producing elements that have not been considered previously. In addition, information could be obtained on the presence and types of nucleon clustering near the nuclear surface and on the breakup of projectiles in the Coulomb field of the target nuclei. In fact, the study of bulk properties of nuclear matter may turn out to be one of the more important aspects of heavy-ion measurements.

e. Compound-Nucleus Reactions

Compound-nucleus formation in heavy-ion reactions differs in two important ways from such formation with light ions in that for heavy-ion reactions (i) very high excitation energies are available because of the low energy per nucleon of the incident projectile and (ii) large amounts of angular momentum can be transferred. In fact, very-heavy-ion reactions are the only known ways of producing compound-nucleus states with very high values of angular momentum, so that these reactions are unique and scientifically important.

The effects of angular momentum and excitation energy have been studied to some extent with projectiles from present heavy-ion accelerators.[21] However, these studies have been limited primarily to projectiles with $Z \leq 10$. A few experiments have been done with argon ($Z = 18$), but the beam currents have been very low. It should be possible to investigate new and interesting facets of compound-nucleus formation and decay with the much heavier projectiles available from the proposed accelerator. In addition, the new accelerator will provide the very valuable asset of variable energy as well as intense beam currents.

For the purpose of the following discussion, the compound-nucleus reaction will be divided into two stages: first the formation of the compound nucleus and then its decay.

(i) Formation cross section. The possibility of large angular-momentum transfer can have an important effect on the formation of a compound nucleus. If the yrast energy[21] (i.e., the energy of the lowest level of spin J for a nucleus) for the angular momentum brought in by a particle exceeds the excitation energy that the compound nucleus would have if formed, then a compound nucleus cannot result since a level with an accessible J does not exist. The cross section for

---

[21] T. D. Thomas, Ann. Rev. Nucl. Sci. 18, 343 (1968).

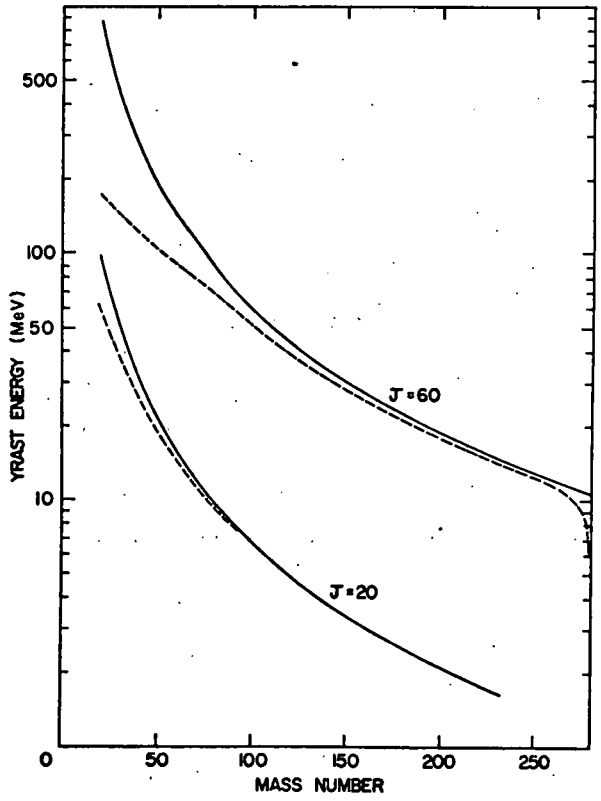

Fig. V. B3-2. Calculated yrast energies for two spin values. Solid lines: for a rigid sphere. Dashed lines: for a spheroidal liquid drop. (From Ref. 21.)

compound-nucleus formation is thus reduced since only those trajectories for which smaller amounts of angular momentum are transferred can participate in this nuclear reaction.

There have been several theoretical calculations of the position of the yrast energy for each value of J, but results disagree by a factor of two or more, depending on the nuclear model used. Figure V. B3-2 shows some yrast energies calculated[22] for a rigid sphere and for a spheroidal liquid drop. Experiments have been performed to measure yrast levels of relatively low angular momentum. However, the nature and implications of yrast energies can be understood only if these measurements are extended to much higher angular momenta for a wide range of projectiles. This requires a range of heavy ions and energies that is unavailable with present machines, but is within the capabilities of the accelerator described in this proposal.

---

[22] R. Beringer and W. J. Knox, Phys. Rev. 121, 1195 (1961).

Yrast levels may have a very important effect on the cross section of "cold nucleus" reactions (as explained in Sec. V.A1d). Since these proposed reactions involve a heavy-ion bombardment in which the resulting compound nucleus has very little excitation energy, cross sections for such reactions could be very sensitive to the locations of the yrast levels.

Because of the instability of a rapidly rotating system, there may be a cutoff in the amount of angular momentum that can be absorbed in a compound state. Calculations by Cohen, Plasil, and Swiatecki[23] indicate that the maximum possible angular momentum deposited in a nucleus by high-energy heavy-ion reactions might be limited to approximately 50 $\hbar$ for nuclei in the region of mass 250—300. These calculations indicate that for larger angular-momentum transfers, centrifugal forces cause the nucleus to be unstable against fission and to break up immediately. If such a cutoff on angular-momentum transfer exists for compound-nucleus formation, then the compound-nucleus cross section for heavy-ion projectiles capable of delivering very high values of angular momentum would be further limited.

Another effect that may limit the cross section of the "cold nucleus" reaction is the Coulomb distortion of the projectile and target nuclei. Because of this distortion, the effective Coulomb barrier during collision may be as much as 30% higher than that calculated for two rigid spheres. If so, this would have a serious effect on proposed "cold nucleus" reactions and on the energy required in order for projectiles to form compound nuclei leading to the production of new elements. Beringer[24] and Wong[25] have discussed this effect from a theoretical point of view, but experimental data are lacking. Wong's calculation of the effective Coulomb barrier for nearly spherical nuclei, with stiffness

---

[23] S. Cohen, F. Plasil, and W. J. Swiatecki, Ref. 12, p. 325.

[24] R. Beringer, Phys. Rev. Letters 18, 1006 (1967).

[25] C. Y. Wong, Phys. Letters 26B, 120 (1968).

determined from experimental data, indicate that the increase in the barrier is only a few percent for particularly stiff nuclei such as the zirconium isotopes. These considerations would indicate that particular combinations of projectile and target nuclei may be especially favorable for low-excitation compound-nucleus formation. The effects of Coulomb distortion have not been estimated for strongly deformed nuclei nor for collisions other than head-on. Even if the increase in effective Coulomb barrier were known, the effect on the cross section for the production of superheavy nuclei is difficult to predict.

A final possibility in compound-nucleus formation is the occurrence of "cooperative energy" phenomena. In these processes, which the new accelerator will make available for study, the speculation is that reactions usually thought of as arising from single-nucleon collisions may be induced in some cluster of nucleons even though the average energy of any single nucleon cluster is below the threshold for the reaction. As an example, one might look for pion production from a bombardment with high-energy heavy ions in which the total energy is well above threshold but the energy per nucleon is below threshold.

(ii) Fluctuation studies. Up to now, very little is known about coherence widths and level spacings particularly of the very-high-angular-momentum states at high excitation energies in the compound nuclei. If one defines compound-nucleus states as quasi-bound states, the density of these levels should decrease above a certain excitation energy and should go to zero as the excitation energy exceeds the total binding energy.

Studies of fluctuations in the excitation functions from heavy-ion-induced reactions and heavy-ion scattering are a useful approach to investigations of the statistical properties of the compound system. As these studies are extended toward heavier nuclei, however, their investigation becomes increasingly difficult as the number of open channels increases and the level width decreases. Nevertheless,

structure accessible to a fluctuation analysis has been observed[2] for S^{32} at excitation energies exceeding 50 MeV in the $O^{16} + O^{16}$ scattering, and an extension to even higher excitation energies seems very feasible.

(iii) Deexcitation of the compound nucleus. Studies of the deexcitation processes of the highly excited, high-angular-momentum states of the compound nucleus formed by heavy-ion reactions can yield valuable information on the validity of various models of nuclear structure, on the position of yrast levels, on the possible existence of clusters, and on the sharing of the total energy among the individual nucleons of the excited nucleus. As mentioned in Sec. V. B3e(ii), yrast levels can play an important role in the formation of a compound nucleus in heavy-ion reactions, and may also influence the mode of deexcitation of the compound nucleus after it is formed.

It has been observed in several cases[26—28] that a compound-nucleus level with angular momentum J_{max} and an energy well above the yrast level for J_{max} will deexcite by fission and by particle and gamma-ray emission. At excitations near the yrast level, where decay by emission of much lighter particles is reduced because no levels of high angular momentum are available in the residual nucleus, the emission of large clusters may be significant since they can carry off large amounts of angular momentum. At excitation energies well above the yrast level, however, deexcitation takes place primarily by nucleon and α emission—with neutron emission favored although alpha-particle emission should become increasingly important as an yrast level is approached. The relative yields of all particles are governed by the transmission coefficients and energies of the outgoing particles, by the level densities available to each, and by the angular momentum of the compound nucleus. There is still only a small amount of data on the competition among

---

[26] J. R. Grover, Phys. Rev. 127, 2142 (1962).

[27] C. D. Williams and T. D. Thomas, Nucl. Phys. 53, 577 (1964).

[28] J. R. Grover and J. Gilat, Phys. Rev. 157, 802 (1967).

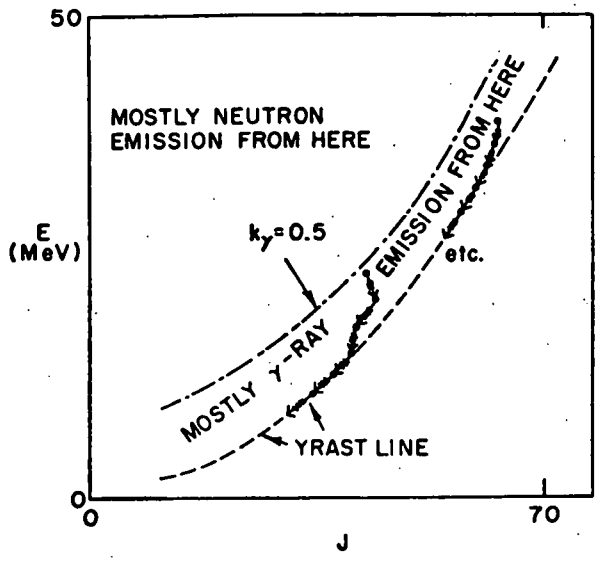

Fig. V.B3-3. Decay sequence of a compound nucleus starting from two excited states of different spin and energy. (From Ref. 28.)

different types of charged-particle emission and almost none on the emission of more complex clusters of nucleons. Much heavier ions with greater energies are required for the observation of some of the effects predicted by present theories. The energies and energy dependences of the emitted particles can also be used to measure the location of yrast levels.

The emission of neutrons and protons normally carries off large amounts of energy but only small amounts of angular momentum. Consequently deexcitation by nucleon emission usually leaves the compound nucleus in an yrast level with spin near that of the initial level. Thus the decay process eventually approaches an yrast energy at which neutron evaporation (normally one of the most probable processes) is hindered because additional emissions would not remove sufficient angular momentum. Deexcitation from this yrast level should proceed by a cascade of gamma rays to successively lower yrast levels. Figure V.B3-3, from a paper by Grover and Gilat,[28] illustrates the sequence expected from compound nuclei at two different states of energy and angular momentum. Production of compound nuclei with angular momenta of the order of 100 $\hbar$ would imply that the gamma cascade would take place over approximately the last 50 MeV of excitation energy. A

study of the gamma-deexcitation process would be very valuable in measuring yrast levels.

Since the last stages of deexcitation of the compound nucleus involve a relatively slow cascade of γ rays from high-angular-momentum states at high excitation energy, fission can be expected to be the major competing mode during this process and also during the particle-emission stage. Furthermore, as the angular momentum of the compound nucleus increases, the fissionability is also expected to increase.[29] Thus, fission is the most probable sequel of heavy-ion reactions.

The compound-nucleus reaction, though one of the first reaction mechanisms studied in nuclear physics, remains a subject that must be investigated further. In particular, the formation and decay properties of compound systems formed in heavy-ion interactions must be understood before the production of new heavy elements can be approached systematically.

---

[29] T. Sikkeland, Phys. Rev. 135, B669 (1964).

V. B4. Studies of Nuclear Fission

Nuclear fission is one of the basic nuclear reactions and clarification of its nature is important in understanding the dynamics of heavy nuclei. For this reason and because of its importance in atomic energy, nuclear fission has been the subject of intensive research at Argonne since the laboratory was founded.

ANL scientists have made important contributions in the determination of the yield of fission-product masses, the charge distribution of the fragments, the x-ray yield as a function of fragment mass, the identification of delayed-neutron emitters, and the measurement of fission cross sections and of the yields of fission neutrons. The spontaneous-fission half-lives of a number of nuclides were measured and the correlation between the spontaneous-fission half-life and the atomic number Z and mass number A of the fissioning nuclide was established. Nuclear fission has been applied as a probe to yield information about the structure of highly deformed nuclei. The distribution of K states and the moments of inertia of transition-state nuclei have been derived from angular-distribution measurements of the fission fragments. Optical-model parameters have been derived by fitting measured fission excitation functions of heavy elements ($Z \geq 90$) with cross sections calculated from optical-model theory. Fission thresholds of nuclides in the region $Z = 81—85$ have also been derived. At energies of several GeV, the breakup of the nucleus has been studied by measuring the mass, charge, and kinetic energy distributions of the fragments.

Nuclear fission has also been studied extensively at many of the universities associated with AUA. Considerable effort has been devoted to measurements of charge and mass-yield distributions of fission products, both in neutron and charged-particle fission. Evidence for ternary fission (the breakup of a particle into three fragments of comparable size) has been obtained for nuclei excited with helium ions of energy greater than 20 MeV. The breakup of nuclei excited

with projectiles of several hundred MeV or more has been studied by measuring the ranges of fission products. These studies have given estimates of the energy deposited in nuclei that fission and have been used to differentiate between fission and fragmentation processes. A number of scientists at both Argonne and the Associated Universities have specialized in studying this important and difficult field and are excited by the possibilities for greatly extending the scope of this work with the new accelerator.

The study of nuclear fission is important because of the significance of the fission process itself and the need to properly understand its mechanism. Fission may be used as a probe to determine the properties of highly deformed nuclei and to gain an improved understanding of nuclear reaction mechanisms. Nuclear fission is a source of radioactive fission products whose nuclear charge is several units from beta stability. The study of these nuclei leads to greater understanding of nuclear excited states.

In the preparation of new elements by heavy-ion bombardments of heavy target nuclei ($Z \geq 90$), fission assumes further importance: it is the principal mode of decay of any excited intermediary nuclei that are formed. A new element may be a fission product of a superheavy element and may itself decay primarily through spontaneous fission.

a. Effect of Angular Momentum on Fission

Heavy-ion bombardments are characterized by high angular-momentum transfer. Theory, supported by a few experimental results, indicates that the probability for fission is greater in the states of higher angular momentum than for other decay processes. This is illustrated schematically[1] in Fig. V.B4-1 in which the deformation energy, the rotational energy, and the sum of the two are plotted against

[1] T. D. Thomas, Ann. Rev. Nucl. Science 18, 343 (1968).

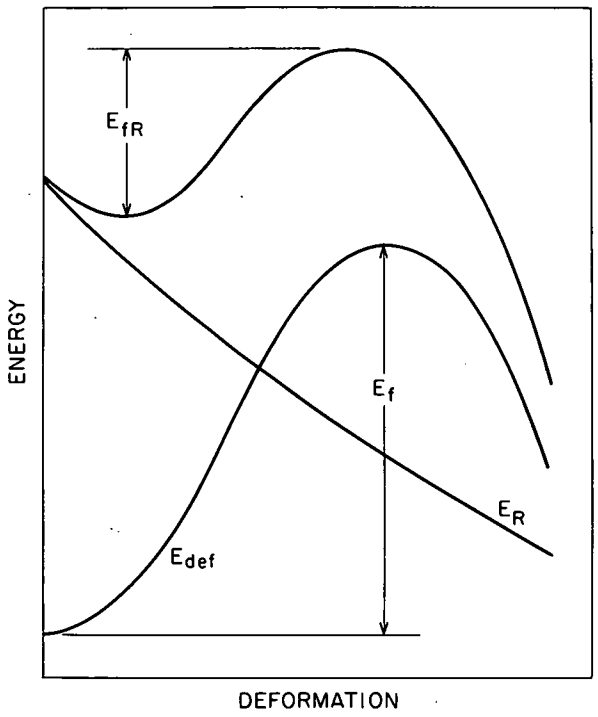

Fig. V. B4-1. The effect of angular momentum on the fission barrier. E_f represents the barrier in the absence of angular momentum. E_{fR} represents the barrier with angular momentum present. (Adapted from Thomas, Ref. 1.)

the deformation of the nucleus. For a nucleus with no angular momentum, the height of the fission barrier is E_f. The rotational energy E_R is defined by the relationship

$$E_R = \frac{\ell(\ell + 1)}{2\mathcal{I}} \approx \frac{\ell^2}{2\mathcal{I}}, \qquad (1)$$

where $\mathcal{I}$ is the moment of inertia of the nucleus. Since $\mathcal{I}$ increases with deformation, E_R decreases. The fission barrier for the rotating nucleus is indicated by E_{fR}. It represents the difference between the minimum and maximum on the curve representing the sum of the deformation and rotational energies. E_{fR} is considerably smaller than E_f. For sufficiently high angular momenta (rotational energies), E_{fR} disappears and the nucleus is unstable with respect to instantaneous fission. The critical angular momentum ℓ_m at which this occurs has been calculated by Cohen et al.[2] and is represented by the solid curve plotted in Fig. V. B4-2 as a function of mass. This figure also shows ℓ_B, the maximum angular-momentum transfer to be expected when a

[2] S. Cohen, F. Plasil, and W. J. Swiatecki, Lawrence Radiation Laboratory Report UCRL-10775, 1963, unpublished.

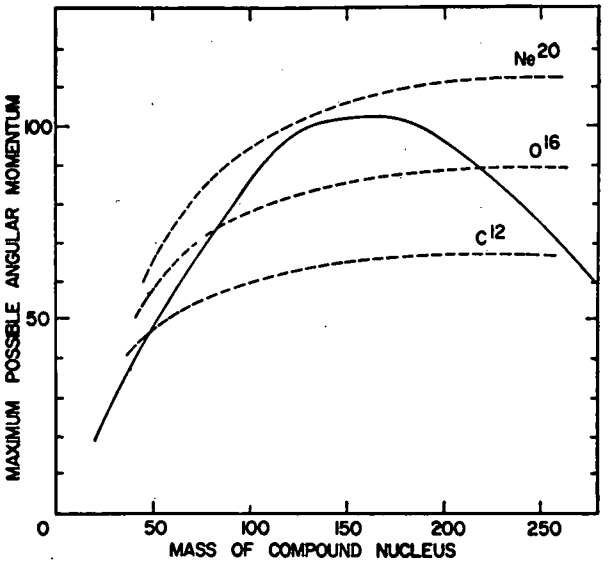

Fig. V. B4-2. Critical angular momentum ℓ_m (solid curve) and maximum angular momentum ℓ_B (dashed curves) of a nucleus, plotted as a function of the nuclear mass. The dashed curves show values of ℓ_B expected when a compound nucleus of the indicated mass is formed by an interaction of a target nucleus with C^{12}, O^{16}, and Ne^{22} accelerated to 10 MeV/nucleon. (From Thomas, Ref. 1.)

compound nucleus of the indicated mass is formed by the interaction of a target nucleus with C^{12}, O^{16}, or Ne^{20} ions accelerated to 10 MeV/nucleon. According to the theory of Cohen et al., all interactions involving ℓ values between ℓ_m and ℓ_B will lead to direct fission with no compound-nucleus formation. For 200-MeV Ne^{20} ions, the theory predicts that there will be some instantaneous fission with all target masses. For 160-MeV O^{16} ions, instantaneous fission will occur only with light and heavy targets.

Let us define the total reaction cross section σ_R to represent any interaction that removes the projectile from the incident channel and define the capture (i.e., compound-nucleus) cross section σ_C to represent complete fusion of projectile and target nucleus. The occurrence of instantaneous fission evidently makes $\sigma_C < \sigma_R$. Even in cases in which ℓ_B is less than ℓ_m, there are other competing direct processes, such as transfer reactions, which further reduce σ_C relative to σ_R. The cross section σ_C may then be only a minor component of the total reaction cross section. Since some proposed methods for making superheavy elements involve compound-nucleus formation, it is important to study the magnitude of σ_C with very heavy ions.

In heavy-ion reactions with heavy element target nuclei ($Z \geq 90$), fission accounts for most of the reaction cross section. Viola

and Sikkeland[3] have measured the fission cross sections σ_f of U^{238} bombarded with projectiles ranging from He^4 through Ne^{20} at energies up to 10.4 MeV/nucleon. These σ_f values have been compared[1] with the values of σ_R calculated for an optical model with potential parameters derived from the scattering of heavy ions from gold and bismuth.[4] The good agreement between these values[1] indicates that σ_f may be used to approximate σ_R when heavy elements are bombarded with heavy ions.

Sikkeland and coworkers[5—7] have devised an ingenious technique to determine the fraction of reactions that lead to compound-nucleus formation. The technique depends on the fact that all of the linear momentum of the projectile enters a compound nucleus, whereas only part of it is transferred in direct interactions. When the compound nucleus fissions, the angular distribution of the fragments is expected to be symmetric about 90° in the center-of-mass system. Fission fragments were measured in coincidence with one detector at a fixed angle relative to the heavy-ion beam and the other detector at variable angles. For heavy-ion bombardments, the angular correlation between fragments from a compound nucleus should give a single maximum, but several maxima should be observed if other reaction mechanisms are also present. The results of Sikkeland and Viola[6] indicate that with C^{12}, N^{14}, O^{16}, and Ne^{20} beams of 10.4-MeV/nucleon incident on U^{238} target nuclei, a substantial amount of the total fission cross

---

[3] V. E. Viola, Jr., and T. Sikkeland, Phys. Rev. 128, 767 (1962).

[4] E. H. Auerbach and C. E. Porter, Proceedings of the Third Conference on Reactions Between Complex Nuclei, edited by A. Zucker, E. C. Halbert, and F. T. Howard (John Wiley and Sons, Inc., New York, 1960), p. 19.

[5] T. Sikkeland, E. L. Haines, and V. E. Viola, Jr., Phys. Rev. 125, 1350 (1962).

[6] T. Sikkeland and V. E. Viola, Jr., Ref. 4, p. 232.

[7] T. Sikkeland, Phys. Rev. 135, B669 (1964).

section, ranging from 25% for C^{12} to 40% for Ne^{20}, does not involve compound-nucleus formation. For lighter targets, only the single peak that corresponds to complete fusion between ion and target nucleus is observed in the angular correlation. This indicates that with target nuclei having $Z \leq 83$ bombarded with heavy ions up to Ne^{20}, fission is not energetically favored unless complete fusion occurs. It would be of great interest to investigate these effects in compound nuclei that have the same mass and charge but differ in excitation energy and angular momentum. This will be possible with the proposed new accelerator.

When $\ell < \ell_m$ and a compound nucleus is formed, this nucleus loses its excitation energy E_x through three competing decay modes—fission, particle emission, and gamma-ray emission. At excitation energies greater than the yrast energies [Sec. V.B3(iii)] it is expected that γ-ray emission is much less likely than particle emission or fission.

The branching ratio Γ_n/Γ_f for neutron emission and fission has been calculated by Huizenga and Vandenbosch[8] on the basis of the theoretical energy dependences of Γ_n and Γ_f. Their results are shown in Fig. V.B4-3, where Γ_n/Γ_f is plotted against the excitation energy in excess of the neutron binding energy. The calculations are for a nucleus that has A = 209 and a fission threshold 5 MeV greater than the neutron binding energy. The dashed and solid curves are drawn for $E_R/E_R^f = 1.75$ and 2.5, respectively, where both E_R and E_R^f are rotational energies read from the E_R curve in Fig. V.B4-1 and are related to angular momentum by Eq. (1); E_R is the rotational energy at equilibrium deformation (minimum in $E_{def} + E_R$, plotted as the upper curve) and E_R^f is the value at the saddle deformation (maximum in $E_{def} + E_R$). The calculated curves indicate that increased angular

[8] J. R. Huizenga and R. Vandenbosch, Nuclear Reactions, edited by P. M. Endt and P. B. Smith (North-Holland Publishing Co., Amsterdam, 1962), Vol. II, p. 42.

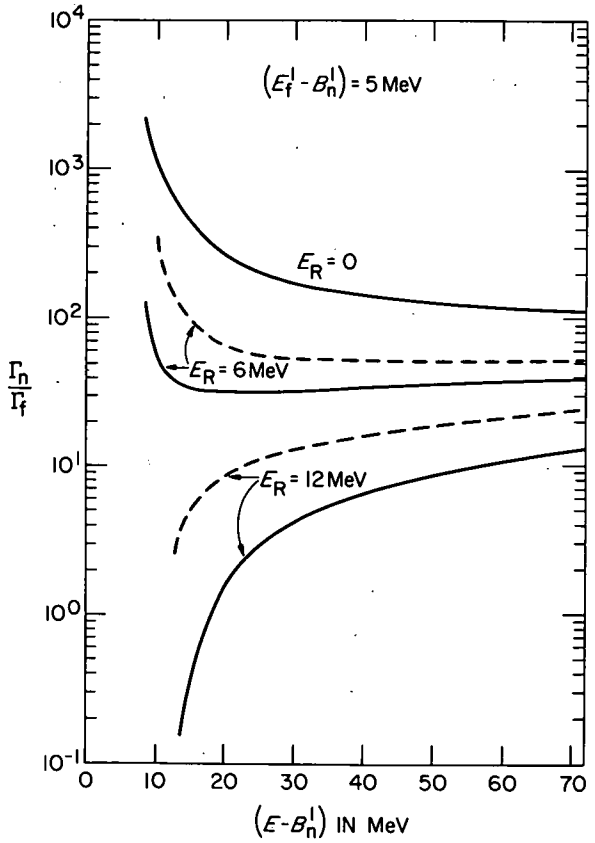

Fig. V. B4-3. Dependence of Γ_n/Γ_f on excitation energy for a nucleus having mass 209 and a fission threshold E_f 5 MeV greater than the neutron binding energy B_n and different amounts of angular momentum. The solid and dashed curves are calculated for estimated ratios $E_R/E_R^f = 2.5$ and 1.75, respectively, where E_R and E_R^f are the rotational energies corresponding to the deformation positions of the minimum and maximum in the upper curve of Fig. V. B4-1. (From Huizenga and Vandenbosch, Ref. 8.)

momentum at a fixed excitation energy indeed favors fission over neutron emission. Since emitted neutrons take away little orbital angular momentum, such emission decreases the excitation energy of the residual nucleus with little change in angular momentum. This further enhances second- and third-chance fission in compound nuclei with high angular momenta.

There has been some investigation of the effect of angular momentum on competition between fission and other decay modes for compound nuclei in the region between rhenium and bismuth.[7,9,10] Results of one of these studies[7] are shown in Fig. V. B4-4, where the ratio σ_f/σ_R is plotted for the Re^{181} compound nucleus formed in three different reactions. For a given excitation energy, the nucleus formed

[9] J. Gilmore, S. G. Thompson, and I. Perlman, Phys. Rev. 128, 2276 (1962)

[10] F. Plasil, Lawrence Radiation Laboratory Report UCRL-11193, 1963, unpublished.

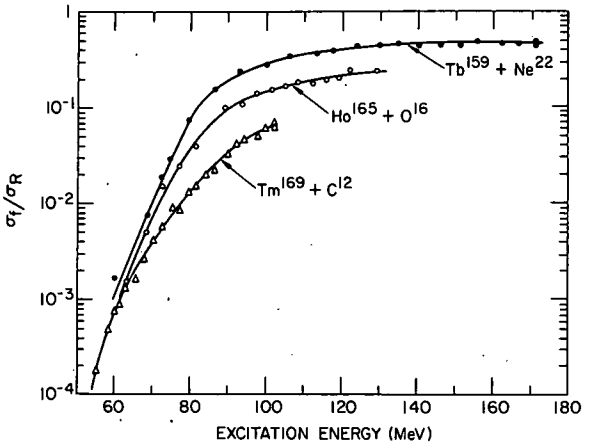

Fig. V. B4-4. Experimental values for the ratio σ_f/σ_R as a function of excitation energy for the compound nucleus Re^{181} formed in the reactions $Tm^{169} + C^{12}$, $Ho^{165} + O^{16}$, and $Tb^{159} + Ne^{22}$. (From Sikkeland, Ref. 7.)

by bombardment with the heaviest ion (Ne^{22}) has the most angular momentum and is the most likely to fission, in agreement with the result expected from Fig. V. B4-3. As the excitation energy is decreased, fission becomes less important, as anticipated from the 0 and 6-MeV curves in Fig. V. B4-3. However, conditions of experiment and calculation are not strictly comparable, since the average angular momentum of the compound nucleus in the experiment decreases with excitation energy.

Interesting as these results are, they are limited by the mass, energy, and angular momentum of the projectiles available with present accelerators. The heaviest ion used is usually Ne^{22} and occasionally Ar^{40}. Experiments so limited leave a number of unanswered questions. Does compound-nucleus formation eventually disappear as a reaction mechanism or does it, as theory suggests, continue to survive for $\ell < \ell_m$? To what extent do transfer reactions and other direct reactions account for fission following incomplete momentum transfer from the projectile? What is the nature of the transferred particle and how does it change with the mass, energy, and angular momentum of the projectile? Although present results indicate that increased angular momentum favors fission as a decay mode, they provide little information about the change in Γ_n/Γ_f with excitation energy for a particular angular momentum. The increased ranges of projectile masses and

energies from the proposed accelerator make possible experiments to answer these questions.

Experiments that might be carried out with the proposed accelerator and would provide answers to some of the above questions are summarized in Table V. B4-I, which gives five different reactions for the preparation of $_{84}Po^{202}$. The Coulomb barrier V_c and reaction Q value are listed also for each of the reactions. The Coulomb barrier has been calculated for spherical nuclei with a nuclear radius parameter $r_0 = 1.4$ F. If projectile and/or target nucleus are appreciably distorted as they approach each other under the conditions of bombardment, then the listed values of V_c are too small and greater projectile energies must be available to give the quoted results for the various cases.

In case I, the projectile energy was taken to be 10 MeV/nucleon. The angular momenta ℓ_B represent the maximum imparted by the various projectiles to the given target nuclei. The quantities ℓ_{av} represent the total angular momenta averaged over all excited nuclei. According to the calculations of Cohen et al.,[2] ℓ_m for $_{84}Po^{202}$ is 96 $\hbar$ when the moment of inertia is assumed to be that of a spherical nucleus. Only the $_8O^{16} + _{76}Os^{186}$ reaction listed in Table V. B4-I has ℓ_B less than this critical value. By measuring the fission-fragment angular correlations for each of the five reactions listed, one can determine the contribution of σ_c to σ_R. If the ideas of Cohen et al.[2] are correct, one would expect the contribution of σ_c to σ_R to be greatest for the $_8O^{16} + _{76}Os^{186}$ reaction and to be successively smaller for the other reactions in the order of increasing ℓ_B.

Cases II and III are examples of reactions in which the calculations of Vandenbosch and Huizenga[8] might be checked in more detail. In case II are listed the ℓ values expected for the various reactions in which the excitation energy of the compound nucleus is kept constant. This is similar to previous experiments[7,9,10] but has the great advantage of including reactions involving larger angular momenta.

TABLE V.B4-I. Coulomb barriers, Q values, and various angular-momentum and energy values associated with different reactions to give $_{84}Po^{202}$.

Reaction	V_c[a]	Q[b]	Case I[c]		Case II[d]		Case III[e]	
			ℓ_B	ℓ_{av}	ℓ_B	ℓ_{av}	E_x[f]	E_{lab}[g]
$_8O^{16} + {}_{76}Os^{186}$	77.2	- 30.1	80	53.5	80	53.5	115.6	158.2
$_{10}Ne^{20} + {}_{74}W^{182}$	92.2	- 37.7	101	67.5	85	56.8	108.4	162.1
$_{18}Ar^{40} + {}_{66}Dy^{162}$	139.8	- 85.6	205	136.8	120	80.2	81.2	208.1
$_{36}Kr^{86} + {}_{48}Cd^{116}$	194.3	-154.4	342	228.2	174	116.2	55.9	366.2
$_{54}Xe^{134} + {}_{30}Zn^{68}$	183.9	-141.4	306	204.2	161	107.5	60.4	599.5

[a] Calculated for spherical nuclei with $r_0 = 1.4$ F.

[b] Calculated from experimental mass values reported by W. D. Myers and W. J. Swiatecki, Lawrence Radiation Laboratory Report UCRL-11980, 1965, unpublished.

[c] Case I: $E_{lab} = 10$ MeV/nucleon.

[d] Case II: $E_x = E_{c.m.} + Q = 117.2$ MeV.

[e] Case III: $\ell_B = 79$, $\ell_{av} = 52.8$.

[f] Excitation energy of compound nucleus.

[g] Energy of projectile in laboratory frame of reference.

Case III represents an experiment which has as yet never been performed. It lists the excitation energies E_x of the compound nuclei for which ℓ_B is 79 ħ and ℓ_{av} is 52.8 ħ in every reaction. The value of ℓ_B is therefore considerably less than ℓ_m which is 96 ħ. Furthermore, the excitation energies of the compound nuclei vary from about 60 to 116 MeV. The determination of the σ_f/σ_R ratio in such experiments would be invaluable in probing the variation of Γ_n/Γ_f vs $(E_x - B_n)$, as in Fig. V.B4-3. In an obvious extension of these proposed experiments, one would reduce ℓ_B to some value less than ℓ_m but maintain the same E_x for each reaction, as in Case II.

b. Formation of New Fission Products and Spontaneously Fissioning Isomers

The realization that a new heavy element may be a fission product of a superheavy element is discussed in Sec. V.A1d. Figure V.A1-11 shows the extrapolated fission-product mass-yield distribution in the reaction $_{92}U^{235} + _{36}Kr^{84}$. This distribution covers an enormous range of masses. The extrapolated cross sections of mass 75—240 exceed one millibarn. As broad as this distribution is, the mass-yield distributions of the U + Xe and U + U reactions are expected to be even broader. Such reactions will produce many new neutron-excess isotopes that can be produced only in the fission process. These fission products may be studied, depending on their half-life, either radiochemically or by physical means. If the new fission products (some of which may be new elements) fission spontaneously with very short half-lives, differences in the mass-yield distributions may be observed by making use of time-of-flight measurements. These techniques are presently being used in the study of isomers that fission spontaneously and in the measurement of x-ray yields. Measurements of spontaneous-fission half-lives less than 10^{-8} sec are possible with these techniques. Nuclei with longer fission or total-decay half-lives (up to minutes) may be studied through mass separation followed by in situ analysis of their decay radiations.

A significant number of spontaneously fissioning isomers with very short half-lives have been reported.[11] These isomers are thought to be associated with a double-humped fission barrier.[12] A number of these isomers have been produced by bombarding various target nuclei with heavy ions up to and including Ne. The double-humped fission barrier has been suggested to explain not only spontaneously fissioning isomers but also certain structural effects in fission cross sections observed with slow and fast neutrons. The existence of a double- or multiple-humped barrier is an extremely important theoretical concept which will necessitate re-examination of much of the data acquired at energies near the fission barrier. For heavy-ion reactions, the double-humped barrier may seriously influence the cross section for compound-nucleus formation, particularly in "cold nucleus" reactions in which the compound nucleus has little excitation energy.

The new accelerator will provide the means for studying reactions of this type. Of particular interest will be reactions (such as Mo + Xe) which represent, in many respects, the inverse fission reaction. The study of these reactions will probe the fission barrier from a direction opposite to fission. Heavy-ion reactions can also provide the means for studying the modes of decay, other than fission, of nuclei found in the excited states thought to exist between the two humps of the fission barrier. With heavy-ion reactions, the investigation of spontaneously fissioning isomers can be extended to new mass regions to determine whether the suggested double-humped fission barrier describes such phenomena over a much wider range of Z, A, and deformation β.

c. Measurements of Coulomb Fission and Fission Lifetime

It has been proposed that the Coulomb field of a heavy ion be used to distort a fissionable, even-even nucleus so that it is

[11] S. M. Polikanov, Usp. Fiz. Nauk 94, 43 (1968) [English transl.: Soviet Phys. Usp. 11, 22 (1968)].

[12] V. M. Strutinski, Nucl. Phys. A95, 420 (1967).

slowly carried over the fission barrier with little internal excitation.[13,14] Such excitation would permit the direct study of the deformation-energy surface and furnish important information on the location of the fission barrier from the equilibrium deformation $\Delta\beta$ and the curvature of the barrier C_b. These quantities are completely unknown at present.

Model-dependent cross sections have been calculated for various values of $\Delta\beta$ and heavy-ion masses.[14] These calculations indicate that the differential fission cross section at 180° in center-of-mass (c.m.) coordinates may be >200 mb for a U^{238} projectile on a U^{238} target nucleus with $\Delta\beta = 1.0$ and $E_{c.m.} = 600$ MeV. The angular distribution of the fragments for this reaction is expected to be concentrated around 90° to the beam, with perhaps some interesting peaks at more forward angles.

The proposed accelerator would allow checking the predictions of this model. The possibility of evaluating the parameters $\Delta\beta$ and C_b is an exciting prospect which would lead to a far more detailed understanding of the fission process.

Another fundamental aspect of the fission process which needs clarification is the time required for fission of a nucleus that has been excited above the fission barrier. Lifetimes $>10^{-4}$ sec for nuclei whose excitation is near the barrier may be measured as a function of nuclear excitation energy in a single experiment using a modified Doppler-shift technique. The very large recoil velocities needed for accurate Doppler-shift measurements of fission-fragment energies can be imparted to a fissioning nucleus by inelastic scattering of very energetic heavy ions. By measuring the energy of the scattered heavy ion in coincidence with a given fission event, the nuclear excitation energy for each fission event for which the Doppler shift is measured can be accurately evaluated.

---

[13] E. Guth and L. Wilets, Phys. Rev. Letters 16, 30 (1966).

[14] L. Wilets, E. Guth, and J. S. Tenn, Phys. Rev. 156, 1349 (1967).

A very low limit on the fission or particle-decay lifetimes of highly excited nuclei may be established by observing whether K x rays of the excited compound nucleus are in coincidence with fission fragments or with emitted particles. The x rays are expected to result from the ejection of electrons from the K shell of the compound-nucleus atom because of the large change in nuclear charge when a heavy ion is absorbed. If characteristic K x rays of the compound-nucleus atom are observed in coincidence with fission, the fission lifetime must be longer than the characteristic "K-electron-shell filling times" of $\sim 10^{-16}$ sec.

d. Ternary Fission

The breakup of a nucleus into more than two fragments has been studied for many years, but experimental results have been modest. Swiatecki[15] has calculated the maximum energy released in the breakup of a uniformly-charged liquid drop into n equal parts. The results of these calculations are summarized in Fig. V. B4-5, in which energy is plotted as a function of the fissionability parameter $x = (Z^2/A)/(Z^2/A)_{cr}$, where the critical value $(Z^2/A)_{cr}$ has been taken to be ~ 50. These calculations suggest that a nucleus with large x may divide into more than two fragments. This effect seems to exist, since the limited available experimental evidence indicates that fission into three fragments occurs more frequently for larger values of Z^2/A for the fissioning nucleus.[16] This evidence is summarized in Table V. B4-II. Some tentative results for the interaction between U^{238} and protons in the GeV energy range may be added to this table. The ratio of ternary

[15] W. J. Swiatecki, Proceedings of the Second International Conference on Peaceful Uses of Atomic Energy, Geneva, 1958 (United Nations, New York, 1958), Vol. 15, p. 248.

[16] R. L. Fleischer, P. B. Price, R. M. Walker, and E. L. Hubbard, Phys. Rev. 143, 943 (1966).

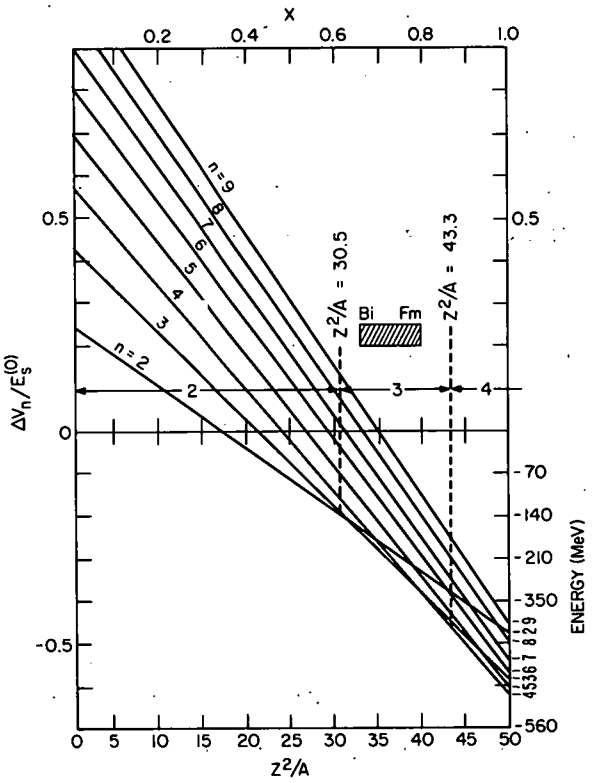

Fig. V.B4-5. Liquid-drop-model calculation of the energy released in the division of a drop into n equal parts as a function of the parameter $x = (Z^2/A)/(Z^2/A)_{cr}$. The ordinate $\Delta V_n/E_s^{(0)}$ indicates the energy difference between n equal fragments at infinity and the original drop in terms of the surface energy $E_s^{(0)}$ of the original drop. Values of the energy released are indicated by ordinate scale labeled in the lower right-hand side of the figure. The numbers 4, 5, 3, 6, 7, 8, 2, 9 indicate the number of fragments into which the original nucleus may divide. The order is that of decreasing energy release. The calculations indicate that energy will be released for division into as many as 20 equal fragments at x = 1.

TABLE V.B4-II. Ternary/binary fission ratios as a function of Z^2/A.[a]

Nucleus	Z^2/A	Ternary/binary
n + U^{235}	35.8	$(7 \pm 3) \times 10^{-6}$
n + U^{235}	35.8	1.3×10^{-6}
Ne + Pb	36.1	$< 6 \times 10^{-4}$
Cf^{252}	38.2	3×10^{-5} to 6×10^{-4}
Cf^{252}	38.2	$< 10^{-4}$
Ar + Pb	40.4	5×10^{-3}
Ar + U	43.5	$\leq 3 \times 10^{-2}$
Ar + Th	43.5	3.3×10^{-2}

[a]From Fleischer et al., Ref. 16. Reference to the original work may be found in this paper.

to binary events for 23-GeV protons is $\sim 5 \times 10^{-3}$ and is $\sim 2 \times 10^{-3}$ for 18-GeV protons.[17] These ratios indicate that ternary fission is enhanced by energy as well as large values of Z^2/A. It has been suggested that ternary fission is asymmetrical binary fission accompanied by subsequent fission of the heavy fragment.[18] With the heavy ions and energies available from the proposed accelerator, the investigation of multiple-fragment fission will be greatly facilitated since both Z^2/A and the energy of the fissioning system will be enhanced. This will permit studies to determine, for example, whether ternary fission proceeds as a one- or two-step process.

e. General Studies of the Fission Process

Many of the still unresolved problems of the fission process concern the extent of statistical equilibrium between the many-nucleon degrees of freedom during the elongation of the nucleus as it proceeds to scission, the deformation of the fragments at the moment of scission, the importance of nucleon configurations and shell structure in fission, and the significance of various phenomenological concepts such as nuclear viscosity. To find answers for these problems will require measurement of the various distributions of fragment mass, charge, kinetic energy, and angle as functions of beam energy, projectile, and target nucleus. Measurements will be made either radiochemically or by physical means. The number and energy distributions of emitted neutrons, charged particles, gamma rays, and x rays will be determined. Such studies will provide valuable fundamental information on the fission process.

---

[17] R. Brandt, University of Marburg, Germany, 1969 (private communication).

[18] S. A. Karamyan, I. V. Kuznetsov, Yu. Ts. Oganesyan, and Yu. E. Penionzhkevich, Yadern. Fiz. 5, 959 (1967) [English transl.: Soviet J. Nucl. Phys. 5, 684 (1967)].

V.B5. Other New Nuclear Species

In addition to the production of new superheavy elements, the proposed accelerator would make possible the production of a number of new isotopes of light and medium-weight elements. The study of these isotopes—and of the reaction mechanism responsible for their production—would be of considerable interest. Brief descriptions of a few such studies are given below.

a. Neutron-Deficient Isotopes: New Regions of Deformation

The shape of a nucleus is primarily determined by the competition between quadrupole and pairing forces. Deformation is expected for nuclei in which the relative strength of the quadrupole force is large, i.e., for nuclei with nucleon numbers far from the magic numbers. Hence, in addition to the known regions of deformation (regions 2, 4, and 5 in Fig. V.B5-1), new regions (1 and 3) are expected. Less qualitative evidence for the existence of deformed nuclei in regions 1 and 3 is given by the calculations of Marshalek et al.[1] and of Kumar and Baranger.[2]

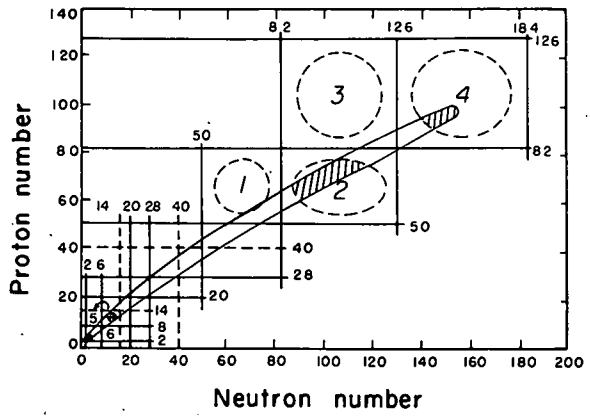

Fig. V.B5-1. A schematic representation of the nuclear periodic table, showing the new regions of deformation (Ref. 1). The cross-hatched areas represent the regions of presently known deformed nuclides.

---

[1] E. Marshalek, L. W. Person, and R. K. Sheline, Rev. Mod. Phys. 35, 108 (1963).

[2] K. Kumar and M. Baranger, Phys. Rev. Letters 12, 73 (1964).

Information as to whether nuclei in regions 1 and 3 are really deformed, as well as the sign of any deformation, can be obtained from their energy-level systematics. In region 1 this information could be obtained by producing odd-odd nuclides and observing the excited states populated in the even-even daughter nuclei. The presence of 0^+, 2^+, $\cdots$ levels and the ratios of their energies would give a measure of the deformation. The energies of excited states of even-even nuclei in region 3 can be obtained from measurements of the α fine structure in their α spectra. Also, since the spin of a compound nucleus formed in heavy-ion reactions is usually highly aligned and this alignment tends to persist in subsequent decays, the angular distribution of emitted γ rays contains information about the spins of levels involved in the transitions.

As shown in Fig. V.B3-1. the possible new regions of deformed nuclei lie on the neutron-deficient side of the β stability line so that they are accessible only by means of heavy-ion-induced reactions. The proposed accelerator would allow the production of many of these nuclei for the purpose of studying their decay schemes.

A number of specific questions about nuclear structure could be answered by studies of these neutron-deficient isotopes. For example, in the N = 81 nuclei there is a series of $h_{11/2}$-$d_{3/2}$ isomers. The ground-state isomers have the configuration $d_{3/2}$. It would be of interest to follow the $h_{11/2}$-configuration state into more neutron-deficient nuclei to determine, for example, the amount and trend of $h_{11/2}$-$d_{3/2}$ configuration mixing.

The probability of α decay relative to that of electron capture for a given element is expected to increase as the mass number decreases. Thus there may be a number of α-active odd-odd nuclei among the neutron-deficient isotopes. Measurements of the α fine structure of these nuclei could provide information about the effective n-p interaction.

b. Nuclei with Proton and Neutron Excesses

During the past few years a number of hitherto unknown light nuclei (e.g., Li^{11} and B^{14}) have been observed[3] as the result of spallation reactions induced by several-GeV protons incident upon heavy nuclei. These nuclei, having a sizeable neutron excess, lie far from the line of stability yet live long enough to be detected electronically. Investigation of the states in these light nuclei is possible by use of heavy-ion-induced reactions, e.g., in $B^{11}(O^{16}, Li^{11})Ne^{16}$ in which the outgoing Li^{11} would be detected. Even if the lifetime of Ne^{16} is too short to allow direct detection, it should be possible to determine its mass and excited states from the spectrum of Li^{11} provided the lifetime of this nucleus is sufficiently longer than the reaction time. Examples of relatively long-lived highly-excited unbound states are known to exist—e.g., the 16-MeV states in Be^{8}.

Proton-rich nuclei may have new and interesting properties. For example, Goldanskii[4] has suggested that the pairing energy in nuclei with large proton excess may be sufficiently large that di-proton emission might be favored over single-proton emission. As in α decay, the Coulomb barrier hinders the di-proton decays so that such nuclei would have long lifetimes. Such delayed-pair emitters would provide a sensitive probe for the study of the pairing interaction. With the proper choice of targets and projectile, it should be possible to produce and investigate these unique proton-rich isotopes.

---

[3] A. M. Poskanzer, S. W. Cosper, E. K. Hyde, and J. Cerny, Phys. Rev. Letters 17, 1271 (1966).

[4] V. I. Goldanskii, Soviet Phys.—Usp. 8, 770 (1966).

V.B6. Nonnuclear Research

Although the proposed accelerator is designed primarily for nuclear research, its unique properties will undoubtedly prove useful in certain special applications in other fields of research. A few such promising applications are presented below.

a. Penetration of Charged Particles Through Matter

Various phenomena related to the penetration of very energetic heavy ions through monocrystalline or polycrystalline solids or through gases should become possible with the use of the TU tandem or the variable-energy cyclotron, or with a combination of both machines (the full MTC).

When energetic ions penetrate through a solid, a variety of physical processes can occur (e.g., nuclear reactions, ion implantation, x-ray emission, sputtering, secondary electron emission, and/or radiation damage). In an amorphous solid the ions undergo successive collisions in randomly distributed directions. For this case it has been observed that the total yield (per unit path length) for any of the secondary processes mentioned above is independent of the direction along which the ion moves. For a monocrystalline solid, however, the ion trajectories can under certain conditions be strongly influenced by the regular arrangement of the lattice atoms, and as a result the ions undergo a nonrandom distribution of successive collisions.

Phenomena connected with the slowing down of charged particles in matter have been of interest in physics for many years; experimental and theoretical studies are associated with such names as Bethe, Bloch, Bohr, Allison, Fano, and Platzmann. At Argonne an extensive research program has been conducted over the past few years to study how the orientation of a monocrystalline metal target with respect to the incident ion beam direction influences the yields of various secondary processes (e.g., sputtering and secondary electron emission)

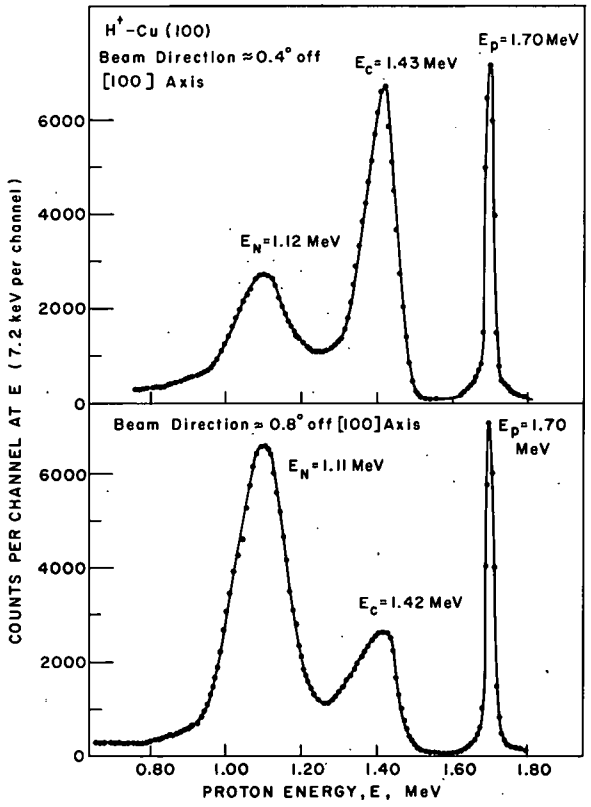

Fig. V.B6-1. Energy spectrum of protons emerging from a monocrystalline copper foil whose surface is a (100) plane. The incoming beam makes an angle of 0.4° (upper curve) or 0.8° (lower curve) with the perpendicular to the (100) planes. The low-energy peak (labeled E_N) comes at the energy expected from the normal rate of energy loss in a polycrystalline target. The high-energy peak (at energy E_c) corresponds to the lower rate of energy loss by a proton traveling along a channel. The energy spectrum of the incoming protons (energy E_p) was obtained with the target foil removed.

as well as the average stopping powers and the distribution of charge states of particles emerging from monocrystalline foils.[1] These studies were conducted for light ions ($Z = 1$ or 2) within the reduced velocity range $0.050 \lesssim V_r \lesssim 2.00$, with $V_r = V/(V_0 Z^{2/3})$, where V is the ion velocity in the laboratory system, $V_0 = e^2/\hbar$, and Z is the atomic number of the incident ion.

When the direction of the incident particles was close to one of the low-index directions of a monocrystalline metal target, two peaks in the energy spectrum of particles emerging from such a target were observed, as is illustrated in Fig. V.B6-1. The rate of energy loss $[(dE/dx)_{av}]_n$ in the low-energy peak is quite closely equal to the "normal" rate in polycrystalline targets of the same thickness. The high-energy

[1] For example, M. Kaminsky, Bull. Am. Phys. Soc. 12, 635 (1967); Proceedings of the 26th Annual Conference on Physical Electronics, MIT, 1966, pp. 316 and 331; Adv. Mass Spectrometry 3, 69 (1966); Atomic and Ionic Impact Phenomena on Metal Surfaces (Academic Press, New York, 1965), Chaps. 10 and 14.

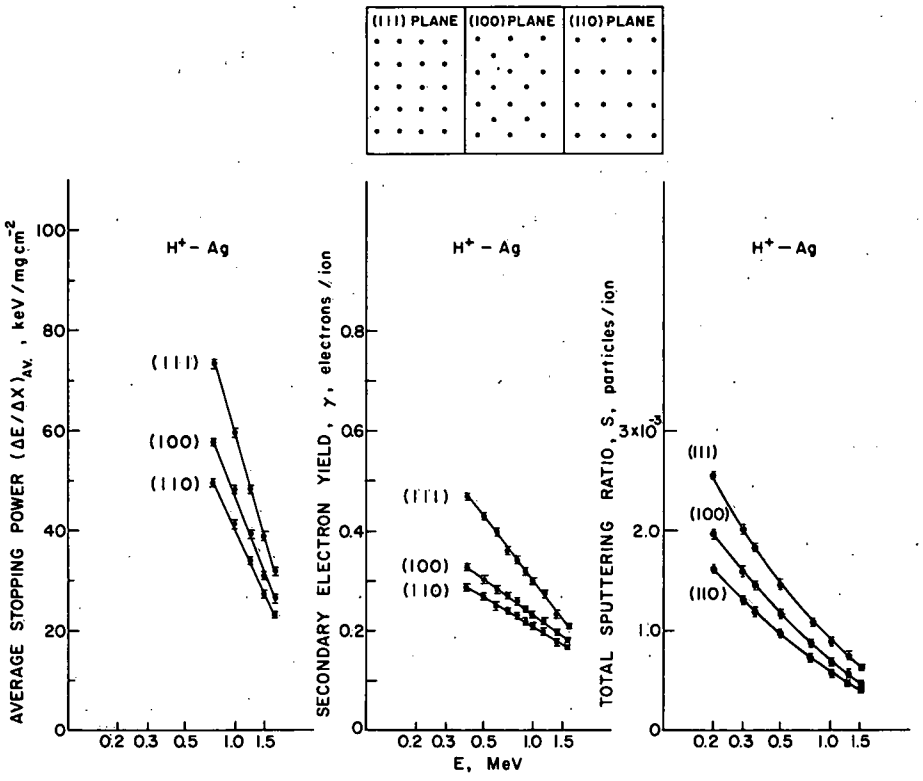

Fig. V.B6-2. Values for the mean stopping power (the average energy loss per unit path length), the total secondary-electron yield γ, and the total sputtering yield S for protons incident with energy E and penetrating through silver monocrystalline foils with their surfaces parallel to the indicated crystal planes.

peak $[(dE/dx)_{av}]_{ch}$ is thought to be due to ions traversing axial channels formed by parallel rows of atoms in the crystal. The yield for sputtering and secondary electron emission also vary with crystal direction.[1]

For the case of protons penetrating silver monocrystals of different orientation (Fig. V.B6-2) the yields decrease in the order [111] > [100] > [110], the order in which the transparency of the lattice along the respective directions becomes larger.

From these results it appears that the observed orientation dependence is determined more by the production mechanism of internal secondary particles (related to the characteristic energy loss of the primary ions) than by the escape mechanism. The observation that

$[(dE/dx)_{av}]_{ch} \approx \frac{1}{2}[(dE/dx)_{av}]_n$ seems to confirm Bohr and Lindhard's equipartition rule,[2,3] which states that particles losing energy predominantly via electronic stopping can lose their energy equally in two processes: (1) close electronic collisions and (2) distant electronic collisions. For the well-channeled ions, process (1) is negligible in comparison to the energy loss due to process (2); but both processes contribute equally to the energy loss of the particles in the "normal peak."

Further insight into the processes that slow down an ion penetrating a solid was gained by studying the charge-transfer processes by which energetic helium-3 ions captured or lost electrons in traversing the [100] axial channel of gold and copper monocrystals.[4] For the low-energy peak $[(dE/dx)_{av}]_n$, the ratio R of doubly to singly charged ions emerging at each energy was close to the ratio observed for a polycrystalline foil (as seen in Fig. V. B6-3); but the ratio R was

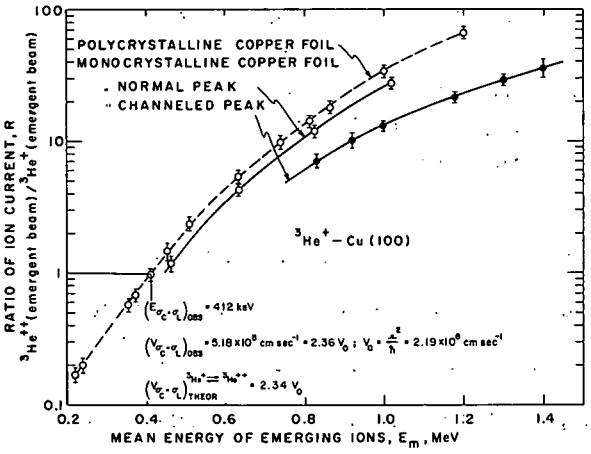

Fig. V. B6-3. The ratio of doubly-ionized to singly-ionized He^3 ions emerging from Cu foils bombarded with singly-charged He^3 ions incident perpendicular to the plane of the foil. The curves show how this ratio depends on the mean energy of the ions as they emerge from the foils. The dashed curve is for a polycrystalline foil. The solid curves are for unchanneled and channeled ions emerging from a monocrystalline foil whose surface is parallel to the (100) planes.

---

[2] N. Bohr, Kgl. Danske Videnskab. Selskab, Mat.-Fys. Medd. 18, 8 (1948).

[3] J. Lindhard and A. Winther, Kgl. Danske Videnskab. Selskab, Mat.-Fys. Medd. 34, 4 (1964).

[4] M. Kaminsky, Bull. Am. Phys. Soc. 13, 1405 (1968).

significantly lower for the high-energy peak characteristic of channeled ions. Thus, ions traversing and escaping through regions of lower electron density (e. g., through the centers of axial channels) have a lower probability of losing electrons than do those traveling at random in the crystal. An extension of such studies (variation of beam direction with respect to channel axis) may permit the mapping of the electron density distribution in channels.

From the scattered information now available, it becomes quite clear that an extension of the present type of studies to heavier ions over a broad velocity range $0.1 \lesssim V_r \lesssim 5.0$ would be highly desirable in order to elucidate the complex nature of the processes involved in the stopping of ions in matter.

While existing energy-loss theories are fairly accurate for the reduced velocity range $V_r > 5.0$ (Bethe-Bloch approximation[5,6]) where the ions are completely stripped of atomic electrons, and for the region $V_r < 0.1$ (approximation of Lindhard et al.[7]) where electron stripping can be neglected and quasi-elastic ion-atom collisions of nearly classical type become important, there are only semi-empirical stopping-power equations for the region $0.1 \leq V_r \leq 2.0$ where ions are usually only partially stripped. Therefore, systematic studies with energetic heavy ions in the velocity range $0.1 < V_r < 5.0$ will provide badly needed information for the development of new and more rigorous theoretical treatments and will open up new frontiers in the field of heavy-ion physics and chemistry (e. g., the production of new materials and devices by ion implantation). Even heavy-ion accelerator technology itself should gain tremendously by such studies by finding, for example, the most efficient way of stripping ions to a given charge for further acceleration.

---

[5] H. Bethe, Ann. Physik 5, 325 (1930).

[6] F. Bloch, Z. Physik 81, 363 (1933); Ann. Physik 16, 285 (1933).

[7] J. Lindhard et al., Kgl. Danske Videnskab. Selskab, Mat-Fys. Medd. 33, Nos. 10 and 14 (1963).

The possibilities are illustrated by the following sets of specific experiments that would be feasible with the propoposed MTC—either the full accelerator or its component TU tandem or cyclotron used alone.

i. Experiments on heavy ions penetrating monocrystalline or polycrystalline solid targets. In studies of the penetration of monocrystalline solids, the availability of heavy ions over a broad range of velocities and atomic numbers will permit one to vary the critical impact parameter b_c over a range extending some orders of magnitude greater and smaller than the typical lattice distance d. In this way it is possible to establish the upper and lower limits of the range of b_c within which the energy loss depends significantly on the angle between the beam direction and the direction of the lattice channel. The strongest orientation dependence would be expected for b_c of the order of the channel dimensions.

Experiments of this type are also well suited to provide a clearer assessment of the relative contributions of nuclear losses and of the various types of electronic losses (e.g., close collisions and distant collisions). In the case of heavier ions, even for energies in the MeV range, nuclear losses can be larger than inelastic losses. However, it would be of special interest to determine to what degree channeling reduces the contributions from both nuclear stopping and close-collision electronic stopping. If the reduction is sufficiently great, measurements on channeled ions may allow the contribution from distant-collision electronic stopping to be studied down to relatively low energies at which the inelastic losses of unchanneled ions (e.g., in polycrystalline targets) normally are completely masked by nuclear stopping. The heavy-ion experiments are especially well suited to obtain more information on the distribution of excited states for partially stripped ions moving through a solid. (The state of any individual penetrating ion changes almost continually since the time between charge-changing collisions is much less than the de-excitation time—e.g., the

half-life for radiative decay.) Such studies would permit a better check of Firsov's model[8] of electronic excitation in quasi-elastic collisions, a model which can be applied to the case of channeled ions. For the lower velocity region, such experiments would also permit a check of Lindhard's model[9] which is based on the Thomas-Fermi interaction between colliding ions and on an estimate of the average electronic excitation over all impact parameters.

It would be of great interest to extend the studies of heavy-ion penetration through monocrystalline targets to higher ion velocities ($V >> V_0 Z^{2/3}$) in order to check whether the dependence of the stopping power on the angle between the beam direction and a crystallographic axis decreases with increasing velocity, as one would expect from a corresponding increase in the value of the critical impact parameter; in the limit of very high energies, the energy loss should become independent of this angle.

Another promising type of experiment would be to extend the present studies of the transverse oscillations (normal to the mean trajectory) of ions traversing planar or axial channels in a monocrystalline target. The rather scarce information available at the moment (e.g., the results of Moak et al.,[10] who studied 60-MeV iodine ions traversing thin Au monocrystalline films) indicates a highly structured energy spectrum of the emerging iodine particles. In part the observed structure could be related to sets of particles that enter the channel at slightly different angles to the channel axis and then traverse the channel with different wavelengths and amplitudes and consequently suffer different energy losses. To what degree differences between the charge distributions of the different sets of particles contribute to the observed structure

---

[8] O. B. Firsov, Soviet Phys.—JETP 9, 1076 (1959).

[9] J. Lindhard, National Academy of Science—National Research Council, Nuclear Science Series Report No. 39, page 1 (1964).

[10] C. D. Moak et al., Phys. Rev. Letters 17, 285 (1966).

has not yet been determined. Further studies along these lines would be expected to yield information on interatomic potentials.

Another experiment on the motion of heavy ions through lattice channels would be a study of the influence of target temperature. For example, in transmission experiments one might expect the stopping power to be proportional to $\exp(2w^2/a^2)$, where w^2 is the mean-square fluctuation of one coordinate of a lattice atom and a is the screening length of the interatomic potential.

Systematic studies of heavy-ion penetration through monocrystalline or polycrystalline solids for the velocity range $V > V_0 Z^{2/3}$ will also be very useful in obtaining better estimates of the inner-shell corrections, which are here defined as all energy-dependent corrections to Bethe's simple stopping-power equation.[5] In the past the importance of the shell corrections was often underestimated and values for the mean ionization energy I were evaluated from experimental data without regard for these corrections. However, because the orbital velocity V_i of a core electron in inner shell i is relativistic in the heavy elements, the condition $V > V_i$ will never be fulfilled and the shell corrections for the heavier elements will not disappear even for $\beta = V^2/c^2 \to 1$. Therefore new experimental results will provide a basis for estimating the errors introduced by the nonrelativistic treatment of the inner-shell electrons of heavy ions, especially since the basic sum rules on which most theoretical treatments rely are not suited for a rigorous relativistic generalization. Furthermore, the accuracy with which the mean ionization energy I can be determined depends in part on the accuracy of the shell corrections. For example, for such heavy elements as uranium it would be very valuable to make measurements at high energies (such that $V > V_0 Z^{2/3}$) in order to obtain an accuracy of better than 2%.

It would also be of interest to study the Thomas-Fermi extensions[11] of Bloch's relation for the mean ionization energy I (the

[11] Reference 9, p. 6.

logarithmic average over the excitation energies weighted by the oscillator strength). With few exceptions the oscillator strengths are not known with sufficient accuracy to calculate values of I, which must therefore be deduced from experimental results such as stopping-power data.

Information about charge-changing phenomena for very heavy ions for energies higher than 1 MeV/nucleon is extremely scarce. The proposed MTC system promises to aid greatly in studies of the basic phenomena and in tests of various practical applications. For example, in accelerator technology the feasibility of Hortig's "pendel accelerator"[12] could be tested more extensively. Systematic studies of heavy-ion channeling in monocrystalline substrates will permit a determination of the degree to which the processes of electron capture and electron loss of the multielectron systems of heavy ions are influenced by axial or planar channeling. The influence of channeling on the attainment of an "equilibrium distribution" of charge states of heavy ions traversing monocrystalline targets of various thickness needs to be studied. It would also be very valuable to study how the "average" charge and the width of the charge-distribution curve for heavy ions varies with velocity, and to determine the velocities at which the average charge will no longer increase with increasing velocity since the K-shell electrons have been removed. It would also be of interest to study the frequency of occurrence of double-ionization processes relative to that of single-ionization processes. In most theoretical analyses of charge-changing data, the later process has been considered as the most likely. Therefore, systematic studies of such ionization processes may lead to a significant modification of the theoretical cross sections for single events.

Studies of the processes involved in the slowing down of very energetic heavy ions in solids would be of special interest near the end of their range, where the predominant stopping process shifts from

[12] G. Hortig, Z. Physik 176, 115 (1963).

electronic to nuclear. Such experiments would also give valuable information on radiation-induced lattice defects near the end of the ion range. For the case of monocrystalline targets, more studies of the "supertail"[13] in the range distribution of channeled heavy ions would be most desirable.

Studies of various secondary phenomena (e.g., sputtering, secondary-electron emission, x-ray emission) connected with the penetration of very energetic heavy ions through solids would also benefit immeasurably from the use of the proposed accelerator system.

The combination of the TU tandem and the variable-energy cyclotron (the full MTC accelerator) would also enable one to produce light charged particles with velocities exceeding about 0.87 c, a velocity at which the kinetic energy of the particles becomes comparable to $m_0 c^2$ and the density effect begins to influence the stopping power appreciably. At these velocities it would also be of interest to test the radiation correction suggested by Tsytovich.[14]

ii. Ion implantation. Another frontier field that undoubtedly will be revolutionized with the aid of the mass- and energy-resolved heavy-ion beams provided by the new MTC facilities is the ion implantation ("doping") of materials. Systematic studies in this field are practically nonexistent, but the scarce information obtained to date (e.g., by Davies et al.[15] at Chalk River and by Mayer[16,17] at the California Institute of Technology) already begins to suggest vast possibilities for production of a new class of materials, surfaces, and devices.

---

[13] For example, J. A. Davies and P. Jespergaard, Can. J. Phys. 44, 1631 (1966).

[14] V. N. Tsytovich, Soviet Phys. —JETP 16, 1260 (1963).

[15] J. A. Davies et al., J. Appl. Phys. 40, 842 (1969).

[16] J. W. Mayer et al., Can. J. Phys. 46, 663 (1968).

[17] J. W. Mayer, review article in "Semiconductor Nuclear Particle Detectors and Circuits," National Academy of Sciences Publication 1593 (1969).

For example, ion implantation adds a new degree of freedom in the doping of semiconducting devices by providing more sharply defined implantation profiles and junction boundaries. Thus junction formation in semiconducting devices is no longer limited to systems having favorable diffusion constants. The result is that, for example, the development of a new class of high-frequency semiconducting devices becomes feasible.

The ion-implantation technique may also provide a new family of solid surfaces with unusual electrical and optical properties. For example, optical materials with zones of different but well-defined index of refraction may be developed.

In the field of surface physics, ion doping provides a new method of producing surfaces with high or low work function. One can also envision the production of new chemical compounds that cannot readily be produced under equilibrium conditions by such other techniques as diffusion. It should be noted that no other known technique permits the doping of chemical additives with comparable chemical purity.

* * *

In conclusion it can be said that the proposed MTC facility will undoubtedly revolutionize the study of charged-particle penetration of matter.

b. Mössbauer Studies

Argonne has been a major center in the development of studies with the Mössbauer effect. For example, the experiments confirming the original discovery were made here in 1959[1]; and interest and effort along these lines has continued since. In the past, experiments employing recoil-free gamma-ray emission and absorption have generally been made with radioactive parents. However, in order to extend this technique to include as many chemical elements as possible, it has been necessary to go to accelerators for sources. The first such experiment at an accelerator, the use of the $K^{39}(d,p)K^{40}$ reaction to make possible Mössbauer studies in potassium, were performed with the 4.0-MeV Van de Graaff at ANL.[2]

i. Production of Mössbauer isotopes in nuclear reactions. It might be expected that the use of nuclear reactions to make short-lived isotopes (whose decay would produce the particular gamma rays desired) would be the most common case. This does not seem to be so, mainly because the usual Mössbauer technique requires milligram amounts of absorber nuclei; and if the isotope under study is too far from the stability line, such nuclei are generally not available. In actual practice, the most useful method seems to be to Coulomb excite stable (and therefore available) nuclei, and to study their de-excitation gamma rays. This presumably will be the dominant way to use accelerators for Mössbauer studies.

Some eight elements have now been studied via Mössbauer-effect measurements with Coulomb-excited sources. Perhaps the most successful are the studies in tungsten; the group at Columbia[3] has made very useful measurements of both nuclear and solid-state properties.

---

[1] L. L. Lee, Jr., L. Meyer-Schützmeister, J. P. Schiffer, and D. Vincent, Phys. Rev. Letters 3, 223 (1959).

[2] S. L. Ruby and R. Holland, Phys. Rev. Letters 14, 591 (1965).

[3] Papers DH10 and DH11 presented at Washington 1969 APS Meeting.

Another successful use of this technique was the study of the second excited state of Ge^{73} at ORNL.[4]

Improvements and extensions of this method to other elements can come about as better accelerators become available. The need is for more energetic particles of higher mass—just the purpose for which the MTC complex is designed. The only concerns are that the Coulomb barrier should not be exceeded and that the multiple-excitation processes do not become too significant. Thus the proposed accelerator should allow a significant increase in the number of usable Mössbauer isotopes, and a large diminution of some of the present hardships in working with the ones presently employed in this fashion.

ii. Recoil implantation. A sub-branch of Mössbauer Coulomb-excitation work involves recoil implantation. In the process of Coulomb excitation by an incident ion of mass m_i and energy E_i, the energy transferred to the recoiling excited nucleus of mass m_r may have any value up to

$$E_r = [4m_i m_r/(m_i + m_r)^2]\, E_i .$$

Thus if the process takes place near the back surface of the target foil, the excited nucleus can be ejected into the vacuum and imbedded in a catcher of arbitrary material—chosen to provide a suitable host environment for the decay of the excited state. The most extensive work of this kind has been that of Sprouse, Kalvius, and Hanna,[5] whose best results were obtained with Fe^{57} Coulomb-excited by 32-MeV oxygen ions.

---

[4] G. Czjzck, J. L. C. Ford, Jr., J. C. Lane, Felix E. Obenshain, and H. H. F. Wegener, Phys. Rev. 174, 331 (1968).

[5] G. M. Kalvius, G. D. Sprouse, and S. S. Hanna, in Hyperfine Structure and Nuclear Radiations (North-Holland Publishing Company, Amsterdam, 1968), p. 686. Included in this volume are the reports of a whole session on implantation studies.

The applicability of recoil implantation is restricted to nuclides whose lifetimes for emission of the Mössbauer γ ray exceeds the time required to traverse the vacuum. For Coulomb excitation by light ions of moderate energies, the recoil nuclei are ejected at velocities $< 10^8$ cm/sec. This is too slow to traverse a vacuum path of $\sim$1 cm during a nuclear lifetime of a few nanoseconds. But with heavy bombarding ions with energies just below the Coulomb barrier, the recoil velocity becomes

$$v_r \approx (10^9 \text{ cm/sec}) \frac{Z_i A_r A_i}{(A_i + A_r)^2} .$$

Thus the use of energetic heavy ions extends the range of applicability to lifetimes an entire order of magnitude shorter than are accessible with light ions. This extension to nanosecond lifetimes clears the way for a number of useful experiments.

Another category of useful experiments is the measurement of the hyperfine magnetic field found at the nucleus of an impurity atom in iron metal. Since this frequently is the largest field that can be found, it may offer the only practicable approach to measurement of such quantities as perturbed angular correlations or nuclear magnetic moments. Such results are also of importance to magnetic theory, in which the disentanglement of various contributions to the total field is a central problem. These measurements may also provide answers to questions about time intervals: How soon after the implanted particle stops in the host material is the magnetic field established?

Mössbauer studies on the implanted atom can also be employed to elucidate problems concerning radiation damage. To date, the experimenters have been mainly interested in "catcher" materials that minimize such effects, and metals have been most used. It will also be useful to employ more rapidly decaying nuclear states, since for some purposes the first 10^{-10} sec after stopping is the most interesting.

iii. Coulomb excitation of projectile nuclei. An unusual possibility is to utilize the Coulomb-excited projectile ions, rather than the target atoms. It is easily shown that the number of Coulomb excitations of bombarding ions is about equal to the number of excitations of target atoms; in fact, for favorable cases the number may be as much as a few per cent of the beam. This would be a copious supply of excited nuclei, which would remain fairly well defined in kinetic energy and direction. Such experiments would complement the more usual "knock-on" technique and would be especially useful for the study of heavy nuclei.

* * *

In conclusion, the heavier and more energetic bombarding ions produced by the MTC will make possible Mössbauer experiments on a number of new nuclei, will facilitate measurements on several already in use (e.g., W^{182} or Ge^{73}), and will make possible a wide and useful class of recoil-implantation experiments.

c. Atomic Spectroscopy by Beam-Foil Excitation

The radiation emitted by excited ions and atoms after passing through thin foils has been used as a spectroscopic source[1] that has yielded many important atomic parameters since its inception five years ago. Indeed this new field of beam-foil spectroscopy, where experimental atomic physics is done with conventional nuclear-physics accelerators, is now a well-established powerful experimental technique in more than 15 laboratories located in the United States, Canada, England, Australia, France, Denmark, and Sweden.

The beam-foil source is obtained with a particle accelerator operating in the keV and MeV range. Work has been done at isotope separator energies[2,3] (10 keV to 150 keV) and with Van de Graaffs (100 keV to 2 MeV with a 2-MeV machine[4,5] and 1 MeV to 6 MeV with a 6-MeV machine[6]). Tandem accelerators[7] have extended the range to 10 and 15 MeV and cyclotron energies to 42 MeV have been used.[8] Every energy region is needed and should be exploited for beam-foil work since many of the parameters that can be measured are highly energy dependent. The experimental arrangement is suggested in Figs.

[1] Proceedings of the Beam-Foil Spectroscopy Conference, November 1967, Tucson, Arizona, edited by Stanley Bashkin (Gordon and Breach, New York, 1968); New Uses for Low-Energy Accelerators, prepared by the committee on Nuclear Science National Radiation Council, National Academy of Science, Washington, D.C., 1968.

[2] W. S. Bickel, Ingmar Bergstrom, Rudolf Buchta, Lennart Lundin, and Indrek Martinson, Phys. Rev. 178, 118 (1969).

[3] W. S. Bickel, I. Martinson, L. Lundin, R. Buchta, J. Bromander, and I. Bergstrom, J. Opt. Soc. Am. (to be published, July 1969).

[4] William S. Bickel and S. Bashkin, Phys. Rev. 162, 12 (1967).

[5] W. S. Bickel, Phys. Rev. 162, 7 (1967).

[6] B. Curnutte, W. S. Bickel, and S. Bashkin (unpublished).

[7] J. A. Jordon, Jr., Ref. 1, paper No. 6.

[8] Research Institute for Physics, Stockholm 50, Sweden (unpublished work with helium).

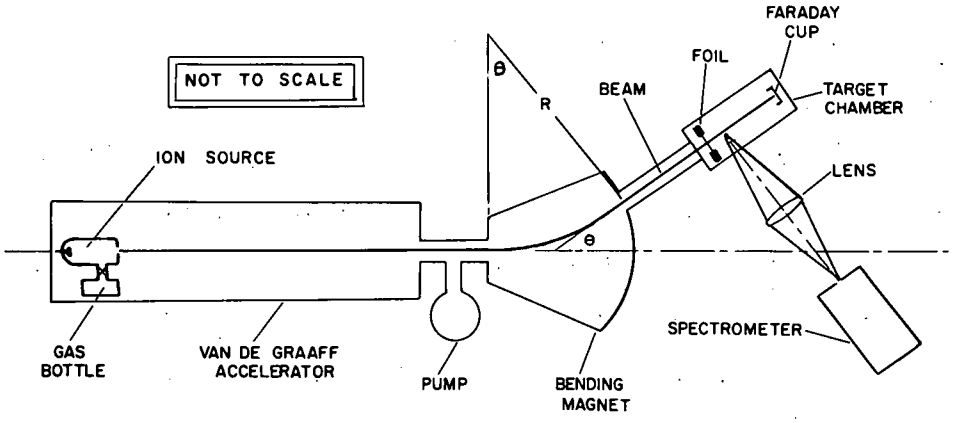

Fig. V. B6-4. A block diagram showing the arrangement of the accelerator, bending magnet, target chamber, and foil for experiments employing the ionic-beam source.

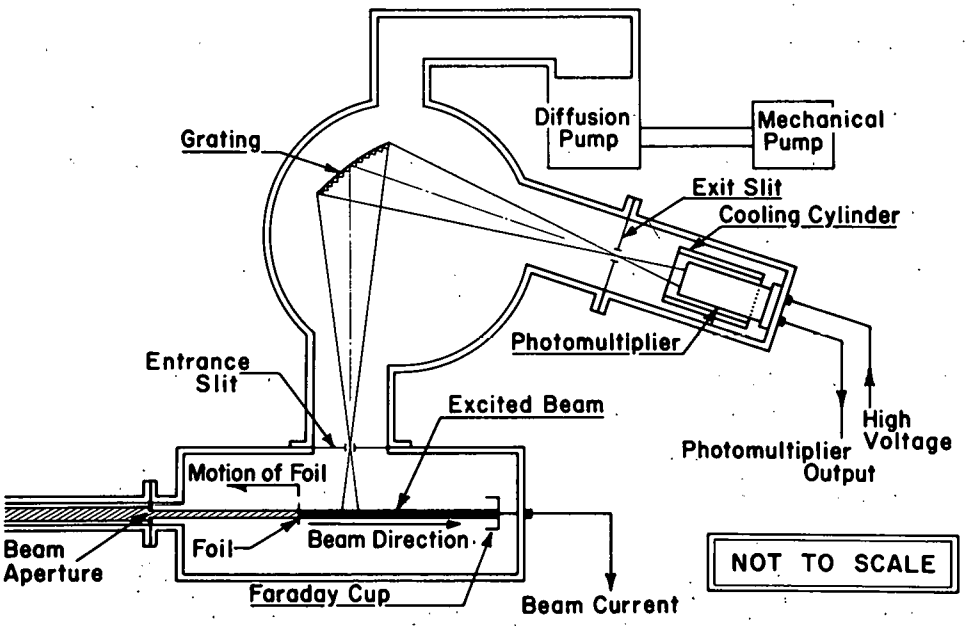

Fig. V. B6-5. An experimental arrangement in which a grating and photomultiplier tube are used to measure intensity variations of the beam. The spectrometer shown here is a Seya-Namioka vacuum-ultraviolet scanning monochrometer. The suppressor plate and grounded shield on the Faraday cup are not shown.

V.B6-4 and 5. Certain properties of the beam-foil source make it useful for studies of the basic properties and structure of atoms.

(i) High degrees of ionization can be obtained and are controlled to a large extent by the incident-particle energy. At low incident-particle energies (10 keV to 150 keV), mostly neutral atoms and singly ionized species appear.[2] From 0.1 to 6 MeV, charge states as high as +9 have been detected.[9] With tandem accelerators U^{+42} has been made,[10] but very little beam-foil work has been done in this energy range.

(ii) The ionic beams exist at room temperature, at ground potential, and in a high vacuum ($< 10^{-5}$ Torr). Therefore external electric and magnetic fields whose values are exactly known can be applied to the beam for Stark[11] and Zeeman[12] effect studies. The atoms and ions radiate in an environment that is free of collisions, electric, magnetic, and radiation fields, and other perturbations. The spectrum is devoid of a continuum or impurity lines. Furthermore, by use of an electric field the beam (which consists of charged ions with a well known velocity) can be separated into its component charge states. Spectral lines emitted by the beam can therefore be assigned unambiguously to a particular charge state.[13] Also isotopically pure beams of a particular charge state can be extracted from the target chamber and directed into another target chamber where interactions

---

[9] W. S. Bickel and Henn Oona, Bull. Am. Phys. Soc. 14, 632 (1969); R. M. Schectman, H. G. Berry, I. Martinson, W. S. Bickel, and S. Bashkin, ibid. 14, 632 (1969).

[10] L. Grodzins, R. Kalish, D. Murnick, R. J. Van de Graaff, F. Chmara, and P. H. Rose, Phys. Letters 24B, 282 (1967).

[11] S. Bashkin, W. S. Bickel, D. Fink, and R. K. Wangsness, Phys. Rev. Letters 15, 284 (1965).

[12] T. Hadeishi, W. S. Bickel, G. Berry, and J. D. Garcia, "Level Crossing in Hydrogen Using Beam-Foil Technique," Phys. Rev. Letters (to be published).

[13] Uwe Fink, J. Opt. Soc. Am. 58, 937 (1968).

between beam particles and atmospheric-type gases, for example, can be studied. This technique has been used to measure electron pickup and ionization cross sections of highly charged species.[14]

(iii) There is virtually no limitation to the kind of element that can be accelerated in preparation for spectroscopic analysis. So far, the elements H, He, Li, Be, B, C, N, O, F, Ne, Al, Si, S, A, Fe, Kr, Xe, Na, Cl, K, I, Br, and U have been accelerated for beam-foil research. It is desirable to have a facility capable of accelerating every element in the periodic table to energies continuously variable up to high values so that atomic properties can be systematically studied along isoelectronic sequences.[15] Of particular importance are studies of the metals and rare earths. However, this program awaits development of more suitable ion sources.

(iv) The radiation emitted by the beams of excited atoms and ions is of greatest importance. Because the beam-foil source exists in a vacuum, studying radiation in the vacuum ultraviolet presents no problems. Therefore all radiations are accessible for study—from the x rays through the infrared. These spectroscopic techniques are now well established and are performed with commercial spectrometers, spectrographs, and detectors. Research with beam-foil-excited spectra has demonstrated the generation of spectral lines that have not been previously reported—even for well-studied elements. For example, over 20 new spectral lines from N have been reported, over 150 from Fe,[16] and in general, over 40% of the spectral lines emitted by S, F,

---

[14] Han Betz, Kansas State University (unpublished work done on a tandem Van de Graaff in Heidelberg, Germany).

[15] W. S. Bickel and S. Bashkin, Phys. Letters 20, 488 (1966); B. Curnutte, W. S. Bickel, Robert Girardeau, and S. Bashkin, Phys. Letters 27A, 680 (1968); W. S. Bickel, R. Girardeau, and S. Bashkin, Phys. Letters 28A, 154 (1968).

[16] W. Whaling, Ref. 1, paper No. 4.

Ne, and O cannot be identified[17] with previously observed lines or with transitions between theoretically predicted energy levels. Many of these lines are attributed to transitions between multiply-excited levels[2] but the research in this area has just begun.

(v) Since all beam particles have the same velocity and the same interaction point (at the foil), the radiation emitted and the spectra obtained are naturally time resolved. At the foil we have N_i^0 atoms formed in excited state i. At a point $x = vt$ downstream from the foil, the number of atoms in excited state i is

$$N_i(t) = N_i^0 \exp(\alpha_i t),$$

where α_i is the mean life of the upper level i.

The intensity of a spectral line with wavelength λ_{if} emitted by the atom when an electron jumps from excited state i to state f is given by

$$I_{if} = N_i(t) A_{if} hc/\lambda_{if},$$

where A_{if} is the spontaneous transition probability per second that the transition $i \rightarrow f$ will occur. By measuring the intensity I(x) as a function of the distance x, we can determine α_i since

$$I_{if}(x) = N_i^0 A_{if} (hc/\lambda_{if}) \exp(-\alpha_i x/v).$$

The quantities A_{if}, α_i, and the mean life τ_i of the state i are related by

$$\alpha_i = \tau_i^{-1} = \sum_f A_{if}.$$

We point out the importance of the beam-foil technique by noting that it allowed the first measurements of the mean lives of multiply ionized emitters (Fig. V.B6-6) with radiations that lie in the vacuum ultraviolet.[18]

---

[17] H. G. Berry, I. Martinson, W. S. Bickel, and S. Bashkin, University of Arizona (unpublished).

[18] S. Bashkin, L. Herous, and J. Shaw, Phys. Letters 13, 229 (1964).

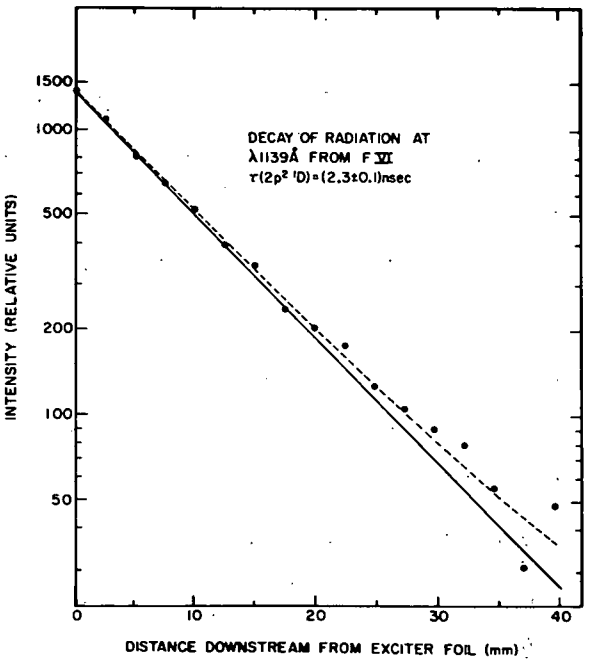

Fig. V.B6-6. Typical intensity decay of a spectral line emitted by the beam-foil source. The dots represent the relative intensity of the λ = 1139 Å radiation from F VI. The curves are best fits to data taken with the experimental arrangement shown in Fig. V.B6-5. The dashed curve is a fit with two exponentials; the straight line is a computer fit to the experimental points after correction for background. The slope of the straight line implies a mean life τ = 2.3 ± 0.1 nsec for the $2p^2\ {}^1D$ level.

Beam-foil spectroscopy at tandem energies (above 6 MeV has yet to be exploited. In addition, the possibility of using electron beams collinear with heavy-ion beams and thus exciting particular atomic resonances has recently been suggested by Morgan and Moore of the University of Texas at Austin.[19] This interesting field of experimentation in atomic physics may well be pursued on the MTC.

---

[19] I. L. Morgan and C. F. Moore, A Study of Atomic Levels in Highly Ionized Light Elements (Center for Nuclear Studies, University of Texas at Austin, 1969), unpublished.

d. Biology and Medicine

Radiological investigations with lower-energy heavy particles of high LET (linear energy transfer = specific energy loss), mainly with the Berkeley and Yale HILAC machines, have established that these particles have some features of unique potential usefulness in medicine. First, the Bragg peak enables a higher dose to be delivered to tissue located within the peak, as compared with the plateau region. Second, the beam can be very precisely localized because of the charged nature of the particles; and third, the reduced effect of oxygen at high LET minimizes the resistance of hypoxic cells in human tumors and thus offers the opportunity for more definitive cancer therapy. These investigations have been confined to radiobiology, because the lack of penetration of the particles available from HILAC machines prohibits clinical studies at depths in tissue.

What is actually required for clinical work is a beam of high-LET particles (50 keV/μ or greater) with a range of 10—20 cm. From Fig. V.B6-7, it is clear that energies of the order of 300 MeV/amu are required for particles having atomic numbers near that of neon. The proposed MTC will approach these requirements. Even with beams of somewhat lesser penetration some animal radiobiology, not now feasible with lower energy particles, will be possible.

The radiobiological experiments to be undertaken on this machine would have three broad objectives: (1) to evaluate the characteristics of the beam for cancer therapy (not necessarily therapy here at ANL), (2) to provide a means of answering specific questions concerning effects dependent upon particle energy or LET (which we expect to arise in the Janus program with neutrons), and (3) to provide more definitive radiobiology with higher LET beams. In (1) the beam must be evaluated for penetration properties, dose rate, field sizes attainable, and its effects upon cells in culture, on animals, and preferably on some animal tumors to establish its relative biological effectiveness, oxygen enhancement ratio, and recovery properties as a basis for radiotherapy. In (2) we anticipate that, in the acute- and chronic-exposure program on

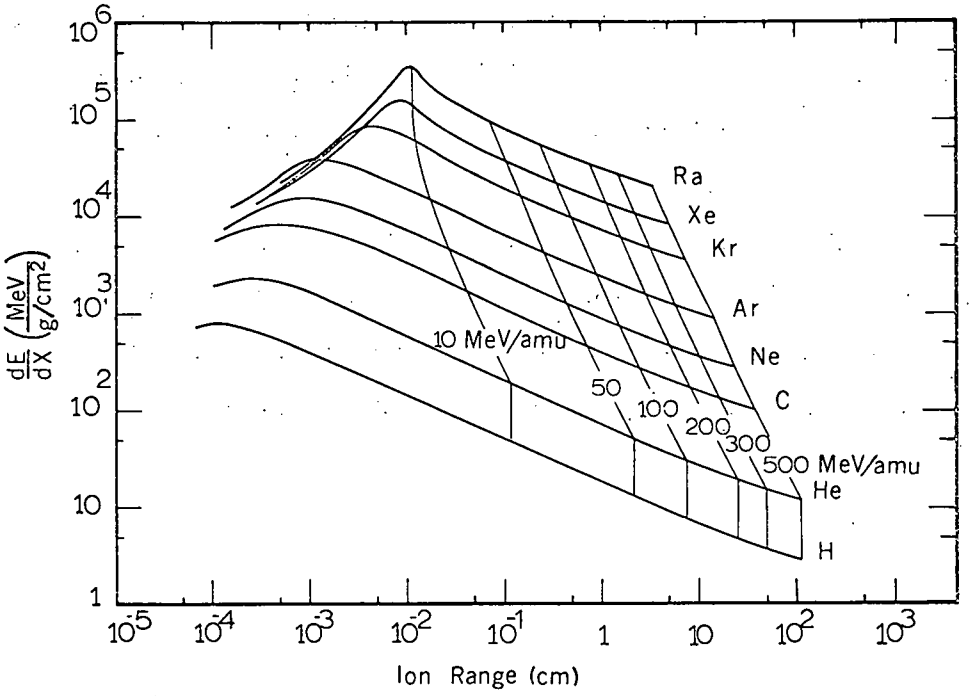

Fig. V.B6-7. Stopping power for heavy ions in water. [From The Omnitron, a Multipurpose Accelerator (Lawrence Radiation Laboratory, Berkeley, 1968, Report No. UCRL-16828, Fig. II-5 facing p. II-19.]

the Janus reactor, various questions relating to the effectiveness of beams of particular LET will arise and that some of these cannot be solved by use of the reactor itself because of the heterogeneous nature of the beam. Some of these questions may be solved with monoenergetic neutrons, others with heavy-particle beams. These include the energy (or LET) dependence of oxygen enhancement ratio, recovery, dose fractionation, RBE (relative biological effectiveness), etc. (3) Radiobiological studies have been extended to the higher LET ranges by the HILAC machines at Berkeley and Yale. Some results on the shape of survival curves in simple cell systems, recovery properties, the oxygen enhancement ratio and its minimum value, and the RBE and the LET at which it occurs shows discrepancies which still require resolution. Furthermore, because of penetration problems it has not been possible to extend these studies to organisms above the cellular level. MTC

will enable animals as large as mice or larger to be irradiated with a penetrating beam of high-LET particles. This would be very desirable since so much other radiobiology has been performed with the mouse as the experimental animal.

The ultimate prospects for better cancer therapy with high-LET particles are being explored via several other, probably less desirable, avenues (viz. fast neutrons and π^- mesons), but the machine proposed here would be very useful for these purposes.

V.C. RESEARCH WITH LIGHT-ION BEAMS

The discussion of research with the proposed accelerator centers of necessity on experiments that are continuations of, or reasonable projections from, what is currently of interest. The hope nevertheless remains that something entirely new and unexpected will be discovered. When proposals for MP-tandem accelerators were being written, little attention was paid to the phenomenon of isobaric-spin analog states. Now that the MP tandems are in operation, analog studies occupy more of their time than any other sort of experiment. A new field of nuclear studies was opened by an unexpected experimental discovery.

In the present state of nuclear physics can we similarly expect the unexpected? The answer is unequivocally yes. Low-energy nuclear physics continues to encounter unexpected and unfamiliar aspects of nuclear behavior. We can cite here the possible existence of super-heavy elements and of other islands of stable nuclei far off the normal stability line. Fission studies, too, have revealed shape isomers—low-lying nuclear states distorted far out of the normal shape of ground-state nuclei. Whole new families of nuclear vibrations—spin-wave excitations, for example—have yet to be seriously investigated. There is therefore every indication that the nucleus can assume shapes and configurations undreamt-of in our present philosophy.

Higher-energy studies of nuclear structure should also yield new sorts of information. Here it is more natural (and more feasible) to probe the correlation structure of ground-state nuclear matter. The quantities of interest are the high-momentum tail of the single-nucleon momentum distribution and the various short-range pair-correlation functions. The significance of these quantities is of course that they reflect the short-range behavior of the nucleon-nucleon interaction—a matter of central importance to the physics of strong interactions. Nothing quantitative is at present known about short-range correlations in nuclei. This situation should change in the next decade as the new field of medium- or intermediate-energy physics develops.

In its higher energy range, the proposed accelerator would play a valuable part in this development.

The present section of the chapter on proposed research deals with experiments that will be possible with the light-ion beams of the TU-tandem and cyclotron components of the proposed accelerator. The term 'light ion' refers here to nucleons, deuterons, tritons, He^3 ions, and α particles. The light-ion beams in question will cover virtually the entire energy range from 0 to 350 MeV (and higher for projectiles other than nucleons). High-quality beams with such a wide range of energy variation will obviously be of enormous value in the study of nuclear structure.

The discussion of light-ion experiments falls into two overlapping parts. The first—Secs. C1 to C5—is mostly concerned with cyclotron experiments in the energy range above 100 MeV. The second—Secs. C5 to C9—centers on lower-energy TU-tandem experiments. The division, however, is not clear-cut. To imply that it is would be to obscure one of the great strengths of the proposed accelerator; for many purposes it will be desirable, and on occasion essential, to use one of the two accelerator components to complement studies carried out with the other.

To conclude, there is need for more precise tests of time-reversal invariance, of parity conservation, and of charge independence in nuclear processes. This is a field of fundamental interest and importance; it was after all in a low-energy nuclear experiment that the nonconservation of parity in weak interactions was discovered. Because of its wide energy range and the variety of the particle beams it can produce, the proposed accelerator is ideally suited to test fundamental conservation laws in nuclear processes.

V.C1. Nucleon-Nucleon Scattering

After nearly three decades of intensive study, several fundamental questions about the nucleon-nucleon interaction have yet to be answered satisfactorily. Knowledge of this interaction is an obvious prerequisite for all nuclear-matter and nuclear-structure calculations. It seems worthwhile, therefore, to consider in some detail experiments that would be feasible with the proposed cyclotron and that could reasonably be expected to yield useful new information about the interaction of two nucleons.

a. Elastic N-N Scattering

The goal of any experimental investigation of scattering is the complete determination of the scattering-amplitude matrix. The difficulty in achieving this goal for N-N scattering can be appreciated from the fact that five separate measurements are necessary to determine the scattering matrix for each isospin state at each angle and at each energy. A complete set of N-N scattering measurements thus must include experiments performed with polarized initial beams and possibly with polarized targets. Because the nuclear interaction is of short range, it is possible to describe the angular dependence of the scattering matrix in terms of a relatively small number of phase shifts so that, at each energy, a set of measurements at a (finite) number of angles is sufficient for the determination of the amplitude matrix.

With one exception, the T=1 phase shifts are reasonably well determined (for energies between 0 and 350 MeV) by existing p-p scattering data. (Detailed sets of experiments are available at the rather widely-spaced beam energies of existing fixed-energy cyclotrons, summarized in Fig. V.C1-1.) The exception[1] is the $^3P_0$ phase shift in

[1] The N-N problem has recently been reviewed by P. S. Signell, in Advances in Nuclear Physics, edited by M. Baranger and E. Vogt (Plenum Press, New York, 1969), Vol. 2.

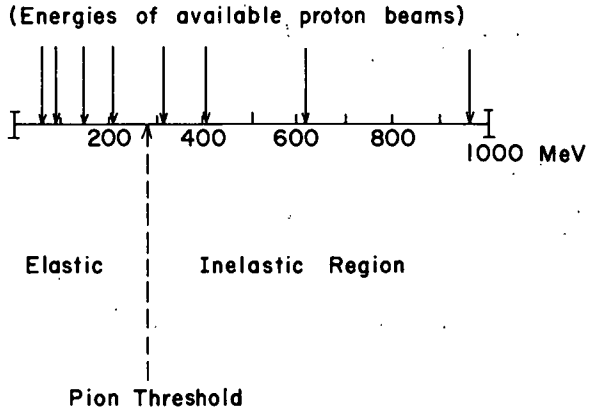

Fig. V.C1-1. Islands of p-p scattering information.

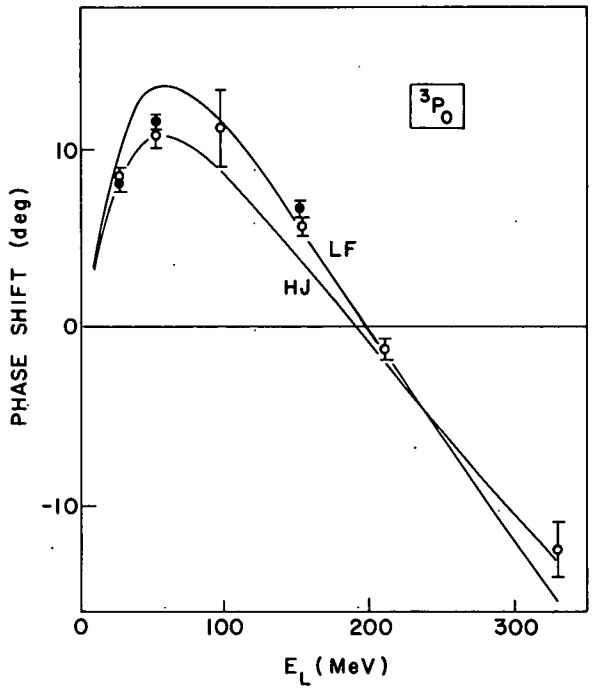

Fig. V.C1-2. The $^3P_0$ p-p phase shift.

the interval 60—120 MeV where $\delta(^3P_0)$ goes through a maximum as shown in Fig. V.C1-2. In order to determine the behavior of $\delta(^3P_0)$ in this interval, it is necessary to make p-p scattering measurements at a number of relatively closely-spaced energies, an experimental program that can reasonably be carried out only with a variable-energy accelerator. This ambiguity in the $^3P_0$ phase shift is significant in nuclear-structure calculations using potentials that are fitted to free N-N data since it occurs at low energy in a partial wave of low relative angular momentum. Furthermore, the energy-dependent behavior of the triplet-P phase shifts is the primary source of information about the short-range spin-orbit force in the T=1 interaction.

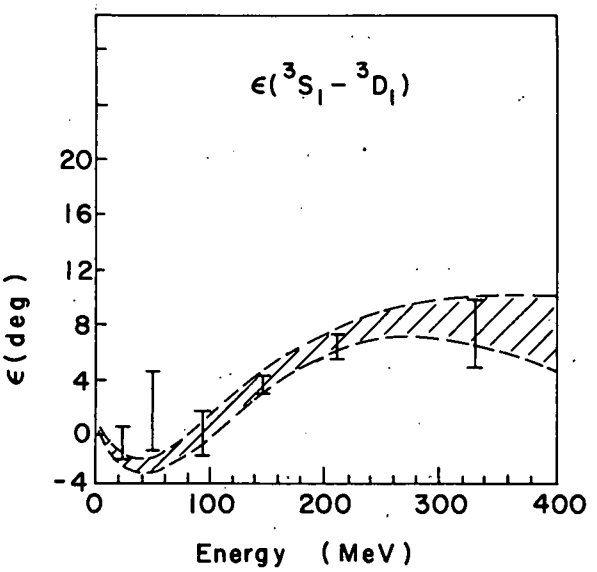

Fig. V.C1-3. The ^3S-^3D mixing parameter.

There are considerably fewer unambiguous p-n scattering data and consequently there is considerably more uncertainty about the T=0 phase shifts. For example, because there exist no p-n data between 210 and 310 MeV, the sign of $\delta(^3S_1)$ above 300 MeV cannot be determined. The value of the $^3S_1$-$^3D_1$ mixing parameter, shown in Fig. V.C1-3, is poorly determined[1] over the entire energy interval. The value of the mixing parameter in the $^3S_1$-$^3D_1$ states (which include the deuteron) is significant for nuclear-matter and nuclear-structure calculations since it is sensitive to the strength of the tensor force in these states. In addition, an accurate determination of the triplet-D phase shifts for energies below ~350 MeV should resolve the present ambiguities concerning the spin-orbit interaction in T=0 states.

Many of the presently available p-n scattering data have been obtained from measurements of proton-deuteron scattering. An impulse approximation is used to relate these measurements to free p-n scattering; this correction is large enough to cast doubt on the reliability of the results. The obvious need for reliable information concerning the T=0 interaction has prompted one well-known experimentalist[2] in the

[2] B. Rose, in Proceedings of the Williamsburg Conference on Intermediate Energy Physics (College of William and Mary, Williamsburg, Virginia, 1966), Vol. II.

field to assert that the time has come to use higher-energy neutron beams extensively in the study of the p-n interaction. This possibility seems to be one of the more interesting experimental programs that could be carried out at the proposed cyclotron. The intensity of the external proton beam from the cyclotron is expected to be of the order of 7×10^{13} particles/sec. If this beam is allowed to strike a thick Al target, neutrons with a continuous spectrum of energies will be produced. The maximum usable energy is ~20 MeV below the energy of the protons. The energy resolution for neutron scattering measurements depends, of course, on the length of the flight path and the length of the neutron burst. It appears likely that a usable neutron beam in the energy range from 150 to 250 MeV with an energy spread (FWHM) of a few percent can be obtained. With a polarized-ion source, a polarized hydrogen target, and a time-of-flight system, it would be realistic to consider not only experiments to determine phase shifts but also experiments designed to give information about such fundamental properties of the nuclear interaction as its charge dependence, its behavior under time-reversal and parity transformations, and its off-energy-shell behavior. Such studies would thus be possible for both p-n and p-p interactions. These possibilities are briefly reviewed below.

b. Charge Dependence

At present there do not exist sufficient n-p scattering measurements at any energy to permit a unique phase-shift analysis. In fact, it is necessary to assume that the T=1 phase shifts have the values obtained from the analysis of p-p scattering and only then to fit the n-p data by adjusting the T=0 phases.

Since both isospin states contribute to the p-n interaction, it is necessary to carry out ten independent measurements at a given energy and angle in order to determine the p-n scattering-amplitude matrix uniquely. Here, however, measurements at the center-of-mass

angles θ and $\pi-\theta$ count as independent so that only five measurements in each quadrant are needed for a complete experiment. With the facility mentioned above, it would be possible to choose among various triple-scattering and correlation measurements to obtain such a complete set of measurements.

To investigate the charge dependence of the nuclear interaction, the n-p and the corresponding p-p measurements should be made at exactly the same energy and, as closely as possible, in the same experimental geometry. Corrections for as many electromagnetic effects as possible should be made before the T=0 phase shifts that describe p-p scattering are compared with the T=0 phases in n-p scattering. Such well-defined separation of specifically nuclear and electromagnetic effects is not possible at small N-N distances where both interactions participate in the determination of the very structure of the nucleon. Observation of departures from charge independence on this level could be important in the study of the structure of the nucleon.

It is obvious that complete n-p measurements at a few energies in the range 100—350 MeV are needed and would be worth the considerable effort that such measurements entail. Whether these measurements can be made with the precision necessary for a meaningful study of the short-range charge-dependence of nuclear forces is a question that can be answered only after initial measurements of this kind have been made.

c. Time-Reversal Invariance and Parity Conservation

Experiments have been suggested[3,4] to test the parity and time-reversal invariance of the N-N interaction, but few such

[3] A. E. Woodruff, Ann. Phys. (N.Y.) 7, 65 (1959).

[4] E. H. Thorndike, Phys. Rev. 138, B586 (1965).

measurements have been carried out.[4,5]

Time-reversal-invariance in p-p scattering implies the inequality $P(\theta) \neq A(\theta)$, where $P(\theta)$ is the polarization that results from the collision of unpolarized particles and $A(\theta)$ is the asymmetry in the scattering of a totally polarized beam by an unpolarized target. Any indication of time-reversal noninvariance in N-N scattering would be most evident at energies at which contributions from coupled states such as $^3P_2$-$^3F_2$ are important; so a measurement of $P(\theta)$ and $A(\theta)$ for p-p scattering at energies $\gtrsim 250$ MeV would be desirable.

The most sensitive tests of parity conservation are indirect ones at relatively low interaction energies. Such measurements are on the borderline of detecting effects of parity nonconservation from weak interactions so that no parity violation in strong interactions is implied. It would be desirable to extend these measurements to higher energy. At the present time, and with present accelerators, however, a direct test of parity conservation in N-N scattering seems unlikely to be successful.

With the proposed facility, many of the suggested measurements (Refs. 3 and 4) to test these transformation properties of the N-N interaction could be carried out to an accuracy that is not presently attainable.

d. p-p Bremsstrahlung

Nuclear-structure and other calculations based on the N-N interaction involve the off-energy-shell behavior of the scattering matrix. The precise determination of all on-shell matrix elements from elastic-scattering data still does not determine completely these off-shell amplitudes. The energy range of interest for nuclear-structure calculations is that below the meson-production threshold; so the only process available for the investigation of off-shell amplitudes is photon

[5] R. Handler, S. C. Wright, L. Pandrom, P. Limon, S. Olsen, and P. Kloeppel, Phys. Rev. Letters 19, 933 (1967).

production. In particular, the reaction $p + p \rightarrow p + p + \gamma$ seems most promising.

The initial indications of large off-shell sensitivity for this process were in error and the task of extracting significant off-shell information from this photon production process has not been carried out. However, accurate measurements of this process have been limited—for the most part—to energies below ~60 MeV, where the expected off-shell contributions are small. Thus a reasonable expectation remains that accurate measurements at energies in the interval 100—300 MeV could yield meaningful information about the off-shell amplitudes—particularly if the protons are detected at angles that emphasize the amplitudes that are far off the energy shell.

Such information is of obvious importance in nuclear-structure calculations that assume an interaction potential in order to extrapolate to the off-shell amplitudes of the N-N interaction. These potentials are far from unique. For example, two potentials (one local and one momentum-dependent) that are Baker transforms[6] of each other give identical on-shell amplitudes but predict different results for processes that involve off-shell amplitudes. N-N bremsstrahlung measurements could provide a basis for a choice among the various potentials that fit on-shell scattering data.

e. Final-State Interactions

At present the only sources of experimental information about n-n scattering are reactions that result in the emission of two neutrons. A systematic program that would measure reactions leading to 2n, 2p, and np in equivalent final states would be of considerable interest. If a reasonable model could be found that gives good agreement with free p-p and n-p parameters, it would be possible to use the model to extract n-n parameters with some degree of confidence.

[6] G. A. Baker, Phys. Rev. 128, 1485 (1962).

f. Summary

The various measurements mentioned above cannot be considered separately. The interpretation of any measurement of the N-N interaction depends on the results of a number of inter-related measurements and calculations that involve not only the N-N system but the three-nucleon and many-nucleon systems as well. Clearly much interesting and important work remains to be done on the basic N-N interaction at energies below the inelastic threshold. There is no doubt that this is a field of study in which the proposed cyclotron could be put to excellent use.

V.C2. Near-Threshold Pion Production

The proposed cyclotron is ideally suited to the study of near-threshold pion production in nucleon-nucleon and in nucleon-nucleus collisions. Such studies are of central importance to nuclear physics for two main reasons. (a) Perhaps the most interesting recent development in strong-interaction physics has been the application of "soft-pion" approximations to express pion-nucleon interaction amplitudes in terms of better-understood weak-interaction currents. Such theories make interesting predictions[1] for low-energy pion production—predictions for which there are as yet no direct experimental tests. (b) Near-threshold pion production on nuclei is sensitive to the high-momentum tail of the single-nucleon momentum distribution. Low-energy nuclear physics tells us nothing about this quantity[2] whose importance to the many-body theory of the nucleus and in distinguishing one sort of nucleon-nucleon interaction potential from another can hardly be over-emphasized.

In this section we summarize the state of experimental and theoretical knowledge of near-threshold pion production—first on nucleons, then on nuclei. It will be clear that there have been so few experiments in this field that studies with the proposed cyclotron can start—to all intents and purposes—with a clean slate.

a. Pion Production in Nucleon-Nucleon Scattering

The possible production reactions in p-p scattering are

$$p + p \rightarrow \begin{cases} \pi^+ + p + n \\ \pi^+ + d \\ \pi^0 + p + p \end{cases} . \qquad (1)$$

---

[1] M. E. Shillaci, R. R. Silbar, and J. E. Young, Phys. Rev. Letters 21, 711 (1968).

[2] K. Gottfried, Ann. Phys. (N.Y.) 21, 29 (1963).

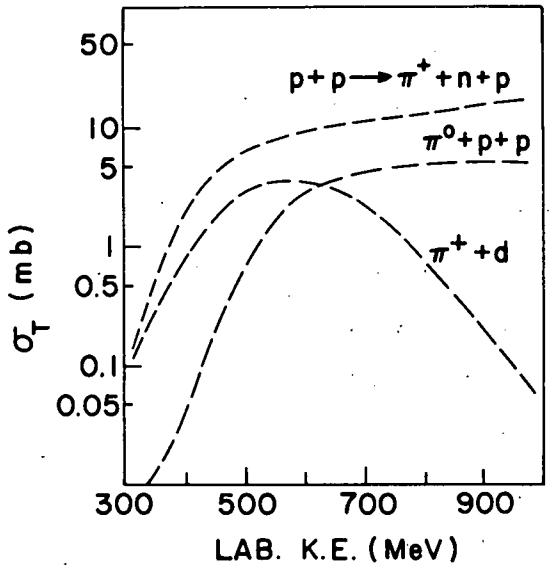

Fig. V.C2-1. Pion-production cross sections.

TABLE V.C2-I. Soft-pion theory of the production reaction $p + p \rightarrow p + n + \pi^+$ near threshold.

E_{lab} (MeV)	Total cross section σ_{tot} (μb)	
	Calc.[a]	Extrapolation of expt.[b]
300	11	10
305	17	17
310	24	28
315	31	42
320	39	66

[a] Reference 1.

[b] Reference 5.

The corresponding total cross sections between the threshold (at 290 MeV) and 1000 MeV are sketched[3] in Fig. V.C2-1. Two points are of particular interest here. First, the cross sections just above threshold are very small—a few microbarns at 300 MeV (Table V.C2-I). Second,

[3] From H. Muirhead, The Physics of Elementary Particles (Pergamon Press, New York, 1965), p. 667.

the fact that the $\pi^+ + d$ cross section up to about 1000 MeV is comparable to that for $\pi^+ + p + n$ is direct evidence of the importance of final-state nucleon-nucleon interactions.

From 350 to 1000 MeV the total production cross sections have been measured with reasonable accuracy and are well understood in terms of Mandelstam's isobar-production model.[4] The dominant process here is

$$p + p \rightarrow N^*(1238) + n \rightarrow (\pi^+ + p) + n. \qquad (2)$$

On the assumption that the p-wave π-nucleon resonance is formed in an s state relative to the neutron, production takes place from the $^1D_2$ partial wave of the two-nucleon system.

In contrast to the situation above 350 MeV, pion production near threshold has not yet been studied carefully. The lowest-energy measurements reported in the literature are those of Rosenfeld[5]—published in 1954—which do not go below 320 MeV. The near-threshold cross sections sketched in Fig. V.C2-1 are Rosenfeld's extrapolations of his data and of data at higher energies. The absence of total-cross-section measurements below 320 MeV and the fact that no experiments have ever been performed on the angular dependence or polarization in pion production, constitute a major opportunity for the proposed accelerator.

There is as yet no generally-accepted theory of near-threshold pion production. Attempts to construct such a theory—which must deal with the weak, nonresonant s-wave pion-nucleon interaction—have followed two different courses. One approach[6] is to use specific nonrelativistic models of the pion-nucleon and nucleon-nucleon interactions and then to devise some approximate means of reducing the three-body problem posed by final-state interactions.

---

[4] S. Mandelstam, Proc. Roy. Soc. (London) A244, 491 (1958).

[5] A. H. Rosenfeld, Phys. Rev. 96, 139 (1954).

[6] D. Koltun and A. Reitan, Phys. Rev. 141, 1413 (1966).

TABLE V.C2-II. Some nuclear production thresholds.

Reaction	Threshold (MeV)
$Be^{9}(p,\pi^{+})Be^{10}$	152
$Al^{27}(p,p\pi^{-})Si^{27}$	151
$Cu^{63}(p,\pi^{0})Zn^{64}$	129
$Cu^{63}(n,\pi^{+})Ni^{64}$	125

The second type of theory involves the application of soft-pion theorems to approximate the pion-nucleon interaction amplitudes by weak-interaction currents. With approximate treatment of the final-state three-body problem, detailed predictions[1] are obtained for pion production. Such approximations are strictly valid only in the limit of zero pion four-momentum so that their application to processes of physical interest involves extrapolation in energy. The results of a recent soft-pion calculation for the reaction $p + p \rightarrow p + n + \pi^{+}$ are compared in Table V.C2-I with Rosenfeld's low-energy extrapolation of the experimental data. While agreement is fairly satisfactory, no definite conclusions are possible without direct measurement of the pertinent production cross sections.

At the upper end of its energy range (290—350 MeV), the proposed cyclotron provides an ideal means of studying pion production in nucleon-nucleon scattering. Such studies are of great interest in their own right since pion production is an important problem in strong-interaction physics. Furthermore, a better understanding of near-threshold production on nucleons is a prerequisite to the extraction of information about nuclear structure from pion production on nuclei.

b. Pion Production in Nucleon-Nucleus Collisions

The threshold for pion production in nucleon-nucleon scattering is at about twice the pion mass since half the laboratory kinetic energy goes into center-of-mass motion. In nucleon-nucleus collisions this kinematic waste of energy does not occur; the threshold for pion production by proton bombardment of nuclei (for $A > 10$) is roughly the pion rest energy (as seen in Table V.C2-II).

When pions are produced on nuclei by protons below 290 MeV, the energy deficit must be supplied by internal nuclear motions. Thus the cross sections below 290 MeV for pion production on nuclei provide a measure of the single-nucleon momentum distribution in the nucleus. The quantity in question here is defined by

$$F(\vec{p}) = \int \left|\psi_0(\vec{p}, \vec{p}_2, \cdots, \vec{p}_A)\right|^2 d^3p_2 \cdots d^3p_A , \qquad (3)$$

where ψ_0 is the momentum-space wave function of the nuclear ground state; the single-nucleon momentum distribution is thus the probability density for finding a nucleon of momentum $\vec{p}$ in the nuclear ground state. The importance of $F(\vec{p})$ in the theory of the nucleus is simply that its high-momentum tail reflects the short-range behavior of the nucleon-nucleon interaction.

Detailed analysis of pion production on nuclei involves four main steps. (a) It is assumed that there is a basic interaction wherein a pion is produced on <u>one</u> of the target nucleons. (b) The propagation of the incident nucleon before the collision and of the ejected nucleon and pion after the collision must be suitably described, possibly by optical-model wave functions. (c) Internal nuclear structure enters through the overlap factor (3). And (d) final-state interactions in three-body production channels must be taken into account.

It is obvious that no quantitative information can be obtained from nuclear pion production until an adequate understanding of the basic production process on nucleons has been achieved. Even then,

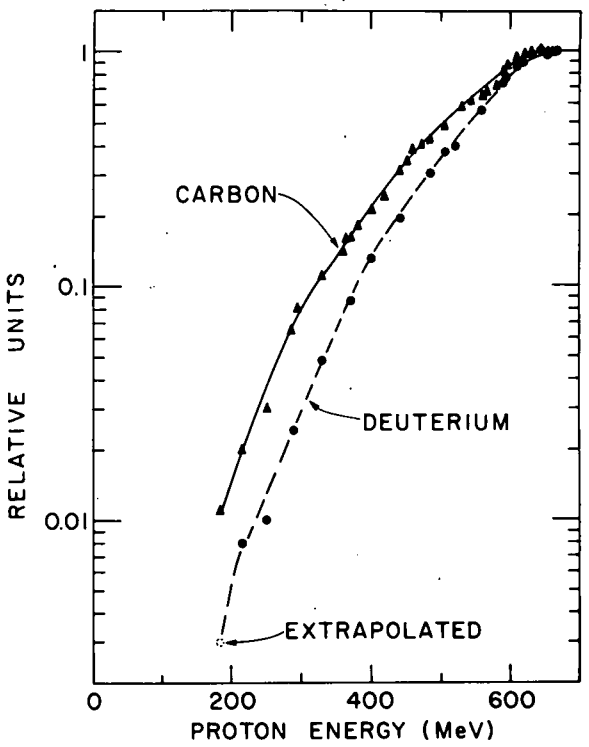

Fig. V.C2-2. Total cross sections for neutral-pion production on carbon and deuterium.

however, formidable difficulties will remain. The final-state three-body problem will still demand attention. Furthermore, particularly in production on very heavy nuclei, the emerging pion will sometimes undergo further interactions, including possible reabsorption.

There have been very few theoretical or experimental studies of near-threshold pion production on nuclei since the publication of the books by Marshak[7] in 1952 and by Bethe and de Hoffmann[8] in 1955. Accordingly, the reviews of nuclear pion production given there are still pertinent.

A more recent experiment of some interest is that of Dunaitsev and Prokoshkin[9] who compared near-threshold production of π^0 on deuterium and carbon. Their results are plotted in Fig. V.C2-2.

---

[7] R. E. Marshak, Meson Physics (McGraw-Hill Book Co., Inc., New York, 1952).

[8] H. A. Bethe and F. de Hoffmann, Mesons and Fields. II. Mesons (Row-Peterson, New York, 1955).

[9] A. F. Dunaitsev and Yu. D. Prokoshkin, Nucl. Phys. 56, 300 (1964); Soviet Phys. —JETP 11, 540 (1960).

Two main points emerge here. The first is that the cross sections below 200 MeV are very small (roughly 300 μb at 175 MeV on C). The second is that the deuterium cross section falls off much more rapidly with decreasing energy, reflecting the greater probability of high nucleon momenta in the heavier C nucleus.

Soft-pion theorems can also be applied to pion production on nuclei.[10] Studies of the accuracy of such approximations for extended nuclear systems are of considerable interest in their own right. It is unlikely, however, that the soft-pion methods in themselves will be a useful means of extracting detailed information about the high-momentum tail of the single-nucleon momentum distribution. The point here is that a real pion can explore the structure of a target nucleus because its Compton wavelength is much smaller than the nuclear radius. In contrast, a zero-mass pion has infinite wavelength and therefore sees the nucleus as a structureless point. Thus all nuclear-structure information will enter through the details of the extrapolation procedure from zero mass. The introduction of specific phenomenological models of the pion-nucleon interaction is probably unavoidable.

To summarize, the study of pion production in nucleon-nucleus collisions is still in its infancy. Such studies promise to yield information on the high-momentum tail of the single-nucleon momentum distribution in nuclei. This quantity is of sufficiently great importance in the many-body theory of the nucleus to repay the extensive experimental and theoretical efforts that are certain to be required.

c. Pion Production by Neutron Bombardment

The availability of a well-collimated neutron beam would make possible studies of pion production in n-p and in neutron-nucleus collisions. The basic ideas here are of course the same as for

---

[10] M. Ericson, A. Figureau, and A. Molinari, Nucl. Phys. B10, 501 (1969).

pion-production by protons. The main new point of interest is that a wide variety of tests of charge independence can be made.[11] Such possibilities exist to a more limited extent if only a proton beam is available. As a particularly simple example, the total production cross sections for π^+, π^-, and π^0 in nucleon bombardment of a T=0 nucleus should be related by

$$\sigma^+ + \sigma^- = 2\sigma^0 . \qquad (4)$$

d. Pion Beams

The existing synchrocyclotrons of the CERN-SREL type have an average internal proton beam current of about 1 μA and produce energy-analyzed pion beams (E_π = 100 MeV, $\Delta E_\pi \approx 10\%$) of the order of 10^5 pions/sec. Since the proposed accelerator will have an external proton beam of approximately 10 μA, it will be possible to obtain a pion beam with a maximum energy of ~50 MeV and an intensity at least comparable to that available from present synchrocyclotrons. This of cource opens up experimental studies of the very wide and little-investigated field of the interactions of low-energy pions with complex nuclei. The interest in probing nuclei with pions is mainly that it is a strongly-interacting elementary particle whose properties are completely different from those of the nucleons which have been the main elementary probes available up to now. Without going into details of possible experimental investigations, one can mention only a few broad categories: absorption, elastic and inelastic interactions, and single and double charge exchange of pions and π-mesic atoms. General theoretical aspects of pion nuclear physics are found in a recent summary by Ericson.[12] A complete description of the experimental situation in the

[11] L. J. Lapidus, Soviet Phys. —JETP 4, 740 (1957).

[12] T. Ericson, in Medium Energy Nuclear Physics with Electron Linear Accelerators, M.I.T. 1967 Summer Study, M.I.T.-2098-No. 470, p. 611.

field has been given by Zupančič.[13] It should be mentioned, finally, that although the proposed accelerator is not designed to accelerate mesons and will not produce pion beams comparable to those from LAMPF, its low-energy beams may nevertheless turn out to be of some value.

e. Conclusion

Near-threshold pion production in nucleon-nucleon and nucleon-nucleus collisions is important both to fundamental strong-interaction physics and to the study of the internal structure of the nucleus. Very few pertinent experiments have so far been carried out. The proposed cyclotron will be of great value in filling this significant gap in present knowledge; in doing so, the upper end (290—350 MeV) of its energy range will be needed.

---

[13] C. Zupančič, in Proceedings of the Second International Conference on High Energy Physics and Nuclear Structure (Weizmann Institute of Science, Rehovoth, 1967).

V.C3. Intermediate-Energy Inelastic Scattering from Nuclei

a. General Features

In inelastic scattering the target nucleus is excited from its ground state to another state, each having definite angular momentum, parity, and isobaric spin. This fact restricts the angular momentum and parity transferred to the nucleus by the scattered projectile and leads to characteristic shapes for the angular distribution of the scattered particles. These characteristic shapes can be used to identify the quantum numbers for the excited states in cases for which these are unknown. An example is shown in Fig. V.C3-1, which gives the

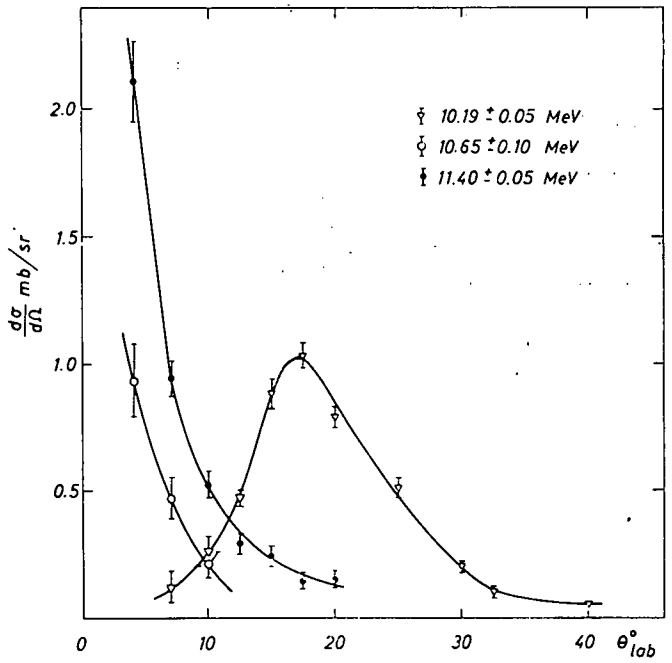

Fig. V.C3-1. Angular distributions for $Si^{28}(p,p')Si^{28*}$, showing two probable M1 excitations and an E3 excitation. [From O. Sundberg et al., Ref. 1, Fig. 11.]

angular distributions for three states in Si^{28} excited by inelastic scattering of 185-MeV protons.[1] Two show the strong forward peak of magnetic-dipole scattering from the 0^+ ground state to 1^+ states, while the third has the form of electric-octopole excitation of a 3^- state.

The restrictions also mean that the matrix elements for inelastic scattering are similar to the matrix elements for

[1] O. Sundberg et al., Nucl. Phys. A101, 481 (1967).

electromagnetic transitions in which a definite multipolarity corresponds to the transfer of a definite angular momentum and parity. Thus a striking feature of inelastic scattering is that the strongly excited states are generally also those that show up strongly in electromagnetic interactions such as gamma decay and inelastic electron scattering. There are differences, but these are strongly masked in the case of heavier projectiles (such as He^3 and He^4) by the contributions to the transition matrix element being localized in the nuclear surface region. If one wants to learn more, the most promising reaction is inelastic scattering of protons.

b. Proton Scattering $A_i(p,p')A_f$

Study of the (p,p') reaction is especially promising, because in the region of 200—300 MeV the technique of theoretical analysis, the distorted-wave impulse approximation[2] (DWIA), should be quite accurate.[3]

(1) The basic approximation is that a single collision between the projectile and a target nucleon is responsible for the change in the state of the nucleus. Furthermore, one assumes that the nucleon-nucleon interaction can be represented by the free nucleon-nucleon scattering amplitude $M(\vec{q})$ at an appropriate momentum transfer $\vec{q}$ given by

$$\vec{q} = \vec{k}_f - \vec{k}_i ,$$

where $\vec{k}_i$ and $\vec{k}_f$ are the initial and final momenta of the incident proton. This is the impulse approximation (IA).

(2) The motion of the projectile before and after the interaction is described by wave functions in an optical potential representing the target. These functions $\chi(\vec{k},\vec{r})$ are the distorted waves (DW).

---

[2] A. Kerman, H. McManus, and R. Thaler, Ann. Phys. (N.Y.) 8, 551 (1959).

[3] R. M. Haybron, M. B. Johnson, and R. J. Metzger, Phys. Rev. 156, 1136 (1967).

(3) The internal nuclear structure of the target states enters through the transition density ρ given by

$$\rho_{if}(\vec{r}) = \int \psi_f^*(\xi, \vec{r})\psi_i(\xi, \vec{r})d\xi,$$

wherein the nuclear wave function overlap is integrated over the coordinates of the other nucleons. The resultant DWIA transition amplitude is then formed by combining these factors, the result being

$$T_{if}(\text{DWIA}) \sim \int d\vec{r}\ \chi_f^{-*}(\vec{k}_f, \vec{r})\ \langle \psi_f | M(\vec{q}) | \psi_i \rangle \chi_i(\vec{k}_i, \vec{r}).$$

The cross section is proportional to the square of this amplitude.

c. Interpretation of Experiments

The free nucleon-nucleon scattering amplitude $M(\vec{q})$ depends on the spin and isospin coordinates of the colliding nucleons as well as on the momentum transfer. Some of these components are much less accurately known than others. The nuclear matrix element $\langle \psi_f | M(\vec{q}) | \psi_i \rangle$ acts as a filter in that transitions with different angular-momentum or isospin changes depend on different components of $M(\vec{q})$. This feature can be utilized in two ways.

(1) For transitions wherein the relevant $M(\vec{q})$ amplitudes are well established in the phenomenological treatment of N-N scattering data, the inelastic proton scattering results provide sensitive tests of the nuclear models that provide the nuclear wave functions.

(2A) In some transitions the nuclear wave functions are quite reliable, such as those wherein the transition density ρ_{if} has been tested by inelastic electron scattering. One can then test whether the ratio of cross sections for two different transitions agrees with the ratio predicted by the different components of $M(\vec{q})$. Another possibility is to test the isospin dependence by studying the scattering of an isospin-changing transition both in (p,p') scattering and in the (p,n) transition to the analog state.

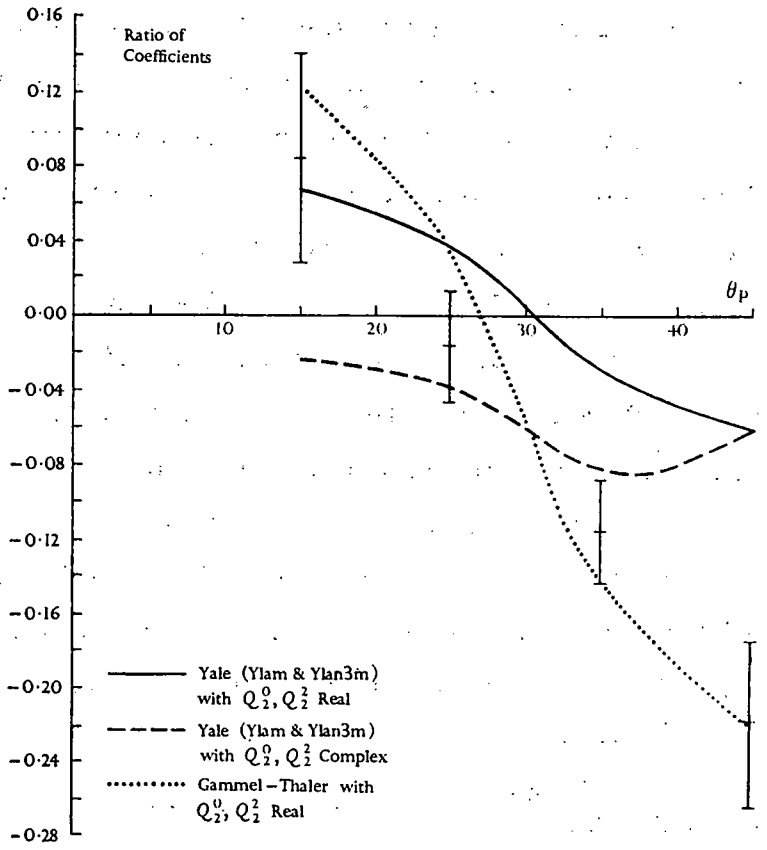

Fig. V.C3-2. The ratio of coefficients of two terms in the gamma-ray angular correlation function following the inelastic scattering of 146-MeV protons from C^{12}, exciting the 2^+ state at 4.43 MeV. The calculated curves result from Yale amplitudes and Gammel-Thaler amplitudes as indicated. [From A. B. Clegg, Ref. 5, Fig. 5 on p. 60.]

(2B) The angular correlation $(p,p'\gamma)$ between the inelastically scattered proton and the resultant nuclear de-excitation gamma ray can be studied with the gamma ray either in the plane of scattering or perpendicular to it. The coefficients in the correlation function are often quite insensitive to the nuclear structure, but can be very sensitive to the amplitudes from $M(\vec{q})$. An example[4] is given in Fig. V.C3-2, where the ratio of two coefficients in the angular-correlation function is plotted as a function of the angle of the emitted proton for $C^{12}(p,p'\gamma)C^{12}$ to the first excited state (2^+). For comparison curves are given which result from two phenomenological fits to the scattering data. In this case, obtained with 146-MeV incident protons, it is uncertain whether the large-angle deviation is due to the amplitudes $M(\vec{q})$ or whether this effect is due to changes in the nuclear amplitude on going off the energy shell (departure from DWIA). Another method of testing the $M(\vec{q})$

[4] D. J. Rowe, A. B. Salmon, and A. B. Clegg, Nucl. Phys. 54, 193 (1964).

amplitudes is to measure the polarization of the inelastically scattered protons.[5] Similar questions arise for large-angle scattering of 146-MeV protons, as occurred in the angular-correlation analysis. Thus by these various means one can test the free nucleon-nucleon scattering amplitudes, particularly parts that are not well established, and perhaps also investigate how these amplitudes change in going off the energy shell.

The chief advantage of doing inelastic proton scattering above 200 MeV is that the DWIA should be a much more reliable and less parameter-ridden reaction theory than the theories at lower energies. A further vital feature is energy resolution sufficient to select excitation of individual states. The proposed resolution width of $\sim$100 keV would enable states in selected heavier nuclei to be isolated and would open a wide field of studies in light nuclei ($A < \sim 50$).

---

[5] A. B. Clegg, High Energy Nuclear Reactions (Clarendon Press, Oxford, 1965).

V.C4. Quasi-Elastic Scattering

If a particle knocks a nucleon out of the nucleus and no further violent interaction occurs between the nucleus and the incident or the two outgoing particles, the process is called quasi-elastic scattering. Such events can be reasonably probable in nuclei because the mean free path of high-energy nucleons in nuclear matter is of the same order of magnitude as the nuclear radius.[1] For such a process to occur, the momentum of the incident nucleon must be high enough that its value of $\lambda\!\!\!^{-}$ (the de Broglie wavelength divided by 2π) is much less than the distance between nucleons in the nucleus. That is, the energy E of the incident nucleon should be ≥ 100 MeV. In order to minimize the effects of absorption, higher energies are desirable. Since the nucleon-nucleon cross section decreases monotonically with increasing energy until $E \approx 200$ MeV (and then remains approximately constant with energy), it is obviously advantageous to have incident nucleons with energy ≥ 200 MeV. At energies of 200 MeV and higher the physical conclusions one can draw from the experimental results are more likely to be valid since the impulse approximation[2] or distorted-wave impulse approximation (DWIA), which is used in the theoretical analysis of the data, is more likely to be valid.

The first experiments that demonstrated quasi-elastic scattering were the 1952 Berkeley results[3] in which light nuclei were bombarded with 340-MeV protons. For the case of free p-p scattering,

---

[1] R. Serber, Phys. Rev. 72, 1114 (1947); M. L. Goldberger, Phys. Rev. 74, 1269 (1948).

[2] G. F. Chew, Phys. Rev. 80, 196 (1950); G. F. Chew and M. L. Goldberger, Phys. Rev. 87, 778 (1952).

[3] O. Chamberlain and E. Segrè, Phys. Rev. 87, 81 (1952); J. B. Cladis, W. N. Hess, and B. J. Moyer, Phys. Rev. 87, 425 (1952).

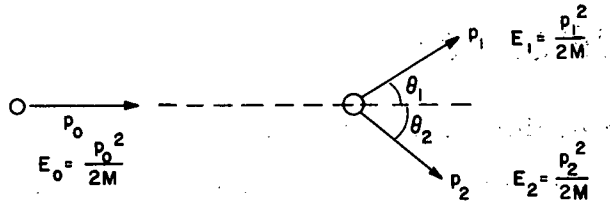

Fig. V.C4-1. Proton-proton scattering.

illustrated in Fig. V.C4-1, conservation of energy and momentum require that

$$\mathcal{P}_0 = \mathcal{P}_1 \cos\theta_1 + \mathcal{P}_2 \cos\theta_2,$$

$$0 = \mathcal{P}_1 \sin\theta_1 - \mathcal{P}_2 \sin\theta_2,$$

$$\mathcal{P}_0^2 = \mathcal{P}_1^2 + \mathcal{P}_2^2 .$$

From these it follows that $\theta_1 + \theta_2$ must be 90° and consequently there must be an angular correlation between the two outgoing particles. The fact that the Berkeley results showed a strong angular correlation between the two outgoing protons when nuclei were bombarded with protons demonstrated clearly the quasi-elastic nature of the knock-out process. The fact that the angular correlation observed in the Berkeley experiments peaked at an angle less than 90° is a manifestation of the fact that protons in the nucleus are bound and have a momentum distribution.

If the shell model has validity, then the cross section for the (p,2p) process should show maxima at energies corresponding to the binding of protons in the various shells. Thus the quasi-elastic scattering process provides an important tool for testing the assumptions that go into one of our most successful nuclear models. If the energies E_i and wave numbers $\vec{k}_i = \vec{\mathcal{P}}_i/\hbar$ of the incident proton, the two outgoing protons, and the recoiling nucleus are denoted by (E_0, k_0), (E_1, k_1), (E_2, k_2), and (E_R, k_R), respectively, then conservation of momentum demands that

$$\vec{k}_0 = \vec{k}_1 + \vec{k}_2 + \vec{k}_R .$$

Furthermore, conservation of energy implies that the binding energy E_s of the knocked-out nucleon is given by

$$E_s = E_0 - E_1 - E_2 - E_R .$$

Since in the quasi-elastic scattering process[4] there is assumed to be no interaction between the incoming proton and the recoiling nucleus and since the target nucleus was initially at rest in the laboratory coordinate system, it follows that the recoil momentum of the final nucleus must be the negative of the momentum of the struck nucleon. That is,

$$\vec{k}_R = -\vec{k},$$

where $\vec{k}$ is the momentum of the struck nucleon in the target nucleus before collision. For the case in which the struck nucleon is in an s state, there is a finite probability that $\vec{k} = 0$, in fact, the most probable situation in this case corresponds to the struck nucleon being at rest. On the other hand, if the angular momentum of the knocked-out nucleon is not zero, there is vanishing probability that $\vec{k} = 0$. Thus the quasi-elastic scattering process should not only be able to detect shell structure, it should also be capable of telling whether or not the knocked-out nucleon had $\ell = 0$.

If one considers the situation in which the incident proton and the two outgoing nucleons lie in a plane and further if (1) the scattering angles θ_1 and θ_2 of Fig. V.C4-1 are equal and (2) the energies of the two outgoing particles are equal, then for the case in which $\vec{k} = \vec{k}_R = 0$, conservation of energy and momentum tells us that

$$2 \cos \theta_1 = (E_0 / E_1)^{1/2}.$$

Thus for $E_1 = \frac{1}{2}(E_0 - E_R)$, the cross section should either peak or have a minimum at this value of θ_1 depending on whether the knocked-out particle had $\ell = 0$ or $\ell \neq 0$.

---

[4] For a detailed derivation of the cross section for this reaction see, for example, Th. A. J. Maris, Nucl. Phys. 9, 577 (1958/59); G. Jacob and Th. A. J. Maris, Rev. Mod. Phys. 38, 121 (1966).

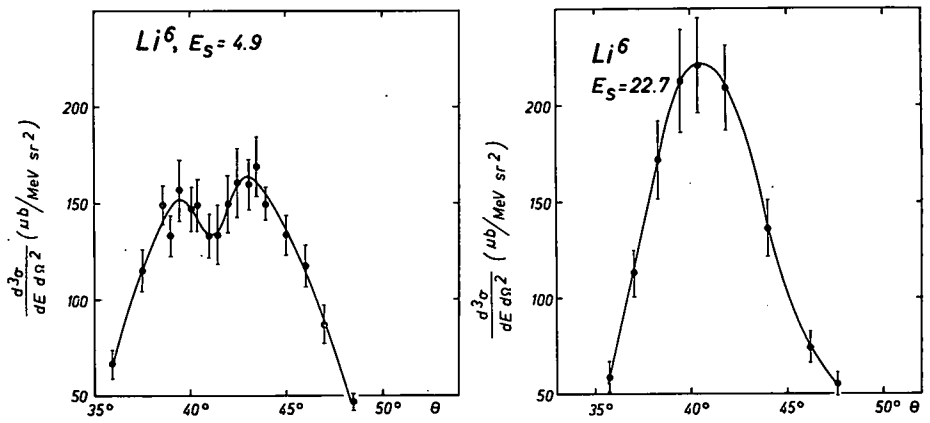

Fig. V.C4-2. Differential cross section as a function of scattering angle for the symmetric coplanar (p,2p) reaction. (From Tyrén et al., Ref. 5.)

The experiments[5] done at the Enrico Fermi Institute of the University of Chicago, where the 460-MeV proton beam was used to bombard Li^6, clearly illustrate the above considerations. In Fig. V.C4-2(b) the experimental cross section for binding energy $E_s = 22.7$ MeV shows a distinct peak near $\theta_1 = 45^\circ$. (The peak position θ_1 would be exactly 45° in the case $E_1 = E_2$ and $E_s = 0$.) For the case $E_s = 4.9$ MeV Fig. V.C4-2(a) shows two peaks with a valley between. Since the initial momentum of the struck nucleon can be directed either toward or away from the incident proton, there will be two peaks corresponding to the fact that for $\ell \neq 0$ the momentum distribution of the knocked-out nucleon has its maximum value for $k \neq 0$, the valley between corresponding to $k = 0$. The knocked-out proton with $E_s = 4.9$ MeV therefore had $\ell \neq 0$. Both these results are, of course, consistent with the fact that the uppermost nucleons in Li^6 are in the 1p state whereas the core nucleons (those in the He^4 core) are in the 1s level.

In addition to this study at the University of Chicago, there have been measurements of quasi-elastic scattering at several other laboratories. Table V.C4-I, taken mainly from the review article of

---

[5] H. Tyrén, S. Kullander, O. Sundberg, R. Ramachandran, P. Isacsson, and T. Berggren, Nucl. Phys. 79, 321 (1966).

TABLE V.C4-I. Experiments on quasi-elastic scattering.

Laboratory	E_0 (MeV)	Energy detector	Beam energy spread (MeV)	Nuclides studied
Uppsala	185	Range telescopes	4.4	Li^7, Be^9, B^{11}, C^{12}, N^{14}, O^{16}
Harwell	150	Total-absorption plastic scintillators	6	Li^7, Be^9, C^{12}, O^{16}, and preliminary results on d-s nuclei
Orsay	155	Total-absorption NaI scintillators	5	Li^6, Li^7, Be^9, B^{10}, B^{11}, C^{12}
Harvard	160	Total-absorption NaI scintillators	7 to 4	Li^7, Be^9, B^{11}, C^{12}, O^{16}, F^{19}, Sc^{45}, V^{51}, Co^{59}, Ni^{58}
Uppsala	185	Range telescopes	3	Li^6, Li^7, Be^9, B^{10}, B^{11}, Mg^{24}, Al^{27}, Si^{28}, P^{31}, Ca^{40}
Chicago	460	Magnetic spectrometers with 4 + 4 plastic telescopes	3	He^4, Li^6, Li^7, Be^9, B^{10}, B^{11}, C^{12}, N^{14}, O^{16}, Al^{27}, Si^{28}, P^{31}, S^{32}, A^{40}, Ca^{40}, V^{51}, Co^{59}
Orsay	155	Magnetic spectrometers with 30 + 8 plastic detectors	4 to 2	Li^6, Ca^{40}, Sc^{45}, Ti^{48}, V^{51}, Cr^{52}, Mn^{55}, Fe^{56}, Ni^{58}, As^{75}
Orsay, Oxford	50—130	Bubble chambers		C^{12}
Orsay	155	Magnetic spectrometers with spark chambers	1.6	H^2, Li^7, Be^9, Na^{23}
Liverpool	387		5	C^{12}, Ca^{40}, Co^{59}, Sn^{120}
MTC	360		$\leq 10^{-3}$ E	

Berggren and Tyrén,[6] lists the various laboratories at which experiments have been carried out. The incident proton energy, energy resolution width, and nuclides studied are also listed in this table. The last line of the table gives the characteristics of the proposed MTC. As far as energy is concerned, only the synchrocyclotrons at the University of Chicago and the University of Liverpool have energies as great as that of the proposed machine. However, neither of these machines has an energy resolution as good as that expected with MTC. In order to be able to differentiate between various single-particle states in the uppermost nuclear shell, it will be important to have this narrow spread in beam energy as well as a particle-detecting system of good resolution for all but the very light nuclei.

The following experiments, which the new MTC facility would make feasible, would be of the highest value in increasing our knowledge of nuclei.

a. (p,2p) Experiments

With the (p,2p) experiments it should be possible to explore the innermost shells in nuclei. This will be particularly interesting since nuclear-structure Hartree-Fock calculations have recently become available[7] and these indicate that for heavy nuclei the innermost 1s shell should be bound by approximately 100 MeV. For light nuclei, the University of Chicago results[5] for C^{12} and O^{16} (Table V.C4-II) are in excellent agreement with the theoretical predictions. The recent results obtained by the Liverpool group,[8] who used a 387-MeV proton beam with an energy spread of 5 MeV to bombard heavier nuclei, are also shown in this table. Only a broad peak corresponding to the innermost levels

---

[6] T. Berggren and H. Tyrén, Ann. Rev. Nucl. Sci. 16, 153 (1966).

[7] R. M. Tarbutton and K. T. R. Davies, Nucl. Phys. A120, 1 (1968).

[8] N. James, University of Liverpool (preprint).

TABLE V.C4-II. Binding energies (MeV) in the 1s and the $1p_{3/2}$ and $1p_{1/2}$ shells in several nuclei.

Shell	Mode of observation	C^{12}	O^{16}	Ca^{40}	Co^{59}	Ni^{56}	Sr^{88}	As^{75}	Sn^{120}
1s	(p,2p)	34 ± 2	44	50 ± 12	56 ± 6				53 ± 8
	(e,e'p)	34		77 ± 14				111 ± 12	
	Theory		44.4	65.1		69.6	77.7		
$1p_{3/2}$	(p,2p)	14.7	18.4 12.1	33 ± 6	43 ± 5				44 ± 7
	(e,e'p)	16		~33				58 ± 14	
$1p_{1/2}$	Theory		17.4 11.7	38.9 34.8		45.9	56.7 56.2		

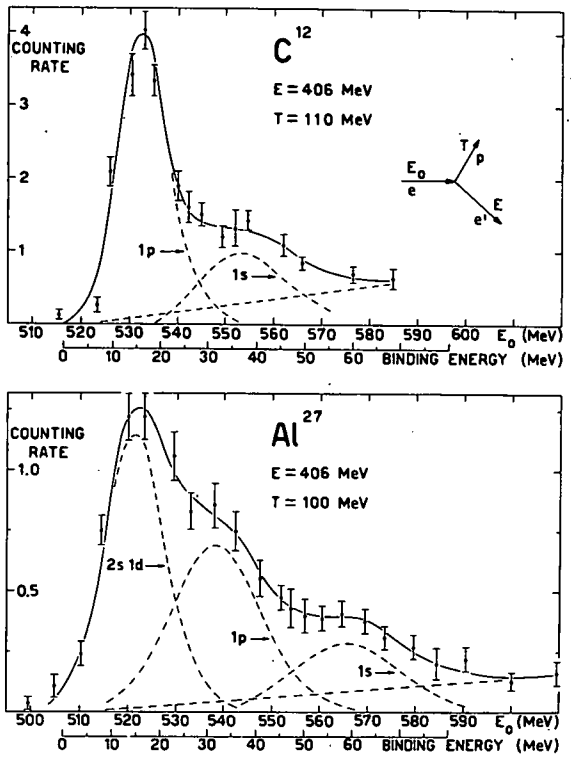

Fig. V. C4-3. Electron-proton coincidence counting rate per 10^{11} equivalent quanta at 550 MeV as a function of the incident energy. The dashed lines indicate the contributions of the various shells and the background. (From Amaldi et al., Ref. 9.)

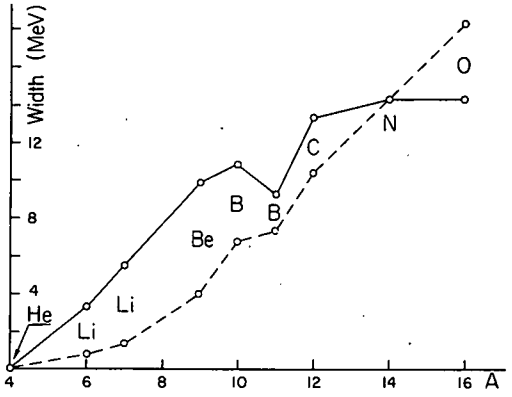

Fig. V. C4-4. Experimental (full line) and estimated (dotted line) widths of the 1s hole states for the 1p shell nuclei. (From Jacob and Maris, Ref. 4.)

is obtained, the center of the peak being uncertain to ±12 MeV in the case of Ca^{40}. The results of the Liverpool group are barely compatible with the Frascatti (e,e'p) results[9] which are also shown in this table and in Fig. V. C4-3. It should be pointed out that a rather large natural width will be associated with the deep-lying nuclear states. Figure V. C4-4 illustrates the increase in the natural width of the 1s state as one goes through the 1p shell.

[9] U. Amaldi, Jr., G. Campos Venuti, G. Cortellessa, C. Fronterotta, A. Reale, P. Salvadori, and P. Hillman, Phys. Rev. Letters 13, 341 (1964).

Turning now to a comparison with theory, we see that both the (p,2p) and the (e,e'p) results could be consistent with theory in Ca^{40}. However, for heavier nuclei theory and experiment tend to disagree. In fact the Sn^{120} results do not show the theoretically anticipated increase in 1s-shell binding. (In Hartree-Fock theory the binding energy of the 1s shell increases with increasing A and is predicted to be slightly greater than 100 MeV for Pb^{208}.) Thus it is imperative that better and more extensive measurements be made on heavier nuclei to test the calculations that are now being made.

So far the (p,2p) experiments that have been done have concentrated on the symmetric coplanar case (i.e., the case in which the incident proton and the two outgoing protons all lie in a plane and both the angles θ_1 and θ_2 and the energies E_1 and E_2 are equal. On the other hand, symmetric noncoplanar experiments have been shown to be sensitive to deformations[10] of the target nucleus. Such studies might shed light on the spatial distribution of bound protons in nonspherical nuclei. This is particularly interesting since despite the spectacular success of the rotational model, the microscopic structure of rotations of deformed nuclei is not well understood. Symmetric noncoplanar experiments probably require proton energies of 300 MeV or more since the more noncoplanar the arrangement, the more energy is lost to the recoiling nucleus.

b. (α,2α) and (α,α'p) Experiments

Since α particles are strongly absorbed, the use of these particles in knock-out experiments should lead to a more effective localization of the reaction in the surface region and hence provide a better tool for the study of the nuclear surface than does the (p,2p) reaction. In fact, Jackson[11] has estimated that in the Ca^{40}(α,α'p)

[10] D. F. Jackson, Phys. Rev. 155, 1065 (1967).

[11] D. F. Jackson, Nucl. Phys. A123, 273 (1969).

reaction initiated by 160-MeV alphas the major contribution to the cross section should come from events occurring at a radius of 6—8 fm—in other words at least 2 fm beyond the radius R_0 at which the nucleon density distribution is half its maximum value. Although the major contribution of the (p,2p) reaction does come from the region beyond R_0, it is less selective in exploring the tail of the nucleon distribution. Thus if one wishes to study the nucleon distribution at large distances from the center of the nucleus, the (α,α'p) and (p,pα) reactions are an invaluable aid.

If there is a high degree of α-particle clustering in the nuclear surface, as has often been suggested,[12] then the (α,2α) and (p,pα) reactions should be a useful means of detecting this clustering. If the impulse approximation is valid, it has been shown[13] that the cross section for the (α,2α) reaction should be proportional to that for the free (α,α) scattering and to the probability that the α particle exists in the nuclear surface. In order to extract reliable information about this probability, it is not only necessary that the DWIA be valid, but also it is necessary to carry out the experiment under such conditions that other factors coming into the theoretical expression for the cross section can be reliably estimated. Jackson[13] suggests that the best arrangement for studying the α clustering in the surface is to do a nonsymmetric coplanar experiment, i.e., to detect one of the alphas near the forward direction and the other (with just enough energy to overcome the Coulomb barrier) at a large scattering angle (near 90°). When the second α fulfills this condition, it is clear that it must have been produced at the nuclear surface; otherwise it could not have escaped from the nucleus. To carry out such experiments and to draw reliable conclusions requires an incident α beam with an energy of at least 300 MeV.

[12] See, for example, D. H. Wilkinson, in Proceedings of the Rutherford Jubilee International Conference, Manchester, 1961, edited by J. B. Birks (Heywood and Co., Ltd., London, 1961), p. 339.

[13] D. F. Jackson, Nuovo Cimento B40, 109 (1965).

The estimates of Guavin, Lefort, and Tarrago[14] show that owing to the height of the Coulomb barrier, α-particle knockout will be small when alphas of less than 150 MeV bombard heavy nuclei. Thus in order to study this process through the entire periodic table, alpha-particle energies in the 300-MeV range are required.

c. (α,αp), (α,αn), and (p,pn) Reactions

In the past fifteen years there has been a controversy as to whether or not there is a neutron "halo" around the nucleus. Johnson and Teller[15] gave a classical argument as to why such a halo should exist. Although the protons in the nucleus repel each other, if one plots the neutron and proton shell-model potentials, as shown in Fig. V.C4-5, it is apparent that the classical turning point of the proton motion lies inside that of the neutron motion if the two particles are bound by the same energy.

Recent high-energy data[16] concerning a possible neutron halo comes from the stopping of K^- mesons in emulsion. In the ratio

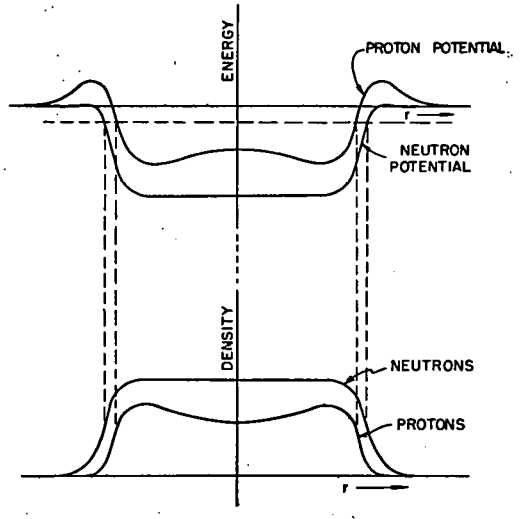

Fig. V.C4-5. Potentials and densities for protons and neutrons inside the nucleus. (From Johnson and Teller, Ref. 15.)

[14] H. Gauvin, M. Lefort, and X. Tarrago, Nucl. Phys. 39, 447 (1962).

[15] M. H. Johnson and E. Teller, Phys. Rev. 93, 357 (1954).

[16] D. H. Davies, S. P. Lovell, M. Csejthey-Barth, J. Sacton, and G. Schorochoff, Nucl. Phys. B1, 434 (1967); E. H. S. Burhop, Nucl. Phys. B1, 438 (1967); S. P. Lovell and G. Schorochoff, Nucl. Phys. B5, 381 (1968).

$$R = \frac{\text{Number of } \Sigma^- \text{ with no visible } \pi}{\text{Number of } (\Sigma^+ + \pi^-) \text{ events} + \text{Number of } (\Sigma^- + \pi^+) \text{ events}},$$

the numerator should involve only absorption of the K^- by neutrons and the processes considered in the denominator should correspond to absorption of the K^- by a proton. This ratio is examined for the heavy (silver and bromine) and light (carbon, nitrogen, and oxygen) emulsion nuclei. The ratio

$$R_{heavy}/R_{light} = 5.0^{+1.2}_{-0.8}$$

indicates a large neutron halo around heavy nuclei.

Further evidence for a neutron halo appears in the spectra of K-mesic atoms.[17] The disappearance of transitions with increasing atomic number is evidence that the K-meson orbit overlaps the nuclear distribution sufficiently for the K meson to undergo a strong reaction. The pattern of missing transitions vs atomic number indicates that the K mesons are interacting at larger radii than are expected from the measured nuclear charge distribution. This implies a neutral halo.

Information on nuclear radii can also be extracted from energies of isobaric analog states. Recent calculations[18] for Pb^{208} indicate an rms neutron radius which is very nearly the same as the rms proton radius. However, the tail of the neutron wave function extends considerably farther than that for the proton and consistency with the K^- results seems to be preserved. In other words, the neutron halo seen by the K^- experiments is a very wispy one.

It is, of course, extremely important to check this fundamental nuclear property in yet another way. The proposed MTC will

---

[17] C. Wiegand, International Conference on Hypernuclear Physics, Argonne National Laboratory, 5-7 May 1969, ANL-HEP Report (to be published).

[18] J. P. Schiffer, Second International Conference on Nuclear Isospin, Asilomar, 13-15 March 1969 (University of California, Lawrence Radiation Laboratory, Berkeley, to be published).

give us the opportunity to do this by measuring either the ratio $(\alpha, \alpha n)/(\alpha, \alpha p)$ or $(p, pn)/(p, 2p)$.

d. $(p, p\alpha)$ Experiments

Newton, Salmon, and Clegg[19] have examined the reaction products from bombardment of Ca^{40} with 150-MeV protons. In one of their runs they observed gamma rays in coincidence with the scattered proton at various energies. In particular, they found that when the proton experienced an energy loss of about 9 MeV, a 2-MeV gamma ray began to appear in coincidence with the proton. If an intact α particle is knocked out of Ca^{40}, the ground state of A^{36} should be produced when the proton energy loss exceeds 7.04 MeV. Thus their experimental finding indicated that the 2^+ state in A^{36} at 1.97 MeV was being appreciably populated via the $Ca^{40}(p, p\alpha)A^{36}$ reaction. Since these experimenters deduced the existence of this reaction through the observation of the gamma rays involved, it was impossible for them to determine whether or not the ground state of A^{36} was appreciably populated in the reaction.

With the narrow energy spread available with MTC and with a high-resolution detecting system, it will be possible to use the $(p, p\alpha)$ reaction to investigate the population of various states of rotational bands in deformed even-even nuclei. The 1d2s-shell experiments, in which both the neutrons and the protons are filling the same Nilsson level, should be extremely interesting since one would expect states in which the two protons and two neutrons are knocked out of the same orbital would show up strongly in this reaction. An experimental test of the validity of this conjecture would be most valuable.

---

[19] D. Newton, G. L. Salmon, and A. B. Clegg, Nucl. Phys. 82, 499 (1966).

e. (p,3p) Reaction

In some exploratory work done at Harwell,[20] the reaction $Ca^{40}(p,3p)A^{38}$ was observed when Ca^{40} was bombarded by 150-MeV protons. The states of A^{38} observed in this reaction were the same as those seen in the $K^{39}(p,2p)A^{38}$ experiment and had much the same relative cross sections. This suggests that an important contribution to the (p,3p) reaction mechanism producing low-lying nuclear states is a process in which the incident proton makes two separate collisions with different protons in the target nucleus and ejects both of them.

It is clear that with the proposed MTC facility processes such as this can be studied in detail. Extensive on-line computing facilities, not available to the Harwell and other earlier groups, will greatly facilitate the study of multiparticle-breakup reactions. The results obtained will provide a foundation on which theories governing the reactions can be formulated.

---

[20] D. Newton, G. L. Salmon, and A. B. Clegg, Nucl. Phys. 82, 513 (1966).

V.C5. Elastic Scattering from Nuclei

Extensive experimental data have been reported on the elastic scattering of nucleons and of the lighter nuclei by heavier nuclei, particularly in the low-energy range. Many of these data have been interpreted in terms of scattering from a purely phenomonological optical potential. For nucleon scattering this potential model can be justified theoretically in considerable detail. On the other hand, it is probable that the simple optical-model concept will prove to be inadequate for the description of the scattering of composite particles. It is convenient, therefore, to discuss these processes separately.

a. Nucleon Scattering

Recently it has been suggested[1] that the real parts of the optical potential that describes nucleon-nucleus scattering can be related to the neutron and proton distributions in the nucleus and to components of the N-N force. This relation is particularly simple in the 20—40 MeV region, in which the dominant contribution to the scattering comes from the surface region of the nucleus where the nucleon separations are relatively large. There is a need for accurate and comprehensive data in this energy region. Such data could be obtained with the XTU tandem with a polarized source.

Because of the relatively long wavelength of the projectile and the dominance of the surface contribution, only macroscopic information about a limited region of the nucleus can be obtained from nucleon-nucleus scattering at energies below 40 MeV. Higher-energy measurements are needed to provide more detailed information, particularly about the interior of the nucleus. At energies $\geq$ 200 MeV the nucleon wavelength becomes less than the range of nonlocality of the nucleon-nucleus interaction and this reduces the importance of absorptive effects. This is of

---

[1] G. W. Greenlees, G. J. Pyle, and Y. C. Tang, Phys. Rev. 171, 1115 (1968).

theoretical interest since the representation of absorptive events is largely phenomenological and hence not entirely satisfactory. To date, however, the available nucleon-nucleus scattering data above 50 MeV are insufficient for a meaningful analysis.

As the optical-model potential assumes more physical content, it becomes increasingly important to resolve ambiguities in the parametrization of the potential as well as in the values of the parameters. Such ambiguities exist—at least in part—because the relevant experimental data are incomplete. There is an obvious need for a facility, such as the one proposed, that would make possible a systematic investigation of the nucleon-nucleus interaction for representative nuclei over a wide range of energies.

b. Scattering of Composite Particles by Heavier Nuclei

An optical-model potential is frequently used to analyze measurements of the elastic scattering of deuterons, H^3, He^3, and He^4 by complex nuclei—the composite projectile being treated as a point particle with no internal structure. Serious questions about the validity of this approximation increase the difficulty of interpreting and evaluating the parameters that define the potential. Nevertheless, this simple potential model has been applied successfully to the analysis of elastic scattering and, in addition, has proved to be extremely useful in the analysis of direct-reaction data. In fact, there is evidence[2] that discrete ambiguities in the potential for a given interaction channel can often be resolved when measurements of reactions that involve that channel are compared with the corresponding direct-reaction calculations. Thus the model seems to merit further investigation both with regard to the specification of the potential and to possible modifications that would enhance its theoretical respectability.

---

[2] L. L. Lee, J. P. Schiffer, B. Zeidman, G. R. Satchler, R. M. Drisko, and R. H. Bassel, Phys. Rev. 138, B68 (1965).

c. Deuteron Scattering

There appears to be a marked difference between the values of the potential parameters that describe elastic deuteron scattering at 82 MeV (Ref. 3) and those obtained at 22 MeV (Ref. 4) and lower energies. It is not clear whether this indicates a basic inadequacy in the potential model or simply an ambiguity in the parametrization of the potential. Basic questions about the parametrization have not been answered definitely. For example, it is not clear whether surface or volume absorption predominates in the scattering of deuterons at energies below 100 MeV.

For incident energies greater than ~150 MeV, existing deuteron scattering data can be fitted by an impulse approximation that uses free N-N scattering amplitudes—provided that the simultaneous scattering of both the neutron and proton in the deuteron is taken into account.[5] Obviously considerable worthwhile information about the deuteron-nucleus interaction could be obtained from a systematic investigation of deuteron scattering in the energy interval from ~20 MeV to ~300 MeV.

d. Scattering of H^3 and He^3

There is also considerable uncertainty about the potentials that describe H^3 and He^3 scattering. For example, the magnitude and shape of the spin-orbit interaction in these channels are completely undetermined. Since highly polarized beams of energetic tritons can be obtained from t-α scattering; the investigation of this term in the triton channel should be reasonably straightforward.

---

[3] H. Doubre, D. Roger, M. Arditi, L. Bembot, N. Frascaira, J. P. Garron, and M. Rion (unpublished).

[4] D. Dehnhard and J. L. Yntema, Phys. Rev. 160, 964 (1967).

[5] M. L. Rustgi, Phys. Letters B24, 229 (1967).

Recent measurements[6] of the elastic scattering of He^3 indicate that the potential in this channel does not depend appreciably on the incident energy. Since the potentials in other channels show a marked energy dependence, this is an unexpected and, as yet, an unexplained result. It would be of interest to determine whether this behavior persists when the incident energy is increased to the 100-MeV/nucleon region.

e. Scattering of He^4

Analyses of experiments in the region of 50-MeV bombarding energy indicate that the important part of the α-nucleus interaction occurs at separation distances at which the nuclear density has fallen to less than ~0.1 of its central value. In this region the internucleon separation is larger than the α particle and it seems reasonable to describe the interaction in terms of an effective potential. Thus α-scattering data are expected to complement nuclear-matter-distribution studies using proton beams.

f. Scattering of Light Nuclei by Light Nuclei

Experimental studies of the interaction of light nuclear systems and resonating-group calculations for these systems have proved to be mutually beneficial. For example, experimental differential cross sections for the scattering of He^3 by He^4 have been explained[7] reasonably well by this type of calculation.

Resonating-group calculations for light systems use a nucleon-nucleon interaction potential that contains exchange terms and describes N-N scattering reasonably well. The Pauli principle is taken into account by employing wave functions that are completely antisymmetric. Thus far, only the elastic channel is included in these calculations

---

[6] B. W. Ridley, T. W. Conlon, and T. H. Braid, Bull. Am. Phys. Soc. 13, 117 (1968).

[7] R. E. Brown and Y. C. Tang, Phys. Rev. 176, 1235 (1968).

so that effects of reactions on the elastic channel are neglected. Furthermore, a central N-N potential has been used so that neither spin-orbit splitting nor polarization effects are predicted by the theory. An attempt is now being made to include a phenomenological imaginary term and a spin-orbit term in these calculations.

The effect of reactions on the elastic channel becomes more important as the energy is increased from low to intermediate values. A systematic experimental study over a wide energy range would be useful to determine whether a phenomenological imaginary potential can accurately account for these effects. Eventually, of course, important reaction channels will have to be included explicitly in the theory. To facilitate this, an experimental study of the partial reaction cross sections would be desirable.

Effective real local potentials for the interaction of light nuclear systems can be derived[7] from resonating-group calculations. These are not usually as simple as the optical-model potentials that are used to describe scattering by heavier nuclei. Instead they behave in many respects like the phenomenological potentials that have been found for very light systems. Such behavior includes an odd-even effect in the ℓ dependence of the potential and a repulsive core in some ℓ states. Sufficient elastic scattering data for a range of energies, projectiles, and target types should contribute to our understanding of the relation between the potentials needed to describe the interaction of very light systems and those used for the description of scattering from heavier nuclei.

Because exchange forces are included in the N-N potential and the Pauli principle is taken into account exactly, the resonating-group calculations predict a variety of "exchange" effects that are free of the usual ad hoc assumptions. For example, a neutron-exchange resonance in $He^3 + He^4$ scattering is predicted to cause a large back-angle peak in the differential cross section. A complete experimental study of this prediction would be possible with a He^3 beam of variable energy over a range of energies up to ~100 MeV.

V.C6. Charge-Exchange Scattering and Analog States

a. The (p,n) Reaction to Isobaric Analog States

The charge-exchange (p,n) reaction has led to one of the most interesting discoveries in modern nuclear physics, the isobaric analog state. This reaction is best described as a quasi-elastic process in which an isospin flip occurs, changing the incident proton into a neutron and replacing the target state by its analog.

The original discovery of isobaric analog states was made by Anderson and Wong[1] in their study of the (p,n) reaction on a variety of targets. The description of the reaction mechanism in terms of a charge-exchange scattering arising from an optical potential of the form

$$V = V_0 + (V_1/A)\,\vec{t}\cdot\vec{T}$$

was first offered by Lane.[2] Here $\vec{t}$ and $\vec{T}$ are the isospin of the scattered nucleon and of the target, respectively. Analysis of experiments in terms of such potentials indicates[3] that $V_1 \approx 24$ MeV. However, our understanding of the detailed behavior of V_1 is very limited, and systematic data over a wide region of incident-proton energy would clearly be of great interest. This will bear not only on our understanding of V_1 but on the whole question of isospin in complex nuclei.

Closely related to the charge-exchange quasi-elastic process is charge-exchange inelastic scattering (to excited analog states) and the charge-exchange reaction to antianalogs (states of the same configuration as the analog state but one lower in isospin). Both these reactions are of considerable interest for a better understanding of both the reaction mechanism and nuclear structure. Our present knowledge of such processes is minimal.

---

[1] J. D. Anderson and C. Wong, Phys. Rev. Letters 7, 250 (1961).

[2] A. M. Lane, Phys. Rev. Letters 8, 171 (1962); Nucl. Phys. 35, 676 (1962).

[3] J. M. Soper, in Isobaric Spin in Nuclear Physics, edited by J. D. Fox and D. Robson (Academic Press, Inc., New York, 1966), p. 565.

b. Isobaric Analog States

Subsequent to the discovery of isobaric analog states in heavy nuclei excited by the (p,n) reaction, it was discovered that such states were also excited as strong resonances in the excitation functions for proton scattering.[4] With such resonances, not only states corresponding to ground states are seen but also analogs of excited states. This discovery has opened the way to many new experiments which have been extremely fruitful in the past few years. Such experiments have been carried out at many laboratories; in particular, Argonne has made a significant contribution to the field.

The isospin formalism was originally introduced by Wigner[5] and later French and Macfarlane[6] developed detailed sum rules relevant to average spectroscopic quantities in nuclear reactions. What had not been realized until the discovery of analog states was that isospin, as a quantum number, was remarkably good in heavy nuclei. Previous authors had always claimed that since the proton is charged and the neutron not, isospin cannot be a good quantum number in heavy nuclei, where Coulomb forces are large compared to nuclear forces. Today we understand this apparent paradox in terms of the long range of the Coulomb force relative to nuclear forces; this makes Coulomb forces much less important in perturbing the isospin symmetry than the strengths would imply.[7]

c. Isospin-Allowed Resonances

In proton-induced reactions, the observed resonances are the analogs of the low-lying states formed by adding a neutron to

[4] J. D. Fox, C. F. Moore, and D. Robson, Phys. Rev. Letters 12, 198 (1964).

[5] E. P. Wigner, Phys. Rev. 51, 106 (1937).

[6] J. B. French and M. H. Macfarlane, Nucl. Phys. 26, 168 (1961).

[7] D. Robson, Phys. Rev. 137B, 535 (1965).

the target [e.g., in a (d,p) reaction]. The analysis of the elastic resonances gives spectroscopic information similar to that from the direct-transfer reactions. The analysis of resonances in inelastic scattering gives the experimental equivalent of direct-transfer reactions on excited target states.

The proton decay of the isobaric analog state results in two classes of inelastic scattering resonances. In one, particle-hole states in the final nucleus are excited.[8] Excitation of such states occurs at the same incident energies as for good single-particle resonances. In the second, collective states of the target are excited.[9] The associated resonances occur most strongly at outgoing proton energies which correspond to single-particle analog resonances. Thus their observation requires higher energies than those necessary to observe resonances in the elastic channel.

At the present time, ground-state analog resonances have been observed in proton reactions on nuclei up to the region of the Pb isotopes for the range of incident energies currently available with tandem Van de Graaffs ($\leq$ 20 MeV). Even for the heaviest stable target, U^{238}, the ground-state analog resonance of U^{239} in Np^{239} should be observed at an incident proton energy of only 15.8 MeV.

For heavy nuclei the availability of proton beams of energy greater than 20 MeV could, however, permit studies of core-excited states by inelastic scattering to be extended to considerably higher excitation energies. In addition, since resonance effects are exhibited in reactions in which the proton energy in either channel is that of a single-particle analog,[10] one can explore reactions other than inelastic

---

[8] C. F. Moore, L. J. Parish, P. von Brentano, and S. A. A. Zaidi, Phys. Letters 22, 616 (1966).

[9] D. L. Allan, G. A. Jones, G. C. Morrison, R. B. Taylor, and R. B. Weinberg, Phys. Letters 17, 56 (1965).

[10] N. Stein, J. P. Coffin, C. A. Whitten, Jr., and D. A. Bromley, Phys. Rev. Letters 21, 1456 (1968).

scattering in which the proton is in the exit channel.

One question that seems rather interesting would be the extent to which the isobaric analogs of states of, say, U^{238} would decay by fission. This bears on the extent of isospin mixing in the fission channel. There are several ways of doing such an experiment. The (p,nf) reaction would be one of them; searching for resonance effects in proton-induced fission may be another.

d. Isospin-Forbidden Resonances

An isospin-forbidden analog resonance is one in which the formation of the analog state in a proton-induced reaction is forbidden by conservation of isobaric spin. Resonances that involve $\Delta T = 1$ forbiddenness have been extensively studied in light nuclei for both $T=\frac{3}{2}$ and $T=2$ analog states at Argonne, Rutgers, and Stanford. These states have also been observed as states in the residual nucleus from allowed reactions, such as (He^3,n) and (p,t) reactions,[11,12] and also from delayed proton emitters.[13] However, the (p,p) and (p,γ) resonance experiments give the best information on location and the only information on width. The positions of such states provide a check on the isobaric mass formulae; the elastic proton width of the resonance measures the isospin impurity.

In general the only allowed decay of such forbidden resonances is by γ emission. However, in some cases (namely those in which the target nucleus has a low-lying T_z+1 state) inelastic proton emission is also allowed. In such a case the resonance may be considerably broader. At present $\Delta T=1$ forbidden resonances have not been observed in nuclei heavier than Ca.

---

[11] E. Adelberger and A. B. McDonald, Phys. Letters 24B, 270 (1967).

[12] G. T. Garvey, J. Cerny, and R. H. Pehl, Phys. Rev. Letters 12, 726 (1964).

[13] P. L. Reeder, A. M. Poskanzer, R. A. Esterlund, and R. McPherson, Phys. Rev. 147, 781 (1966).

The pursuit of these studies of forbidden resonances to heavier nuclei will be feasible with the high energies available from the TU tandem. In addition, it may be possible to look for resonances of a higher order of forbiddenness, e.g., $\Delta T = 2$. In these resonances, to first order, only the iso-tensor part of the Coulomb perturbation can produce the necessary mixing. Of course, in all cases of isospin-forbidden resonances their observation depends on their being narrow; this depends on whether all possible decay channels are isospin forbidden. Jänecke[14] has systematically examined the location of higher isobaric analog states in odd-A and even-A nuclei.

In the search for T-forbidden resonances on heavier nuclei, the study of allowed two-nucleon-transfer reactions leading to the analog state may be necessary to locate the position of the expected resonance, just as for the lighter nuclei. Then the observed charged-particle decay of these states can be used to determine the relative decay width in the various channels and hence the feasibility of the resonance study. A good example is the recent study[15] of the $Si^{30}(p,t)Si^{28}$ reaction to the T=2 state in Si^{28}. Measurements of the subsequent charged-particle decay in coincidence with the prompt triton has shown that $\Gamma_\alpha >> \Gamma_p$ for the lowest T=2 state. This has been confirmed by the fact that the resonance is observed[16] only in the $Mg^{24}(\alpha,\alpha)$ reaction. An extension of such coincidence studies to heavier nuclei will be possible with the TU tandem.

At the higher energies available on the TU, one will not be limited to two-nucleon transfer. The recent observation of

---

[14] J. Jänecke, Proceedings of the Third International Conference on Atomic Masses (University of Manitoba Press, Winnipeg, 1967), p. 583.

[15] R. L. McGrath, J. C. Hardy, and J. Cerny, Phys. Letters 27B, 443 (1968).

[16] K. A. Snover, D. W. Heikkinen, F. Riess, H. M. Kuan, and S. S. Hanna, Phys. Rev. Letters 22, 239 (1969).

three-nucleon[17] and four-nucleon[18] transfers greatly increases the possibilities for extending such studies to higher analog states. In addition, there is the possibility of using more exotic reactions to populate higher analog states. For example, reactions such as (Li^7, He^6) can lead to $\Delta T=\frac{3}{2}$ transitions. Similarly, double-charge-exchange reactions such as (O^{18}, Ne^{18}) can lead to $\Delta T=2$ transitions. With the intense heavy-ion beams of high energy available from the TU tandem, it will be feasible to look for such reactions.

It may be that in heavier nuclei the observation of the subsequent delayed protons $\bar{p}$ from the analog states produced in the proton decay of the isospin-forbidden resonance will be the only way to locate the positions of these states. From the known systematics of the analog states, the $\bar{p}$ energy can be precisely determined. Such studies are an obvious extension of the original allowed $(p, n\bar{p})$ studies[19] on such nuclei. As in the latter reaction, the decay proton can be distinguished from other direct protons in the spectrum in that its energy remains constant although the incident energy changes. Thus an increase in the yield of decay protons would characterize the position of the forbidden resonance.

e. The (He^3, t) Reaction

This process is basically the same as the (p,n) reaction and the same selection rules apply. It has the advantage that with an emerging charged particle, much better energy resolution is possible. This allows one to determine the Coulomb energy difference between parent and analog states with very good accuracy. Such experiments

[17] J. Cerny, R. H. Pehl, F. S. Goulding, and D. A. Landis, Phys. Rev. Letters 13, 726 (1964).

[18] J. Cerny, S. W. Casper, G. W. Butler, R. H. Pehl, F. S. Goulding, D. A. Landis, and C. Détraz, Phys. Rev. Letters 16, 469 (1966).

[19] A. I. Yavin, R. A. Hoffswell, L. H. Jones, and T. M. Noweir, Phys. Rev. Letters 16, 1049 (1966).

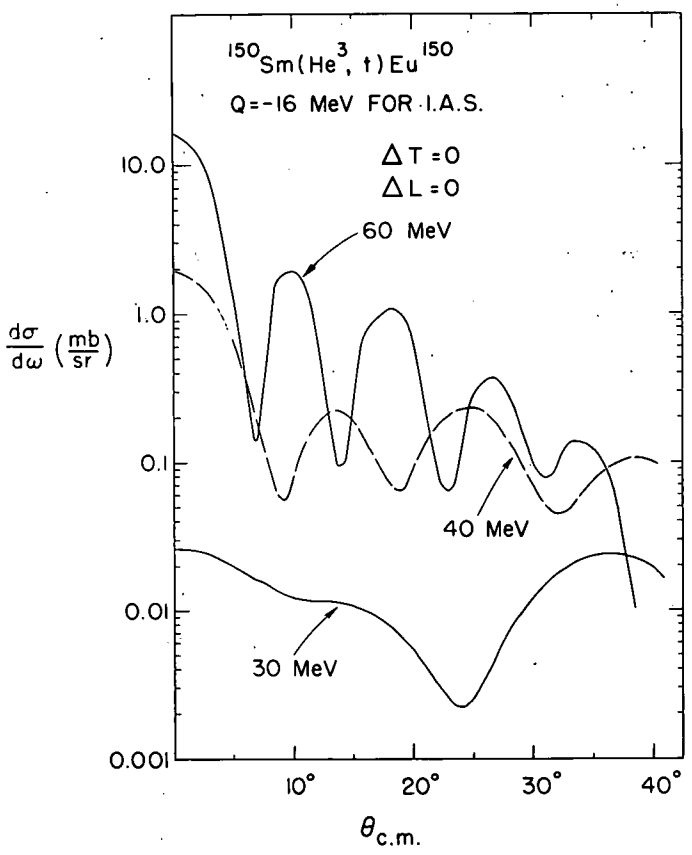

Fig. V.C6-1. DWBA calculations of the angular distributions of the (He^3,t) reaction on Sm^{150} for several incident energies.

have been carried out at Minnesota, Los Alamos, and Argonne. Precise knowledge of this difference has become of increasing interest recently in work at Argonne, Princeton, and elsewhere, since it carries important and unique information on nuclear radii. In heavy nuclei, the (He^3,t) reaction leading to the highly excited isobaric analog states is very strongly inhibited by the negative Q value (typically -16 MeV for the Sm isotopes) and the higher Coulomb barrier.

DWBA calculations have been performed to obtain an estimate of the differential cross sections of the (He^3,t) reaction on Sm^{150} at three different energies: at E(He^3) = 30 MeV (the highest energy obtainable with the existing MP tandem accelerators), at 40 MeV, and at 60 MeV. While the cross section at 30 MeV is only 27 μb/sr at 0°, it increases 70-fold to 1.9 mb/sr at 40 MeV, and by another factor of 8 to 15 mb/sr at 60 MeV, as is shown in Fig. V.C6-1. Thus the higher energies available with the proposed accelerator should greatly facilitate these studies.

f. Antianalog States

French and Macfarlane have pointed out[20] that such states would not be populated in a charge-exchange reaction if the two-body interaction were just of the form $\vec{\tau}_1 \cdot \vec{\tau}_2$. However, it is now clear that the interaction is not that simple and hence one might expect that the antianalogs will be populated. Such states are extremely interesting and our present knowledge of them is minimal. There is some indication that the (He^3,t) and (p,n) reactions indeed favor such states and other states of closely related configurations[21] but it remains to be seen whether this is, in fact, so. A study of the (p,n) charge-exchange process to analog and antianalog states simultaneously would be extremely interesting. The study of the (He^3,t) reaction on heavy nuclei with good resolution could be of very great importance in locating and understanding such states; the required He^3 energies would probably be >40 MeV

g. Relationship Between the (p,n) Reactions and β Decay

Nucleon-charge-exchange reactions can be treated as similar to elastic and inelastic scattering of nucleons. In particular, if the impulse approximation is valid, the monopole part of the interaction (s-wave transfer) is directly proportional to the matrix element[22] for allowed β decay. Hence the study of high-energy (≥ 150 MeV) s-wave charge exchange between isobaric analog states allows a test of the current-algebra relations in which nucleons are considered as elementary particles.

---

[20] J. B. French and M. H. Macfarlane, Phys. Letters 2, 255 (1962).

[21] H. Ohnuma, J. R. Erskine, J. A. Nolen, Jr., J. P. Schiffer, and N. Williams, Proceedings of the International Conference on Nuclear Structure, Tokyo, 1967, Suppl. J. Phys. Soc. Japan 24, 647 (1968).

[22] W. M. Visscher and R. A. Ferrell, Phys. Rev. 107, 781 (1957).

V.C7. Nucleon-Transfer Reactions

This section concerns direct reactions wherein a single nucleon or a cluster of nucleons is transferred from one nuclear state to another. Reactions of this sort include stripping reactions [(d,p), (He^3,d), (α,p), etc.] wherein the transferred cluster is captured by the target and pickup reactions [(p,d), (p,t), (d,α), etc.] wherein the transferred cluster is removed from the target. Summed strengths for transfer reactions measure the extent to which clusters in the same internal state as the transferred cluster are already present in the target ground state; angular distributions yield information about the angular-momentum quantum numbers of the transferred cluster; relative cross sections to different final states reveal the relationship of these final states to the target ground state.

Studies of this sort began around 1950 with single-nucleon transfer—more precisely, with deuteron stripping reactions. Many of the pioneering experimental studies were carried out at the cyclotrons of the Universities of Michigan, Pittsburgh, and Indiana, of Washington University in St. Louis, and at Argonne National Laboratory. This early work[1—5] and its spirit is described in the 1960 review article of Macfarlane and French.[6] Since then, technical innovations in both experiment and theory have radically altered the field. The advent of high-energy tandem Van de Graaff accelerators and of variable-energy

[1] W. C. Parkinson, E. H. Beach, and J. S. King, Phys. Rev. 87, 387 (1952).

[2] B. L. Cohen, S. Mayo, and R. E. Price, Nucl. Phys. 20, 360 (1960).

[3] M. T. McEllistrem, H. J. Martin, D. W. Miller, and M. B. Sampson, Phys. Rev. 111, 1636 (1958).

[4] F. B. Shull and A. J. Elwyn, Phys. Rev. 112, 1667 (1958).

[5] B. Zeidman, J. L. Yntema, and B. J. Raz, Phys. Rev. 120, 1723 (1960).

[6] M. H. Macfarlane and J. B. French, Rev. Mod. Phys. 32, 567 (1960).

isochronous cyclotrons, together with the development of solid-state detectors, transistorized multichannel analyzers, and broad-range magnetic spectrographs has permitted detailed study of heavier nuclei with closely-spaced levels. The distorted-wave Born approximation (DWBA)[7,8] has placed the theoretical analysis of single-nucleon transfer on a sounder and more quantitative basis.

It is perhaps surprising, but is nevertheless true, that after twenty years of extensive study, much remains to be done in the field of direct nucleon transfer. For example, single-proton pickup on nuclei with $A > 90$ (including deformed nuclei) still awaits the higher-energy, high-precision studies that will be possible with the proposed TU tandem. The field of many-nucleon transfer has now developed roughly to the stage attained in single-nucleon transfer around 1960. Since in principle many-nucleon transfer contains more information about nuclear states than does single-nucleon transfer, the situation is very promising.

In the following, we draw attention to those aspects of nucleon transfer in which the high energy and high precision of the TU tandem will be of particular value.

a. Single-Nucleon Transfer

Single-nucleon-transfer reactions yield information about the occupation-probabilities of single-particle states and about the fragmentation of single-particle and single-hole excitations. Such information is of course critical to all variants of the nuclear shell model, for both spherical and deformed nuclei.

Angular distributions in single-nucleon transfer identify not only the orbital angular momentum ℓ of the transferred nucleon

[7] G. R. Satchler, Nucl. Phys. 55, 1 (1964).

[8] L. L. Lee, Jr., J. P. Schiffer, B. Zeidman, G. R. Satchler, R. M. Drisko, and R. H. Bassel, Phys. Rev. 136, B971 (1964).

but also its total angular momentum j. The small yet systematic features of (d,p) angular distributions that reveal j values were first noticed by Lee and Schiffer at Argonne.[9] Similar effects have now been identified in nearly all single-nucleon-transfer reactions.

Such studies have yielded a reasonably comprehensive view of single-neutron levels throughout the periodic table, with the important restriction that most of the available information concerns the few active (i.e., valence) orbits close to the Fermi surface. Serious gaps in our knowledge exist for unbound levels and for deeply-bound core orbits. Since most pickup reactions have unfavorably negative Q values, studies of strongly-bound orbits demand higher bombarding energy than has been available until recently. The TU tandem and the lower energy range of the proposed cyclotron will be very valuable in continuing the kind of detailed study[10—12] of hole states already started with the linear accelerator at the University of Minnesota and the high-energy cyclotrons at the University of Michigan and at Michigan State University.

Far less is known about proton levels. Although (d,n) studies were started at the same time as (d,p), the difficulty of neutron detection has inhibited spectroscopic applications. The main source of information has been the (d,He^3) and (He^3,d) reactions. Here unfavorable Q values [for (d,He^3)] and Coulomb barriers have until recently restricted studies to nuclei with $A < 90$. Our knowledge of single-particle and single-hole structure in heavy nuclei is accordingly seriously lopsided in favor of neutrons. The higher-energy beams from the TU tandem will do much to redress the balance.

---

[9] L. L. Lee, Jr., and J. P. Schiffer, Phys. Rev. 136, B405 (1964).

[10] C. D. Kavaloski, G. Bassani, and N. M. Hintz, Phys. Rev. 132, 813 (1963).

[11] G. Muehllehner, A. S. Poltorak, W. C. Parkinson, and R. H. Bassel, Phys. Rev. 159, 1039 (1967).

[12] L. A. Kull, Phys. Rev. 163, 1066 (1967).

Much work—particularly with proton transfer—remains to be done on single-particle and single-hole states in deformed nuclei. There have been many studies[13–15] of neutron structure in the rare-earth region, and a series of recent studies[16,17] at Argonne on neutron structure in the actinides, but no detailed experiments at all on proton structure. Spherical single-particle states in deformed nuclei are fragmented in a way that tells us much about the interplay of collective and single-particle modes in nuclei.

When a single proton is added to (or a single neutron removed from) a nucleus with positive neutron excess, the resulting single-particle excitation splits into two widely-separated isobaric-spin components. The component with $T = T_> = T_{target} + \frac{1}{2}$ is simply the isobaric analog of the corresponding single-neutron excitation. These isobaric analogs have been studied as compound-nucleus resonances in proton-induced reactions; analysis of such reactions has confirmed the reliability of DWBA as a means of extracting spectroscopic information from direct-transfer reactions. Both $T_>$ (analog) and $T_<$ (antianalog) components can be excited directly in (He^3,d) reactions. Studies of this sort, wherein the part of the proton excitation that is a mere replica of the corresponding neutron excitation is identified and removed, have so far been confined to light nuclei and to heavy nuclei near closed shells. With the TU tandem antianalogs and their fragmentation can be studied throughout the periodic table.

---

[13] J. R. Erskine, Phys. Rev. 138, B66 (1965).

[14] D. G. Burke, B. Zeidman, B. Elbek, B. Herskind, and M. Olesen, Kgl. Danske Videnskab. Selskab, Mat.-Fys. Medd. 35, No. 2 (1966).

[15] M. N. Vergnes and R. K. Sheline, Phys. Rev. 132, 1736 (1963).

[16] T. H. Braid, R. R. Chasman, J. R. Erskine, and A. M. Friedman, Phys. Letters 18, 149 (1965).

[17] J. R. Erskine, A. M. Friedman, T. H. Braid, and R. R. Chasman, Proceedings of the Third International Conference on Atomic Masses (University of Manitoba Press, Winnipeg, 1967).

It has been found that whereas the simpler single-nucleon-transfer reactions [(p,d), (d,t), (d,p), etc.] strongly favor low values of ℓ, those such as (α, He^3) and (He^3, α) favor larger values of ℓ ($\ell \approx 4$ or 5).[18] Thus single-nucleon transfer with heavier projectiles frequently reveals transitions too weak to be detected (or at least too weak for quantitative study) in (d,p) or (d,t) reactions. In the same way, (α, t) and (t, α) studies provide a valuable supplement to (He^3, d) and (d, He^3). The possibilities here have not yet been seriously exploited since, at the low bombarding energies attainable at present, the angular distributions for the various ℓ values (and a fortiori for the possible j values) are not sufficiently distinctive for experimental identification.

Finally, although DWBA is clearly a reliable basis for the analysis of most single-nucleon-transfer reactions, there no doubt are a few cases in which competing processes are significant. One such competing process is that in which either the ingoing or the outgoing projectile excites the target to a low-lying collective state which then participates in stripping or pickup. Identification and detailed analysis of reactions of this sort—currently honored with the name 'anomalous'—will require systematic experimental study over as wide a range of bombarding energies as possible and perhaps with several different projectiles [e.g., with (d,n), (He^3, d), and (α, t) reactions].

To summarize, although single-nucleon transfer has been studied extensively for close to 20 years, there still remain areas wherein very little is known because of limitations in the available bombarding energies. In such situations, the higher energies and great precision of the TU tandem will be very valuable. Furthermore, these studies at the upper end of the TU's energy range will support and be supported by parallel studies in the lower energy range of the proposed variable-energy cyclotron.

---

[18] D. D. Borlin, Thesis, Washington University, St. Louis, 1967 (unpublished).

b. Two-Nucleon Transfer

In two-nucleon transfer, the transferred object is a pair of nucleons in a definite quantum state. Although the logical steps in the analysis of such reactions are the same as in single-nucleon transfer, the situation is intrinsically more complicated and therefore intrinsically contains more information. Furthermore, a two-nucleon wave function cannot be constructed until the single-particle wave functions are known. In this sense, a study of multi-nucleon transfer must follow an understanding of single-nucleon transfer; this, indeed, is how the subject has developed.

Until recently, analyses of two-nucleon transfer were of the semi-phenomenological sort characteristic of single-nucleon transfer in its early years. The work of Glendenning[19] and of Bayman[20] in adapting single-nucleon DWBA to two-nucleon reactions promises to provide a sounder theoretical framework. So far, quantitative understanding has been achieved only for $L = 0$ (and $T = 1$) transfer in (p,t) and (t,p) reactions, where L is the orbital angular momentum of the mass-center of the transferred pair. $L = 0$ transitions have now been studied by (p,t) and (t,p) reactions in many regions of the periodic table[21—23]; the results have been interpreted in terms of seniority-coupling schemes and theories of pairing vibrations.[24—27]

[19] N. K. Glendenning, Nucl. Phys. 29, 109 (1962).

[20] B. F. Bayman and A. Kallio, Phys. Rev. 156, 1121 (1967).

[21] G. Bassani, N. Hintz, and C. D. Kavaloski, Phys. Rev. 136, B1006 (1964).

[22] J. H. Bjerregaard et al., Nucl. Phys. A103, 33 (1967).

[23] E. R. Flynn, G. Igo, and P. D. Barnes, Phys. Rev. Letters 22, 142 (1969).

[24] S. Yoshida, Nucl. Phys. 33, 685 (1962).

[25] D. R. Bes and R. A. Broglia, Nucl. Phys. 80, 289 (1966).

[26] A. Bohr, in Nuclear Structure, Dubna Symposium, 1968 (International Atomic Energy Agency, Vienna, 1968), p. 179.

[27] O. Nathan, in Ref. 26, p. 191.

The situation for other two-nucleon reactions—$L \neq 0$ transfer in (p,t) and (t,p), and all T=0 transfers—is still uncertain. The available experimental data reveal a variety of systematic features but no detailed theoretical interpretation can be given, largely because of the extreme sensitivity of the cross sections to phase relations and to the interplay of small components in the pertinent nuclear wave functions. When a good two-nucleon theory becomes available, however, this apparent vice will stand revealed as a virtue—for it is simply a manifestation of the fact that two-nucleon-transfer reactions contain more information about nuclear states than do single-nucleon transfer.

Although the transfer of a p-n pair by means of a reaction such as (He^3,p) or (α,d) does not have the selectivity of an L=0 transfer, these reactions may be used extensively to provide spectroscopic information.[28,29] At Pittsburgh, recent work[30] on (d,α) reactions has provided detailed information concerning the levels and spins of odd-odd nuclei. Other recent work[31] with (He^3,p) reactions has provided similar, though not as unambiguous, results. The (He^3,p) reaction on nuclei near closed shells exhibits an unusual aspect of correlated behavior that has proved useful. Since the transfer of the p-n pair results in enhanced cross sections for levels in which both particles are in the same major shell, reactions on nuclei having a single hole will selectively populate 2p-1h states which are otherwise difficult to identify.[32] The (He^3,p) reaction also populates states which are the isobaric analogs of states observed in (t,p) reactions. A study[33]

[28] B. Zeidman and J. L. Yntema, Nucl. Phys. 12, 298 (1959).

[29] B. G. Harvey and J. Cerny, Phys. Rev. 120, 2162 (1960).

[30] W. W. Daehnick, Phys. Rev. (to be published).

[31] T. A. Belote, W. E. Dorenbusch, and J. Rapaport, Nucl. Phys. A109, 666 (1968).

[32] T. A. Belote, F. T. Dao, W. E. Dorenbusch, J. Kuperus, J. Rapaport, and S. M. Smith, Nucl. Phys. A102, 462 (1967).

[33] J. A. Nolen, Jr., J. P. Schiffer, N. Williams, and D. von Ehrenstein, Phys. Rev. Letters 18, 1140 (1967).

performed at Argonne resulted in the determination of Coulomb energy differences not obtainable otherwise; but the same p-n transfer in an (α,d) reaction would not have populated these states. It is therefore highly desirable to use both reactions so as to distinguish T values. Because of the highly negative Q value of (α,d) reactions, high energies are required together with good resolution.

Much work remains to be done. Clearly two-nucleon-transfer reactions, particularly T=0 transfer, requires additional data and a great deal of work on the underlying reaction theory.

(p,t) and (He^3,n) reactions have the useful feature of transferring 1 unit of isobaric spin to the target nucleus. For targets with isobaric spin $T_0 > \frac{1}{2}$, this allows final states with $T = T_0 \pm 1$ to be populated.[34] Thus two-nucleon transfer is a useful complement to other studies of analog states; its $\Delta T=1$ branch in particular can provide a means of completing isobaric-spin multiplets.

It is clear, then, that two-nucleon-transfer reactions will some day provide very detailed information about the two-nucleon parentage of nuclear wave functions. At present, with the exception of L=0 transfer in (p,t) and (t,p) reactions, there have been few systematic series of experimental studies. In particular, relatively little is known about two-nucleon transfer in deformed nuclei, though some recent Minnesota work on Yb(p,t) reactions reveals interesting systematic features. Many of the two-nucleon studies on heavy nuclei will need high energies to overcome negative Q values and high Coulomb barriers; variable energy will also be essential to establish the details of the reaction theory.

c. Three-Nucleon Transfer

Let us confine attention here to (α,nucleon) reactions. Very little data have so far been obtained in energy ranges where

[34] G. J. Garvey, J. Cerny, and R. H. Pehl, Phys. Rev. Letters 12, 726 (1964).

compound-nucleus formation is not dominant. A study[35] of (p,α) reactions at 17 MeV reveals that this reaction shows many of the features of a simple proton pickup such as (d,He^3). It appears that the neutron pair behaves as a spectator, serving merely to shift the mass of the target nucleus. It may be possible to calibrate this reaction to provide reliable spectroscopic factors. Various studies have shown that (α,nucleon) reactions exhibit pronounced j-dependent effects, which makes them suitable as spectroscopic probes. Since three nucleons are transferred, (α,nucleon) reactions provide a means for doing the equivalent of single-nucleon transfer on unstable nuclei. Since it is essential to avoid compound-nucleus effects, the high variable energy of the proposed accelerator is necessary.

d. Transfer of Clusters with $A \geq 4$

Here we consider reactions induced by light-ion bombardment, in which clusters of four or more nucleons are transferred. Early work of this sort with (d,Li) reactions was carried out at Pittsburgh[36] and at Argonne.[37] Only in recent years have such cluster-pickup studies begun to yield information that can be interpreted in terms of the structure of the nuclear states involved.

At present, cluster pickup is being studied with two rather different aims in mind. On the one hand, a group at Berkeley[38] has used cluster pickup to study nuclear species well off the stability line and to excite levels of exotic isobaric spin in less-than-exotic nuclei.

---

[35] J. A. Nolen, Jr., Thesis, Princeton University, 1966 (unpublished).

[36] L. J. Denes, W. W. Daehnick, and R. M. Drisko, Phys. Rev. 148, 1097 (1964).

[37] D. S. Gemmell, IEEE Trans. Nucl. Sci. NS-11, 409 (1964).

[38] G. W. Butler, J. Cerny, S. W. Casper, and R. L. McGrath, Phys. Rev. 166, 1096 (1968).

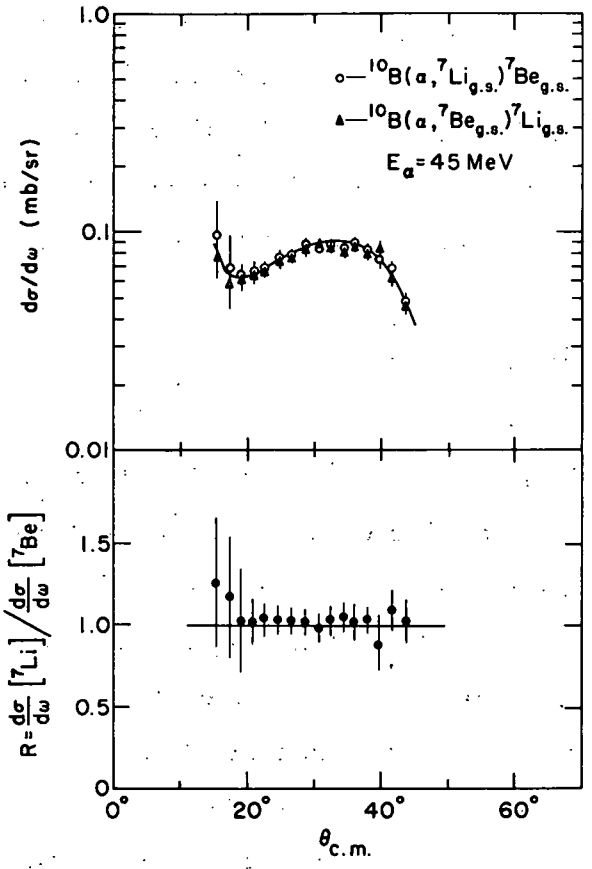

Fig. V.C7-1. Comparison of the angular distributions of Li^7 and Be^7 ions in the reaction $B^{10} + \alpha \rightarrow Li^7_{g.s.} + Be^7_{g.s.}$

On the other, groups at Argonne[39] and elsewhere are studying angular distributions and relative yields in cluster pickup to clarify the underlying reaction mechanism and to establish cluster pickup as a quantitative means of studying nuclear structure. It is only because the field is so new that little overlap has yet developed between the two approaches.

Another recent Argonne experiment[40] illustrates the possibilities in using appropriate cluster transfers to test conservation laws. The reaction involved is $B^{10}(He^4, Be^7)Li^7$, in which the outgoing nuclei form a mirror pair. If isobaric spin is conserved, and if the residual nuclei are left in isobaric analog states, then the angular distributions of the residual nuclei should be identical. The resulting angular distributions (Fig. V.C7-1) are consistent (within error) with conservation of isobaric spin.

[39] B. Zeidman and H. T. Fortune, Bull. Am. Phys. Soc. 14, 507 (1969).

[40] H. T. Fortune, A. Richter, and B. Zeidman, Phys. Rev. Letters (to be published).

It is clear that the cluster-pickup experiments carried out to date do no more than skim the surface of a promising field of study. Future work will demand great flexibility both in type of projectile and in variability of energy; such flexibility will clearly be provided by the proposed accelerator.

e. Summary

The study of various aspects of nucleon-transfer reactions has been seriously inhibited by a lack of beams with sufficiently high bombarding energy and sufficiently narrow energy spread. Several such fields have been cited above—for example, (1) deeply-bound hole states, (2) proton single-particle and single-hole states in heavy nuclei, (3) two-nucleon transfer other than (p,t) or (t,p) with L = 0, and (4) (α, nucleon) reactions at energies high enough to avoid overwhelming compound-nucleus effects.

Taken by itself, the TU tandem would be of great value in shedding light on these and similar problems. Combining the TU with the lower energy range of the proposed cyclotron, we have a research tool with unique power to solve some of the main outstanding problems in the study of nucleon-transfer reactions.

V.C8. Radiative-Capture Reactions

The giant dipole resonance observed in the interaction of photons with nuclei is one of the most interesting and best-known of nuclear collective phenomena. It has been the subject of many studies with the bremsstrahlung from electron accelerators; in the Midwest, in particular, such studies have been carried out at the University of Illinois, at the University of Chicago, and at Iowa State University at Ames.

Tandem Van de Graaff accelerators have made it possible to study the dipole resonance through the inverse radiative-capture reaction. Many such experiments have been carried out at Argonne, Chalk River, Oxford, and elsewhere. Typical results[1]—those for the reaction $Al^{27}(p, \gamma)Si^{28}$—are shown in Fig. V.C8-1. Similar (p, γ) studies have been reported from Canberra and Rice with Li^{7} as a target, from Oxford with N^{15} targets, from the University of Illinois and S.U.N.Y. (Stonybrook) with K^{39}, and from Argonne[2] with B^{11}, F^{19}, Na^{23}, and Cl^{37}.

Such experiments have revealed a great deal of fine structure in the giant dipole resonance in not-too-heavy nuclei. In addition, they give some indications of an intermediate structure—grosser than that of the individual compound-nucleus levels from which the dipole resonance is built, yet still a substructure of the giant-resonance envelope itself. These results pose the problem of interpreting the intermediate structure in terms of simple excitations of the core nucleus. No such detailed understanding has yet been achieved and it is clear that further detailed experimental study is needed.

A very striking fact has emerged from studies of the angular distribution of (p, γ) reactions. It is found that the shape of the (p, γ)

---

[1] P. P. Singh, R. E. Segel, L. Meyer-Schützmeister, S. S. Hanna, and R. G. Allas, Nucl. Phys. 65, 577 (1965).

[2] R. G. Allas, S. S. Hanna, L. Meyer-Schützmeister, and R. E. Segel, Nucl. Phys. 58, 122 (1964); R. E. Segel, Z. Vager, L. Meyer-Schützmeister, P. P. Singh, and R. G. Allas, Nucl. Phys. 93, 31 (1967); R. C. Bearse, L. Meyer-Schützmeister, and R. E. Segel, Nucl. Phys. A116, 682 (1968).

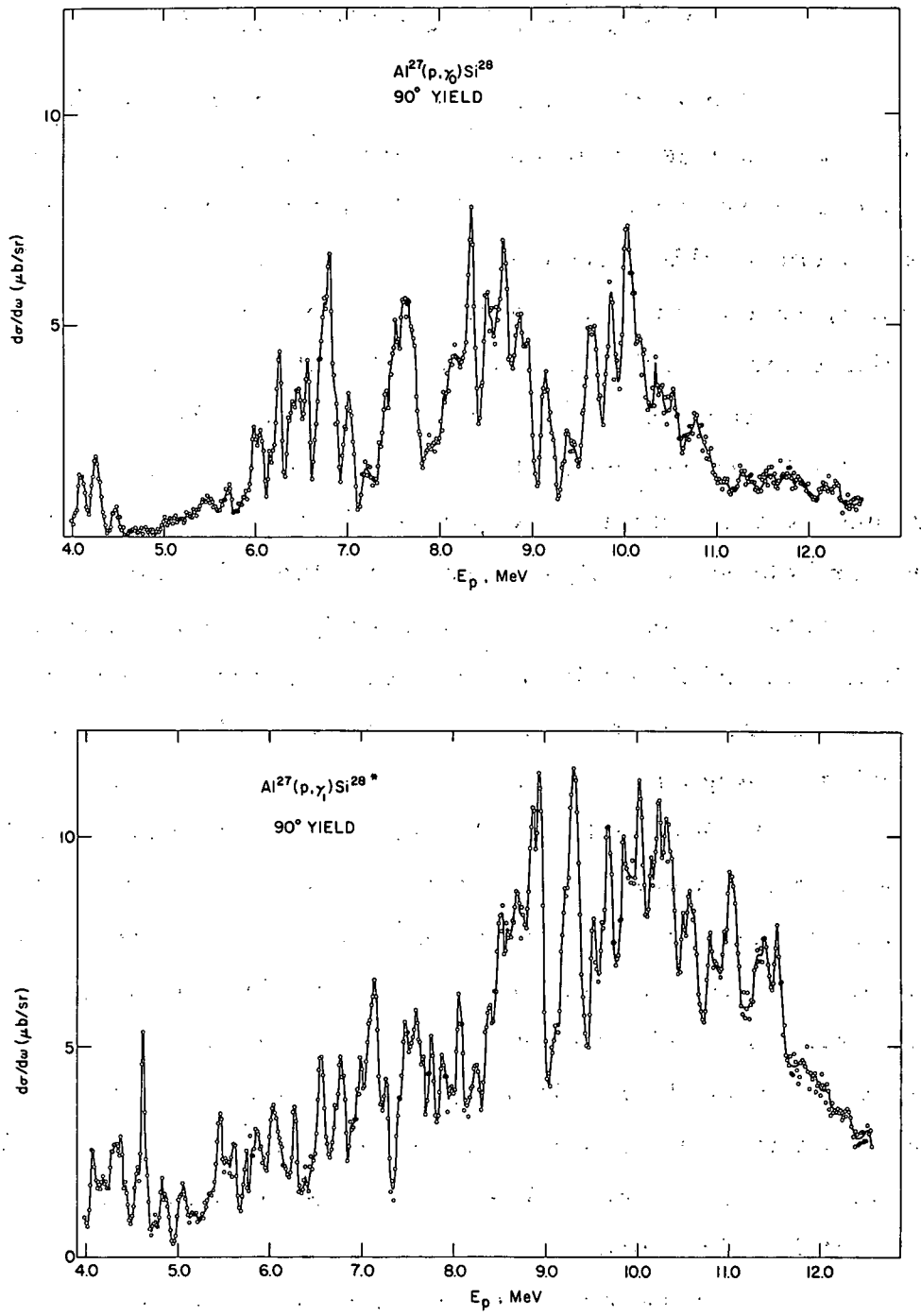

Fig. V.C8-1. Differential yield curve for $Al^{27}(p,\gamma_0)Si^{28}$ and $Al^{27}(p,\gamma_1)Si^{28}$. (From Bearse et al., Ref. 2c.)

differential cross section does not vary significantly as the proton bombarding energy is varied across the dipole resonance. It is clear that we do not yet understand the full significance of this phenomenon for the structure of the dipole resonance; in some sense it implies that of the many configurations or particle structures that can contribute to the dipole state, one supplies most of the strength.

Recent (γ, n) and (γ, p) studies at Iowa State University[3] have permitted detailed comparisons with (p, γ) studies of the giant dipole resonance in C^{12}. Figure V.C8-2 compares the results of the $B^{11}(p, \gamma_0)C^{12}$ and $C^{12}(\gamma, p)B^{11}$ experiments. Such comparisons yield estimates of proton emission from the giant dipole resonance to excited states of the daughter nucleus. Studies at Argonne[1] have revealed giant resonances built on excited states of nuclei, very similar to the ground-state resonances but displaced upwards by roughly the excitation energy of the pertinent excited state.

In most Van de Graaff work to date, the giant dipole resonance has been excited by proton capture. In a few cases, however, excitation of the dipole resonance by alpha capture has also been studied.

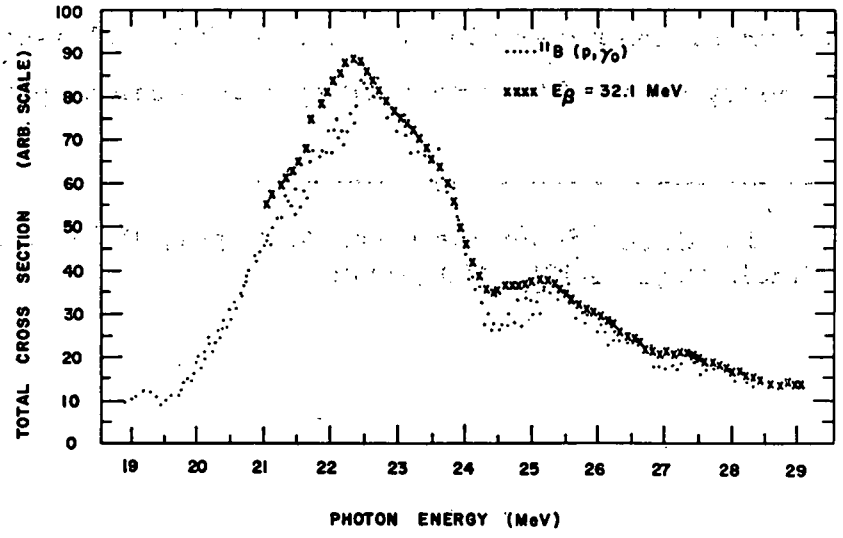

Fig. V.C8-2. Comparison of cross sections for the reactions $B^{11}(p, \gamma_0)C^{12}$ and $C^{12}(\gamma, p)B^{11}$. (From Frederick and Sherick, Ref. 3b.)

[3] B. C. Cook, J. E. E. Baglin, J. N. Bradford, and J. E. Griffin, Phys. Rev. 143, 724 (1966); D. E. Frederick and A. Daniel Sherick, Phys. Rev. 176, 1177 (1968).

This work[4] has yielded insight into the manner in which the giant-dipole excitation distributes its strength over the compound-nucleus levels in its neighborhood. Since the alpha-particle has T = 0, the (d, α) reaction is a useful way of studying the isobaric-spin purity of the dipole resonance.

Two particular directions are indicated for future research. (1) Most available data concern even-even nuclei with N = Z. Experiments are beginning on nuclei with two excess neutrons and should be extended in the future to nuclei with larger neutron excess. A major point of interest here is the detection and study of the isobaric-spin splitting of the giant dipole resonance. (2) It will be of great interest to study proton capture at much higher bombarding energies, where capture will no longer be dominated by the giant dipole resonance. At such energies, it may be possible to distinguish the giant quadrupole resonance. Some technical innovations will no doubt be necessary in such studies. For instance, where enough momentum is transferred to the daughter nucleus, it should be possible to separate the recoiling nucleus by magnetic analysis since the recoil momentum will be well defined. Different types of gamma-ray detector will probably be needed for $E_\gamma > 100$ MeV.

It is clear that in achieving such significant extensions of current experimental knowledge, both the TU tandem and the lower energy range of the proposed cyclotron can be put to excellent use.

---

[4] L. Meyer-Schützmeister, Z. Vager, R. E. Segel, and P. P. Singh, Nucl. Phys. A108, 180 (1968).

V.C9. Polarized-Beam Experiments

It is well known that polarization experiments are vital to studies of the spin-dependence of nuclear processes. This is well illustrated in Los Alamos work on the spin-orbit term in the proton-nucleus optical potential.[1] This section discusses the prospects for polarized-beam experiments with the XTU tandem.

Systematic information on polarization effects in nuclear reactions has been limited because, until recently, polarization experiments have involved tedious double-scattering techniques. Over the last few years, however, rapid progress has been made in the development of polarized-ion sources.[2] These are devices that make use of atomic interactions to produce polarized ions which are then injected into the accelerator. Polarized beams have been accelerated successfully in both cyclotrons and tandem accelerators. Particularly rapid progress has been made recently in the preparation of polarized beams of negative ions. The application of these beams to an XTU tandem would offer a unique facility to study the spin dependence in almost any type of nuclear reaction. The combination of the energy range of the XTU, which is ideal for any direct-reaction process, with the expected large intensity of polarized beams opens a vast new area to experimental investigation. Polarized negative-ion beams of 0.2 μA have been obtained at Wisconsin and 0.6 μA has been observed at Los Alamos.[3] Experience with another source of the same type[4] has shown that as much as 50% of the injected beam may be available on target. On the basis of these figures, it seems entirely realistic to expect at least a 0.1-μA polarized beam after acceleration from an XTU tandem. The probability is great that even

---

[1] L. Rosen, J. G. Beery, A. S. Goldhaber, and E. H. Auerbach, Ann. Phys. (N.T.) 34, 96 (1965).

[2] W. Haeberli, Ann. Rev. Nucl. Sci. 17, 373 (1967).

[3] G. P. Lawrence, G. G. Ohlsen, and J. L. McKibben, Bull. Am. Phys. Soc. 13, 1443 (1968).

[4] T. B. Clegg, G. R. Plattner, L. G. Keller, and W. Haeberli, Nucl. Instr. Methods 57, 167 (1967).

larger polarized beam currents will be feasible by the time this accelerator is operating. This intensity is not only sufficient to perform scattering and reaction experiments on a routine basis, but makes it feasible in certain circumstances to consider double-scattering experiments; thus experiments that would normally have required triple scattering now become possible. This will allow the determination of the various Wolfenstein parameters (spin-rotation and spin-correlation parameters). Some possible applications of the XTU polarized beam are given below.

a. Very Light Nuclei and the Few-Nucleon Problem

There is considerable interest in the determination of the scattering amplitudes for systems consisting of a few nucleons. The hope is that such systems may be particularly simple and can be understood in terms of nucleon-nucleon forces. To provide sufficient data for a phase-shift analysis (e.g., for proton scattering from deuterium), an extensive collection of polarization data is needed. Scattering of polarized 15-MeV protons from deuterium and scattering of 30-MeV vector- and tensor-polarized deuterons from hydrogen would give five pieces of information for each scattering angle instead of just one (cross section only). Triple-scattering and spin-correlation parameters will also be of interest. Similar experiments should also be considered for $He^3(p, p)He^3$, $He^3(d, d)He^3$, $He^3(d, p)He^4$ with unpolarized and with polarized targets. The unexpected observation[5] that scattering of deuterons by deuterons show little or no polarization below about 20 MeV should be investigated at higher energies.

b. Elastic and Inelastic Scattering

Very little is known about the spin dependence of the deuteron nucleus interaction. Scattering of vector- and tensor-polarized deuterons should be studied over a wide range of deuteron energies and atomic weights

---

[5] G. G. Ohlsen, Los Alamos (private communication).

of the target. Measurements with tensor-polarized beams are essential to determine which of the three possible forms of tensor coupling are the important ones and to find the strength and radial dependence of the tensor potential. This information is presently unavailable. Measurements of the polarization in proton elastic scattering are still needed, because earlier measurements[1] were often of poor accuracy and did not have sufficient energy resolution to separate elastic and inelastic scattering. Measurements of the asymmetry in the inelastic scattering of polarized protons for several bombarding energies provide an excellent test of coupled-channel calculations.

c. Transfer Reactions

Pronounced polarization effects have recently been discovered when vector-polarized deuterons were used to initiate (d, p) reactions.[6] The effects permit unique angular-momentum assignments and also contribute an additional test of the theoretical description of the reaction mechanism. There is much interest in extending such measurements to a wider range of bombarding energies. In particular, it would be interesting to determine whether the distorted-wave theory can account for the energy dependence of cross sections and polarizations with consistent values of the appropriate nuclear matrix elements. No studies have yet been reported with tensor-polarized beams. Such measurements would yield additional information; in particular they would test for the effect of the deuteron D state. At the same time, the inverse (p, d) reaction should be studied at the corresponding center-of-mass energy; this is not readily possible with present tandem machines because of the limited energy range. Similar effects presumably exist in other transfer reactions but none of them has been investigated with polarized beams. The energy range and polarized-beam capabilities of an XTU tandem would be ideally suited for such studies.

---

[6] T. J. Yule and W. Haeberli, Nucl. Phys. A117, 1 (1968).